

COMPARATIVE STUDY OF CONTIGUOUS PILE WALL AND STEEL
SHEET PILE WALL AS SHORE PROTECTION SYSTEM USING
NUMERICAL TECHNIQUE



A thesis Submitted by

Istiakur Rahman

Student No. 0416042211

A thesis submitted to the Department of Civil Engineering in the Partial Fulfillment of the
Requirement for the Degree of

MASTER OF SCIENCE IN CIVIL ENGINEERING

BANGLADESH UNIVERSITY OF ENGINEERING AND TECHNOLOGY

May, 2019

The thesis titled “COMPARATIVE STUDY OF CONTIGUOUS PILE WALL AND STEEL SHEET PILE WALL AS SHORE PROTECTION SYSTEM USING NUMERICAL TECHNIQUE”, submitted by Student- Istiakur Rahman, Roll No.: 0416042211, Session: April 2016, has been accepted as satisfactory in partial fulfillment of the requirement for the degree of Master of Science (Civil & Geotechnical Engineering) on 22 May, 2019.

BOARD OF EXAMINERS

<hr/> <p>Dr. Mehedi Ahmed Ansary Professor Dept. of Civil Engineering BUET, Dhaka-1000.</p>	<p>Chairman (Supervisor)</p>
<hr/> <p>Dr. Ahsanul Kabir Professor & Head Dept. of Civil Engineering BUET, Dhaka-1000.</p>	<p>Member (Ex-Officio)</p>
<hr/> <p>Dr. Abu Siddique Professor Dept. of Civil Engineering BUET, Dhaka-1000.</p>	<p>Member</p>
<hr/> <p>Dr. Md. Abu Taiyab Professor Dept. of Civil Engineering DUET, Gazipur-1700</p>	<p>Member (External)</p>

DECLARATION

I certify that this thesis or any part of it has not been submitted elsewhere for the award of any degree or diploma. To the best of my knowledge and belief, the thesis contains no material previously published or written by another person except where due reference is made in the thesis itself.

Istiakur Rahman

TABLE OF CONTENTS

DECLARATION	iii
TABLE OF CONTENTS	iv
LIST OF FIGURES	viii
LIST OF TABLES	xi
NOTATIONS	xiii
ACKNOWLEDGEMENT	xv
ABSTRACT	xvi
CHAPTER 1: INTRODUCTION	1
1.1 General	1
1.2 Background and present state of the problem	3
1.3 Objectives	4
1.4 Organization of the thesis	5
CHAPTER 2: LITERATURE REVIEW	6
2.1 Introduction	6
2.2 Theoretical methods	6
2.2.1 Classical earth pressure hypothesis	6
2.2.2 Stability analysis	7
2.2.3 Stress Path Method	8
2.3 Empirical Method	9
2.3.1 Basal Stability Calculation	12
2.3.2 Predicting Wall Deflection, Ground Settlement and Apparent Earth Pressure.	14
2.4 Laboratory tests and field measurements	23
2.5 Numerical modeling	24
2.5.1 Model details and simulation process	24

2.5.2	Effect of retaining wall stiffness	26
2.5.3	Effect of the support system of retaining wall	27
2.5.4	Effects of construction process	28
2.5.5	Effect of geometry of the excavation	28
2.5.6	Effect of wall installation	29
2.5.7	Effect of soil-structure interaction	30
2.6	Constitutive models of soil behavior	31
2.6.1	Mohr Coulomb (MC) Model	35
2.6.2	Hardening Soil (HS) Model	40
2.6.3	Difference between the Mohr-Coulomb model and Hardening soil model in general	49
2.7	Drainage conditions: Undrained A/ B/ C/ D	49
2.7.1	Advantages and limitations of Undrained A, B, C and D	51
2.8	Review on Sheet Pile Wall and Contiguous Pile Wall	54
2.8.1	Sheet Pile Wall	54
2.8.2	Contiguous Pile Wall	61
2.9	Summary	63

CHAPTER 3: DATA COLLECTION AND THE VALIDATION OF FEM MODEL

	MODEL	66
3.1	Introduction	66
3.2	Geological and geotechnical engineering properties of study areas	67
3.2.1	Generalized geotechnical properties of the site in Dhaka	67
3.2.2	Generalized geotechnical properties of a site in Chittagong	70
3.3	Parametric studies of an excavation	73
3.3.1	Geometry of the excavation	73
3.3.2	Construction sequence	75
3.3.3	Finite element model	75
3.3.4	Material Models and input parameters	76
3.4	Influence of meshing in the output result	77
3.5	Influence of soil-structure contact and interface properties	83

3.6 Influence of failure factor on wall deformation	85
3.7 PLAXIS 3D model versus field instrumentation data	86
3.8 PLAXIS 3D model versus data from the available literature	92
3.9 Summary	97
CHAPTER 4: NUMERICAL MODELING	98
4.1 Introduction	98
4.2 PLAXIS 3D Modeling	98
4.3 Derivation of soil stiffness parameters	99
4.3.1 Derivation of soil parameters from field test	99
4.3.2 Derivation of soil parameters from laboratory test	99
4.3.2.1 Tri-axial test	100
4.4 Design Parameters	100
4.4.1 Introduction	100
4.4.1.1 Parameters for Mohr Coulomb (MC) model	100
4.4.1.2 Parameters for Hardening Soil (HS) model.	102
4.5 Numerical Analysis	103
4.6 Modeling	109
4.6.1 Modeling of Soils and Excavation Sequences	109
4.6.2 Modeling of Structural Elements	112
4.7 Summary	113
CHAPTER 5: RESULTS AND DISCUSSIONS	114
5.1 Introduction	114
5.2 Retaining wall deflections	114
5.2.1 Sheet pile wall and contiguous pile wall deflections for Dhaka site for single basement system	115
5.2.2 Sheet pile wall deflections in Dhaka soil for double basement system	125

5.2.3 Sheet pile wall and contiguous pile wall deflections for Dhaka site for triple basement system	133
5.2.4 Sheet pile wall and contiguous pile wall displacement for Chittagong site having single, double and triple basement	143
5.2.5 Comparison between the sheet pile wall and the contiguous pile wall	165
5.3 Internal forces of retaining wall	166
5.4 Effect of adjacent structure near to the excavation zone	173
5.5 Effect of the number of struts in each bracing level	176
5.6 Ground settlement	179
5.7 Basal Heave	181
5.8 Cost comparison of steel sheet pile wall and contiguous pile wall in the context of Bangladesh	183
CHAPTER 6: CONCLUSIONS AND RECOMMENDATIONS	185
6.1 Conclusions	185
6.2 Recommendations for Future Work	189
REFERENCES	191
APPENDIX A	203
APPENDIX B	209

LIST OF FIGURES

Fig. 2.1 Basal Stability- Terzaghi Method	12
Fig. 2.2 Modified Terzaghi Method (Wong and Goh, 2002)	13
Fig. 2.3 Summary of settlements adjacent to open cuts in various soils, as function of distance from edge of excavation (Peck 1969)	15
Fig. 2.4 Typical Profile of Movements (Clough and O'Rourke 1990)	15
Fig. 2.5 Relationships between Maximum Lateral Wall Movements and Ground Surface Settlements for different Stiffness Supporting Systems in Clay and Factor of Safety Against Basal Heave (Clough and O'Rourke, 1990)	16
Fig. 2.6 Observed Maximum Wall Movements and Ground Settlements Verses Excavation Depth for Various In-situ Walls (Clough and O'Rourke, 1990)	17
Fig. 2.7 Apparent Earth Pressure Diaphragms (Peck 1969)	18
Fig. 2.8 Hyperbolic Model	32
Fig. 2.9 Mohr-Columb Failure Criterion	36
Fig. 2.10 Mohr-Coulomb Yield Surface in Principal Stress Space ($c'=0$)	37
Fig. 2.11 Definition of E_{50}	38
Fig. 2.12 Hyperbolic Stress-Strain Relation in Primary Loading for a Standard Drained Triaxial Test (Schanz et al., 1999).	42
Fig. 2.13 Shear Hardening and Cap Yield Surfaces in the Hardening Soil Model	44
Fig. 2.14 Definition of E_{oed} in Oedometer Test Results	45
Fig. 2.15 Resulting Strain Curve for a Standard Triaxial Test when Including Dilatancy Cut-off	46
Fig. 2.16 Illustration of Double Yield Surface of the Hardening Soil Model (a) in p - q plane; (b) in 3D with $c'=0$	48
Fig. 2.17 Effective stress path using c' and ϕ' - MC model (Wong 2009)	52
Fig. 2.18 Undrained shear strength predicted by undrained method A for normally consolidated and over consolidated clays (Wong 2009)	52
Fig. 2.19 Cantilever Sheet Pile Wall	55
Fig. 2.20 Anchored Sheet Pile Wall	55
Fig. 2.21 Steel sheet piles in excavation of a bridge foundation pit.	60
Fig. 2.22 Bored Pile Walls	61
Fig. 2.23 Earth pressure distribution proposed by Peck (1974)	62
Fig. 3.1 Soil profile of a site in Dhaka	68
Fig. 3.2 Soil profile of a site in Chittagong	71
Fig. 3.3 Plan and section view of a four level excavation system	74
Fig. 3.4 Meshing of the model	76
Fig. 3.5 Deformed meshing of a) Fine meshing b) Medium meshing c) course meshing and d) very course meshing	79
Fig. 3.6 Total displacement of sheet pile in long side for a) fine meshing b) medium meshing c) coarse meshing d) very course meshing.	82
Fig. 3.7 Wall deflection at center in the long side for different meshing	83
Fig. 3.8 Wall deflection at center in the long side of sheet pile wall for different interface factor	84
Fig. 3.9 Wall deflection at the long side of sheet pile wall for different failure factor	85
Fig. 3.10 Cross-section of bridge pier (No 12)	86

Fig. 3.11 Actual footage during construction work	87
Fig. 3.12 Arrangement of struts in two levels	88
Fig. 3.13 Field instrumentation of a strut by strain gauge	89
Fig. 3.14 Deformed mesh of the model	90
Fig. 3.15 Axial forces acting on the struts	91
Fig. 3.16 Field instrumented data obtained for strut force (kN)	92
Fig. 3.17 Layout of Siam Machine Motor Building (Chhunla Chheng and Suched Likitlersuang, 2017)	93
Fig. 3.18 Connectivity plot of the excavation zone.	95
Fig. 3.19 Displacement of the Sheet pile wall	96
Fig. 4.1 Plan layout of a) Excavation zone b) Placement of Sheet pile wall c) Placement of Contiguous pile wall	105
Fig. 4.2 Cross-sectional view of sheet pile wall retaining pile system a) Single basement b) Double basement c) Triple basement.	106
Fig. 4.3 Cross-sectional view of Contiguous pile wall retaining pile system a) Single basement b) Double basement c) Triple basement.	107
Fig. 4.4 Connectivity plot of finite element model containing sheet pile wall retaining system	108
Fig. 4.5 Connectivity plot of finite element model containing contiguous pile wall retaining system	108
Fig. 5.1 Sheet pile wall and Contiguous pile wall displacement of Dhaka site having single basement system in the long side –MC model	116
Fig. 5.2 Sheet pile wall and Contiguous pile wall displacement of Dhaka site having single basement system in the short side –MC model	117
Fig. 5.3 Sheet pile wall and Contiguous pile wall displacement of Dhaka site having single basement system in the long side –HS model	118
Fig. 5.4 Sheet pile wall and Contiguous pile wall displacement of Dhaka site having single basement system in the short side –HS model	119
Fig. 5.5 Sheet pile wall and Contiguous pile wall displacement of Dhaka site having double basement system in the long side -MC model	125
Fig. 5.6 Sheet pile wall and Contiguous pile wall displacement of Dhaka site having double basement system in the short side -MC model	126
Fig. 5.7 Sheet pile wall and Contiguous pile wall displacement of Dhaka site having double basement system in the long side –HS model	127
Fig. 5.8 Sheet pile wall and Contiguous pile wall displacement of Dhaka site having double basement system in the short side –HS model	128
Fig. 5.9 Sheet pile wall and Contiguous pile wall displacement of Dhaka site having triple basement system in the long side –MC model	134
Fig. 5.10 Sheet pile wall and Contiguous pile wall displacement of Dhaka site having triple basement system in the short side –MC model	135
Fig. 5.11 Sheet pile wall and Contiguous pile wall displacement of Dhaka site having triple basement system in the long side –HS model	136
Fig. 5.12 Sheet pile wall and Contiguous pile wall displacement of Dhaka site having triple basement system in the short side –HS model	137
Fig. 5.13 Sheet pile wall and Contiguous pile wall displacement of Chittagong site having single basement system in the long side –MC model	144

Fig. 5.14	Sheet pile wall and Contiguous pile wall displacement of Chittagong site having single basement system in the short side –MC model	145
Fig. 5.15	Sheet pile wall and Contiguous pile wall displacement of Chittagong site having double basement system in the long side –MC model	146
Fig. 5.16	Sheet pile wall and Contiguous pile wall displacement of Chittagong site having double basement system in the short side –MC model	147
Fig. 5.17	Sheet pile wall and Contiguous pile wall displacement of Chittagong site having triple basement system in the long side –MC model	148
Fig. 5.18	Sheet pile wall and Contiguous pile wall displacement of Chittagong site having triple basement system in the short side –MC model	149
Fig. 5.19	Sheet pile wall and Contiguous pile wall displacement of Chittagong site having single basement system in the long side –HS model	150
Fig. 5.20	Sheet pile wall and Contiguous pile wall displacement of Chittagong site having single basement system in the short side –HS model	151
Fig. 5.21	Sheet pile wall and Contiguous pile wall displacement of Chittagong site having double basement system in the long side –HS model	152
Fig. 5.22	Sheet pile wall and Contiguous pile wall displacement of Chittagong site having double basement system in the short side –HS model	153
Fig. 5.23	Sheet pile wall and Contiguous pile wall displacement of Chittagong site having triple basement system in the long side –HS model	154
Fig. 5.24	Sheet pile wall and Contiguous pile wall displacement of Chittagong site having triple basement system in the short side –HS model	155
Fig. 5.21	Sheet pile wall and contiguous pile wall displacement in the long side of Dhaka site having double basement system - with presence of adjacent structure	174
Fig. 5.22	Sheet pile wall and contiguous pile wall displacement in the short side of Dhaka site having double basement system - with presence of adjacent structure	175
Fig. 5.23	Sheet pile and contiguous pile wall displacement of Dhaka site having double basement system in the long side – reducing the number of struts in both X and Y direction in each bracing level.	177
Fig. 5.24	Sheet pile and contiguous pile wall displacement of Dhaka site having double basement system in the short side – reducing the number of struts in both X and Y direction in each bracing level.	178
Fig. 5.25	Ground surface settlement profiles of Dhaka site having a double basement system	180
Fig. 5.26	The basal heave of Dhaka soil having double basement system	182

LIST OF TABLES

Table 2.1 Summary of the conventional empirical method conducted by different researchers.	19
Table 2.2 Mohr-Coulomb Model input parameters.	38
Table 2.3 Hardening Soil Model Parameters	41
Table 2.4 Summary of analyses for undrained materials	51
Table 3.1 Engineering properties of the site in Dhaka	69
Table 3.2 Engineering properties of the site in Chittagong	72
Table 3.3 Construction sequence	75
Table 3.5 Generated nodes for different type of meshing	77
Table 3.6 Properties of soil	90
Table 3.7 Properties of structural components	90
Table 3.8 Soil parameters used to model the soil (Chhunla Chheng and Suched Likitlersuang, 2017)	94
Table 3.9 Parameters used to model the structural component (Chhunla Chheng and Suched Likitlersuang, 2017)	94
Table 3.10 Construction Sequences	95
Table 4.1 A Summary of Input Parameters for MC Model for the site in Dhaka	101
Table 4.2 A Summary of Input Parameters for MC Model for the site in Chittagong	101
Table 4.3 A Summary of Input Parameters for HS Model for the site in Dhaka	102
Table 4.4 A Summary of Input Parameters for HS Model for the site in Chittagong	103
Table 4.5 Stage Construction- Various phases in PLAXIS modeling	110
Table 4.6 Summary of Structural Elements Properties	112
Table 5.1 A comparison between MC model and HS model for sheet pile displacement of Dhaka site having single basement system	121
Table 5.2 A comparison between MC model and HS model for contiguous pile displacement of Dhaka site having single basement system	122
Table 5.3 A comparison of output result with available literature for the displacement of sheet pile wall and contiguous pile wall for Dhaka site having single basement system for MC model.	123
Table 5.4 A comparison of output result with available literature for the displacement of sheet pile wall and contiguous pile wall for Dhaka site having single basement system for HS model.	124
Table 5.5 A comparison between MC model and HS model for sheet pile displacement of Dhaka site having double basement system	130
Table 5.6 A comparison between MC model and HS model for contiguous pile displacement of Dhaka site having double basement system	130
Table 5.7 A comparison of output result with available literature for the displacement of sheet pile wall and contiguous pile wall for Dhaka site having double basement system for MC model.	131
Table 5.8 A comparison of output result with available literature for the displacement of sheet pile wall and contiguous pile wall for Dhaka site having double basement system for HS model.	132
Table 5.9 A comparison between MC model and HS model for sheet pile displacement of Dhaka site having triple basement system	139

Table 5.10	A comparison between MC model and HS model for contiguous pile displacement of Dhaka site having triple basement system	140
Table 5.11	A comparison of output result with available literature for the displacement of sheet pile wall and contiguous pile wall for Dhaka site having triple basement system for MC model.	141
Table 5.12	A comparison of output result with available literature for the displacement of sheet pile wall and contiguous pile wall for Dhaka site having triple basement system for HS model.	142
Table 5.13	Sheet pile wall displacement of Chittagong site having single, double and triple basement system	157
Table 5.14	Contiguous pile wall displacement of Chittagong site having single, double and triple basement system	158
Table 5.15	A comparison of output result with available literature for the displacement of sheet pile wall and contiguous pile wall for Chittagong site having single basement system for MC model.	159
Table 5.16	A comparison of output result with available literature for the displacement of sheet pile wall and contiguous pile wall for Chittagong site having single basement system for HS model.	160
Table 5.17	A comparison of output result with available literature for the displacement of sheet pile wall and contiguous pile wall for Chittagong site having double basement system for MC model.	161
Table 5.18	A comparison of output result with available literature for the displacement of sheet pile wall and contiguous pile wall for Chittagong site having double basement system for HS model.	162
Table 5.19	A comparison of output result with available literature for the displacement of sheet pile wall and contiguous pile wall for Chittagong site having triple basement system for MC model.	163
Table 5.20	A comparison of output result with available literature for the displacement of sheet pile wall and contiguous pile wall for Chittagong site having triple basement system for HS model.	164
Table 5.21	Comparison between Sheet pile wall and contiguous pile wall	165
Table 5.22	Axial force of retaining wall in Dhaka soil having different basement system	167
Table 5.23	Axial force of retaining wall in Chittagong Site having different basement system	168
Table 5.24	Shear force of retaining wall in Dhaka Site having different basement system	169
Table 5.25	Shear force of retaining wall in Chittagong Site having different basement system	170
Table 5.26	Bending moment of retaining wall in Dhaka Site having different basement system	171
Table 5.27	Bending moment of retaining wall in Chittagong Site having different basement system	172
Table 5.28	Comparison of ground settlement of the current study with the conventional methods	181
Table 5.29	Factor of safety against basal heave compared with available literature	183

NOTATIONS

Symbol	Description
CU	Undrained triaxial test
UU	Unconsolidated undrained triaxial test
c'	Cohesion
e_{init}	Initial void ratio
e_{max}	Maximum void ratio
E	Young's modulus
E_{50}	Secant elastic modulus at 50% peak strength
E_{oed}	Oedometer modulus
E_{ur}	Unloading/reloading modulus
H	Excavation depth
I	Moment of Inertia
k	Coefficient of permeability
k_o^{nc}	Coefficient of earth pressure at rest for normally consolidated soil
m	Power for stress level dependency stiffness
OCR	Over Consolidated Ratio
P_a	Resultant of active earth pressure
P_p	Resultant of passive earth pressure
p^{ref}	Reference Pressure
q	Deviatoric stress
q_a	Asymptotic value of deviatoric stress
q_f	Deviatoric stress at failure
R_f	Failure ratio
R_{int}	Strength reduction factor
S_u	Undrained shear strength

Symbol	Description
α	Adhesion factor
α	Cap parameter
β	Cap parameter
δ_{hm}	Maximum horizontal surface settlement behind wall
δ_{vm}	Maximum vertical surface settlement behind wall
ε	Axial strain
ε_1	Major Principal strain
ε_a	Axial strain
ε_1^p	Plastic shear strain
ε_v^p	Plastic volumetric strain
ε_v^{pc}	Volumetric cap strain
φ	Angle of friction
φ'_{mob}	Effective mobilized angle of friction
γ	Unit weight of soil
ν	Poisson's ration
ν_{ur}	Unloading/reloading poisson's ratio
σ_1, σ'_1	Major total, effective principal stress
σ_3, σ'_3	Minor total, effective principal stress
σ_h, σ'_h	Total, effective horizontal stress
σ_v, σ'_v	Total, effective vertical stress
τ	Shear stress
ψ	Dilatancy angle
ψ'_{mob}	Effective mobilized dilatancy angle

ACKNOWLEDGEMENT

At first gratefulness, to Almighty Allah, for His blessings to give me the ability for completing this thesis work successfully.

I want to express my sincere appreciation to my supervisor, Dr. Mehedi Ahmed Ansary, Professor, Department of Civil Engineering, BUET for his guidance, encouragement, and support throughout this research project. Without his guidance and enthusiasm, this research project would not have reached completion. I am fortunate to have him as my supervisor, and this experience will stay in my memory forever. He often went beyond the call of duty in encouraging and supporting the goals of the research and providing his expertise.

I also would like to acknowledge with appreciation the opportunity provided by Bangladesh University of Engineering and Technology (BUET) to carry out the research work.

I would like to express my gratitude to Dr. Ahsanul Kabir, Professor & Head, Department of Civil Engineering, BUET, for the valuable time he provided as member of my advisory committee. I would also like to take the opportunity of expressing sincere appreciation to Dr. Abu Siddique, Professor, Department of Civil Engineering, BUET and Dr. Md. Abu Taiyab, Professor, Department of Civil Engineering, DUET, for their kind consent to be the member of my advisory committee. Their co-operation and essential suggestions helped me to understand the importance of research.

I want to express my gratitude to my beloved family especially my parents for their love, tolerance, support, and encouragement as I worked to complete this endeavor.

ABSTRACT

Deep excavations have been used globally for underground construction, but they inevitably alter the ground conditions and induced ground deformation which may cause damage to adjacent building structures and utilities. Previously, conventional soil mechanics and empirical data were used by geotechnical engineers to predict the performance of shallow excavations, but those methods were not suitable for deep excavations. However, the advanced numerical method is proved to be capable of simulating the excavation process, investigating the mechanism of soil-structure interaction, estimating ground and retention system movements nowadays. This study aims to conduct numerical analysis in order to compare in between the sheet pile wall and contiguous pile wall-the two retaining systems available in Bangladesh. The feasibility of both the retaining system has been checked based on the comparison. This thesis uses advanced numerical analysis by employing a finite element code PLAXIS 3D to simulate the construction sequences of deep excavation, using a range of foreseeable soil parameters to carry out predictions of sheet pile wall and contiguous pile wall deflections. Also, the numerical model is validated by two case studies, and a parametric study of the model is also been carried out. In general, the results indicate that contiguous pile wall exhibits a better performance in resisting wall movement with or without the presence of nearby structures, reducing internal forces and bracing components and also offers economic benefits through reducing cost.

On average, Contiguous pile wall offers 19% and 43% more resistance to wall movements than the sheet pile wall in the Dhaka site and Chittagong site respectively in case of single basement system by incorporating Mohr-Columb as a soil model. Moreover, the resistance of contiguous pile wall to wall movements in Dhaka site is almost 42.5% and 21% higher than the sheet pile wall in case of double and triple basement systems respectively and the resistance is also higher in the Chittagong site. However, it is observed from the results that HS model predicts lower than the MC model due to the incorporation of three different stiffnesses (tri axial loading secant stiffness, tri axial unloading/reloading stiffness and oedometer loading tangent stiffness).

Contiguous pile wall also shows better performance than sheet pile wall in the comparison of study results with the available literatures. The effectiveness of countering wall displacements in case of contiguous pile wall is also higher than the sheet pile wall in the presence of adjacent structures. Besides, the effect of reducing the number of bracing components is also negligible in case of contiguous pile wall which helps to reduce cost associated with deep excavation.

CHAPTER 1

INTRODUCTION

1.1 General

Due to the inadequate land for the construction in the urban area, underground infrastructures have been extensively constructed for purposes such as deep basements, subways, tunnels, underground car parks, and shopping centers. In order to maximize the use of limited land space, underground structures are usually required to be designed very close to the boundary. Many deep excavations are also needed to be carried out in deplorable subsoil conditions and close proximity to the existing buildings and infrastructures. Excessive ground deformations induced by deep excavations will inevitably damage the surrounding near-by surface and sub-surface structures, resulting in delays, dispute or even litigation and cost overrun. The failure of excavation may have catastrophic consequences, and special care must be taken to avoid such failure. One disaster of this sort in Bangladesh is the collapse of the foundation pit of National Bank Limited (NBL) Twin Tower near the intersection of Sonargaon Hotel in Dhaka city on May 27, 2015. The main causes of this types of failure are various, e.g., unexpected soil conditions, rupture of the bracing system (e.g., buckling or poor connection to the wall), violating the designed construction sequences (e.g., over-excavation). In these types of circumstances, the ability to predict ground deformations with precise accuracy and to tolerable limits has become an essential and challenging geotechnical design issue.

In most cases, however, the pre-performance is more vital, and considerable efforts have been made to understand the characteristics of the soil and structural deformations. To reduce the excavation-induced deformations, an appropriate retaining wall and support system should be designed, as well as employing adequate construction methods. As the excavation becomes deeper and more significant in scale and may be constructed in problematic soils, challenges arise for the research, design, and construction of deep excavations. Therefore, the performance of deep excavations should be better understood through more sophisticated approaches, e.g., real-time field monitoring systems, and numerical predictions.

Ground movements around deep excavations critically depend on the ground conditions (e.g. initial stress states, stiffness and strength properties, and groundwater regime), retaining structures (e.g. types of the retaining wall and support system, rigidity of retaining structures), and the methods of construction (e.g. top-down, bottom-up, open-cut, and excavation sequences). Excessive lateral wall displacements are mainly due to an inadequate support design (e.g., insufficient strut system), and can also result from construction errors (e.g., excessive excavation).

Numerical analysis is proven to be a viable solution for the solution of problems related to deep excavations. Numerical analysis can consider both the geotechnical and structural aspects in the deep excavations such as the soil properties, details of structures, and construction sequences, and provide necessary information on the performance of deep excavations for design purpose. It can also be used to predict the behavior of deep excavation and provide guidance for the construction. A significant development has been made in the numerical technique for the prediction of the ground deformations induced by deep excavations since Peck (1969) published his comprehensive review of a deep excavation. Many researchers now use a finite element method to study the various factors that control deep excavation performances. Indeed, the improving agreement between computed performance and observed performance measured from geotechnical instrumentation is boosting the confidence that we can now push excavation technology to new depths in poorer grounds.

The finite element code PLAXIS 3D has been chosen for this study. This is because of its popularity and experience gained over the past years. Analysis of deep excavation is one of the intended applications of PLAXIS. PLAXIS can simulate staged construction. A number of constitutive soil models, such as a simple elastic perfectly plastic Mohr-Coulomb model and an elastic-plastic non-linear stress dependent stiffness Hardening Soil model are available in PLAXIS for deep excavation design. Applying this program to complex deep excavation work would allow us to solve problems related to deep excavation design and provide better performance predictions for future projects. This thesis, therefore, has strong practical implications.

The practical demonstration will be demonstrated by validating a case study of Siam Motor building in Bangkok and also validating with field monitoring data of strut force in excavation using vibrating wire strain gauge obtained from the construction of a Pier in 2nd Bridge over Gumti River.

In this study, after the successful validation of the program, a detailed numerical comparison has been conducted between contiguous pile wall and sheet pile wall to check the feasibility of these two retaining structures in the urban areas of Bangladesh especially in the capital city Dhaka and the port city Chittagong.

1.2 Background and present state of the problem

Construction projects involving deep excavations are widespread in many urban areas around the world. The commonly used systems for the support of such deep excavations to minimize lateral and vertical ground movements are secant and contiguous pile walls, diaphragm walls, and steel sheet piles. The above soil retention systems are used in combination with horizontal struts, corner struts, and anchors, etc. (Ou, 2006). The behavior of a deep excavation support system is defined and analyzed by using a number of measures, mainly: (a) the displacement of wall elements, (b) the movement of soil masses surrounding the excavation, (c) the movement of existing adjacent structures, and (d) the forces acting on the lateral support elements (Ng et al., 2004). The above measures can be evaluated by the following methods: (1) performance of numerical analyses (Zdravkovic et al., 2005), (2) analyzing physical models of small and medium scale (Laefer et al., 2009) and (3) collecting performance data from instrumented large scale deep excavation projects (Zekkos et al., 2004). Numerical modeling is an effective way to investigate the performance of deep excavations. A significant amount of numerical analyses have been conducted on deep excavations to approximate real deep excavations in the design process by adopting 2D analyses (Clarke et al., 1984; Hubbard et al., 1984; Finno et al., 1991; Hashash et al., 1996). Most of these analyses rely on simplifying assumptions, and therefore the information they can provide is limited and sometimes misleading. In reality, all geotechnical problems involving retaining structures are three dimensional, and ideally, three-dimensional analyses, fully representing the structure's geometry, loading conditions and variations in ground conditions across the site, should be undertaken. Three-dimensional analyses have some advantage over two-dimensional

analyses. For instance, a 2D analysis is not able to consider the corner effects in deep excavations, which indicate that the wall deformation and ground movement are smaller close to the wall corner than around the wall center. Besides, 2D plane strain analysis tends to overestimate the wall deflection and ground settlement behind the wall compared to the simplified 3D symmetric square or rectangular analysis (Gouw et al., 2014; Ou et al., 1996).

Among the options available for retaining structures, Sheet pile wall has been used extensively during the excavation process throughout the world. Meanwhile, two dimensional and three dimensional finite element analyses of sheet pile wall has been widely used as a numerical tool to predict wall movements during excavation (Athanasopoulos et al., 2011; Day et al., 1993; Chheng et al. 2017; Chowdhury et al. 2019, Bhatkar et al. 2017, Jesmani et al. 2018).

However, a sheet pile wall is quite expensive in the context of Bangladesh. In Bangladesh, reinforced retaining system, i.e., contiguous pile wall is common and relatively economical to be used in cohesive soil. Based on the economic advantages of contiguous pile wall compared to a sheet pile wall, there is a scope of intensive research to prove it as a viable option for the excavation process. In this research based on 3D numerical analyses for contiguous pile wall and sheet pile wall, a detailed comparison have been made considering several factors such as soil-structure interaction, stress analysis, pore-water pressure analysis, foundation type, etc.

1.3 Objectives

The following are the main objectives of the research:

- a) To conduct a numerical analysis of steel sheet pile wall for a single, two and three basement systems to obtain lateral displacements, forces, bending moments etc.
- b) To conduct a numerical analysis of contiguous pile wall for a single, two and three basement systems to obtain lateral displacements, forces, bending moments etc.
- c) To compare lateral displacements, forces, bending moments etc. between steel sheet pile wall and contiguous pile wall.

1.4 Organization of the thesis

The main focus of this research was to compare between steel sheet pile wall and contiguous pile wall based on the context of Bangladesh considering several factors such as lateral displacements, forces, stresses, bending moments, etc. The research work conducted for achieving the stated objective is presented through several chapters of this thesis.

Chapter two reviews the previous studies and recent progress in the analysis of deep excavations, including the theoretical and empirical methods, laboratory tests and field observations, and numerical analyses and also the review of the different constitutive model for soil is presented in this chapter.

Chapter three represents a series of parametric studies are conducted on this chapter. The influence of a number of important aspects of deep excavations is also investigated in this chapter. The parametric studies also provide useful preparatory information for the complex modeling procedure described in the subsequent chapters. Validation of the FEM model by taking field instrumentation data of Siam Motor Building in Bangkok and construction of Pier in 2nd Bridge over Gumti River has also been shown in this chapter.

Chapter four describes the modeling procedures using finite element analysis of deep excavations based on the commercial software PLAXIS, and addresses various vital aspects which should be considered in the analysis.

Chapter five presents several case studies using sub-soil properties of a site in Dhaka and another in Chittagong as input to PLAXIS software for both the sheet pile wall and contiguous pile wall. Results obtained through this analysis are presented along with related discussions. A summary of the chapter is also given at the end where results are summarized again.

Chapter six presents the findings of the research program and related discussions are presented in this chapter. This chapter also includes scopes for future researches with specific recommendations.

CHAPTER 2

LITERATURE REVIEW

2.1 Introduction

The deep excavation is a complex subject in geotechnical engineering and has been studied using various methods, e.g., theoretical and empirical methods, laboratory tests, field measurements, and more sophisticated numerical analysis. However, all these methods have their limitations, although they have contributed in various degrees to the understanding of the performance of deep excavations. Some of these methods are reviewed and discussed in this Chapter. The emphasis, however, is to put on the various aspects of observed performance of deep excavations in the field and the capability of finite element analysis to replicate these observed behaviors. A complete review on the constitutive model of soil especially Mohr-Colomb model and Hardening soil model is also presented in this chapter. Moreover, a detailed analysis of the design and numerical analysis related study of sheet pile wall and contiguous pile wall is also shown in this chapter.

2.2 Theoretical methods

Theoretical and empirical methods offer some basic understanding of the performance of deep excavations in a completely different manner. However, they even have boundaries because of their simplicity and assumptions. A number of these ways are reviewed in this section.

2.2.1 Classical earth pressure hypothesis

The design of retaining walls requires the assessment of active earth pressure which is to a great extent in light of the exemplary arrangements of lateral earth pressure given by Coulomb (1776) and Rankine (1857). Coulomb (1776) first concentrated the earth pressure issue utilizing the limit equilibrium method to consider the stability of a wedge of soil between a retaining wall and failure plane. It is very much checked for the frictional soil in active state, however isn't the situation for either the cohesive soil or for the passive state. The point of application of active thrust is assumed at a distance of one-third of the

height of the wall from its base and independent of various parameters such as soil friction angle, angle of wall friction, backfill angle, and wall inclination angle. Rankine (1857) exhibited an answer for lateral earth pressures in retaining walls based on the plastic equilibrium. He expected that there is no friction between the retaining wall and the soil, the soil is isotropic and homogenous, the friction resistance is uniform on the failure surface, and both the failure surface and therefore the backfilled surface is a planer. Caquot and Kerisel (1948) presented tables of active earth pressure coefficients derived from a technique that directly integrates the equilibrium equations on the combined planer and logarithmic spiral failure surface. They included the friction factor between the retaining wall and also the soil and assumed a curved failure surface that is recognized to be very close to the actual failure surface. The active and passive coefficients were developed for cohesion less soils; however, they'll be used for evaluating long term conditions in cohesive soils wherever complete dissipation of pore water pressure happens.

These classical earth pressure theories and their further development form the premise of earth pressure calculations used these days; however, they're solely applicable underneath certain conditions to estimate roughly the earth pressures on the wall. Moreover, they do not consider the construction process and provides no indications on the wall deformations, and ground movements in the more complex braced deep excavations.

2.2.2 Stability analysis

Stability analysis is vital in the design of retaining structures in clay and is regularly directed utilizing limit equilibrium methods or finite element methods. Limit equilibrium calculations are sometimes administered in the design and involve assuming the classical active and passive earth pressure distributions on the back and front of the wall and taking moments about the position of the prop.

Terzaghi (1943) proposed a mechanism comprising of a soil column outside the excavation which creates a bearing capacity failure. The failure is resisted by the weight of a corresponding soil column inside the excavation and also by adhesion acting along the vertical edges of the mechanism. Bjerrum and Eide (1956) expected that the base of the excavation could be dealt with as negatively loaded perfectly smooth footing and gathered

data on total or partial failure cases to analyses the basal heave failure of deep excavations in soft clays. The calculated factor of security is appeared to be below 1.0 for the situations where failure happened, and directly over 1.0 for the cases wherever partial failure occurred, or no failure was observed. Clough and Hansen (1981) further thought of the strength anisotropy of the clay within the expression of factor of safety proposed by Terzaghi (1943), and recommended that the basal heave factor of safety outlined in isotropic soil would overestimate the factor of safety for an anisotropic soil, and this impact becomes significant because the degree of anisotropy will increase. O'Rourke (1993) further changed the basal stability calculations to incorporate flexure of the wall below the excavation level and assumed that the embedded depth of the wall doesn't amendment the geometry of the basal failure mechanism. However, a rise in stability was anticipated because of the elastic strain energy stored in flexure. This gave stability numbers that were functions of the yield moment and assumed boundary conditions at the bottom of the wall.

However, the limit equilibrium approach doesn't contemplate the initial stress state within the soil, the retaining structures, the construction methods, and soil and wall movements.

2.2.3 Stress Path Method

The soil behavior depends on the current stress state, as well as on the stress history. The exclusion of soil in deep excavations results in a reducing of the vertical stress in the soil inside the excavation and loss of lateral constraint for the soil on the retained side. As the excavation behavior is affected by the stress state of the soil, understanding the stress path in the field during the excavating procedure is important to distinguish basic components affecting the shear strength and decide appropriate strength and stiffness parameters through laboratory tests for design and analysis. The stress path technique (Lambe 1967) gives a sound way to deal with comprehend the varieties of effective stress in the soil components at some typical areas caused by both horizontal and vertical stress relief during the excavation.

Ng (1999) understood the field stress paths adjacent to a diaphragm wall during a deep excavation and compared with some relevant laboratory triaxial stress path tests. It had been found that the field effective stress paths in front of the wall are almost similar to the

laboratory stress paths in undrained extension tests, whereas field stress paths behind the wall don't correspond well with those from laboratory undrained compression tests. The potential reason is that the soil at the soil-wall interface had already reached, or was about to, the active condition after wall installation, ensuing from a considerable horizontal stress relief throughout the wall construction. This may indicate that the standard undrained assumption doesn't hold for the soil situated instantly behind the wall throughout a comparatively fast excavation in stiff clay.

Hashash and Whittle (2002) utilized nonlinear finite element analysis to translate the development of lateral earth pressure acting on the well-braced diaphragm walls for deep excavations in soil and clarify the soil arching mechanism. It was exhibited that the stress path experienced by a soil in front of the wall at the final excavation level takes after a typical path of plane strain passive method of shearing, though the soil components behind the wall on the retained side take after more complicated pressure paths because of rotation of the principle stress directions and inversion in shear direction caused by the soil arching mechanism. Results additionally demonstrated that lateral earth pressures can surpass the initial stress at elevations above the excavation grade, delivering apparent earth pressures higher than those forecasted from empirical design methods (Peck 1969).

2.3 Empirical Method

Empirical methods are used to interpolate the performance of deep excavations from the analysis of previously published field data in different areas of the world and local experiences.

Terzaghi (1943) proposed that the average earth pressure is approximately uniform with depth and has small reductions at the top and bottom of the wall based on field measurements. Terzaghi and Peck (1967) proposed the apparent earth pressure envelopes based on field measurements from various locations for predicting maximum strut loads in a braced excavation. However, these diagrams do not represent the real distribution of earth pressures at any vertical section in an excavation and this method has been evaluated by many different researchers such as Wong, Poh et al. (1997), Charles (1998), and Hashash and Whittle (2002).

Peck (1969) summarized excavation in various regions of the world arranged the settlement bend into three zones depending upon the kind of soil and workmanship, and this strategy was normal for unpleasant appraisals of ground surface settlements under different conditions. Be that as it may, the general depiction of settlement curve ignores imperative factors, for example, soil conditions, wall establishment techniques, types of retaining structures, and the construction sequence. What's more, these case narratives are previous to 1969, and the excavation is supported by flexible sheet piles or soldier piles with lagging which result in substantially more significant ground developments than those upheld by considerably stiffer diaphragm walls with top-down construction techniques. Subsequently, it is hard to utilize this empirical method for the prediction of a specific deep excavation project. Clough and O'Rourke (1990) proposed that the settlement profile is triangular for an excavation in sandy soil or stiff clay with the maximum ground settlement occurring at the wall. Non-dimensional profiles demonstrate that the corresponding settlement extends out to 2 and 3 times the excavation depth for sandy soil and stiff to very hard clays, respectively. For an excavation in soft to medium clay, the maximum settlement usually occurs at some distance from the wall, and a trapezoidal shaped settlement trough was proposed. The impact zone extends up to 2 times the excavation depth.

Hsieh and Ou (1998) summed up the ground settlement profiles into two types (i.e., the spandrel type and the concave type) and proposed an experimental technique for anticipating these two sorts of settlement profiles because of regression analysis of the field observations. They partitioned the settlement profiles into the essential impact zone which expands to 2 times of the unearthing profundity, and the auxiliary impact zone which reaches out to times the excavation depth. The maximum ground settlement happens around at half of the excavation depth behind the wall, and the settlement at the wall is about half of the maximum ground settlement. This exact technique might be utilized for the forecast of ground surface settlement profiles, yet the exactness of the prediction relies upon various factors, for example, soil profiles, retaining structures, and construction methods. Kung(2007) developed a semi-empirical model to determine the maximum wall deflection and ground surface settlement caused by a braced excavation in soft to medium clays, based on a database of 33 case histories and results from a large number of finite element analyses. The created model mainly comprises of three parts to assess the maximum wall deflection, the deformation ratio between maximum lateral wall

deflection and maximum ground surface settlement, and the ground surface settlement profile. Regression-based equations were used to break down the relationship of the input variables which may include the maximum wall deflection and the deformation ratio. Model bias was surveyed, and the accuracy of this model was respected to be sufficiently high for functional application. The proposed model was verified using case histories not used in the development of the model.

Mana and Clough (1981) related the normalized maximum observed wall movements over the excavation depth with the factor of safety against basal heave by Terzaghi (1943), based on the analyses of many case histories in soft to medium clays. The constant non-dimensional movement at a high factor of safety is a sign of mostly elastic response, whereas the rapid increases in changes at a lower factor of safety are the result of yielding in the subsoil. Upper and lower limits were suggested for estimating the expected wall movement. Wong and Broms (1989) proposed an upfront procedure to evaluate the lateral deflection of strutted or anchored sheet-pile walls in clay with average to excellent quality. The system was developed based on the assumption that the walls are flexible and the lateral deflections are governed by plastic yielding of the soil below the bottom of the excavation. There were no net volume changes during the excavation, and the volume corresponding to the ground settlement is equal to the volumes associated with the heave and the lateral wall displacement above the bottom of the excavation. The excavation width, excavation depth, and secant or tangent moduli of the soil were included in the analysis. Clough, Smith et al. (1989) premeditated a semi-empirical procedure to estimate wall movement evoked by excavation in clay. The most lateral wall deflection is evaluated relative to factor of safety against basal heave by Terzaghi (1943) and system stiffness. The derived curves are based on average condition, good quality, and therefore the assumption that cantilever deformation of the wall contributes only a small fraction of the total movement.

Generally the design of a deep excavation support system must ensure that the excavation is stable against bottom heave in clay and piping in sand, there is no failure of the supporting system, both the lateral support provided by the bracing system and the retaining wall itself, and that the limit wall and adjacent ground movement is to acceptable limits. In the empirical approach, stability is normally assessed using limit equilibrium methods and deformation entirely relies on empirical co-relationships. Further discussion

on some parameters necessary for the stability and deformation check related to conventional empirical/semi-empirical approaches will be discussed elaborately in the following sections.

2.3.1 Basal Stability Calculation

Limit equilibrium methods are commonly used to assess basal stability of deep excavations. The failure mechanism, proposed by Terzaghi (1943), is given in Fig. 2.1. This method is identical to bearing capacity failure mechanism. Bjerrum and Eide (1956) pointed out that Terzaghi's method is reliable for homogeneous soil with excavation depth $B \geq H$, and is unreliable for narrow ($B < H$) excavation or presence of stiff desiccated crust on the surface. Bjerrum and Eide used inverted bearing capacity concept, whereby the unloading behavior caused by excavation is analogous to building foundation being subjected to upward loading, by using the bearing capacity equation for deep foundation, so that then ultimate unloading pressure can be obtained. Bjerrum and Eides' method considered the effects of excavation shape, width, and depth and is therefore applicable to various shapes and depths (deep and shallow) of excavation.

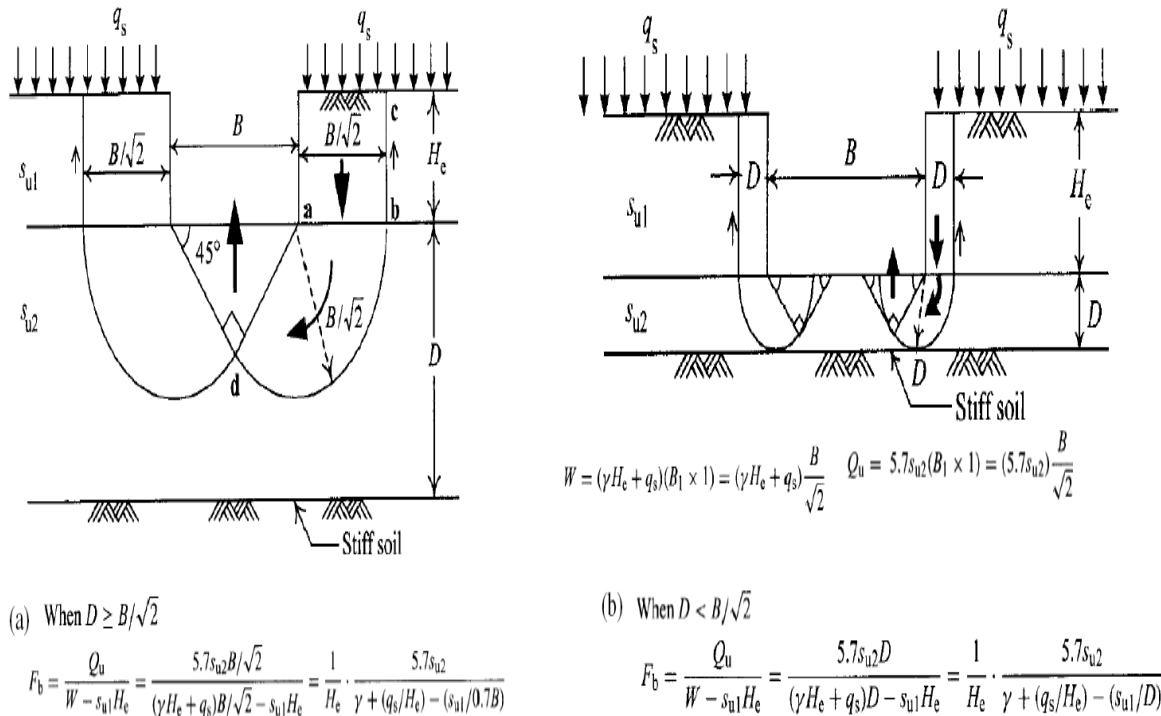


Fig. 2.1 Basal Stability- Terzaghi Method

Mana and Clough (1981) reported cases where the factor of safety calculated using Terzaghi's method, even though this was less than unity, did not result in the excavations failing. This study concluded that Terzaghi's approach might be conservative in certain situations. Hashash and Whittle (1996) summarized several alternative methods to determine the factor of safety against basal heave. They concluded that the penetration depth of the support wall has a significant influence on the overall stability of the excavation and that failure of the soil is constrained by the presence of the wall (unless structural failure of the wall occurs).

Wong and Goh (2002) extended Terzaghi's method to include the effect of rigid wall penetration below the base of excavation as shown in Figure 2.2. They demonstrated that the factor of safety obtained by this method is in close agreement with two examples computed using finite element method.

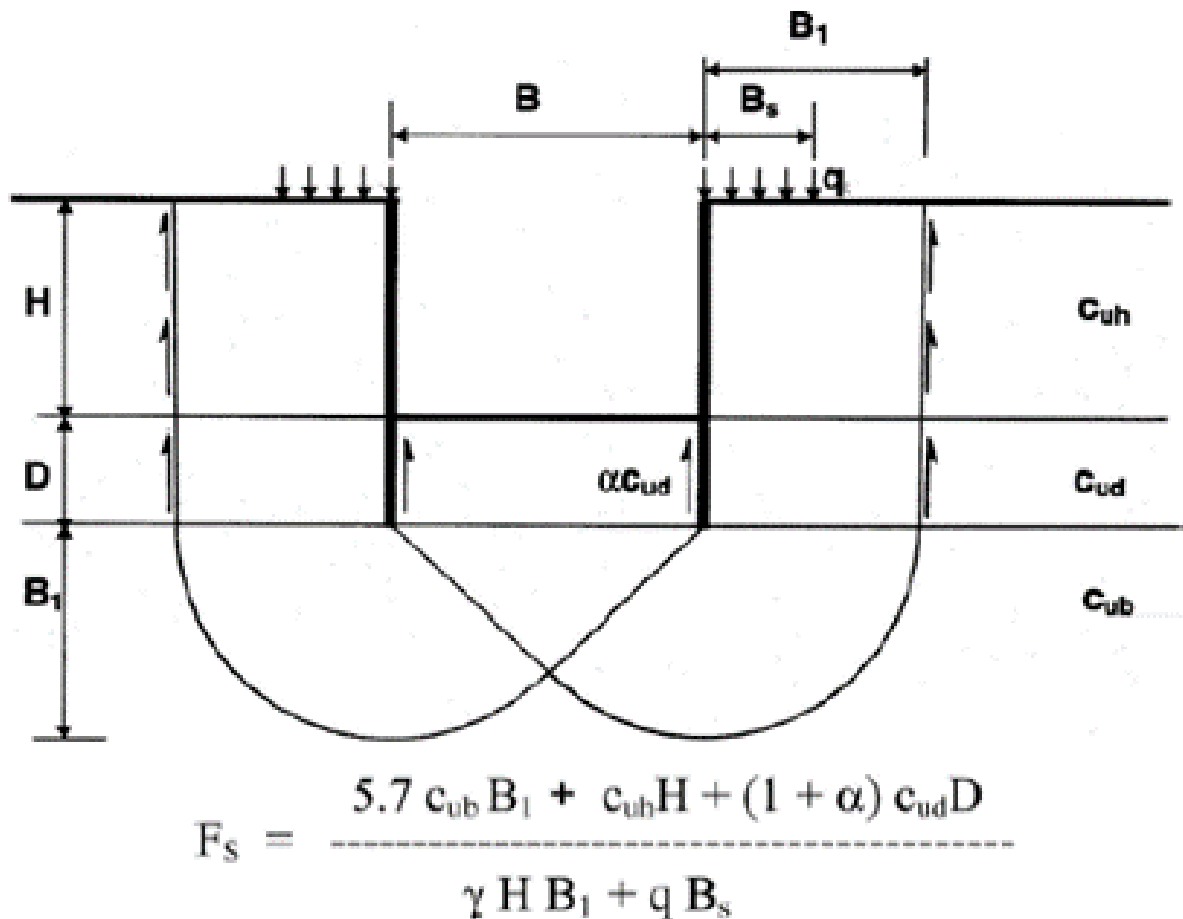


Fig. 2.2 Modified Terzaghi Method (Wong and Goh, 2002)

Ou (2006) commented that the basal heave calculation proposed by Terzaghi has nothing to do with the existence of the retaining wall. However, the presence of a rigid retaining

wall should improve the factor of safety, (i.e., the actual factor of safety with the presence of the rigid retaining wall should be higher than the one calculated using Terzaghi's formula). He further commented that Terzaghi's method did not yield consistent results because the assumptions made in the technique, such that the failure surface extends up to ground surface and the shear strength is fully mobilized along the failure surface, are not necessarily valid for deep excavations. Bjerrum and Eides' method, however, considered the effects of excavation shape, width, and depth, and is therefore applicable to various shapes and depths (deep and shallow) of excavation. In terms of calculation of factor of safety against basal heave, Bjerrum, and Eides' method, therefore, is comparatively better than Terzaghi's method.

2.3.2 Predicting Wall Deflection, Ground Settlement and Apparent Earth Pressure.

The magnitude and distribution of the ground surface settlement induced by deep excavations are related to many factors: soil and groundwater condition, excavation geometry, excavation sequences, duration of excavation, method of retaining wall construction, quality of workmanship, surcharge condition, existence of adjacent buildings, penetration depth, wall stiffness, type and installation of lateral support, spacing and stiffness of struts etc. All these influential factors cannot be included in any of the methods derived purely from a theoretical basis. Several empirical methods to predict ground surface settlement have been developed in the past based on field observations and local experiences. Several commonly used empirical methods in engineering practice are presented as follows:

Peck (1969) compiled ground surface settlement data measured adjacent to temporarily braced sheet pile and soldier pile wall with struts or tieback support, and summarized the data normalized by the excavation depth as shown in Figure 2.3. The Figure defines three zones, each representing certain ground conditions. The data suggest that excavations within a thick layer of soft to medium clay can produce large settlements, often greater than 0.2% of the excavation depth adjacent to the support wall, and extend laterally up to four times the excavated depth from the wall. The case histories used in the development of the Figure are earlier to 1969, and the excavations are supported by sheet piles or soldier piles with lagging. With the use of a much stiffer retaining wall, the maximum settlements are expected to be generally smaller than those defined in the Figure.

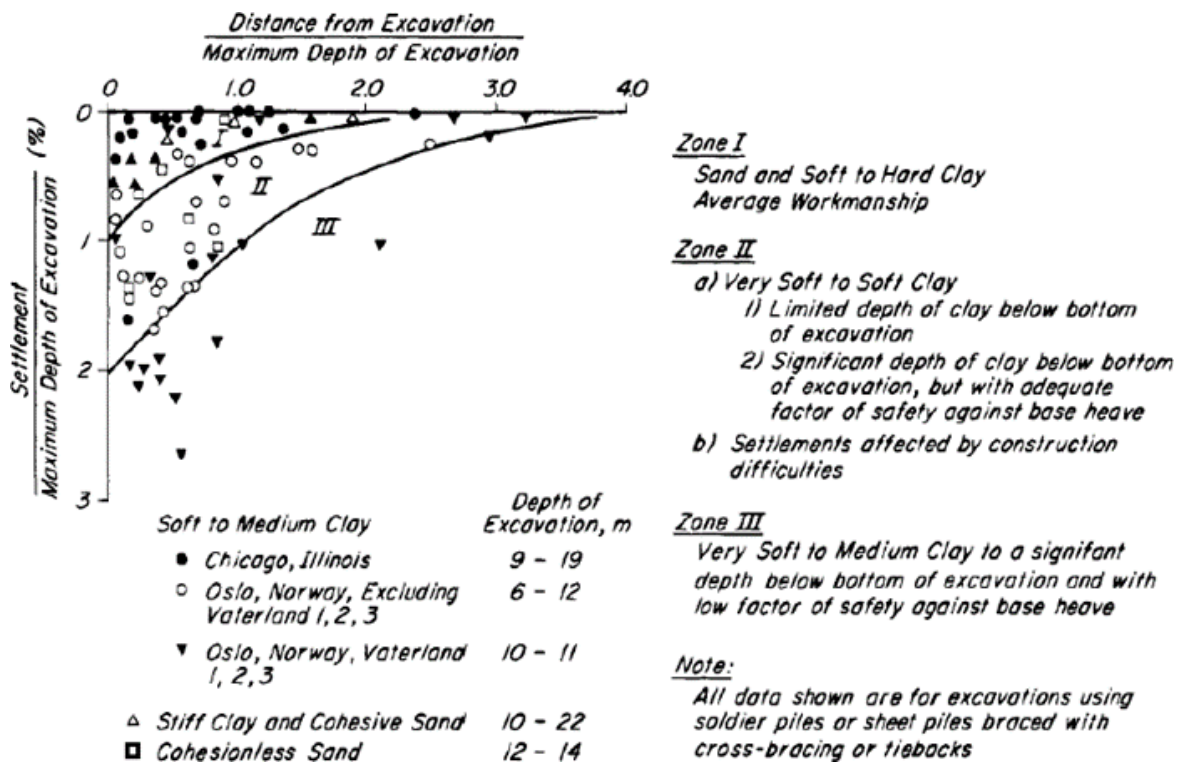


Fig. 2.3 Summary of settlements adjacent to open cuts in various soils, as function of distance from edge of excavation (Peck 1969)

Clough and O'Rourke (1990) conferred a semi-empirical method for estimating excavation deformations in soft clays. Fig. 2.4 depicts the general pattern of ground movements related to wall deformations as observed in typical excavations.

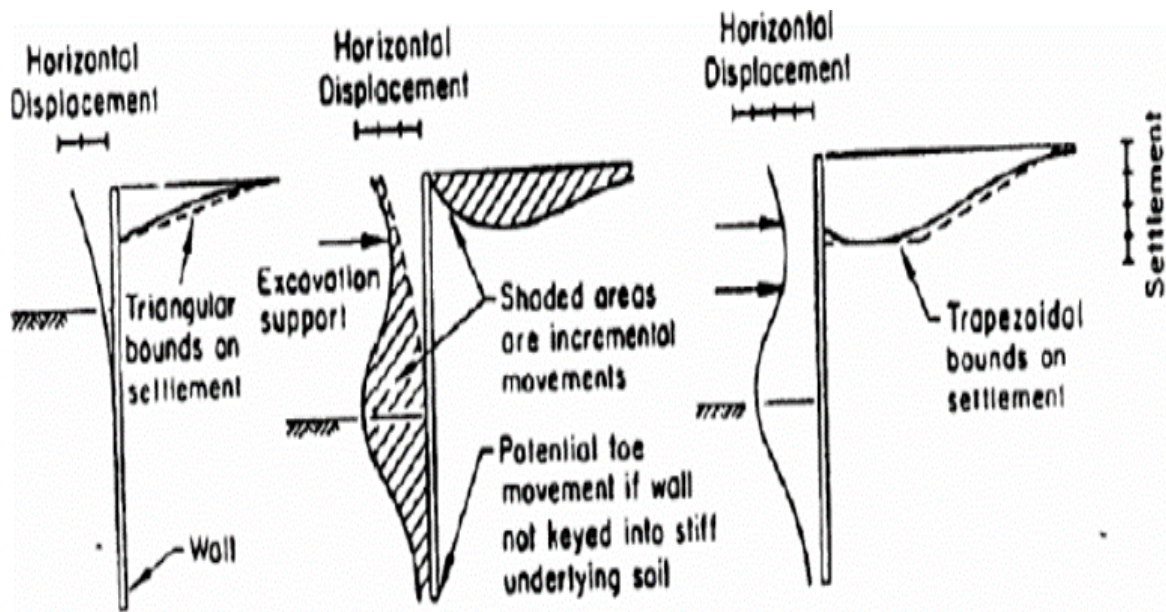


Fig. 2.4 Typical Profile of Movements (Clough and O'Rourke 1990)

The maximum lateral deformation caused by the excavation depends on the system stiffness and the factor of safety against basal heave. The overall stiffness of the support system is typically expressed in terms of a sufficient stiffness of the system and is defined in Fig. 2.5. Clough and O'Rourke noted that when the factor of safety against basal heave is less than 1.5, the system stiffness can significantly influence the soil movements. Fig. 2.5 demonstrates allowance of the estimation of maximum lateral deformation as a percentage of the depth of the excavation, once the system stiffness has been selected and the factor of safety against basal heave has been estimated.

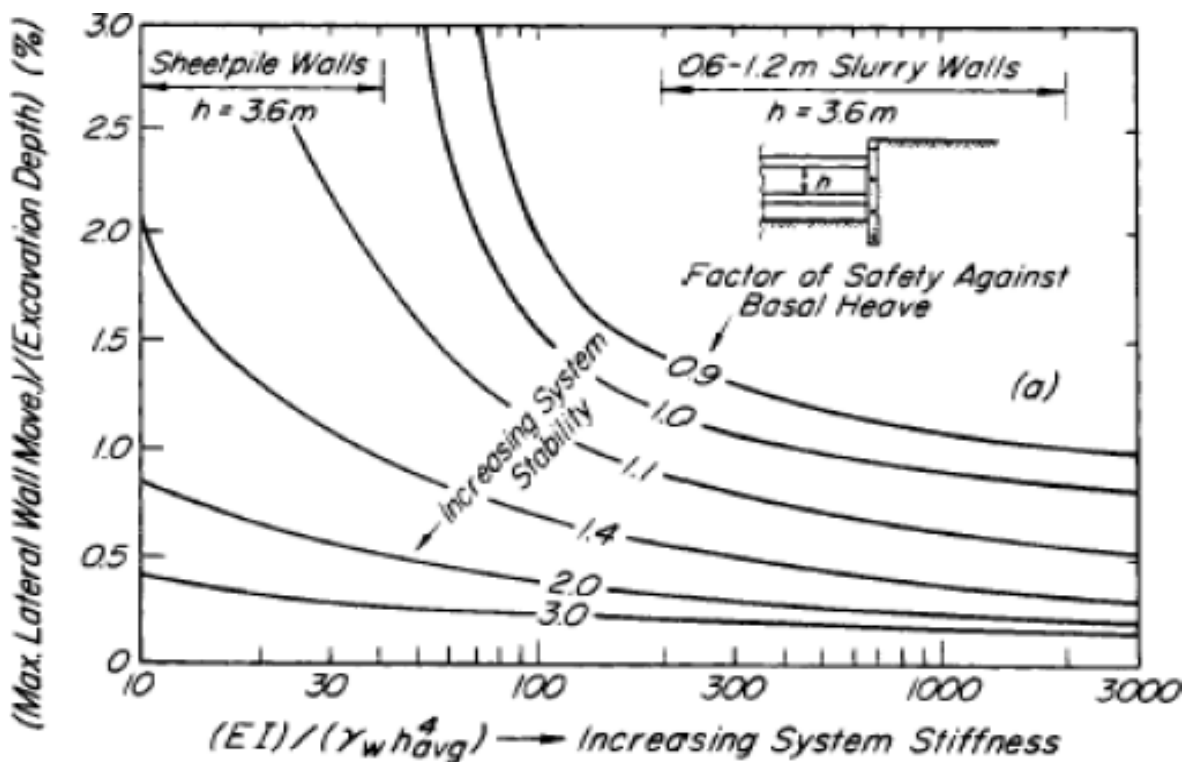
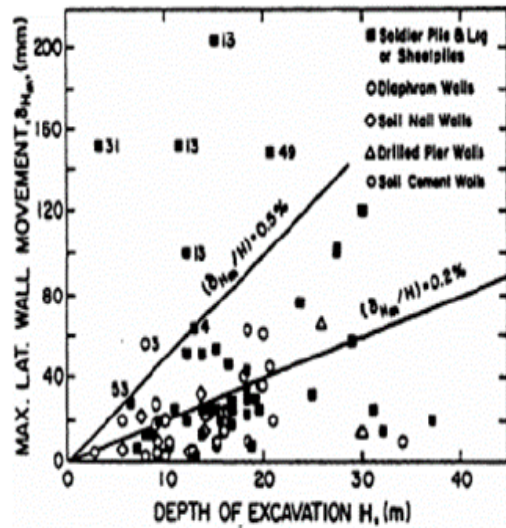
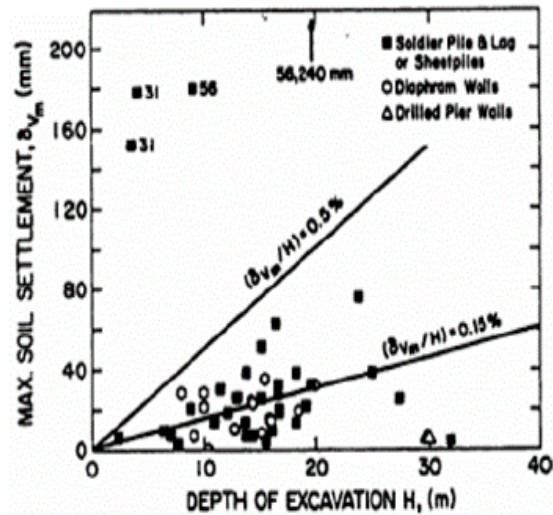


Fig. 2.5 Relationships between Maximum Lateral Wall Movements and Ground Surface Settlements for different Stiffness Supporting Systems in Clay and Factor of Safety Against Basal Heave (Clough and O'Rourke, 1990)

Fig. 2.6 proposed by Clough and O'Rourke (1990) shows maximum lateral wall deflection and surface settlements respectively as a function of excavation depth. These Figures are commonly used as design tools to estimate maximum wall and soil movements. Based on the graphs, the lateral movements are mostly 0.2% of H, while the settlements show a tendency to 0.15% of H.



(a) Max. Lat. Movement versus Excavation Depth



(b) Max. Soil Settlement Movement versus Excavation Depth

Fig. 2.6 Observed Maximum Wall Movements and Ground Settlements Verses Excavation Depth for Various In-situ Walls (Clough and O'Rourke, 1990)

Kung (2009) also pointed out that, the lateral movements are nearly the 0.2% of excavation depth. Kung (2009) made the comparison of diaphragm wall deflection caused by excavation of the top-down method (TDM) and the bottom-up method (BUM). It has been concluded from the study is that in general, the wall deflection of BUM cases is smaller than that of TDM cases.

For the cantilever sheet pile wall, the bottom of the wall is assumed not to displace, whereas the top of the wall at the ground assumed to have enough movement to allow the active and passive earth pressure to be generated (Yandzio 1998). On the other hand, the displacements at the anchor level are limited when the anchors are used. Although the wall can bend between these positions, the overall wall displacements will be quite small compared to cantilever wall of the same height (Yandzio 1998).

No firm guidelines exist for acceptable deflection in retaining walls, and values ranging from 1 to 5 inches (25mm to 125mm) are typically considered acceptable. It is recommended that the deflection be limited to 1 to 3 inches (25mm-75mm) (National Engineering Handbook 2007). There are different methods used to reduce sheet pile wall deformations. Bilgin and Erten (2009) stated that while having multiple anchor levels is the most efficient way to reduce anchored wall deformations.

Design of a retaining wall requires estimation of strut loads and sizing of retaining structures from the inception of the project. Because of their simplicity, apparent earth pressure diagrams are commonly used to estimate strut loads and initial sizing of retaining structures and are generally conservative concerning overall shoring stability. The most widely used apparent earth pressure diagrams are those proposed by Peck (1969) as compare to those by, for example, Schnabel (1982) and Sabatini et al. (1999). Peck's diagrams are based on field measurement of strut loads on various soils supported by sheet piles and soldier piles. For excavation using stiff diaphragm wall in soft soils, the above apparent earth pressure diagrams may not be appropriate. Higher apparent earth pressures could be expected; see, for example, Goldberg et al. (1976) and Hashash and Whittle (2002). Despite its limitations, apparent earth pressure diagrams are useful for preliminary bracing loads estimation, for sizing of struts or anchors and retaining structures.

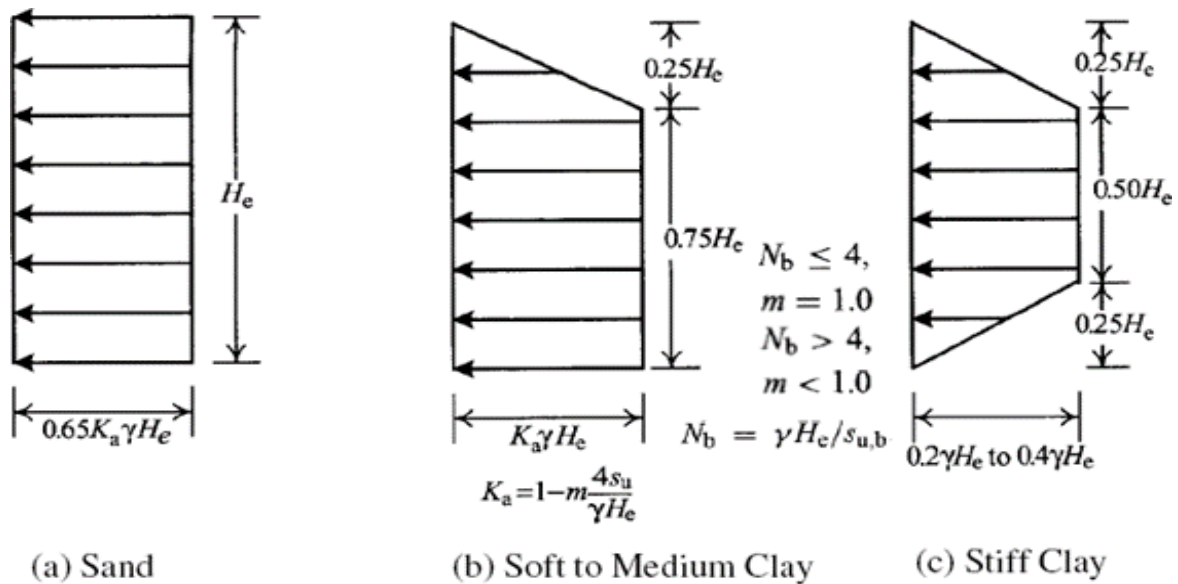
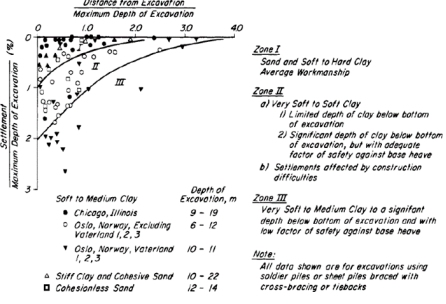
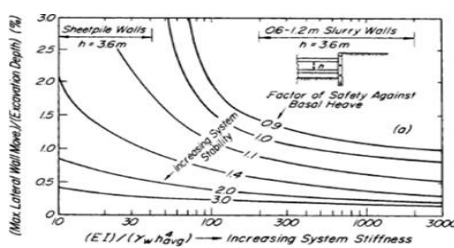


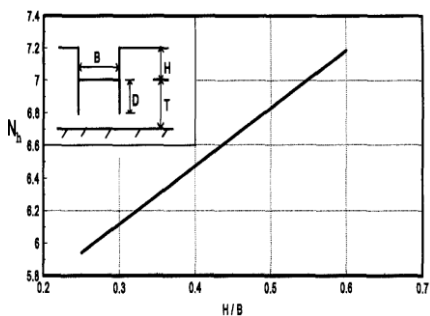
Fig. 2.7 Apparent Earth Pressure Diagrams (Peck 1969)

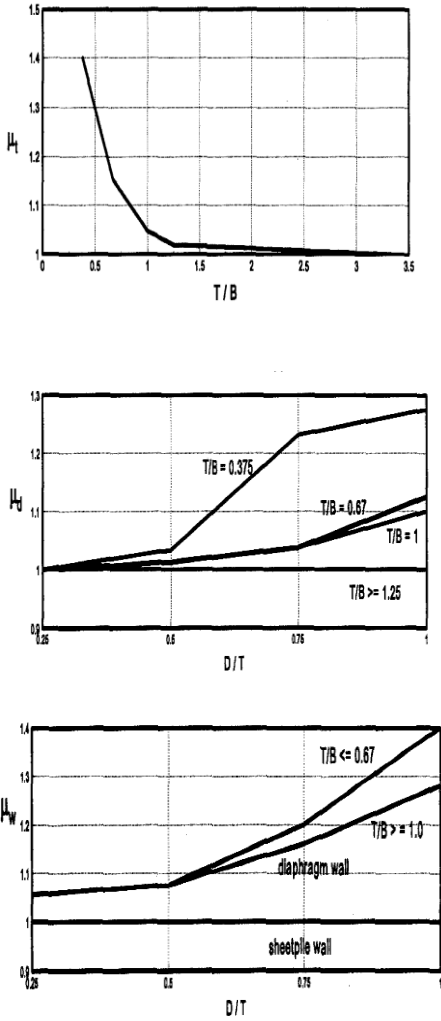
Table 2.1 presents a summary of the conventional empirical method conducted by different researchers which will be used as measure of checking of the current study.

Table 2.1 Summary of the conventional empirical method conducted by different researchers.

Researcher/ Research Group	Stability or Deformation Check Criteria	Basis of the criteria	Information extracted from the literature	Year
Clough and O'Rourke	Deformation	Lateral Displacement	Based on the graph obtained by different case histories, it is observed that the maximum lateral displacement should be within 0.2 % of excavation depth	1990
Clough and O'Rourke	Deformation	Lateral Displacement	<p>Based on the relationship between the system stiffness and the maximum lateral movement, the system stiffness was used to derive lateral movement.</p> <p>System stiffness was derived from the following formula:</p> $\text{System Stiffness} = \frac{EI}{\gamma h^4}$ <p>E= Young's Modulus I= Moment of Inertia γ= Unit Weight h=Vertical spacing between struts</p>	1990
Yandzio	Deformation	Lateral Displacement	The bottom of the wall is assumed not to displace, whereas the top of the wall at the ground assumed to have enough movement. However, displacement at the anchor or strut level is limited.	1998

Researcher/ Research Group	Stability or Deformation Check Criteria	Basis of the criteria	Information extracted from the literature	Year
National Engineering Handbook	Deformation	Lateral Displacement	Lateral displacement should be within 25mm-75mm	2007
Kung	Deformation	Lateral Displacement	Lateral movements are nearly the 0.2% of excavation depth	2009
Bilgin and Erten	Deformation	Lateral Displacement	Multiple anchor or strut levels is the most efficient way to reduce lateral wall deformations.	2009
Peck	Deformation	Ground Settlement	Developed a graph based on a lot of case histories for various soil from which maximum ground settlement and extension of the settlement from the wall could be gained empirically. 	1969
Clough and O'Rourke	Deformation	Ground Settlement	Based on the graph obtained by different case histories, it is observed that the maximum ground settlement should be within 0.15 % of excavation depth	1990
Clough and O'Rourke	Stability	Basal Heave	Factor of safety against basal heave can be obtained from a relationship between lateral displacements and system stiffness 	1990

Researcher/ Research Group	Stability or Deformation Check Criteria	Basis of the criteria	Information extracted from the literature	Year
Terzaghi	Stability	Basal Heave	<p>Formula for factor of safety in case of wide excavation (i.e. excavation length (B) is greater than the excavation depth (H))</p> $F.S = \frac{5.7 c}{H(\gamma - \frac{c}{0.7 B})}$ <p>c = cohesion H= excavation depth B= excavation width γ=unit weight</p>	1943
Bjerrum & Eide	Stability	Basal Heave	<p>Formula for factor of safety</p> $F.S = \frac{c N_c}{\gamma H + q}$ <p>q= Surcharge N_c can be obtained by the excavation depth by excavation width ratio chart.</p>	1956
Goh	Stability	Basal Heave	<p>Formula for factor of safety derived based on several finite element model</p> $F.S = \frac{c N_h}{\gamma H + q} \mu_t \mu_d \mu_w$ <p>N_h= Modified bearing capacity factor obtained from the following chart</p>  <p>$\mu_t, \mu_d, \text{ and } \mu_w$ are clay thickness modification factor, wall-embedment factor and wall-stiffness factor</p>	1994

			<p>respectively obtained from the following graphs:</p>  <p>* T = Distance between the excavation bottom to the underlying hard stratum</p>	
Ou	Stability	Basal Heave	<p>The actual factor of safety with the presence of the rigid retaining wall should be higher than the one calculated using Terzaghi's formula</p>	2006

2.4 Laboratory tests and field measurements

The performance of deep excavations has been studied through each laboratory tests and field measurements by a variety of researchers, and therefore the main findings are summarized during this section.

The advantage of laboratory tests is that the factors are affecting results. Small-scale centrifuge model tests have been applied in an attempt to gain a consistent view of the soil-structure interaction behavior of deep excavations (Bolton and Powrie 1987, Bolton and Powrie 1988, Bolton and Stewart 1994, Richards and Powrie 1998, Takemura, Kondoh, et al. 1999). Centrifuge modeling allows a correctly scaled physical model to enable the prototype behavior of excavation so that it can be effectively used to investigate soil deformation mechanisms during the excavation process. The tests can be repeated and continued until failure, which is not possible in the full-scale projects. Moreover, the tests are time-efficient and can observe the long-run behavior of a geotechnical construction in the soil of low permeability over a relatively short amount of time. However, it ought to be noted that centrifuge testing has its limitations and therefore the conditions it will model are comparatively easy.

Field measurement is an effective method, but it is also expensive and takes a long time to obtain the data and this process is not repeatable. Various case narratives of deep excavation have been accounted for worldwide with all around archived field information, e.g., in the UK (Skempton and Ward 1952, Wood and Perrin 1984, Simpson 1992), in Chicago (Wu and Berman 1953, Finno, Atmatzidis et al. 1989, Finno and Nerby 1989), in Shanghai (Liu, Ng et al. 2005, Xu 2007, Wang, Xu et al. 2010, Liu, Jiang et al. 2011, Ng, Hong et al. 2012), in Singapore (Wong, Pohet al. 1996, Lee, Yong et al. 1998), in Hong Kong (Leung and Ng 2007), and in Taiwan (Ou, Hsieh et al. 1993, Ou, Liao et al. 1998, Ou, Shiau et al. 2000). These case narratives vary starting with one then onto the next in topographical conditions, retaining structures, and retaining structures, which makes the correlation and comparison troublesome. Generally, they recorded the main excavation behavior, such as wall bends, ground movements, earth and pore water pressures, strut loads and wall bending moments, and deformation of adjacent infrastructure. Therefore, they supply valuable resources for understanding a lot of general behavior of deep excavations, and additionally for calibrating the numerical analyses.

2.5 Numerical modeling

Numerical modeling is a compelling method to examine the soil structure mechanisms in deep excavations and can give all the expected data to outline purposes. A portion of the numerical modeling forms are depicted in this section, and the initial discoveries are likewise summarized.

2.5.1 Model details and simulation process

2D simulations (i.e. plain strain, and axisymmetric analysis) have been generally used to estimated real deep excavations in the design process and inquired for research purposes (Clarke and Wroth 1984, Hubbard, Potts et al. 1984, Potts and Fourie 1984, Finno, Harahap et al. 1991, Powrie and Li 1991, Simpson 1992, Whittle, Hashash et al. 1993, Hashash and Whittle 1996), because of the constraint of software abilities and computational resources available. Be that as it may, the confinements of 2D analyses ought to be perceived, and completely 3D analyses are required if necessary. For instance, the 2D analysis is not able to consider the corner effects in deep excavations, which indicate that the wall deformation and ground movement are smaller closes to the wall corner than around the wall center. Additionally, 2D plane strain analysis tends to overestimate the wall deflection and ground settlement behind the wall compared to the simplified 3D symmetric square or rectangular analysis (Ou, Chiou, et al. 1996, Lee, Yong et al. 1998, Finno, wood warbler et al. 2007), and therefore the distinction depends on factors like geometry of the excavation, the length to depth ratio, the stiffness of the retaining system, the excavation depth, soil properties, and the factor of safety against basal heave.

Zdravkovic, Potts et al. (2005) investigated many issues related to the modeling of retaining structures used to support an excavation in 3D finite element analysis and compared results with equivalent plain strain and axisymmetric modeling. Results demonstrated that the plain strain investigation over predicts the wall deflection diversion and ground movement contrasted with the 3D analyses, though the axisymmetric analysis is nearer to the 3D analysis. Both shell components and active components were utilized to show the retaining wall, and it was discovered that the wall deflection is more prominent when the wall is modeled with shell components, resulting from the lack of beneficial

action of shear stresses mobilized on the back of the wall. The anisotropic wall approach was utilized to consider the discontinuities in the retaining wall, and the wall deflection and bending moment at the wall corner are incredibly enhanced contrasted with those from the isotropic wall. Analysis of rectangular excavations was directed, and 3D impacts were observed to be apparent. Distinctive wall depth was analyzed yet the effect on the developments and necessary powers is insignificant.

The advances in hardware and software these days have empower the utilization of completely 3D investigation in deep excavations, which can incorporate more geotechnical and structural details (e.g. ground profile, excavation geometry, retaining system, and construction sequence) and deal with large scale case studies (Hou, Wang et al. 2009, Lee, Hong et al. 2011, Dong, Burdet al. 2012, Dong, Burd et al. 2013, Dong, Burd et al. 2013). Lee, Hong et al. (2011) showed the utilization of extensive 3D finite element analysis to two case studies, the long trench excavation of Nicoll Highway Station, and the excavation-pile interaction in Common Services Tunnel. The geometry and conveyance of retaining structures, for example, the diaphragm wall, the sheet pile wall, joints between diaphragm wall panels, the soldier piles, and horizontal struts, were presented correctly in the analysis. The outcomes were promising in these investigations, and the results with field estimation were sensibly great considering the vulnerabilities and complexities included in the analyses.

Previous research has indicated that the plane strain analysis may not be able to predict the excavation behavior accurately due to the inability to account for the effects of the length of excavation and the associated secondary walls which span the two extreme ends of the excavation. With recent improvements in computer technology, it is logical to conduct 3D analysis by considering these effects. Ng and Yan (1999) presented results of a 3D back-analysis of retaining wall installation sequence at Lion Yard and identified the critical stress transfer mechanisms and ground deformations. Zdravkovic et al. (2005) investigated some issues related to the modeling of a retaining structure used to support an excavation in 3D finite element analyses and provided a detailed assessment of wall and ground movements and structural forces in the wall in the light of different modeling assumptions. Finno et al. (2007) studied the effect of the excavation length of the braced excavations by conducting a 3D FE parametric study of braced excavations in soft clay overlying medium and stiff clay. Arai et al. (2008) conducted 3D total stress elasto-plastic FEM analysis to

examine ground movement and stress after the installation of circular diaphragm walls and soil excavation within the walls. Hsieh et al. (2013) performed 3D numerical analyses for four deep excavation cases with different installations of cross walls and demonstrated the effectiveness of cross walls in reducing lateral wall deflection. Orazalin et al. (2015) highlighted the effects of the 3D excavation and support geometry on wall and ground movement through 3D analyses of excavation support system for the Stata Centre Basement on the MIT Campus. Goh A.T.C et al. (2017) conducted a series of two dimensional and three-dimensional analyses on the braced excavation. The results showed that the 3D maximum wall deflections were generally much smaller than those for 2D. Comparisons were also made with other commonly used semi-empirical charts. They also developed a simple wall deflection equation was developed for estimating the maximum wall deflection that considers the 3D effects through different ratios of excavation length over excavation width. However, because of the increased processing time required to perform a three-dimensional finite element analysis, it is more economical to use plane strain analysis in the industry. Therefore, it is useful to examine in what situations three-dimensional analysis should be conducted and when plane strain analyses will give reliable results.

2.5.2 Effect of retaining wall stiffness

A change of the stiffness of the wall within practical limits for a given soil has a negligible effect on the ground movements (Clough and Tsui 1974, Burland et al. 1979, Mana 1978, and Hsieh 1999). Clough and Tsui (1974) showed that an increase in wall stiffness by a factor of 32 had resulted in the corresponding reduction of the movements by a factor of 2 only. However, an increase in the rigidity of the wall increases the bending moment and support loads. Potts and Bond (1994), however, commented that the effect of wall stiffness is preferably a function of the initial stress condition. It is higher for soils with $K_0 = 2$ than for soils with $K_0 = 0.5$. For instance, with $K_0 = 0.5$, the effect is minimal on bending moment and almost negligible on support load.

2.5.3 Effect of the support system of retaining wall

Stiffer lateral support systems tend to reduce the deflection of the wall at the support levels, and increases strut loads and bending moment accordingly (Burland et al. 1979, Clough & O'Rourke 1990, Clough & Tsui 1974, Mana 1978). However, surface settlement is inevitable. This is because deformations which occur below the excavation are not affected much by the rigidity of the support.

Ou (2006) points out that most horizontal movement occurs at the embedded portion of the walls between the completion of excavation and the installation of the supports at each level. To reduce the magnitude of the load acting on the unsupported portion of the wall, it is necessary to reduce the distance between the supports to be installed and the bottom of the excavation for each level. By doing so, the stiffness of the system is also improved.

Pre-stressing of the struts has the benefit of tightening the supporting system and reducing the ground movements. The pre-stress loads should be limited by the yield properties of the soft clay soil (McRostii et al. 1972). A large amount of pre-stress may not provide additional benefits (Clough & Tsui 1974, Mana 1978, Palmer & Kenny 1972). This is because a great deal of the wall deflection occurs well below the excavation level before the installation and pre-stressing of the supporting system. Bose and Sun (1998) reported that increasing the excavation width generates a large zone of plastic deformation, and eventually the wall deflection and ground settlement increase without altering the lateral force equilibrium on the diaphragm wall. Strut pre-stressing was found to affect considerably the deviation of the upper portion of the wall while virtually no significant change is evident at the bottom of the wall, and the ground settlement also reduces with the increase in the magnitude of strut pre-stress.

A recent study was performed by Armani (2019) on the anchored retaining wall in deep excavations to protect and support the multilayer soil structure. In this research, a reference model was established; then a parametric study was carried out. The final obtained model of the case study was of a good approximation to the reality (the instrumental data of wall displacement). In the parametric study, several calculation parameters (discretization and precisions) and geotechnical parameters (the interface, water pressure, and the anchor system) were varied individually and finally compared

from the anchored to the non-anchored wall. It is evident from this study that the variation of the parameters in a reasonable interval has considerable effects of horizontal displacement and moments on the wall. In the end, it was concluded that the use of numerical analysis procedures could provide more efficient and more economic geotechnical project design.

Valentina and Francesco (2019) carried out a study on a full-scale anchored piles diaphragm used to supporting deep excavation in the urban area devoted to the new Library of the University of Enna “Kore” Enna (Italy). Instrumented data obtained with conventional inclinometer cases and embedded piezoelectric accelerometers have been used to check the harmony with numerical analysis conducted by PLAXIS 2D. It has been observed that this model allows for a satisfactory simulation of the displacement of the wall during the construction phases under a static loading scenario. The results in terms of horizontal displacements obtained by numerical modeling are in good agreement with those derived by measurements.

2.5.4 Effects of construction process

Potts and Fourie (1984) assumed two different types of construction method, excavated and backfilled, and found that the excavation behavior was mostly mixed. However, Arai, Kusakabe et al. (2008) reported that the sequence of soil removal inside the excavation has little effect on the performance of the excavation. Due to limited published information regarding the impact of construction sequence, the influence of construction sequence on the excavation behavior is still unclear.

2.5.5 Effect of geometry of the excavation

Mana (1978) showed that the more extensive the excavation, the larger the magnitude of ground movements are and the size of the yield zones as expected. Clough and O'Rourke (1990) found that the more extensive the excavation, the more significant the deformation of the retaining wall due to larger the unbalanced forces. Moreover, the factor of safety against basal stability decreases with increases in excavation width for soft clay (Bjerrum and Eide 1956). Kempfert and Gebreselassie (2006) concluded the wall deflection increases with the increase of the width of excavation. The main factor that influences the

heave at the bottom of the excavation and settlement at the surface is the height of the model rather than the width of the model. Another general observation is that with the deflection of the wall, the heave at the excavation bottom increases with increases in the width of excavation, whereas the settlement at the surface tends to decrease with increasing width of excavation. Ou (2006) stated that the surface settlement influence zone is affected by the width of excavation. The wider the width, the longer the influence zone.

In reality, deep basements are in different shapes, such as the rectangular basement, cylindrical basement and triangular basement (Liu et al. 2011, Tan and Wang 2013, Shi et al. 2015). Several simplified prediction methods were proposed to evaluate the effects of rectangular excavation by simplifying rectangular basement as a plane strain problem (Liang et al. 2017 and Zhenget al. 2018). Tan and Wang (2013) investigated deformation characteristics of retaining wall and ground movement due to a cylindrical basement excavation by conducting a field study. It is found that deformation behaviors of cylindrical basements were controlled by the excavation diameter rather than the wall penetration depth ratio. Shi et al. (2015) conducted a field study to explore the deformation mechanisms of a large-scale triangular basement. Recently, Shi et al. (2019) conducted a numerical parametric study to investigate the geometric effects on three-dimensional excavation. They found that if three-dimensional effects in a small basement are ignored, the heave and transverse tensile strain of tunnels are overestimated by up to 160% and 50%, respectively.

2.5.6 Effect of wall installation

Wall installation will change the ground stress conditions and movements may be developed as a result of wall installation. O'Rourke and Clough (1990) presented data to show that settlements which arose from the installation of five diaphragm walls were up to 0.12% of the depth of the trench. Poh and Wong (1998) reported that the maximum settlements induced by single panel excavation in sand-clay alternated layer and Singapore marine clay was 10-15 mm and 24 mm respectively. Ou and Yang (2000) studied the monitoring results of Taipei Rapid Transit System and concluded that the maximum settlement caused by single trench panel excavation was about 0.05% of trench depth, and for multiple panels, up to 0.07% trench depth. Upon completion of the panels, the

maximum settlement could be as much as 0.13% trench depth. Most of the settlements occurred within 0.3-time trench depth and spread to 1.0 trench depth.

The excavation for diaphragm wall panels or bored piles is certain to result in significant in situ total stress relief which will alter the level of total horizontal stress applied to the retained side of a wall. It was expected that the change would influence the actual values of prop or anchor forces and the maximum bending moment in the wall (Gunn and Clayton 1992). Substantial ground movement and reduction of in situ lateral stress have been observed in the field measurements during the construction of embedded retaining walls (Symons and Carder 1992). The installation effects of bored piles and diaphragm walls have been investigated using numerical analyses in 2D (De Moor 1994, Ng, Lings et al. 1995) and 3D (Gourvenec and Powrie 1999, Ng and Yan 1999, Schäfer and Triantafyllidis 2004). Gourvenec and Powrie (1999) found that the magnitude and extent of both lateral stress reduction and soil lateral movement in the vicinity of a diaphragm wall during construction depend on the panel length and are over predicted in-plane strain analyses, which indicates that 3D analyses are required and the panel length should be considered.

2.5.7 Effect of soil-structure interaction

In order to understand the soil–structure interaction mechanisms, many researchers have carried out field monitoring studies (Mair et al. 1993, Boonyarak et al. 2014), full-scale and physical model tests (Selemetas et al. 2006, Lee and Bassett 2006, Ng et al. 2013) and analytical studies (Huang et al. 2009, Xiang and Feng 2013). Also, there have been numerous studies which have focused on the influence of excavation on the foundation by numerical methods like (Mroueh and Shahrour 2002, Kitiyodom et al. 2005, Lee and Bassett 2007, Liu et al., 2008, Lee 2012, Jongpradist et al. 2013). Freiseder (1998) showed that the variation of the interface reduction factor has insignificant influence on earth pressure and horizontal wall deflection at the wall toe, whereas it has a slight influence on the bending moment of the wall and considerable effect on the horizontal wall deflection and vertical displacement of the top of the wall. Recently, Mojtaba and Daniel (2019) investigated the influence of the soil/structure interaction in terms of surface settlements, forces induced and forces along the piles. They concluded that the MC model could not

accurately estimate the ground settlements and the forces; therefore it is necessary to use advanced constitutive models for design purposes.

2.6 Constitutive models of soil behavior

The soil is a multi-phase material. Natural soils are anisotropic. Its reactions to loading are nonlinear, path-dependent, influenced by its stress history, and exhibit time-dependent behavior. Deformations include irreversible plastic strains and may dilate or compact. Ideally, a perfect soil model would be capable of predicting these soil behaviors under all types of loading conditions.

In recent years, numerical methods have become widespread in the analysis of geotechnical problems. This is mainly due to the availability of inexpensive computer hardware and improved software capability to carry out complex numerical analyses. The continuous achievements being made in the development of the constitutive soil models are another contributing factor to this. There are many constitutive models available for simulating soil behavior. Some of these models have been developed for specific types of soils or for research purposes, while others can be used for both cohesive and non-cohesive soils and for practically oriented purposes. The practical oriented constitutive models can generally be grouped into the following categories (Chanaton2010, Potts et al. 2002, Schweiger et al. 2009):

1. Linear and non-linear elastic model
2. Linear elastic-perfectly plastic model
3. Elasto-plastic model
4. Elastic-plastic model with kinetic hardening

The first category, the isotropic elasticity model is based on Hooke's law. The material is characterized by a stiffness parameter and the Poisson's ratio or preferably, for soil skeletons, the bulk modulus and the shear modulus. Because of its simplicity, this method has been widely applied in conventional soil mechanics where the boundary value problem has to be solved analytically. It was used as a soil model in the early years of the finite element method. However, the elastic model does not reproduce any of the essential features of real soil behaviors and thus is not suitable to model soil. However, it may be used to model stiff volume in the soil such as for a concrete diaphragm wall or bored piles.

The non-linear elastic model is a substantial improvement over the linear model as the non-linear relationship of the shear stress, and shear strain can be captured. A widely used model of this type is the hyperbolic one (Kondner&Zelasko1963), in which the shear modulus decreases from an initial value to a zero value at failure (Fig. 2.8a). Such a shear response corresponds well to the shear curve obtained for normally consolidated clays and loose sands.

This method was implemented into a finite element code for the first time by Duncan and Chang (1970). Duncan and Chang combined Kondner’s idea to approximate the drained triaxial compression test stress-strain curve by a hyperbolic method and Ohde’s formulation of soil stiffness as a stress-dependence parameter using a power law (Ohde 1939). The hyperbolic model requires two parameters (Fig. 2.8b) which can be determined from experimental results.

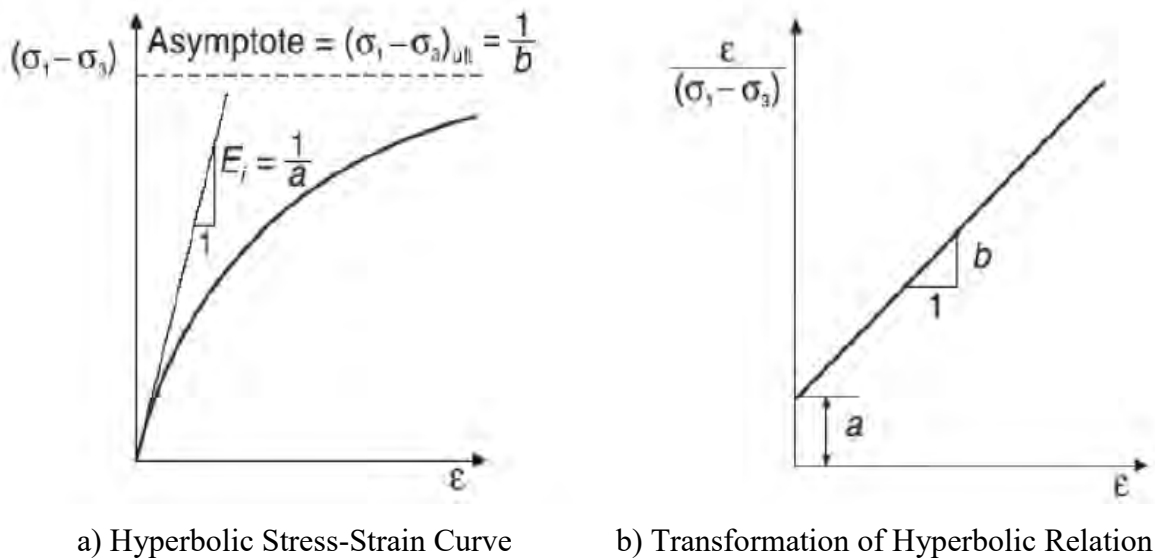


Fig. 2.8 Hyperbolic Model

Non-linear-elastic models can simulate well monotonic curves of experimentally measured stress-strain relations for specific loading paths (triaxial and oedometric). However, their extrapolation beyond the calibration curves is practically impossible. These models are mostly focused on a single feature of the soil behavior (stress-strain curve) and do not take into account other important aspects (e.g., stress paths dependence, or volume change during shear). They also share many of the disadvantages of linear

elastic models (e.g., no hysteretic behavior during cyclic loading) and, in contrast to linear elastic models, they lack a sound theoretical background.

The second category, the elastic-perfectly plastic (Mohr-Coulomb) model, is relatively simple and is considered the most widely used model among practicing engineers. This model is a combination of Hooke's Law and the generalized form of Coulomb's failure criteria. The elastic-perfectly plastic model seems to be sufficient for some areas of geotechnical problems, primarily when being used by experienced engineers. For example, the deformation of the diaphragm wall induced by excavation can be predicted when used in conjunction with total stress analysis and a back analyzed stiffness parameter (Lim et al. 2010, Phienwej 2008). However, care must be taken because the stress path predicted by this model, especially for soft clay, can be misleading and results in an over-prediction of soil strength in the case of soft clays.

The third category, the elasto-plastic model, includes the isotropic hardening single surface plasticity model category and the isotropic hardening double surface plasticity model. The isotropic hardening single surface plasticity model is the first step to modeling real soil behavior. The principal soil model of this category is the Modified Cam-Clay (MCC) model (Roscoe & Burland 1968). The MCC model introduced an elliptic yield surface which separates the elastic behavior from the plastic behavior. The application of this model has been widely accepted, especially for cases of embankments on soft clay modeling. Where there is an unloading problem, such as excavation, the soil stress path generally remains inside the yield surface. Thus, the predicted deformations in excavation are governed by elastic behavior.

In relation to the isotropic hardening double surface plasticity model, the predominant model in this category is the Hardening Soil model (Schanz et al. 1999), which was developed from the double hardening model, introduced by Vermeer (1978). This type of model gives more realistic displacement patterns for the working load conditions, especially in the case of an excavation. An extension of the Hardening Soil (HS) model to incorporate the small strain behavior of soils, is also available in the Hardening Soil model with Small Strain Stiffness: (HSsmall) model (Benz 2006).

The fourth category is the kinematic hardening multi-surface plasticity models. These models are generally able to capture more complex soil behavior, including softening, small strain, anisotropy, and structured soils. Examples of soil models in this category are the Kinematic Hardening model or Bubble model (Al Tabbaa & Wood 1989, Wood 1995), and the Three Surface Kinematic Hardening (3-SKH) model (Atkinson &Stallebrass1991). Such models have been developed from the Cam-Clay model and, therefore, share the underlying assumptions of linear behavior within the elastic (recoverable) state, while the associated flow rule at the yield surface is applied. Other more complex soil models, such as the MIT-E3 Model (Whittle &Kavvadas1994), use different assumptions, for example, non-linear behavior in recoverable state and non-associated flow rule. These models require large numbers of complicated input parameters which are not easily obtained from conventional soil tests. For example, the MIT-E3 model simulates important features of soil behavior including anisotropic stress-strain–strength relationship, small strain nonlinearity, and hysteretic response upon load reversal. The most general form of the MIT-E3 model uses 15 input parameters that are evaluated, for given clay, using a strict hierarchy in which some of the constants are determined from predefined parametric studies. Not all of these parameters can be determined from conventional laboratory tests. A recent case history using MIT-E3 for deep excavation in Singapore is given by Corral and Whittle (2010).

Since PLAXIS has been chosen to be used for this study, the review of constitutive soil models will be focus on those associated with PLAXIS. Only those related to the chosen models will be reviewed. Complete coverage and greater details can be found in PLAXIS manuals.

PLAXIS is a geotechnical soil simulation tool, with soil behaviors qualitatively represented by soil models and model parameters used to quantify the soil characteristics. A total of seven soil models are available in PLAXIS. They are the Linear Elastic (LE) model, Mohr-Coulomb (MC) model, Hardening Soil (HS) model, Hardening Soil model with Small-Strain Stiffness (HSsmall), Soft Soil (SS) model, Soft Soil Creep (SSC) model, Modified Cam-Clay (MCC) model, and NGI_ADG model.

Despite its known limitations (Teo and Wong 2011, Wong 2009), the MC model is still widely used in conventional excavation design by practicing engineers. It is simple to use, and the required soil parameters can be obtained from routine in-situ or laboratory tests or empirical correlations. In cases where there is a lack of specific laboratory or field characterization of the soils, and thus a simple approach is desirable, this model is also advantageous. The Hardening Soil model (HS) is an advanced soil model that can generate more realistic soil response in terms of non-linearity, stress dependency, and inelasticity. However, it suffers the same problems as the MC model in using effective stress parameters c' and ϕ' to determine the undrained shear strength. The HS model is the most likely to be used to replace the MC model. The quick and simple MC model can be used as a first approximation, and then followed by the HS model as an additional analysis to provide a 'second opinion.' The LE model is mainly for modeling of structures such as piles, diaphragm walls, and structures. All these models will be used to evaluate their performances relative to field measurements of a real problem.

The rest of the models are not considered because they are either not better than or not developed primarily for excavation analysis. The SS model and SSC model are more capable of modeling loading behavior of very soft soils; the MCC model is meant mostly for the modeling of near normally consolidated clayey soil, and NGI-ADP is not a popular model for excavation modeling. Further details of their limitations to simulate excavation works are given in the PLAXIS Material Models Manual.

2.6.1 Mohr Coulomb (MC) Model

The MC model is an elastic perfectly-plastic model which combines linear isotropic elasticity Hooke's law and the generalized form of Coulomb's failure criterion. In the Mohr-Coulomb yield surface, the soil is assumed to behave as a linear elastic-perfectly plastic material. The failure criterion for the model is shown in Fig. 2.9 and can be expressed as:

$$\tau_f = \sigma'_{nf} \tan \phi' + c' \quad (2.1)$$

Where τ_f and σ'_{nf} are the shear and the normal effective stresses on the failure plane, respectively. ϕ' and c' are the two plastic model parameters friction angle and cohesion from Coulomb's failure criteria, respectively.

The Mohr-Coulomb yield function, when formulated in term of effective principal stress, is given as:

$$f = \frac{1}{2}(\sigma'_1 - \sigma'_3) + (\sigma'_1 + \sigma'_3)\sin\phi' + c'\cos\phi' \quad (2.2)$$

Where, σ'_1 and σ'_3 are the major and minor effective principal stresses, respectively.

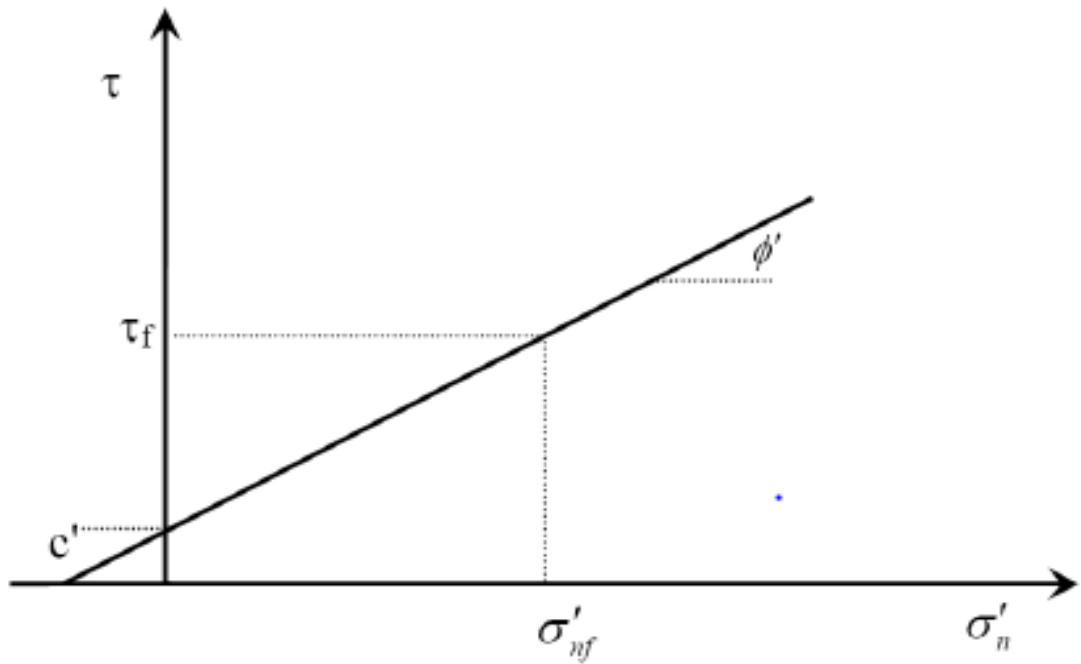


Fig. 2.9 Mohr-Columb Failure Criterion

The full Mohr-Coulomb yield condition can be defined by six yield functions when formulated in terms of principal stresses (Smith and Griffith, 2013). It can be represented by a hexagonal cone in the principal stress space as, shown in Figure 2.10.

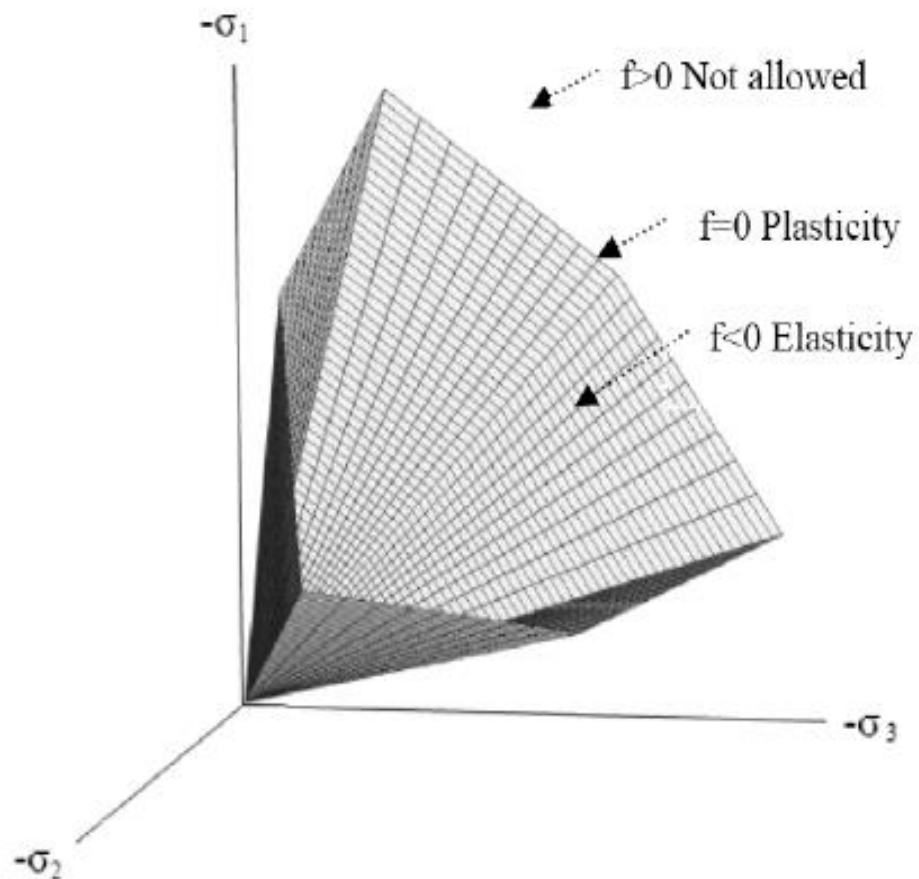


Fig. 2.10 Mohr-Coulomb Yield Surface in Principal Stress Space ($c'=0$)

In addition to Hooke's law and Coulomb's failure criterion, a dilatancy angle ψ is used to model a realistic irreversible change in volume due to shearing (non-associated flow rule).

The MC model requires a total of five parameters (Table 2.2). The following sections summarize the details of these parameters.

Table 2.2 Mohr-Coulomb Model input parameters.

Parameter	Description	Parameter evaluation
φ'	Internal friction angle	Slope of failure line from MC failure criterion
c'	Cohesion	y-intercept of failure line from MC failure criterion
ψ	Dilatancy angle	Function of ε_a and ε_v
E_{50}	Reference secant stiffness from drained triaxial test	y-intercept in $\log(\sigma_3 p^{ref}) - \log(E_{50})$ space
ν	Poisson's ratio	0.3-0.4 (drained), 0.495 (undrained), 0.15-0.25 (unloading)
K_0^{nc}	Coefficient of earth pressure at rest (NC state)	$1 - \sin\varphi'$ (default setting)

a) Young's Modulus (E)

The Young's modulus is a basic stiffness modulus which relates the soil stress and the strain. It is defined for uniaxial loading. Generally, the secant modulus at 50% strength, denoted as E_{50} , is suitable for soil loading conditions. It is a constant in bi-linear stress-strain relationships (Fig.2.11).

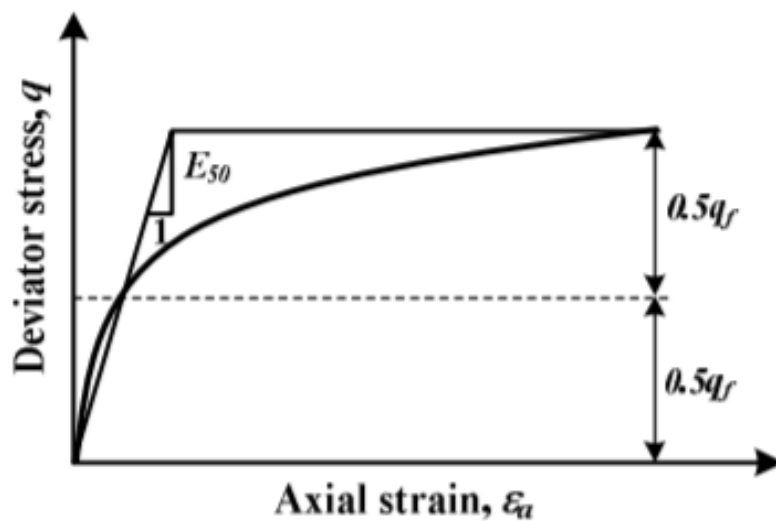


Fig. 2.11 Definition of E_{50}

The relationship between Young's modulus (E), shear modulus (G) and bulk modulus (K), is given as:

$$\frac{1}{E} = \frac{1}{9K} + \frac{1}{3G} \quad (2.3)$$

$$\frac{-\theta}{E} = \frac{1}{9K} - \frac{1}{6G} \quad (2.4)$$

Equations (2.3) and (2.4) can be rearranged and give:

$$G = \frac{E}{2(1+\theta)} \quad (2.5)$$

$$K = \frac{E}{3(1-2\theta)} \quad (2.6)$$

$$E_{\text{oed}} = \frac{(1-\theta)E}{(1-2\theta)(1+\theta)} \quad (2.7)$$

Where, E_{oed} refers to the Young's modulus in the oedometer test under constrained conditions.

b) Poisson's Ratio (ν)

The drained Poisson's ratio of soils in the loading condition ranges in a narrow band from 0.3 to 0.4 (Bowles 1988). For unloading, the values are between 0.15 and 0.25. For an undrained condition, the undrained Poisson's ratio is 0.5. However, using the exact undrained Poisson's ratio of 0.5 leads to numerical difficulty, and so $\nu_u = 0.495$ is suggested. Bishop and Hight (1977) state that one of the fundamental difficulties associated with the measurement of Poisson's ratio is the high degree of accuracy with which one must make measurements of strain and / or the calibration relationship. In this case study, recommendations given in PLAXIS Material Model manual are used so to be in consistent with the formulation of PLAXIS.

c) Cohesion (c')

The cohesion (c') has the dimension of stress. In the PLAXIS software, even for cohesionless materials ($c' = 0$), it is advised to adopt a small value of cohesion (at least $c' > 0.2 \text{ kN/m}^2$) to avoid computational complications.

d) Friction Angle (ϕ')

The friction angle (ϕ') is obtained from a plot of shear stress versus normal stress, as shown in Figure 2.2 (Mohr-Coulomb failure criterion). The unit of friction angle is in degrees.

e) Dilatancy Angle (ψ)

The dilatancy angle (ψ) is specified in degrees. In general, the dilatancy angle for quartz sands is in the order ($\phi'-30^\circ$). For cohesive materials, apart from heavily over-consolidated layer, clayey soils tend to have a small dilatancy. The value of $\psi = 0$ would be realistic for use in a general case.

2.6.2 Hardening Soil (HS) Model

Hardening Soil Model (Brinkgreve & Vermeer 1998, Schanz & Vermeer 1998) is a true second order soil model for soils in general for any type of application. The model involves shear hardening to model the irreversible plastic shear strain in deviatoric loading, and compression hardening to model the irreversible volumetric strain in primary compression in oedometer loading and isotropic loading. Failure is defined by means of the Mohr-Coulomb failure criterion.

In the model, the total strains are calculated using power law formulation stress-dependent stiffness similar to those used in the Duncan-Chang hyperbolic model. Different stiffness moduli are used in both loading and unloading/reloading. Hardening is assumed to be isotropic, depending on the plastic shear and volumetric strains. A non-associated flow rule is adopted when related to frictional hardening and an associated flow rule is assumed for the cap hardening.

The HS Model surpasses the hyperbolic model by using theory of plasticity instead of theory of elasticity, by including soil dilatancy and introducing a yield cap due to compression hardening.

Schanz et al. (1999) explained in detail, the formulation and verification of the HS model. The essential backgrounds of the model are summarized in this section. A total of ten input parameters are required in the HS Model, as tabulated in Table 2.3.

Unlike the MC Model, the stress-strain relationship due to the primary loading is approximated by a hyperbolic curve in the HS Model. The hyperbolic function, as given by Kondner & Zelasko (1963), for the drained triaxial test can be formulated as:

$$\varepsilon_1 = \frac{q_a}{2E_{50}} \cdot \frac{q}{q_a - q}, \text{ for } q > q_f \quad (2.8)$$

Where, ε_1 is the axial strain, and q is the deviatoric stress.

Table 2.3 Hardening Soil Model Parameters

Parameter	Description	Parameter evaluation
φ'	Internal friction angle	Slope of failure line from MC failure criterion
c'	Cohesion	y-intercept of failure line from MC failure criterion
R_f	Failure ratio	$(\sigma_1 - \sigma_3)_f / (\sigma_1 - \sigma_3)_{ult}$
ψ	Dilatancy angle	Function of ε_a and ε_v
E_{50}^{ref}	Reference secant stiffness from drained triaxial test	y-intercept in $\log(\sigma_3/p^{ref}) - \log(E_{50})$ space
E_{oed}^{ref}	Reference tangent stiffness for oedometer primary loading	y-intercept in $\log(\sigma_1/p^{ref}) - \log(E_{oed})$ space
E_{ur}^{ref}	Reference unloading/reloading stiffness	y-intercept in $\log(\sigma_3/p^{ref}) - \log(E_{50})$ space
ϑ_{ur}	Unloading/ reloading Poisson's ratio	0.2 (default setting, pure elastic parameter)
K_0^{nc}	Coefficient of earth pressure at rest (NC state)	$1 - \sin\varphi'$ (default setting)

The ultimate deviatoric stress (q_f) is defined as:

$$q_f = \frac{6\sin\phi'}{3-\sin\phi'} \cdot (\sigma'_3 + c' \cos\phi') \quad (2.9)$$

and the quantity (q_a) is:

$$q_a = \frac{q_f}{R_f} \quad (2.10)$$

Where q_f is the ultimate deviatoric stress at failure, which is derived from the Mohr-Coulomb failure criterion involving the strength parameters c' and ϕ' . q_a is the asymptotic value of the shear strength. R_f is the failure ratio, if $q_f = q_a$ ($R_f = 1$), the failure criterion is satisfied and perfectly plastic yielding occurs. The failure ratio (R_f) in PLAXIS 3D is given as 0.9 for the standard default value. Fig. 2.12 shows the hyperbolic relationship of stress and strain in primary loading.

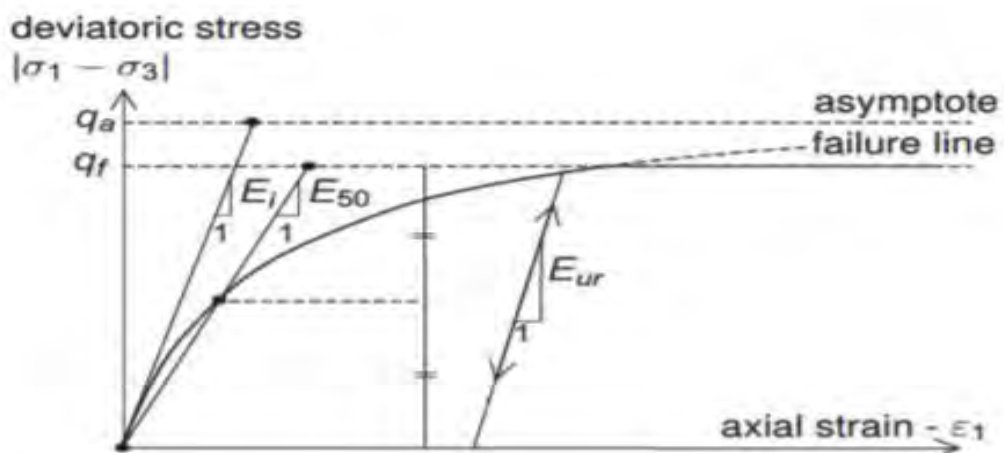


Fig. 2.12 Hyperbolic Stress-Strain Relation in Primary Loading for a Standard Drained Triaxial Test (Schanz et al., 1999).

The stress-strain behavior for primary loading is highly non-linear. The parameter E_{50} is a confining stress σ'_3 dependent stiffness modulus for primary loading. E_{50} is used instead of the initial tangent modulus E_0 for small strain because E_0 is more difficult to determine experimentally.

$$E_{50} = E_{50}^{\text{ref}} \left(\frac{c' \cos\phi' - \sigma'_3 \sin\phi'}{c' \cos\phi' + p^{\text{ref}} \sin\phi'} \right) \quad (2.11)$$

Where E_{50}^{ref} is a reference stiffness modulus corresponding to the reference stress p^{ref} . In Plaxis, a default setting $p^{\text{ref}} = 100 \text{ KN/m}^2$ is used. The actual stiffness depends on the minor principal stress σ'_3 , which is the effective confining pressure in a tri-axial test. Note that σ'_3 is negative in compression. The amount of stress dependency is given by the power m . Soos and Boháč (2002) reported a range of m values from 0.5 to 1 in different soil types with the values of 0.9 to 1 for the clay soils. In order to simulate a logarithmic stress dependency, as observed for soft clay, m is recommended to be taken as 1.

The stress dependent stiffness modulus for unloading and reloading stress paths is calculated as:

$$E_{\text{ur}} = E_{\text{ur}}^{\text{ref}} \left(\frac{c' \cos \phi' - \sigma'_3 \sin \phi'}{c' \cos \phi' + p^{\text{ref}} \sin \phi'} \right)^m \quad (2.12)$$

Where $E_{\text{ur}}^{\text{ref}}$ is the reference modulus for unloading and reloading, which corresponds to the reference pressure $p^{\text{ref}} = 100 \text{ kN/m}^2$. For a practical case, PLAXIS 3D gives the default setting of E_{ur} equal to $3E_{50}^{\text{ref}}$. This is an average for various soil types.

The shear hardening yield function (f_s) in the HS Model is given as:

$$f_s = \bar{f} - \gamma^p \quad (2.13)$$

$$E_{\text{oed}} = \frac{q_a}{E_{50}} \cdot \frac{(\sigma'_1 - \sigma'_3)}{q_a - (\sigma'_1 - \sigma'_3)} - \frac{2(\sigma'_1 - \sigma'_2)}{E_{\text{ur}}} \quad (2.14)$$

Where, σ'_1 and σ'_3 are the major and minor principal stresses, E_{50} is 50 per cent secant stiffness modulus, q_a is the asymptotic value of the shear strength, and γ^p is the plastic shear strain, and can be approximated as:

$$\gamma^p \approx \varepsilon_1^p - \varepsilon_2^p - \varepsilon_3^p = 2\varepsilon_1^p - \varepsilon_v^p \approx 2\varepsilon_1^p \quad (2.15)$$

Where, ε_1^p , ε_2^p and ε_3^p are plastic strains and ε_v^p is plastic volumetric strain.

From the formulations of the shear hardening yield function, it can be seen that the triaxial moduli (E_{ur} and E_{50}^{ref}) are parameters that control the deviatoric or shear hardening yield

surfaces. In addition to the shear hardening yield surfaces, the cap yield surfaces are also used in the HS Model. These cap yield surfaces are related to the plastic volumetric strain measured in the isotropic compression condition. Fig.2.13 shows the shear hardening and the cap yield surfaces in the HSM for soil with no cohesion ($c' = 0$).

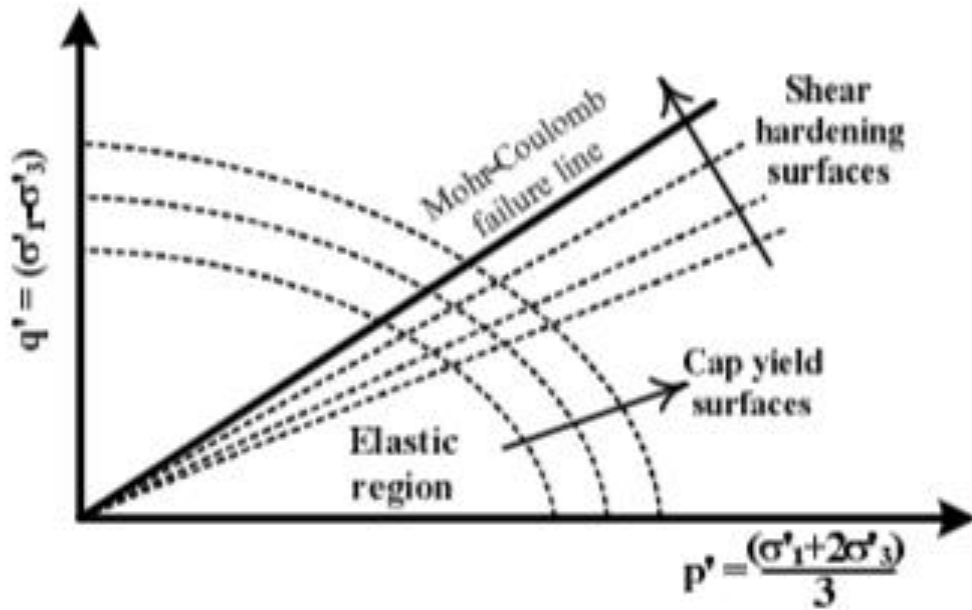


Fig. 2.13 Shear Hardening and Cap Yield Surfaces in the Hardening Soil Model

The reference oedometer modulus ($E_{\text{oed}}^{\text{ref}}$) is used to control the magnitude of the plastic strains that originate from the yield cap $\varepsilon_v^{\text{pc}}$, i.e., control of volumetric hardening. In a similar manner to the tri-axial moduli, the oedometer modulus (E_{oed}) obeys the stress dependency power law:

$$E_{\text{oed}} = E_{\text{oed}}^{\text{ref}} \left(\frac{c' \cos \varphi' - \sigma'_1 \sin \varphi'}{c' \cos \varphi' + p^{\text{ref}} \sin \varphi'} \right)^m \quad (2.16)$$

Where E_{oed} is the tangent stiffness modulus as indicated in Fig. 2.14 with reference to $p_{\text{ref}} = 100$ kPa.

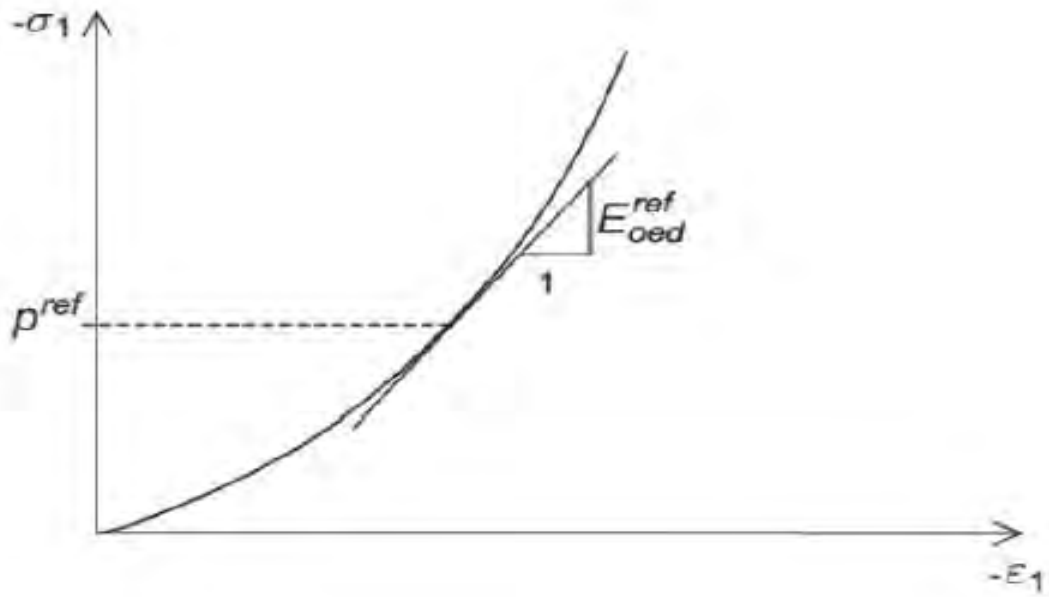


Fig. 2.14 Definition of E_{oed} in Oedometer Test Results

Similarly the stress dependent stiffness modulus for unloading and reloading stress paths is calculated as:

$$E_{ur,oed} = E_{ur}^{ref} \left(\frac{c' \cos \phi' - \sigma'_1 \sin \phi'}{c' \cos \phi' + p^{ref} \sin \phi'} \right)^m \quad (2.17)$$

Note that σ'_1 is the effective consolidation stress in oedometer test. It is negative in compression.

After extensive shearing, dilating materials arrive in a state of critical density where dilatancy has come to an end. In the Hardening-Soil model, a dilatancy cut-off is introduced. In order to specify this behavior, the initial void ratio, e_{init} and the maximum void ratio, e_{max} , of the material must be entered as general parameters. As soon as the volume change results in a state of maximum void, the mobilized dilatancy angle, ψ'_{mob} is automatically set back to zero, as indicated in Fig.2.15.

For $e < e_{max}$

$$\sin \psi'_{mob} = \frac{\sin \phi'_{mob} - \sin \phi'_{cv}}{1 - \sin \phi'_{mob} \sin \phi'_{cv}} \quad (2.18)$$

$$\text{Where: } \sin\phi'_{cv} = \frac{\sin\phi' - \sin\psi'}{1 - \sin\phi' \sin\psi'}$$

$$\text{For } e \geq e_{max}: \quad \psi'_{mob} = 0$$

The definition of the cap yield surface can be given as:

$$f^c = \frac{\tilde{q}^2}{\alpha^2} + p^2 - p_p^2 \quad (2.19)$$

Where, α is an auxiliary model parameter.

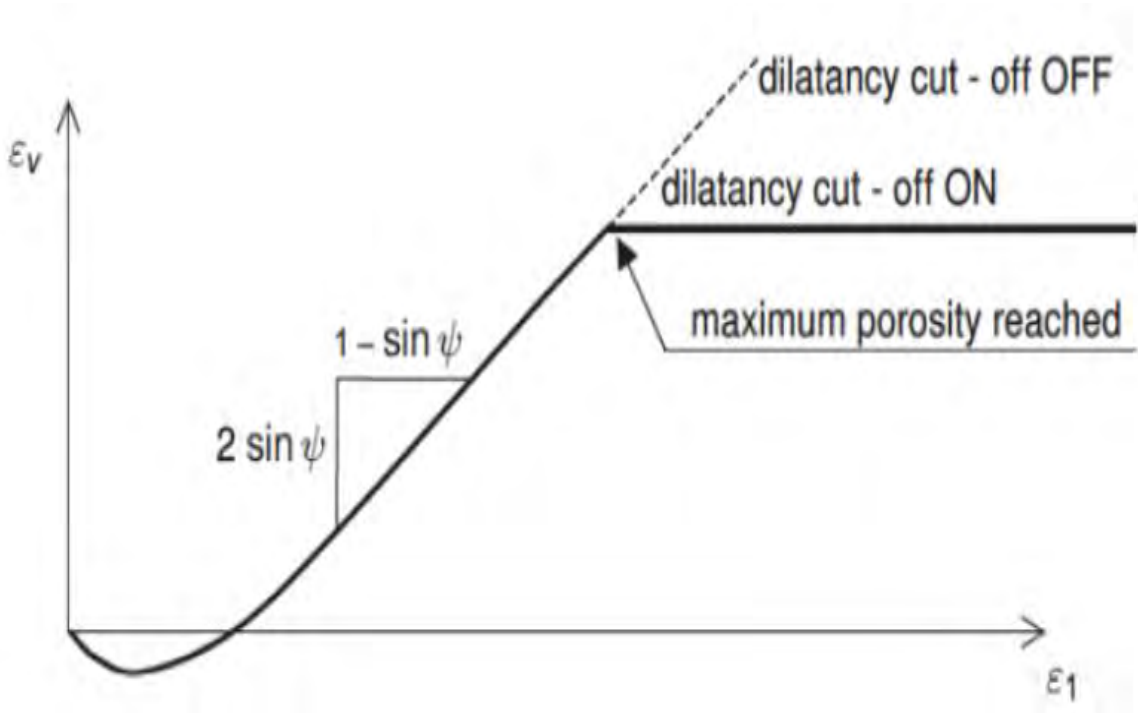


Fig. 2.15 Resulting Strain Curve for a Standard Triaxial Test when Including Dilatancy Cut-off

The parameters p and \tilde{q}^2 are expressed as:

$$p = \frac{-(\sigma_1 + \sigma_2 + \sigma_3)}{3} \quad (2.20)$$

$$\tilde{q}^2 = \sigma_1 + (\delta - 1)\sigma_2 - \sigma_3 \quad (2.21)$$

$$\delta = \frac{3 + \sin\phi'}{3 - \sin\phi'} \quad (2.22)$$

Where, \tilde{q} is the special stress measure for deviator stresses. In the case of the triaxial compression \tilde{q} reduces to $\tilde{q} = (\delta)(\sigma_1 - \sigma_3)$.

The magnitude of the yield cap is determined by the isotropic pre-consolidation stress P_p . Importantly the hardening law, which relates the pre-consolidation pressure (P_p) to the volumetric cap-strain (ϵ_v^{pc}) can be expressed as:

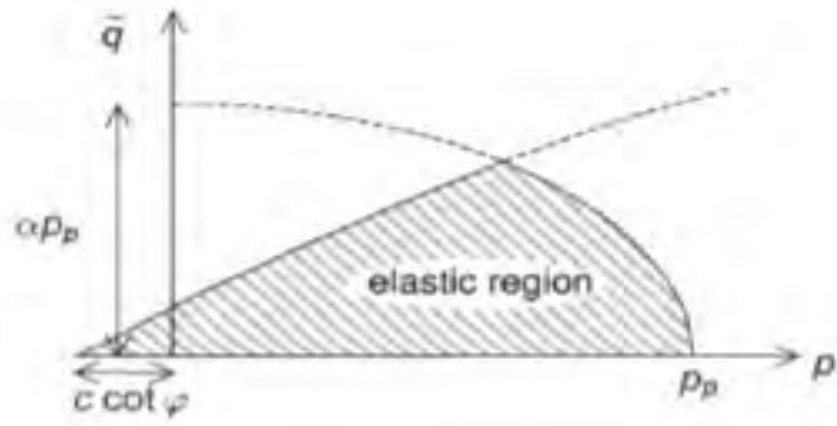
$$\epsilon_v^{pc} = \frac{\beta}{1-m} \left(\frac{p_p}{p^{ref}} \right)^{1-m} \quad (2.23)$$

Where, ϵ_v^{pc} is the volumetric cap strain, which represents the plastic volumetric strain in isotropic compression. In addition to the constants m and p^{ref} , which have been discussed earlier, there is another model constant β . Both α and β are cap parameters, but PLAXIS does not adopt them as input parameters. Instead, their relationships can be expressed as:

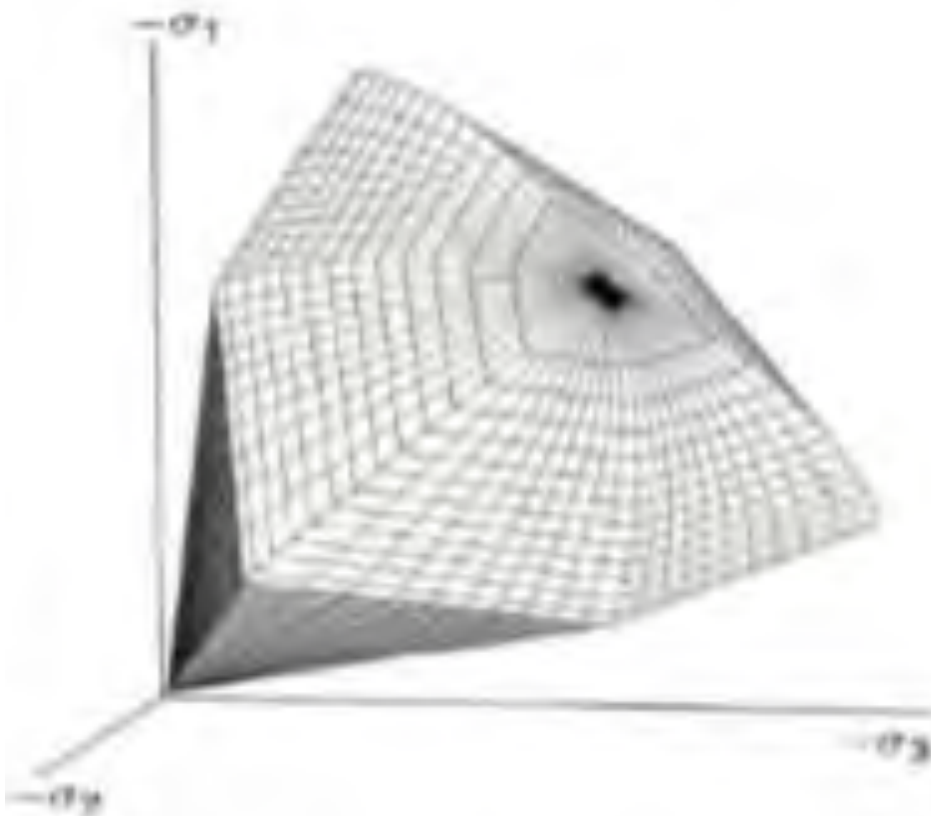
$$\alpha \leftrightarrow K_0^{nc} \quad (\text{By default } K_0^{nc} = 1 - \sin\phi) \quad (2.24)$$

$$\beta \leftrightarrow E_{oed}^{ref} \quad (\text{By default } E_{oed}^{ref} = E_{50}^{ref}) \quad (2.25)$$

Such that K_0^{nc} and E_{oed}^{ref} can be used as input parameters that determine the magnitude of α and β , respectively. Fig. 2.16 (a & b) shows the ellipse shape cap surface in the p - \tilde{q} plane.



(a)



(b)

Fig. 2.16 Illustration of Double Yield Surface of the Hardening Soil Model (a) in p - \bar{q} plane; (b) in 3D with $c'=0$

2.6.3 Difference between the Mohr-Coulomb model and Hardening soil model in general

- The Mohr-Coulomb model only use a single Young's modulus and also not able to distinguish between loading and unloading stiffness. In the Hardening Soil model, soil stiffness is calculated much more accurately by using three different stiffness (tri-axial loading secant stiffness, tri-axial unloading/ reloading stiffness, and oedometer loading tangent stiffness).
- The Mohr-Coulomb model represents Young's modulus of soil in the in situ stress state. On the other hand, the Hardening Soil model represents its three moduli at the reference pressure, and these moduli at the in situ stress state are automatically calculated as a function of the current stress state.
- In contrast to the Mohr-Coulomb model, the Hardening Soil model can control stress-dependency of stiffness moduli.
- Mohr-Coulomb model can be used for clay in undrained condition or hardening soil model for loose sand.
- Practical cases have proven that for different types of excavations, where the unloading behavior of the soil is significant, the Hardening Soil (HS) model gives more realistic and accurate results than the Mohr-Coulomb (MC) model.

2.7 Drainage conditions: Undrained A/ B/ C/ D

There are two approaches for analysis of short term undrained behavior of cohesive soils, namely effective stress analysis and total stress analysis. In the effective stress analysis, pore water pressure and soil are treated separately; in the total stress analysis, pore water pressure and soil are treated as a single unit. The total stress approach for short term undrained condition in clay has the advantage of avoiding the cumbersome need to predict the excess pore pressure. If the excess pore pressure is known or can reasonably be anticipated, then the short term undrained behavior of soils may be written in terms of effective stress parameters.

Several constitutive soil models have been developed using the effective stress approach. Two of these models, namely the Mohr-Coulomb (MC) model, and Hardening Soil (HS)

model will be discussed here. The MC model is formulated using the combination of linear elastic Hooke's law and the Mohr-Coulomb failure criterion. The HS model (Schanz et al. 1999) is based on the elastic-plastic hardening rule. These two models have been implemented in PLAXIS. Advantages and limitations undrained analysis methods discussed herein are based on those applied in PLAXIS. (Brinkgreve 2005; Chanaton 2010; Schweiger et al. 2008; Wong 2009).

The behavior of soils is primarily governed by the effective stresses independent of the drainage condition (Brinch-Hansen and Gibson 1949; Schmertmann 1975). Janbu (1977) concluded that the short term undrained behavior of saturated clays are governed by the effective stresses. Since the soil behavior is governed by effective stress rather than total stress, the parameters for total stress models should consider the development of pore water pressure and influence of stress history, that is, the principle of effective stress should be completely defined in the parameters.

There are four methods (Undrained Method A, B, C, and D) available in PLAXIS 3D to model undrained soil behavior. Undrained Method A, B, and C are used in combination MC model. Undrained Method D is used in the HS model.

Undrained Method A, B and D model undrained behavior using effective stiffness parameters. Method C uses total stress undrained stress stiffness parameters; Undrained Method A and D use effective strength parameters; Undrained Method B and C use total stress undrained strength parameters. A summary of analyses for models is given in Table 2.4.

Table 2.4 Summary of analyses for undrained materials

Undrained Method	Material Behavior type	Material model	Computed stresses	Parameters	
				Stiffness	Strength
A	Undrained (MC)	Mohr-Coulomb	Effective stress and pore pressure	Effective (E' , $\nu' \leq 0.35$)	Effective (ϕ , c' , ψ')
B	Undrained (MC)	Mohr-Coulomb	Effective stress and pore pressure	Effective (E' , $\nu' \leq 0.35$)	Total (ϕ_w , c_u , $\psi=0$)
C	Non-porous/ Drained (MC)	Mohr-Coulomb	Total stress	Total (E' , $\nu' \leq 0.495$)	Total (ϕ_w , c_u , $\psi=0$)
D	Undrained (HS)	Hardening Soil	Effective stress and pore pressure	Effective parameters depending on soil model selected	

2.7.1 Advantages and limitations of Undrained A, B, C and D

a) Undrained Method A

Method A utilizes both effective stress and stiffness parameters to model undrained behavior of soils, (i.e., material behavior type). As shown in Figure 2.17, the predicted pore pressure is much smaller than the actual one and the effective stress path (ESP) predicted rose up vertically until the failure envelope is reached (elastic soil). This stress path is unlikely to be identical to the real soil stress path especially in case of normally consolidated clay. As a result, it over-estimates the undrained shear strength and underestimates the excess pore pressure. Method A does not necessarily always over-estimate undrained shear strength. For a given clay layer with constant undrained shear strength, Undrained Method A underestimates undrained shear strength at low stress and overestimates it at high stress and however, it is the opposite in over-consolidated clay (see Figure 2.18).

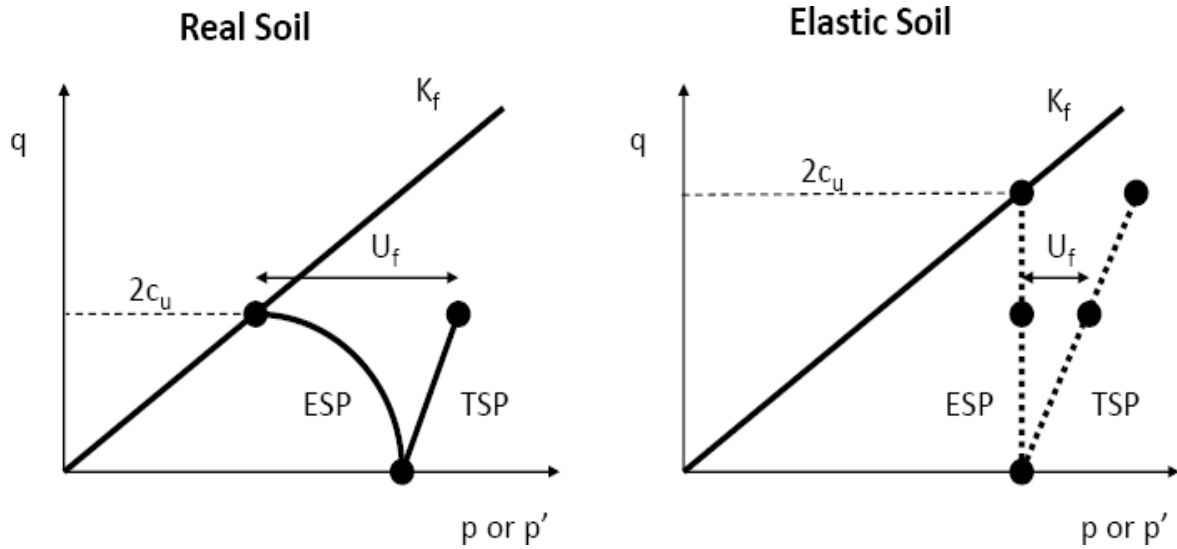


Fig. 2.17 Effective stress path using c' and ϕ' - MC model (Wong 2009)

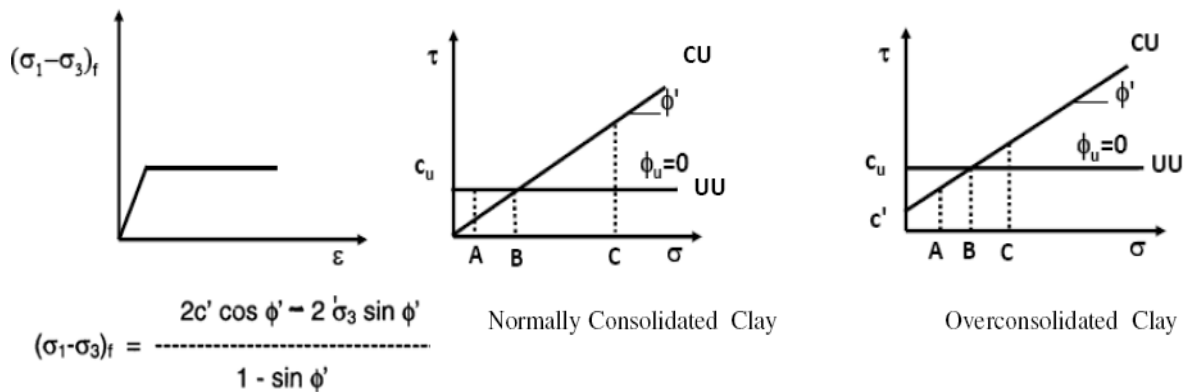


Fig. 2.18 Undrained shear strength predicted by undrained method A for normally consolidated and over consolidated clays (Wong 2009)

Undrained shear strength in Undrained Method A is a consequence of modeling, not an input parameter. Since pore pressure is predicted, the undrained analysis may be followed by consolidation and increase in shear strength is obtained due to dissipation of excess pore pressure. However, the increase in shear strength may also be quantitative wrong due to incorrect excess pore pressure estimation.

b) Undrained Method B

Similar to Undrained Method A, this method analysis is in terms of effective stress and Mohr- Coulomb model is used. Material behavior type is undrained. Effective stiffness parameters and total strength parameter (the undrained shear strength) are both used as input parameters. Constitutive equations are formulated in terms of effective stress. Calculated stress path from Undrained Method B is identical to that of from Undrained Method A. Undrained shear strength is an input parameter and is not a consequence of the model; it will not be affected by effective stress path. The prediction of pore pressure is generally unrealistic and thus it should not be followed by a consolidation analysis.

c) Undrained Method C

Undrained Method C is a total stress approach. Material behavior type is drained. It adopts both undrained strength and undrained stiffness parameters E_u . Undrained Poisson's ratio ν_u is selected between 0.495 and 0.499. K_0 -value to generate initial stresses refers to total stresses. Pore pressure is not calculated. Material type of Undrained Method C is set to "Non-porous" which means neither initial nor excess pore pressure will be taken into account. The disadvantage of this approach is that no distinction is made between effective stress and pore water pressures are equal to zero. An alternative to this is that the material type is set to "Drained". Initial pore water pressure is carried over to the analysis. Nevertheless, there is no change of pore water pressure computed afterward.

d) Undrained Method D

Input parameters of Undrained Method D for both stiffness and strength parameters are the same as Undrained Method A. The only diversion from these two methods is Undrained Method D utilizes a more sophisticated advanced model (such as HS or HSsmall models). Undrained shear strength computed from this method depends on the accuracy of effective stress part as obtained from the advanced model used.

In the present study, method A has been used for both the MC & HS model.

2.8 Review on Sheet Pile Wall and Contiguous Pile Wall

The commonly used systems for the support of deep excavations to minimize lateral and vertical ground movements are secant and contiguous pile walls, diaphragm walls, and steel sheet piles (Ou, 2006). In this study, a numerical comparison has been done between the steel sheet pile wall and contiguous pile wall. Steel sheet pile wall and contiguous pile wall have designed by classical design methods using Columb theory and Rankine theory throughout the years. The numerical analysis is proved to be an effective way to investigate the performance of retaining structure on deep excavations. This thesis is concerned with evaluating the capability of finite element analysis in reproducing various aspects of observed deep excavation behavior in the field. So, in this section, significant research work regarding finite element application on sheet pile wall and contiguous pile wall has been discussed and also the ongoing scenario of the use of both the retaining structure in Bangladesh has been discussed.

2.8.1 Sheet Pile Wall

Retaining structures are commonly categorized into two families:

- Rigid retaining structures, where the stability is provided by the use of a large volume of mass. Only rigid body movements can occur.
- Flexible retaining structures, where other properties of the materials, such as stiffness, strength and wall thickness are exploited to provide stability. Bending and rigid body movements are found.

Sheet pile walls are classified as flexible retaining structures. The stability is provided through an embedment of the wall on the ground working as a cantilever structure (Fig. 2.19) and eventually a system of anchors (Fig. 2.20), so the wall is subject to shear stresses and bending moments. One of the main advantages is the minimization of used material, in contrast to the needs of rigid retaining structures.

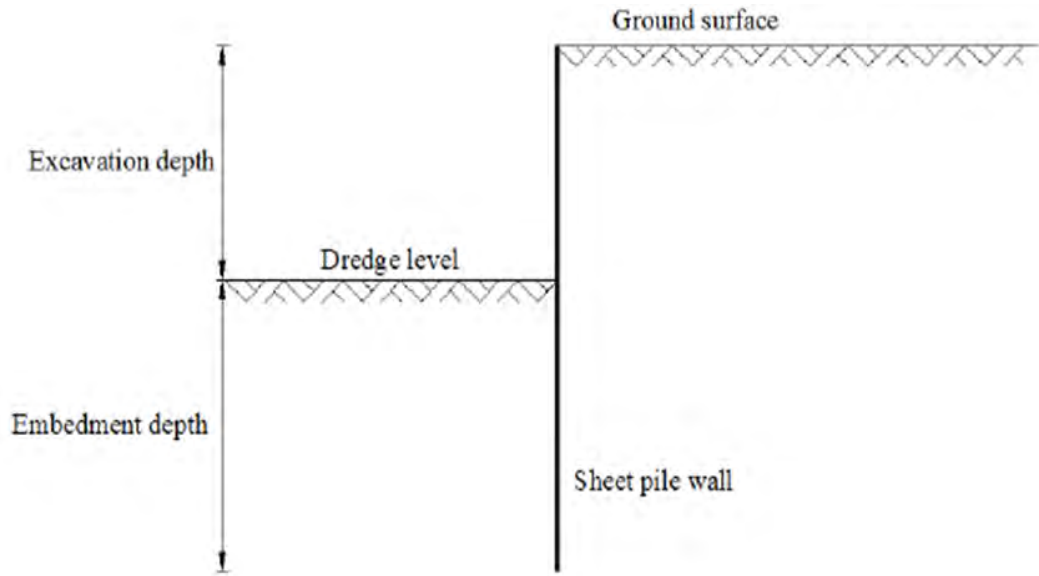


Fig. 2.19 Cantilever Sheet Pile Wall

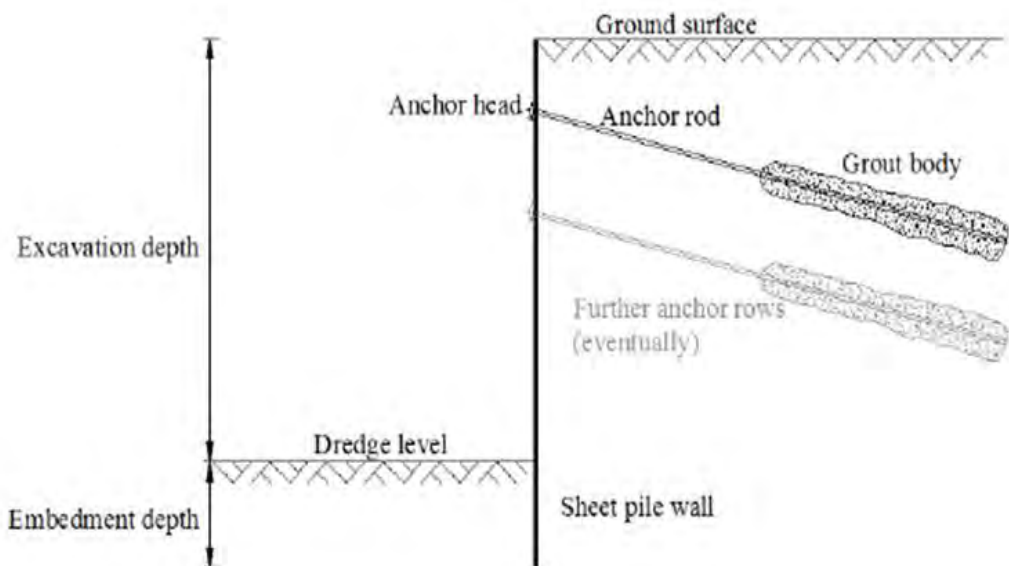


Fig. 2.20 Anchored Sheet Pile Wall

Sheet pile walls are in essence walls built before excavating, with the double aim of resisting the earth pressure generated by the excavation, and limiting or preventing the water inlet. The execution of a sheet pile wall consists of an excavation of a trench, broad and deep, without the need of shoring, but usually stabilized with bentonite slurries. Then, reinforcement bars are placed, and the concrete is laid, or prefabricated elements are placed instead. Sheet pile walls are not only able to resist earth pressures and prevent the

water inlet, but also to receive vertical loads transmitted by other structural elements. Moreover, sheet pile walls are an efficient solution to limit ground movements associated with the excavation. Thus, four main functions can be carried out by a sheet pile wall (Jimnez 1980):

- i. Resist the thrust generated by the excavation.
- ii. Limit the movements in the back of the wall, in the unexcavated zone.
- iii. Prevent from the water inlet.
- iv. Support vertical loads.

There are a good number of design methods for sheet pile walls. The original proposals date back from the first half of the 20th century and have been constantly reviewed. Some of them are still evaluated and studied nowadays. Analytical methods can be found under the name “classical methods” or “limit-stage design methods” (King, 1995). Regardless the name adopted, geotechnical design calculations in either cantilever or anchored sheet pile walls establish equilibrium of horizontal forces and moments to define the failure state and the reference embedment below the dredge line (before applying the safety factor).

The main analytical methods for cantilever walls are the full method, simplified method and gradual method and the main analytical methods for anchored walls are the free earth support method and the fixed earth support method. A significant amount of research work has been found on the analytical method (Padfield & Mair 1984, Day 1999, Škrabl 2006).

First applications of the Finite Element method date from the early 1980s. The discretizations of the geometry were coarse, and the results were limited. Fourie & Potts (1989) presented a comparison of finite element and limit equilibrium analysis for a cantilever wall. The soil behavior was modeled through an elasto-plastic constitutive law, under drained conditions. The classical methods used were the full method and the simplified method. In the finite element model, Young’s modulus is considered to increase linearly with depth. Drained conditions, with zero pore water pressures everywhere, zero cohesion and a single soil friction angle of 25° were considered. One hundred sixty-five eight-noded isoparametric elements discretized the domain. The effect of the initial stress was studied as well. Two extreme cases, with $K_0=0.5$ and $K_0=2$, were performed. Results showed that larger horizontal movement of the wall occurs with $K_0=2$ than with $K_0=0.5$,

for the same depth of excavation. Further results of the comparison indicated that both the limit equilibrium method used in the Paper and the finite element approach give similar predictions of the embedment depth required to ensure stability. The finite element analysis justifies the 20% increase in embedment depth arbitrarily assumed in the limit equilibrium approach, which was showed again by Cuadrado (2010). Results displayed as well that in excavations with low K_0 values limit equilibrium methods overestimate the maximum bending moments in almost 50%. Some reduction of the bending moment must, therefore, be guaranteed.

Day & Potts (1993) showed that while working with a Finite Element model, beam elements are appropriate to represent sheet pile walls. However, since the effect of the wall the element type is significant, beam elements are not recommended for the analyses of thick concrete retaining walls (referring to rigid structures); in which 2D elements are appropriate as they more accurately describe the geometry of the structure.

Bilgin and Erten (2009) conducted a Finite Element Analysis on the different loading and unloading variation of soils around the wall and showed that the location of anchored sheet pile wall has a significant effect on wall behavior. Although the existence of stress concentration at the anchor level, the conventional design methods do not consider the stress concentrations along the wall height, and they assume that lateral earth pressures linearly increase with depth. Because the whole design depends on the lateral earth pressures, a design based on an inaccurate earth pressure distribution will result in models that are either conservative or, more importantly, unsafe. A Comparative parametric study using the conventional design method and the FEM was performed to investigate the lateral earth pressures, bending moments, and anchor forces of single-level anchored sheet pile walls in soils. According to obtained results, neither active nor passive earth pressures linearly increase with depth as assumed in conventional design methods. Also, the conventional design methods resulted in approximately 50% more wall bending moments compared with the FEA results but the anchor forces obtained from the FEAs were about 40% more than the ones derived from the conventional design method.

Sahajda (2014) conducted a study to consider the determination of anchor loads. In this study, the measurement was carried out on a sheet pile wall supporting an excavation in mixed clay or sand soil. The forces measured were in average 68 % of the values

calculated in the design with the assumption of fully drained conditions in clay. The calculation made with undrained clay led in turn to calculated forces significantly smaller than measured. Since this lies on the unsafe side, it is not recommended to assume undrained conditions in the firm and stiff clay. The actual anchor forces were shown to depend more on the value of the lock-off load than the e.g. surface load at the retained side.

Guha Ray and Baidya (2015) conducted a study on reliability-based analysis of cantilever sheet pile backfilled with different soil types using the finite-element approach. According to the survey, it was found that cohesion of the foundation soil is the most sensitive parameter. Loose layer location might have variable effects on forces acting on sheet pile wall and strut system. This issue has not investigated precisely yet in studies related to sheet pile walls. Authors of previous studies in clay deposits depicted that existence of loose layer in the bottom of stiff layers increased struts axial forces and sheet piles bending moments (Ahmadpour and Amel Sakhi 2019). Other previous studies showed that for retaining walls that retain a significant thickness of soft material, maximum lateral and vertical movements values increased significantly from the stiff soil cases (Long, 2001).

A significant amount of numerical analyses have been conducted on deep excavations to approximate real deep excavations in the design process by adopting 2D analyses (Clarke et al. 1984, Hubbard et al. 1984, Finno et al. 1991, Hashash et al. 1996). Most of these analyses rely on simplifying assumptions, and therefore the information they can provide is limited and sometimes misleading. In reality, all geotechnical problems involving retaining structures are three dimensional, and ideally, three-dimensional analyses, fully representing the structure's geometry, loading conditions and variations in ground conditions across the site, should be undertaken. Three-dimensional analyses have some advantage over two-dimensional analyses. For instance, a 2D analysis is not able to consider the corner effects in deep excavations, which indicate that the wall deformation and ground movement are smaller closes to the wall corner than around the wall center. Besides, 2D plane strain analysis tends to overestimate the wall deflection and ground settlement behind the wall compared to the simplified 3D symmetric square or rectangular analysis (Gouw et al. 2014, Ou et al. 1996).

Numerical simulation is often used in the stress analysis of sheet pile wall (Lee et al. 2011, Chowdhury et al. 2013; Guha Ray and Baidya 2015; Golaitet al. 2018; Van Baars2018). Under symmetrical loading conditions, the sheet pile wall can be simplified as a two-dimensional (2D) plane strain problem. Chowdhury et al. (2013) adopted the Mohr-Coulomb model to describe the soil behavior and beam elements to simulate the pile, and the effects of the design parameters of the support structure on the excavation process were obtained. Using a similar route, Azzam and Elwakil (2017) simulated a pile wall subjected to axial forces, and the calculated values agreed well with the experimental results. Athanasopouloset al. (2011) performed a 2D finite-element analysis of a foundation pit supported with steel sheet piles in an urban area. It was also shown in this analysis that measured values were in close agreement with theoretical values. In most cases, the sheet pile wall suffers asymmetric loads due to the complicated topography so the use of 2D simulation was insufficient and a detailed 3D analysis.

Among the options available for retaining structures, Sheet pile wall has been used extensively during the excavation process throughout the world. A typical retaining structure supported by steel sheet pile comprises steel sheet piles, ring beams, middle struts, and corner struts (Fig.2.21).



Fig. 2.21 Steel sheet piles in excavation of a bridge foundation pit.

Under symmetrical loading conditions, horizontal loads such as earth pressure and water pressure are transferred to struts by steel sheet piles. In this case, reducing the space between the braces can effectively reduce the stress in these steel sheet piles. By contrast, under asymmetric loading conditions, the behavior of a support structure is similar to a cantilever beam. The steel sheet piles mainly resist the unbalanced load. Even increasing the number of struts cannot effectively reduce the bending moment of steel sheet piles. In this situation, the composite action of the steel sheet piles has a significant influence on the behavior of the pit support structure.

Though sheet pile wall has been used widely throughout the world, it is rarely used in Bangladesh. A sheet pile wall is quite expensive in the context of Bangladesh. However, a

significant number of researches have been found on the numerical analysis of sheet pile wall, but no research work regarding the finite element application of sheet pile wall in the context of Bangladesh have not found. In this study extensive three-dimensional finite element analysis has been done using PLAXIS 3D on sheet pile wall through variable consideration of different factors. This study has been done using soil profile from the two major cities (Dhaka and Chittagong) of Bangladesh to check the viability of using sheet pile wall.

2.8.2 Contiguous Pile Wall

In-situ pile retaining walls which are also known as column piles are rows of concrete piles constructed either in cast-in-situ or precast pile method. Advantages of using column piles are less disturbance or vibration than produced by the installation of soldier piles or sheet piles. Column piles have a higher stiffness than soldier piles or steel sheet piles. They prevent excessive bulk excavation and help to control ground movements. Three commonly used bored piles are Contiguous wall, Secant wall, and tangent wall (Fig. 2.22)

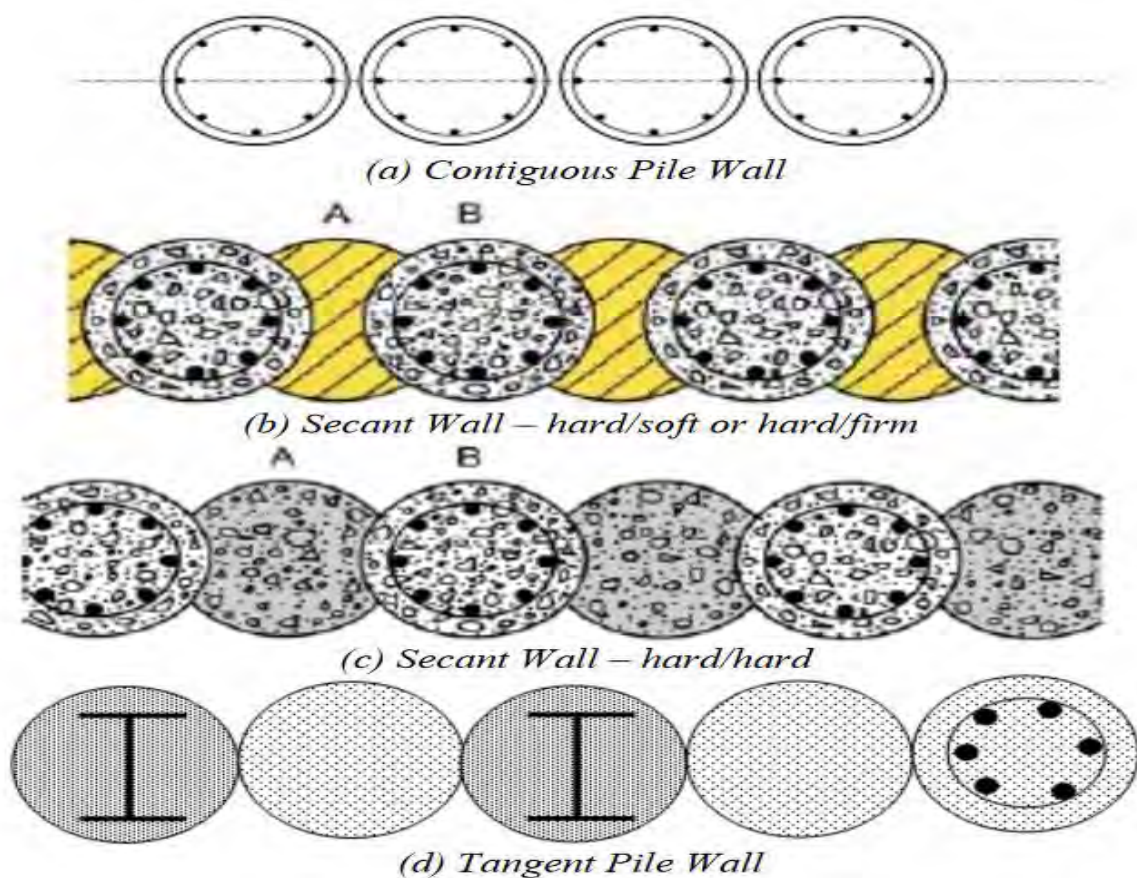


Fig. 2.22 Bored Pile Walls

Contiguous pile walls constructed with small gaps between adjacent piles. The use of low-cost drills and, more particularly, Contiguous Flight Auger (CFA) rigs to drill successive unconnected piles provide an economical wall. Diameter and spacing of the piles are decided based on soil type, groundwater level and magnitude of design load. Large spacing is avoided as it can cause in caving of soil through gaps. CFA pile diameters range from 300mm to 1000mm. CFA piles are considered more economical than diaphragm wall in small to medium scale excavations due to the reduction in cost and time of site operations. Besides, no bentonite mud is needed for the excavation. Contiguous piles are suitable in crowded urban areas, where traditional retaining methods would otherwise invade the adjoining properties; these piles restrict ground movements on the backfill side.

Contiguous pile is proposed to be used as permanent retaining wall, contiguous piles were analyzed for two types of phase namely temporary analysis and permanent analysis. The temporary analysis is carried out till the final excavation level whereas the permanent analysis is done considering all the floor slabs in position. Normally, contiguous pile wall are designed by using Classical Conventional method such as earth pressure theory proposed by Peck (1974). Figure 2.23 gives the apparent pressure distribution diagrams as proposed by Peck.

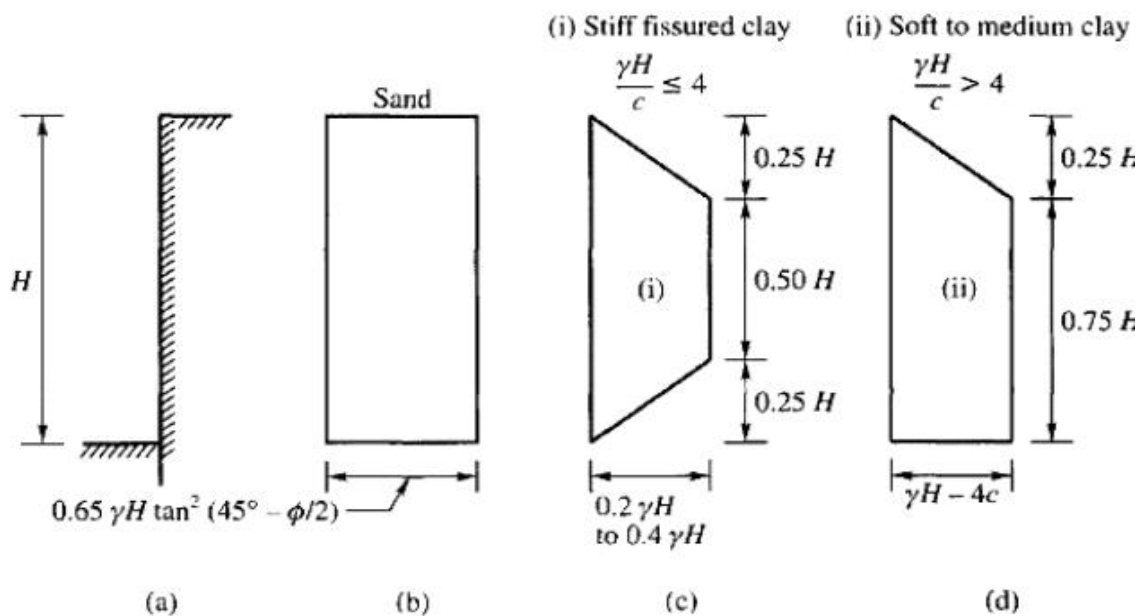


Fig. 2.23 Earth pressure distribution proposed by Peck (1974)

There is a scarcity of research work regarding the finite element application on contiguous pile wall. Recent work has been done by Vinoth and Ghan (2018) to present a case history on the use of temporary support of excavation using contiguous bored piled wall technique for deep basement excavation in Chennai. They conducted a two-dimensional finite element analysis using PLAXIS 2D and monitored the data with a total station. They concluded by observing the Total station measurements that contiguous pile moved towards retaining side (negative deflection) at the top of the contiguous pile wall due to the development of tension zones behind the contiguous pile.

In Bangladesh, reinforced retaining system, i.e., contiguous pile wall is common and relatively economical to be used in cohesive soil. Based on the economic advantages of contiguous pile wall compared to a sheet pile wall, there is a scope of intensive research to prove it as a viable option for the excavation process. In this Study, a three-dimensional analysis of Contiguous pile wall has been conducted using PLAXIS 3D. Moreover, In this research based on 3D numerical analyses for contiguous pile wall and sheet pile wall, a detailed comparison have been made considering several factors such as soil-structure interaction, stress analysis, pore-water pressure analysis, foundation type, etc.

2.9 Summary

Numerical analyses have been useful to examine the performance of deep excavations in many aspects for example wall deflections, ground movements, wall bending movements, strut loads, and earth and pore water pressures. Some answers have been found, and lessons are acknowledged which is stated below in short.

- 2D analyses could distort the matter and cause unreliable or inaccurate results, as discussed in Gourvenec, Powrie et al. (2002), Zdravkovic, Potts et al. (2005) and Lee, Hong et al. (2011), though they need to be contributed to the understanding of some aspects of deep excavations. 3D effects are evident and significant in deep excavations, and 3D analyses are entirely feasible nowadays due to the advances of hardware and software. Therefore, 3D analyses are encouraged within the analysis, and vital aspects like the ground profile, the geometry of the excavation, the retaining structures, and also the construction sequences, should be portrayed suitably within the modeling procedure. However, there are only a few journals

relating to elaborated 3D analyses of deep excavations and comparison with field data from case histories.

- Accurate soil constitutive models are pivotal to catch the observed execution of deep excavations in the field estimation. Conventional linear elasto-plastic soil models (e.g. Mohr-Coulomb) without considering the small-strain stiffness nonlinearity of the soil perform rather poorly in reproducing the observed ground movement in the field (Burland and Hancock 1977, Potts and Zdravkovic 2001), while advanced soil models which incorporate more practical soil practices, e.g., the small-strain stiffness nonlinearity, stress history change, anisotropy can enhance the computed results (Simpson 1992, Whittle, Hashash, et al. 1993, Hashash and Whittle 1996, Dong, Burd et al.2013).
- The soil-structure interface properties affect the wall deformation and ground movement, and a genuine contact model is needed to anticipate their effects (Day and Potts 1998). However, a detailed study of the influence of interface properties on the performance of braced excavations is never seen in research publication.
- The impact of construction sequence on the execution of braced excavations is as yet vague, because of limited data accessible in written works. Besides, it is rarely seen in any publications regarding incorporating adjacent infrastructure in the model and investigating their response to braced excavations.
- It is significant to calibrate the numerical results with laboratory tests and field measurements to appraise the competence of numerical analyses in replicating the observed behavior in the experiments or the field. Discrepancies between the numerical analysis and laboratory tests or field measurements can be attributed to variety of reasons, e.g. limitations of the numerical analysis, simplifications and assumptions created within the analysis, the capability of the material models and the reliability of input parameters, and uncertainties in the tests and measurements. Parametric studies are helpful to investigate how significant the influence of a particular factor is and identify which factors are the most important ones.
- Among the options available for retaining structure, Sheet pile wall has been widely used throughout the world, but it has been used barely in Bangladesh due to economical reason. A significant number of two-dimensional analysis has it has been conducted on a sheet pile wall, and a few three-dimensional analysis has been conducted as well. In Bangladesh most commonly used retaining structure is

contiguous pile wall as it is economical to use. There is still lacking in the finite element application on contiguous pile wall thorough out the world. In this study, a detailed numerical comparison has been made in between sheet pile wall and contiguous pile wall based on the subsoil characteristics of two major cities of Bangladesh.

However, some conclusions ought to be treated with caution due to the simplifications and assumptions created within the analyses.

CHAPTER 3

DATA COLLECTION AND THE VALIDATION OF FEM MODEL

3.1 Introduction

Deep excavations in the urban areas of Bangladesh are usually close to adjacent infrastructure, e.g., buildings, deep foundations, and buried pipelines, which are sensitive to the excavation-induced ground movement. In such conditions, the design and construction of deep excavations must consider the possible adverse effect of the excavation and control it within a permissible level. The design of the excavation, therefore, is entirely dominated by the more restricted deformation criteria, rather than the failure. The bottom-up construction method is widely used in Bangladesh. In our study, we choose two prominent cities of Bangladesh, e.g., Dhaka and Chittagong as a good number of the tall buildings are being constructed in the both cities in recent years.

Deep excavations in Dhaka and Chittagong soil are challenging and influenced by some factors such as geological conditions, retaining structures, construction methods, and workmanship. Finite element analysis is a useful tool to investigate the excavation behavior, but its capacity in replicating the observed performance in the field needs to be evaluated through calibration with the field data. Also, some undetermined parameters can be estimated through parametric studies.

This chapter will present the geological and geotechnical engineering properties derived from the soil investigation on Dhaka and Chittagong soil. Field tests are also described here. An idealized excavation geometry is adopted in this chapter to conduct the parametric studies. Some useful findings and conclusions are generated for practical applications in the design and construction of deep excavations. Also, validation of the FEM model by taking field instrumentation data of Siam Motor Building in Bangkok and construction of a Pier in 2nd Bridge over Gumti River have also been presented in this chapter.

3.2 Geological and geotechnical engineering properties of study areas

In our study, we have selected two sites: one in Dhaka and the other in Chittagong. The generalized geotechnical engineering properties that are based on the sub-soil investigation will be described in the following sections.

3.2.1 Generalized geotechnical properties of the site in Dhaka

This section reviews the generalized geotechnical properties of the site in Dhaka. The information is extracted mainly from the sub-soil investigation report of the project area. The project area is situated in Purbachal. Two borings conducted at the site in the present study. The geological profile from the site investigation of this project is shown in Fig. 3.1.

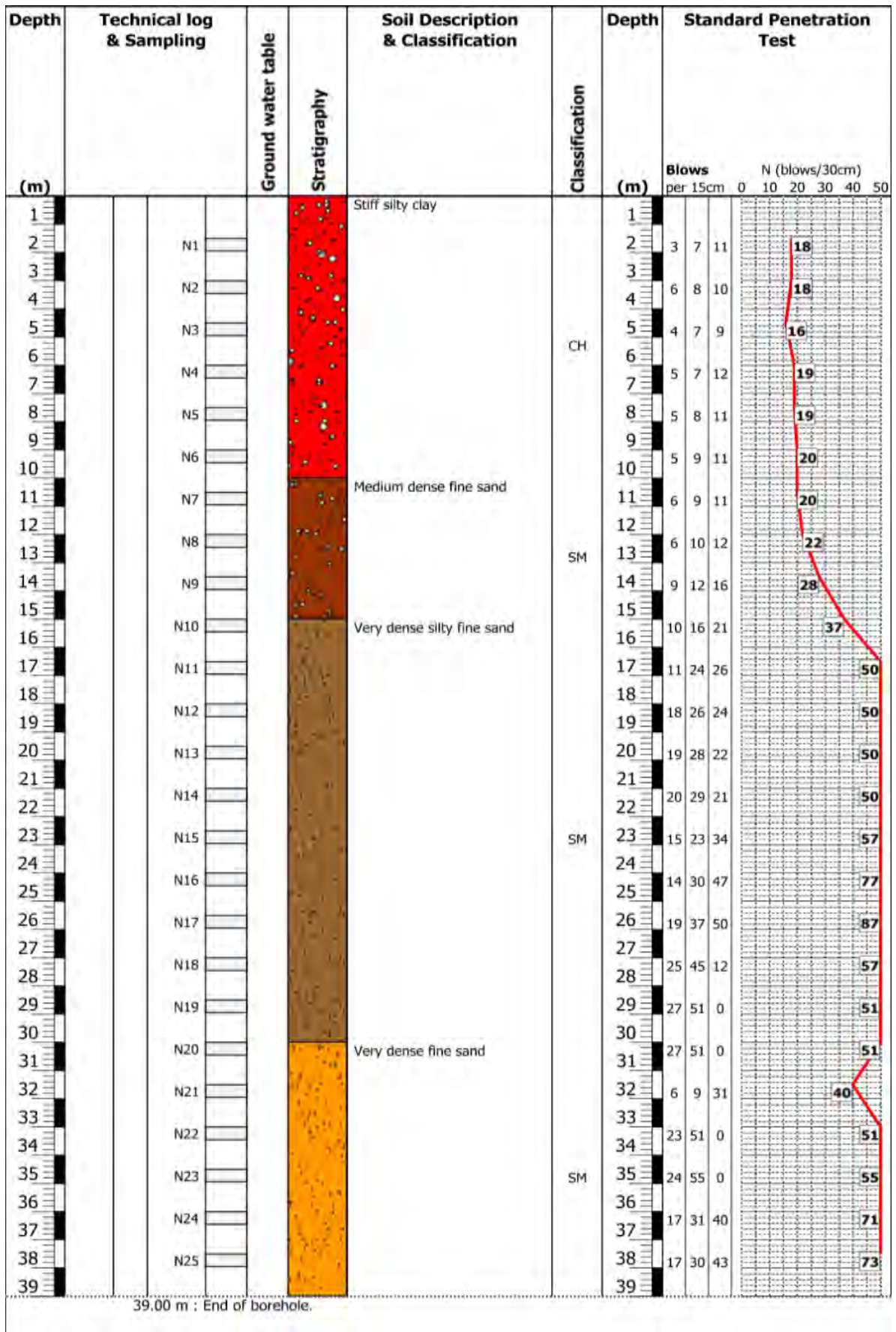


Fig. 3.1 Soil profile of a site in Dhaka

According to the site investigation report, the site is underlain by alluvial deposits. The groundwater table was well below the borehole depth of 39m. The soil profile is divided into 4 sub-layers according to the difference in soil characteristics, physical and mechanical properties. The subsurface consists of a 10m layer of stiff silty clay and 5 m thick layer of medium dense fine sand. Underlying is a 15m thick very dense silty fine sand. Underneath the silty fine sand is a 9.5m thick layer of very dense fine sand.

A summary of engineering properties of the site in Dhaka are given in Table 3.1:

Table 3.1 Engineering properties of the site in Dhaka

Parameter	Unit	Formation		
		Stiff Silt with little fine sand	Medium dense fine Sand	Very dense fine sand
Avg SPT N		16	37	>50
Unit weight	kN/m ³	19	18	20
Dry unit weight	kN/m ³	15.8	16	17
Liquid limit	%	50	-	-
Plasticity index	%	22	-	-
Undrained Shear Strength, S _u	kPa	19	-	-
Cohesion, c'	kPa	31	0	0
Angle of friction, ϕ	Degree	14	31	33
Dilatancy angle, ψ	Degree	0	1	3
Poisson's ratio, ν		0.3	0.3	0.3
Co-efficient of Permeability	m/s	7×10^{-10}	5.27×10^{-6}	5.78×10^{-6}
Young Modulus, E	kPa	26500	27000	28000
Secant Modulus, E ₅₀	kPa	35000	43000	35000
Oedometer Modulus, E _{oed}	kPa	33000	22000	35000
Unloading reloading Modulus, E _{ur}	kPa	105000	129000	105000

3.2.2 Generalized geotechnical properties of a site in Chittagong

This section analyses the generalized geotechnical properties of a site in Chittagong. The information is extracted mainly from the sub-soil investigation report of the project area. The project area is situated in the vicinity of Chittagong Port Authority Headquarter. Two borings were conducted at the site in the present study. The geological profile from the site investigation of this site is shown in Fig.3.2.

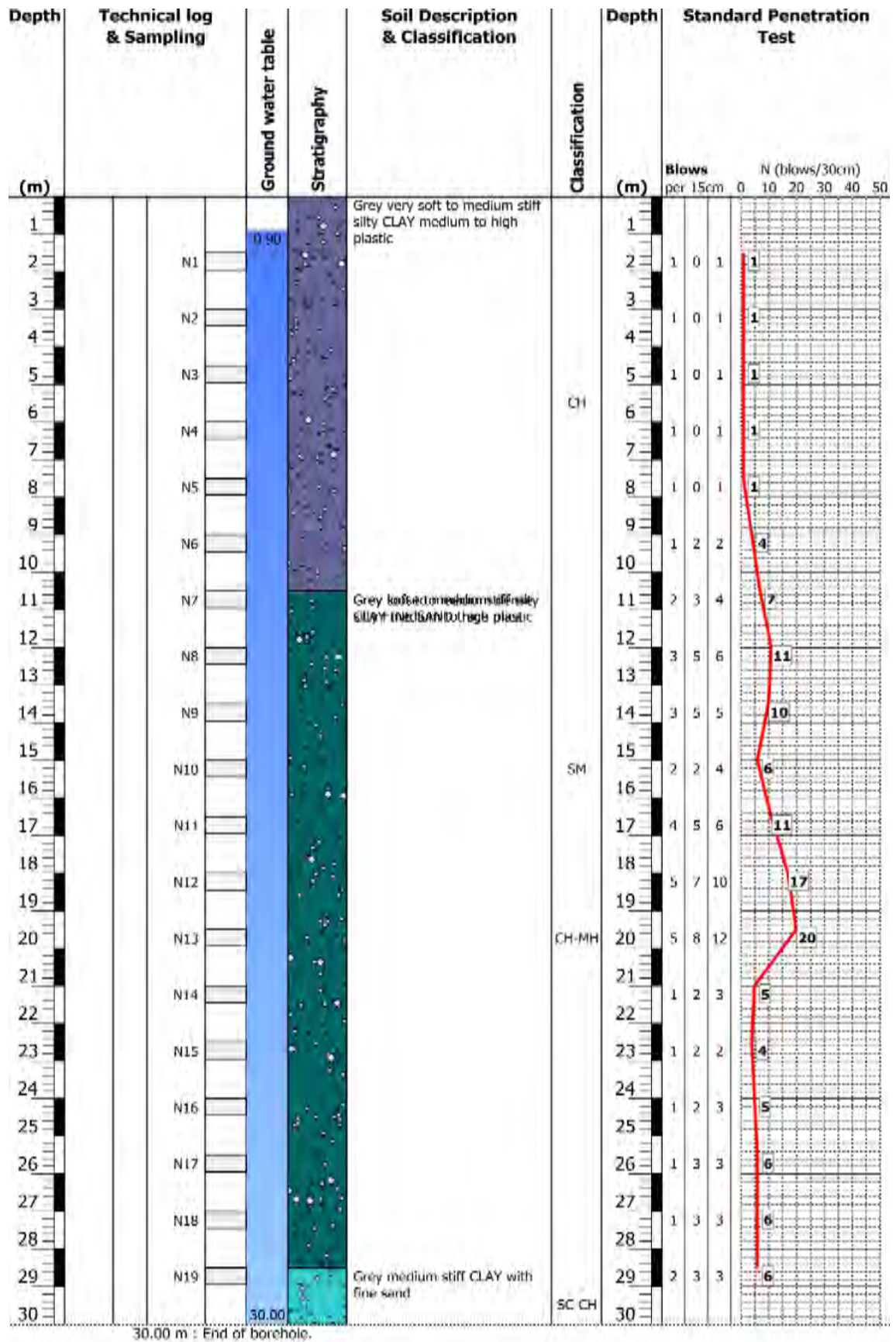


Fig. 3.2 Soil profile of a site in Chittagong

According to the site investigation report, the study area consists of mainly coastal deposits. The groundwater table which may vary with the season was found to be at 0.9m below the ground surface at the time of boring. The soil profile is divided into three sub-layers according to the difference in soil characteristics, physical and mechanical properties. The subsurface consists of a 10.5m layer of soft clay below which there is a 9.5m thick layer of dense silty fine sand. Underneath the silty fine sand is a 10.5m thick layer of stiff silty clay.

A summary of engineering properties of the site in Chittagong are given in Table 3.2

Table 3.2 Engineering properties of the site in Chittagong

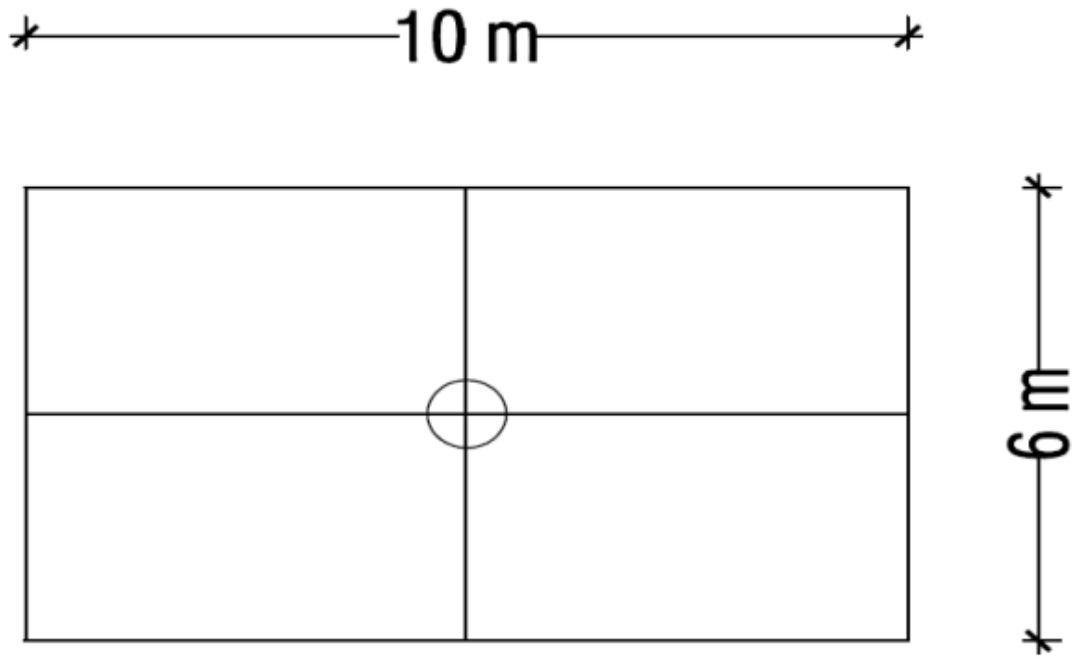
Parameter	Unit	Formation		
		Stiff Silt with little fine sand	Medium dense fine Sand	Very dense fine sand
SPT N		4	20	6
Unit weight	kN/m ³	17	20	17
Dry unit weight	kN/m ³	16	17	15
Cohesion, c'	kPa	5	0	1
Angle of friction, ϕ	Degree	30	34	18
Dilatancy angle, ψ	Degree	0	4	0
Poisson's ratio, ν		0.3	0.3	0.3
Co-efficient of Permeability	m/s	8.58×10^{-6}	5.10×10^{-6}	5.79×10^{-6}
Young Modulus, E	kPa	27500	31000	31000
Secant Modulus, E_{50}	kPa	21000	43000	43000
Oedometer Modulus, E_{oed}	kPa	21000	43000	43000
Unloading reloading Modulus, E_{ur}	kPa	63000	129000	129000

3.3 Parametric studies of an excavation

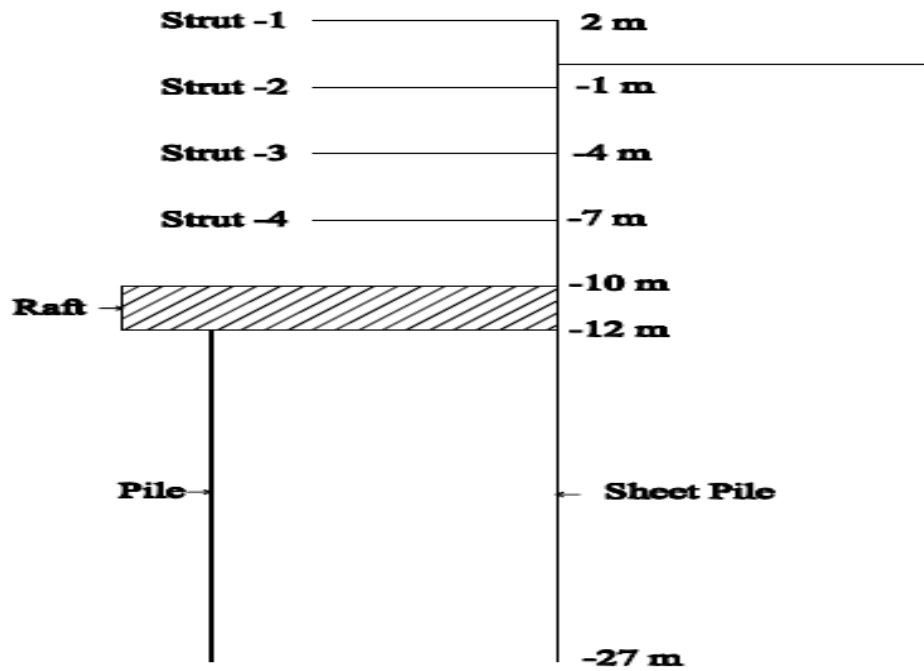
The deep excavation is a very complex soil-structure interaction problem, and its performance is affected by some factors such as the ground condition, the excavation geometry, the excavation depth, the type and stiffness of the retaining system, and the construction method. However, considering all of these features in a single analysis is difficult and cumbersome for practical use in the design and analysis of deep excavations. Also, it is expensive and time-consuming to investigate the influence of these features through complex case history studies. Therefore, it is more reasonable and practical to conduct a series of parametric studies based on one simplified model to understand the influence of several main factors for general purposes. Moreover, the pieces of information obtained in this process are suitable preparations for the more complex case studies. An idealized excavation is adopted in this chapter to conduct the parametric studies. Some useful findings and conclusions are generated for practical applications in the design and construction of deep excavations.

3.3.1 Geometry of the excavation

The idealized excavation, as shown in Fig.3.3, is the simplification of a typical four-level basement excavation (10m x6 m in the plan, 12m deep) using a bottom-up construction method. The excavation is retained by a sheet pile wall (0.370m thick, 24m deep) which is supported by four levels of horizontal wallings and struts and vertical king post. The foundation of the building is 2m thick raft with the combination of vertical piles. The vertical distance between each basement is 3m. A six-storied adjacent building has been considered in one side of the building, and the total load of the building is calculated to be approximately 86 kN/ m².



Plan



Section

Fig. 3.3 Plan and section view of a four level excavation system

3.3.2 Construction sequence

The construction sequence follows a typical bottom-up construction method which is widely adopted all over the world due to the relatively small wall deflection and ground movement induced by the excavation. The main activities of construction are summarized in the Table 3.3.

Table 3.3 Construction sequence

Step	Description
1	Install the sheet pile wall and king post
2	Excavate soil at 0m
3	Install the first level walling and struts at 2m
4	Excavate soil at -3m
5	Install the second level walling and struts at -1m
6	Excavate soil at -6m
7	Install the third level walling and struts at -4m
8	Excavate soil at -8m
9	Install the fourth level walling and struts at -7m
10	Excavate soil at -12m
11	Install the piles and construct the raft portion of the foundation

3.3.3 Finite element model

The finite element model considers the critical structural components in the braced excavation and follows closely the bottom-up construction sequence. The mesh for the model is shown in Fig.3.4. The sheet pile wall is modeled as a plate element, while the horizontal struts, wallings, and vertical king post are modeled as beam elements. Piles attached with raft portion of the foundation is modeled as embedded elements. It is to be noted that the piles are embedded into the soil without any interface properties and that's why they are modeled as an embedded element. A positive and negative interface has been considered around the sheet pile wall in order to reduce soil-structure interaction

problems. A large family of element types (e.g. linear and quadratic elements, with full or reduced integration) is available in PLAXIS 3D, but they may have the difference in terms of the accuracy and efficiency in the computation. The difference is compared through parametric studies. Influence of different types of meshing and influence of stiffness is analyzed through some case studies. The influence of the soil-structure interface properties is also investigated in the parametric analysis.

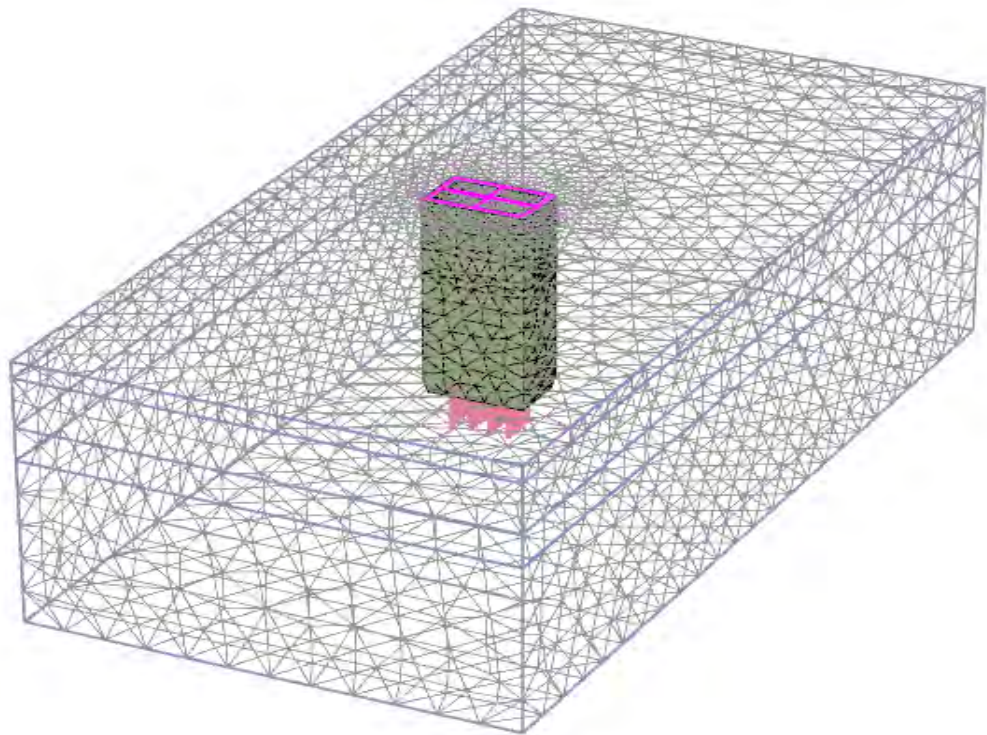


Fig. 3.4 Meshing of the model

3.3.4 Material Models and input parameters

Throughout the analyses, the soil is represented by the Mohr-coulomb model to consider the small-strain stiffness nonlinearity of the soil, associated with the input parameters attached in the following table. The structural components (i.e., the king post, piles, and raft) are assumed to be reinforced concrete materials and behave linearly elastic for simplicity. The water table is considered to be at the ground surface. The coefficient of

earth pressure at rest is assumed to be 0.5. All the analyses are conducted in undrained conditions.

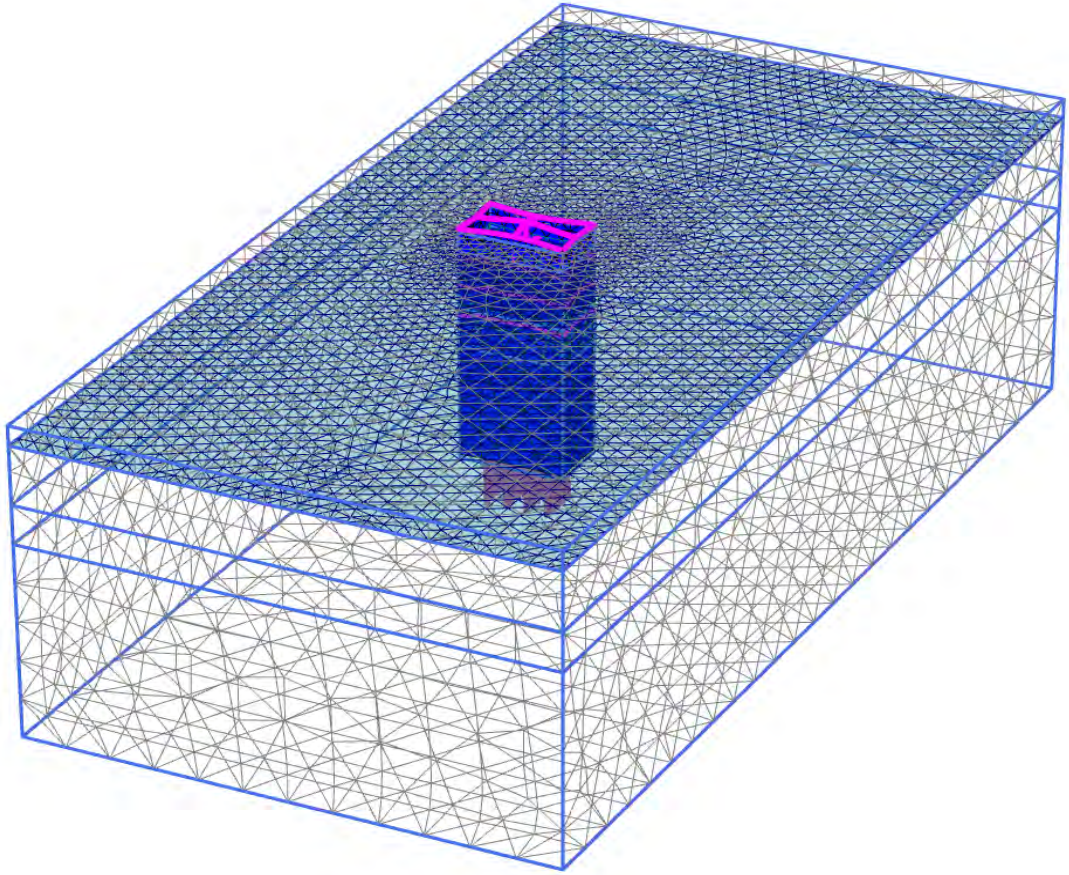
3.4 Influence of meshing in the output result

Mesh generation is the practice of generating a mesh that approximates a geometric domain. Meshing is a collective term to denote the pre-processing phase of the Finite Element Analysis (FEA). It is a tool that engineers use to complete their analysis of a particular design. In this parametric study, we have calculated the same model using four types of meshing namely very course meshing, course meshing, medium meshing, and fine meshing. We used 0.25 as a coarseness factor for all kinds of meshing. It is noticeable that the finer the meshing system, the more time has been required for the computation. The number of nodes generated for each type of meshing is shown in Table 3.5.

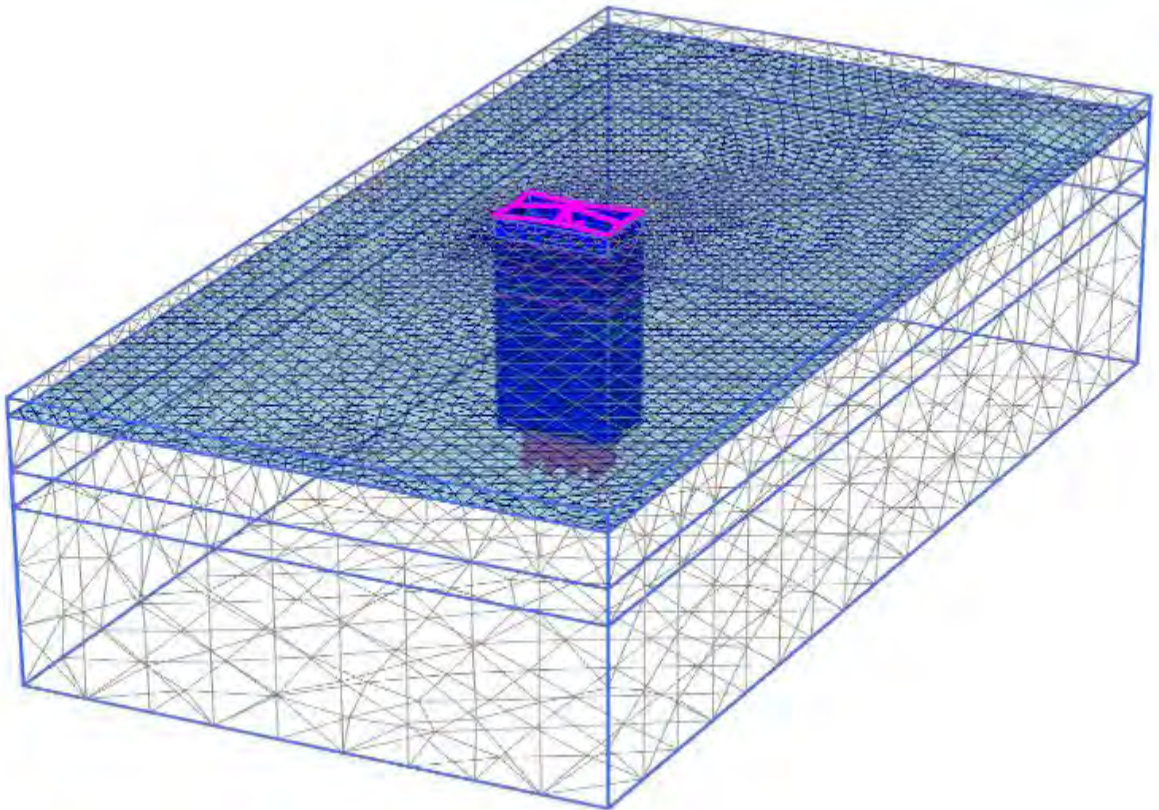
Table 3.5 Generated nodes for different type of meshing

Types of meshing	Number of nodes
Very course meshing	31778
Course meshing	32906
Medium meshing	64118
Fine meshing	132327

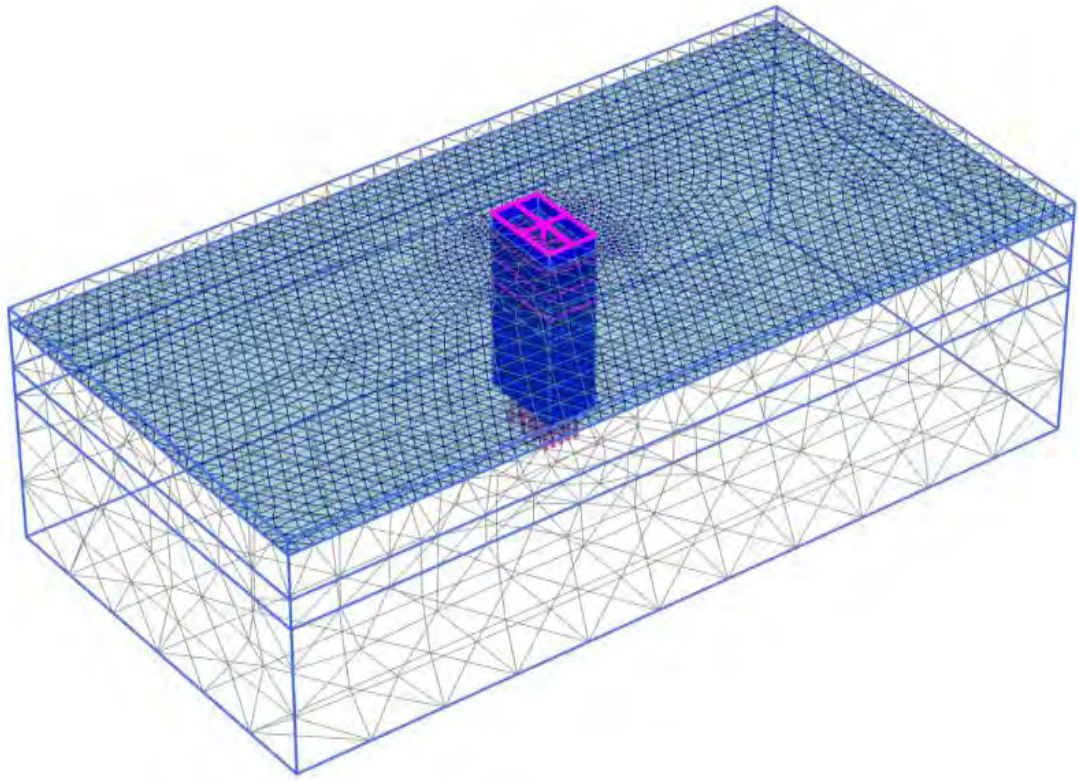
The deformed mesh of all types of meshing is also shown in Fig. 3.5



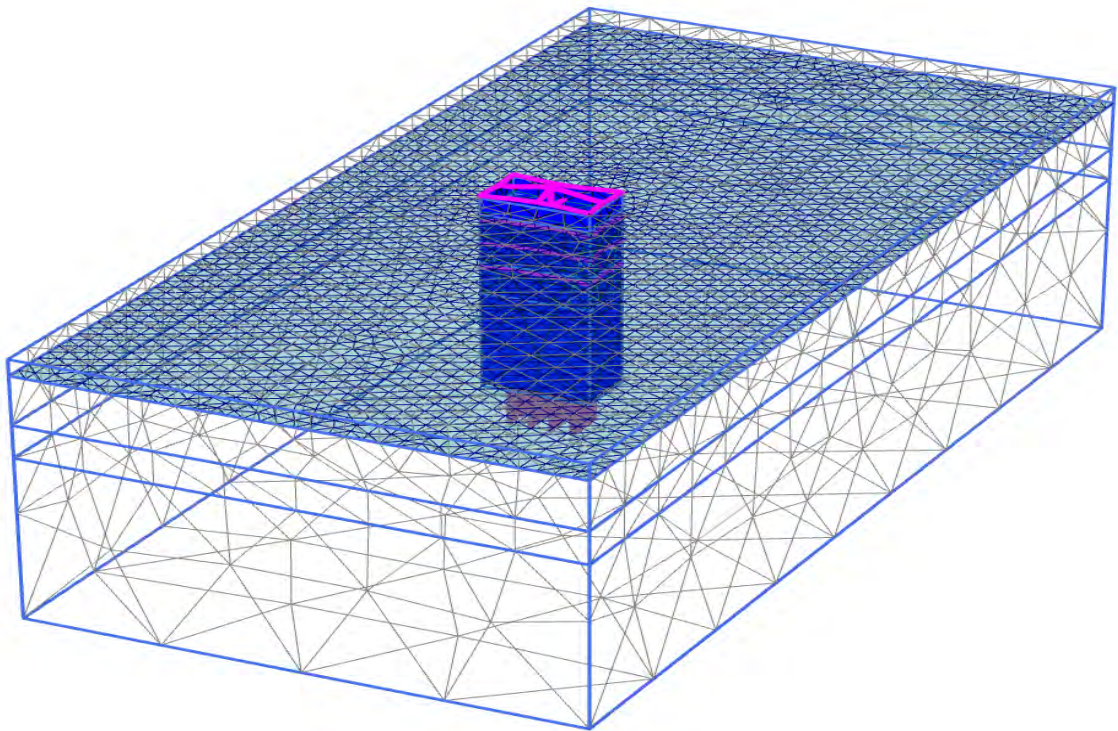
(a)



(b)



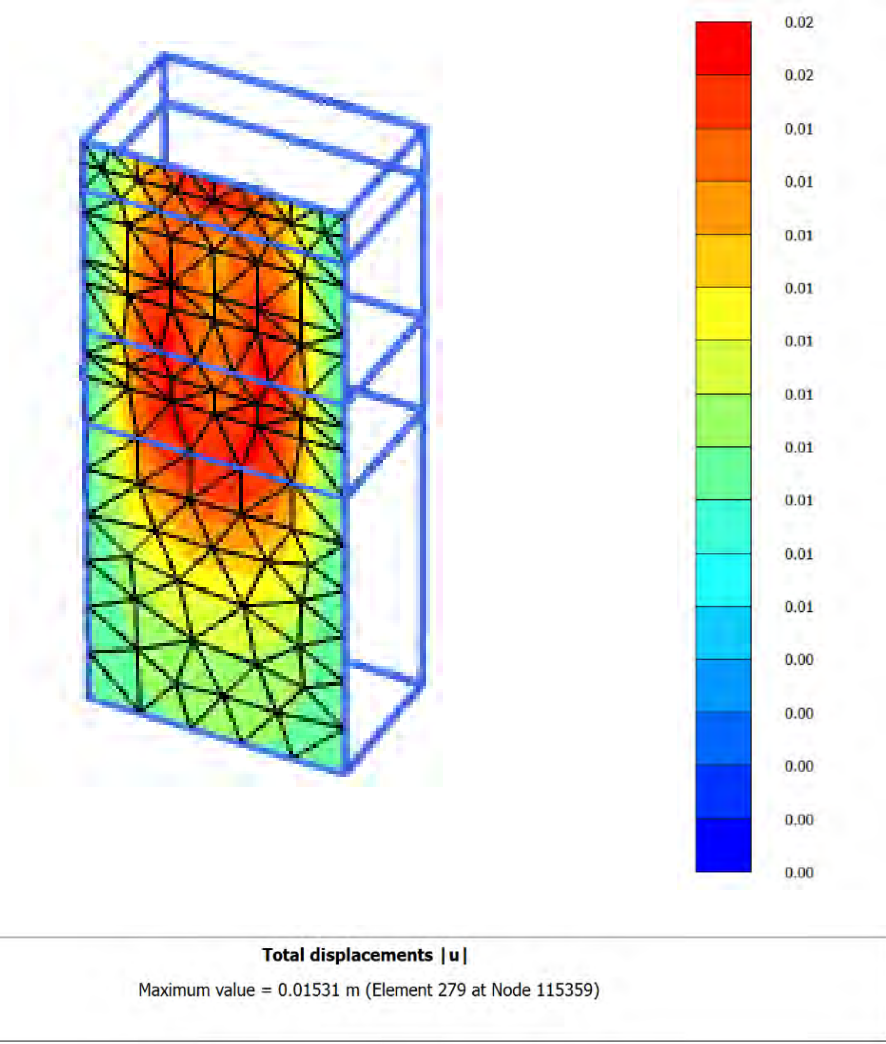
(c)



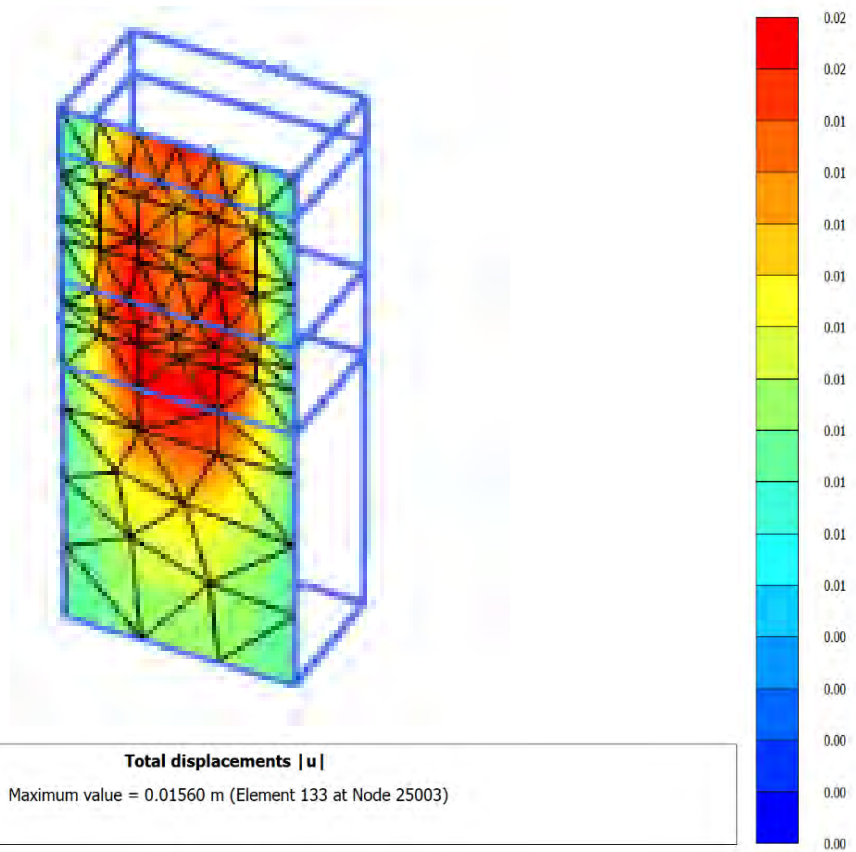
(d)

Fig. 3.5 Deformed meshing of a) Fine meshing b) Medium meshing c) course meshing and d) very course meshing

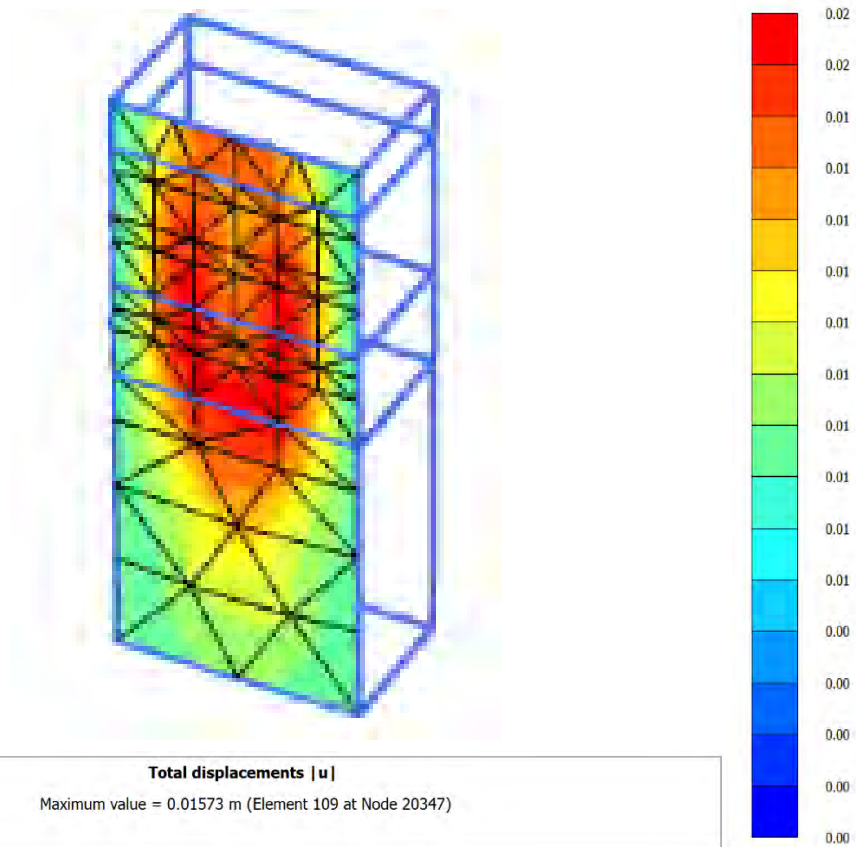
It has been observed from the computed output result that total maximum displacement of sheet pile wall occurs in the long side of the sheet pile wall. The total maximum displacement of sheet pile is shown in Fig. 3.6 for different types of meshing.



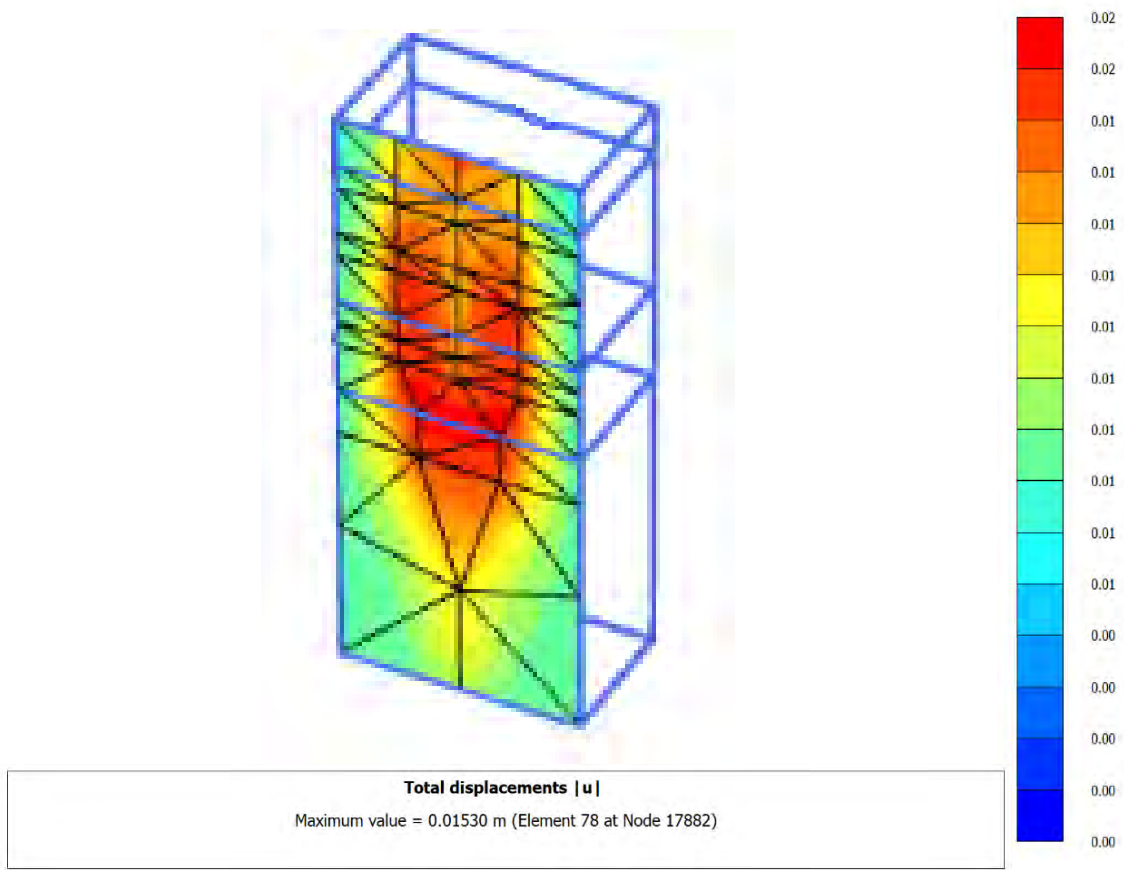
(a)



(b)



(c)



(d)

Fig. 3.6 Total displacement of sheet pile in long side for a) fine meshing b) medium meshing c) coarse meshing d) very course meshing.

The computed result for the wall deflection at the long side of the wall center is shown in Fig. 3.7.

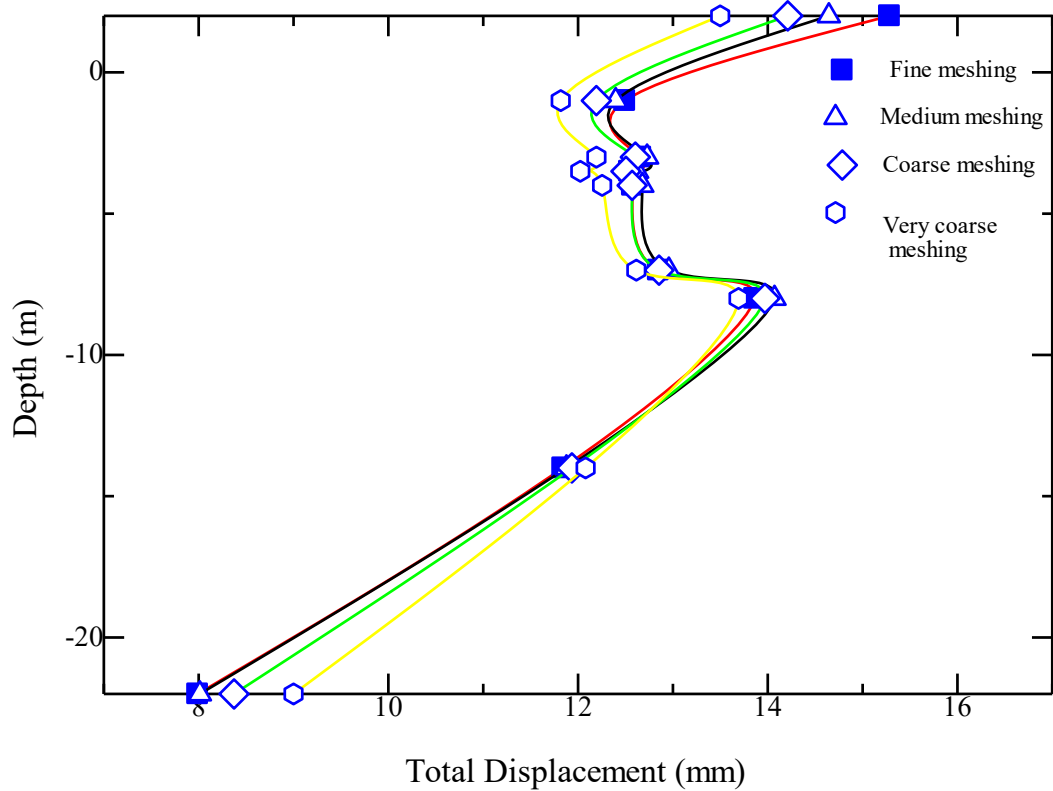


Fig. 3.7 Wall deflection at center in the long side for different meshing

It is observed from the above-plotted graph that the output results are close to each other. So, it can be said that the variation of different types of meshing in the output results is quite insignificant. As the differences between different kinds of meshing are of little importance in this study coarse meshing has been chosen for modeling the site in Dhaka and Chittagong.

3.5 Influence of soil-structure contact and interface properties

The contact between the soil and structures is a critical problem in geotechnical engineering. In deep excavations, there are large areas of interface between the soil and structures (e.g., the soil/wall interface and the soil/pile interface), and the interface properties may affect the excavation behavior. It is difficult to investigate their influence through in-situ tests or laboratory experiments but is straightforward through numerical analyses. In PLAXIS 3D the impact of the interface has been utilized by using interface factor (R_{int}) which is taken as the ratio of wall friction to the friction of soil. The interface

elements take the mechanical property from the nearby soil cluster after reducing all the parameters by an interface factor. The value of interface factor ranges from 0.1 to 0.9. The influence of the value of interface factor has been analyzed through parametric studies.

Three analyses were conducted to investigate the influence of soil/wall interface properties on the excavation behavior, and to understand what is the difference if the contact is not considered and how sensitive is the result to the value of interface factor. The three values of (0.1, 0.5, and 0.9) have been selected to represent three possible contact conditions. The result of the total displacement at the long side of the sheet pile wall considering three interface factors is shown in Fig. 3.8.

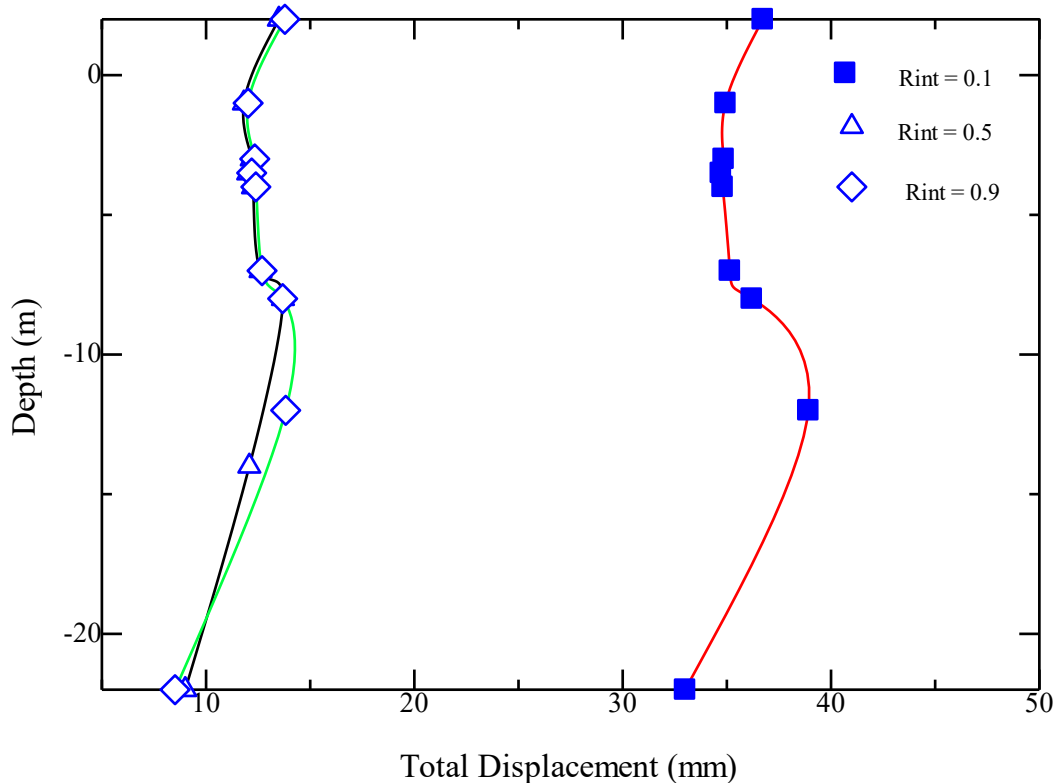


Fig. 3.8 Wall deflection at center in the long side of sheet pile wall for different interface factor

It is observed from the output result in case of lower interface factor value (0.1) the value of maximum displacement is almost 2.5 times higher than the result considering interface factor 0.5 and 0.9. Reducing the interface factor value will cause more massive deflection in the retaining system. So, in this study, we will use 0.7 as interface factor.

3.6 Influence of failure factor on wall deformation

Failure factor (R_f) is the ratio between ultimate deviator stresses at the failure by asymptotic value of the shear strength. When both the value of deviator stress at failure and asymptotic value of shear strength becomes equal, it denotes that failure criterion is satisfied and perfectly plastic yielding occurs. We have analyzed three conditions for the parametric study by considering three failure factors (R_f) such as 0.5, 1 and 1.5. These three value indicates before reaching yielding state, at the yielding point and beyond yielding condition respectively. The influence of R_f on the idealized excavation, however, seems to be minimum. The output result is shown in Fig. 3.9.

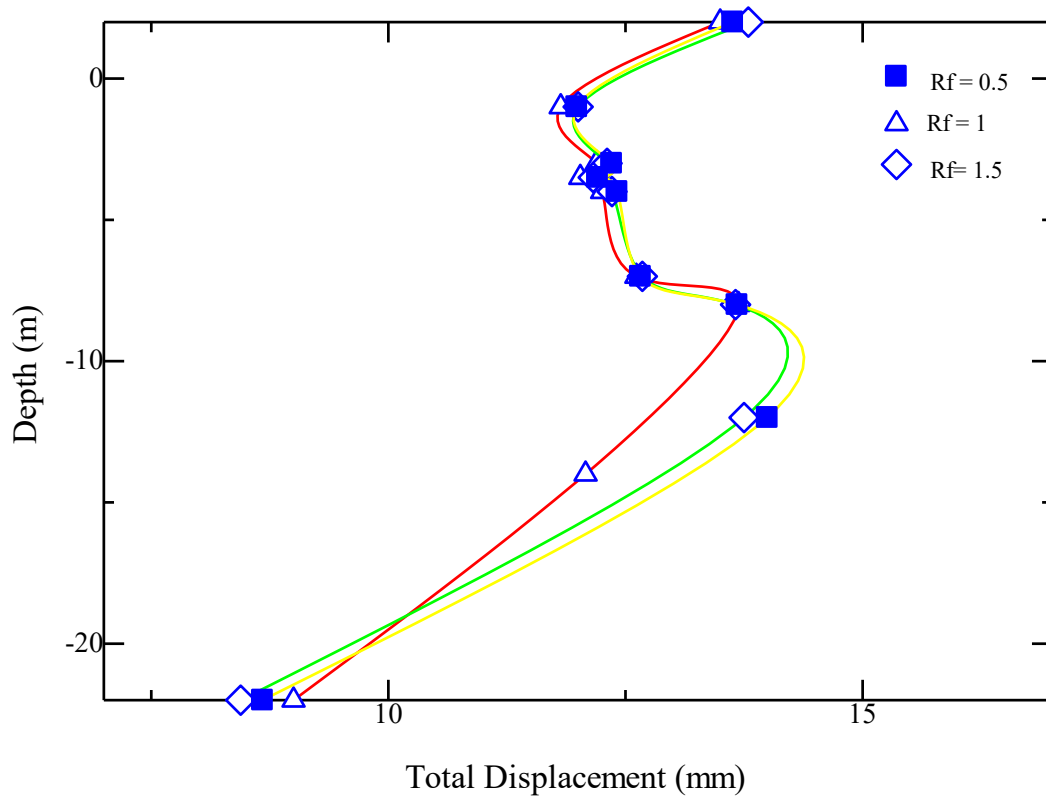


Fig. 3.9 Wall deflection at the long side of sheet pile wall for different failure factor

Standard value of failure factor recommended by PLAXIS 3D manual is 0.9. In this study value of failure factor will be considered 0.9.

3.7 PLAXIS 3D model versus field instrumentation data

In this study, validation of the model has been done by taking field instrumentation data of the construction of a pier in the 2nd bridge over the Gumti River. Vibrating wire strain gauge has been used in the investigation of lateral movement of soil supported by sheet pile wall with eight horizontal struts. The struts were installed at the corners of two different levels. The forces in all the eight struts were estimated from frequency reading taken every five seconds over six months. Various patterns of strut force variation and lateral soil movement were observed with time and the ambient temperature. The variation of strut forces at a given level demonstrates the importance of continuous monitoring of excavation using such advanced technology. A model of the bridge pier has been done using PLAXIS 3D. The cross-section of the bridge pier is shown in Fig. 3.10.

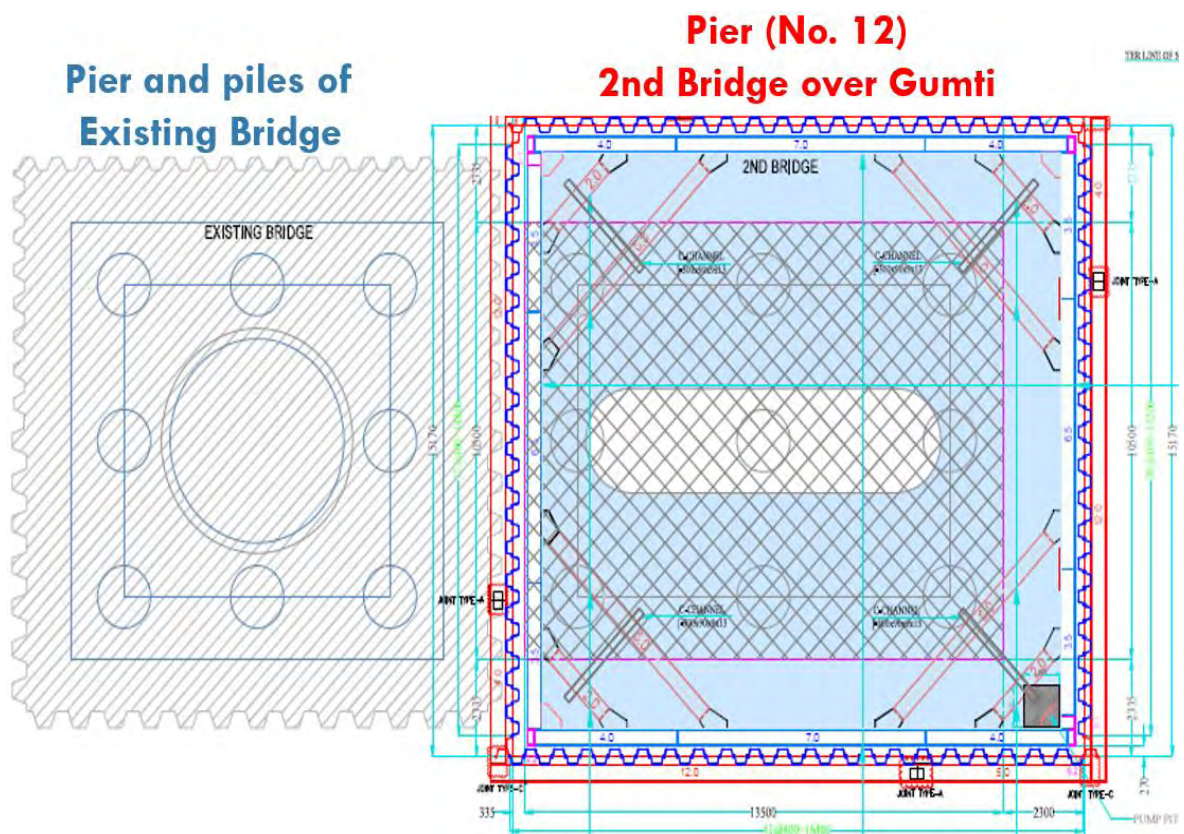


Fig. 3.10 Cross-section of bridge pier (No 12)

An actual footage during the construction work is shown in Fig. 3.11



Fig. 3.11 Actual footage during construction work

In total eight horizontal struts have been used in the pier to support the sheet pile wall. They were arranged in two levels each having four struts. Forces acting on the upper-level struts were mainly due to the water pressure, flow and tides whereas forces on the lower level strut were due to soil pressure working on them. A glimpse of the arrangement of struts is shown in Fig. 3.12.



Fig. 3.12 Arrangement of struts in two levels

The cross-sectional area of each strut is 197.70 cm^2 , and weight is 200kg/m . H-40 model is used for the strut. Field instrumentation has been done using strain gauge, vibrating wire cable, channel relay multiplexer, data logger and 12 V power supply with a regulator. Field instrumentation of a strut with a strain gauge is shown in Fig. 3.13.

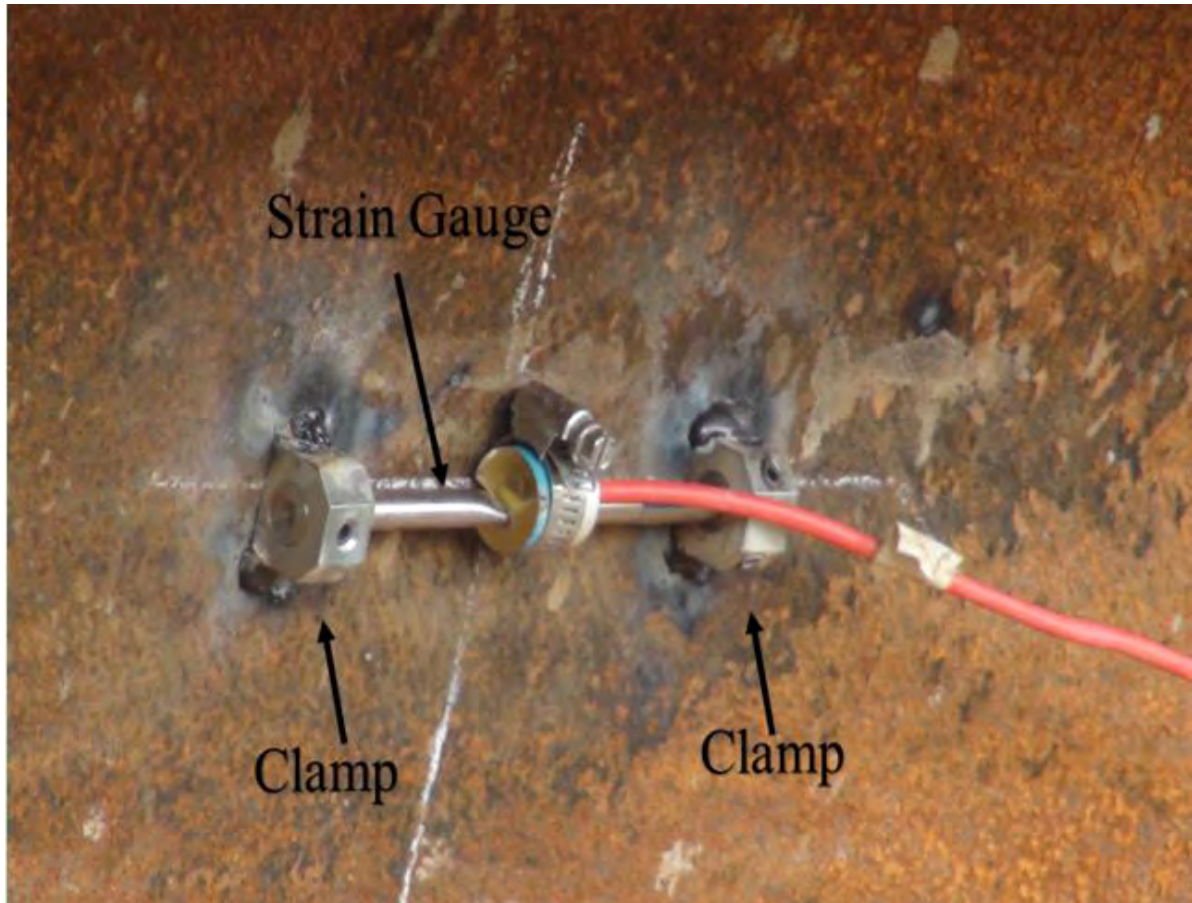


Fig. 3.13 Field instrumentation of a strut by strain gauge

In this study, finite element model of the pier was created by using PLAXIS 3D. The pier was 16.135 x 15.170m in plan. Sheet pile wall was used as a retaining structure which was supported by eight horizontal struts. The total depth of the penetrated sheet pile was 20m. Struts were placed in two levels and firmly attached with the walling. The first level of struts was set 1m below the water level and the second level of struts was placed 6m below the water level. The upper 10m of the sheet pile was continuously prevented the lateral water pressure, and lower 10m of the sheet pile was used to retain the lateral soil movement. The river bed mainly consists of fine silty sand. Mohr-Coulomb model was used to model the soil. The soil properties used in the model is shown in Table 3.6, and the features of structural components are shown in Table 3.7.

Table 3.6 Properties of soil

Properties	Unit	Value
Unsaturated Unit Weight (γ_{unsat})	kN/m ³	15
Saturated Unit Weight (γ_{sat})	kN/m ³	19
Modulus of elasticity (E)	kN/m ²	10000
Poison's ratio (ν)		0.3
Cohesion (c)	kN/m ²	1
Angle of friction (ϕ)	Degree	30

Table 3.7 Properties of structural components

Properties	Unit	Sheet pile wall	Strut	Walling
Area	m ²	-	0.0197	8.682
Thickness	m	0.335	-	-
Unit Weight	kN/m ³	2.550	78.50	78.50

The meshing of the model is done by using coarse meshing and coarseness factor as 0.25. Deformed mesh of the model is shown in Fig. 3.14.

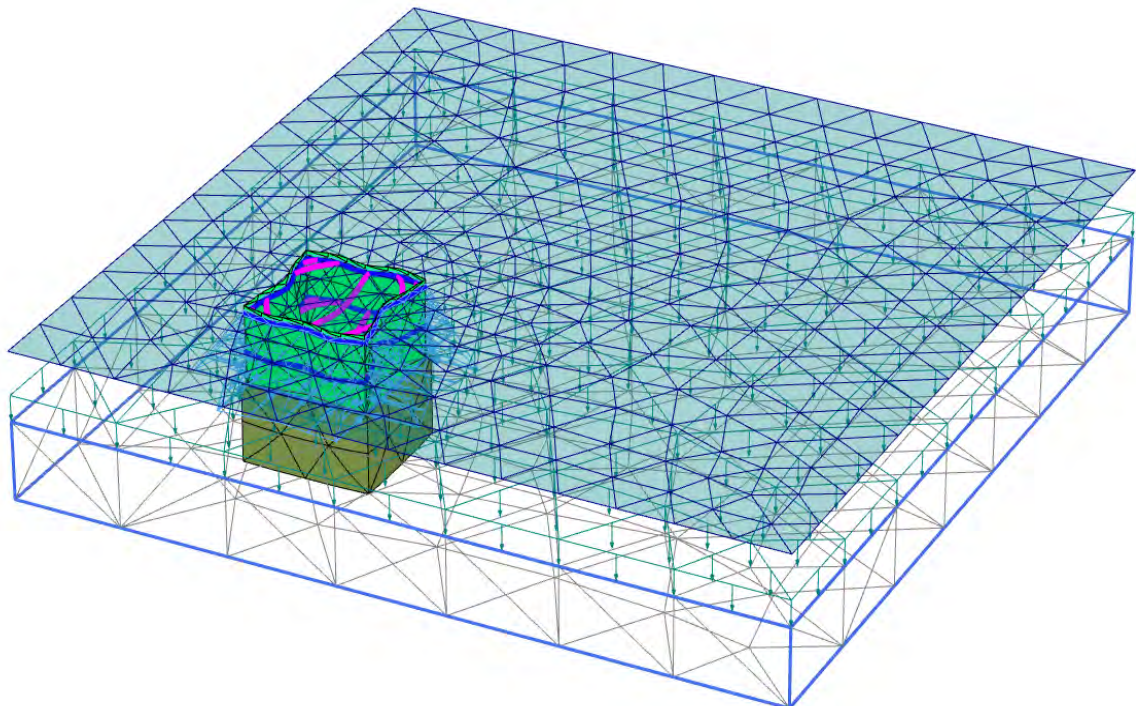


Fig. 3.14 Deformed mesh of the model

The calculation was done using staged construction strategy. Firstly the sheet pile was installed followed by the installation of the first level of struts installation. Finally, the second level of struts was installed. The output results of the axial force acting on the struts are shown in Fig. 3.15.

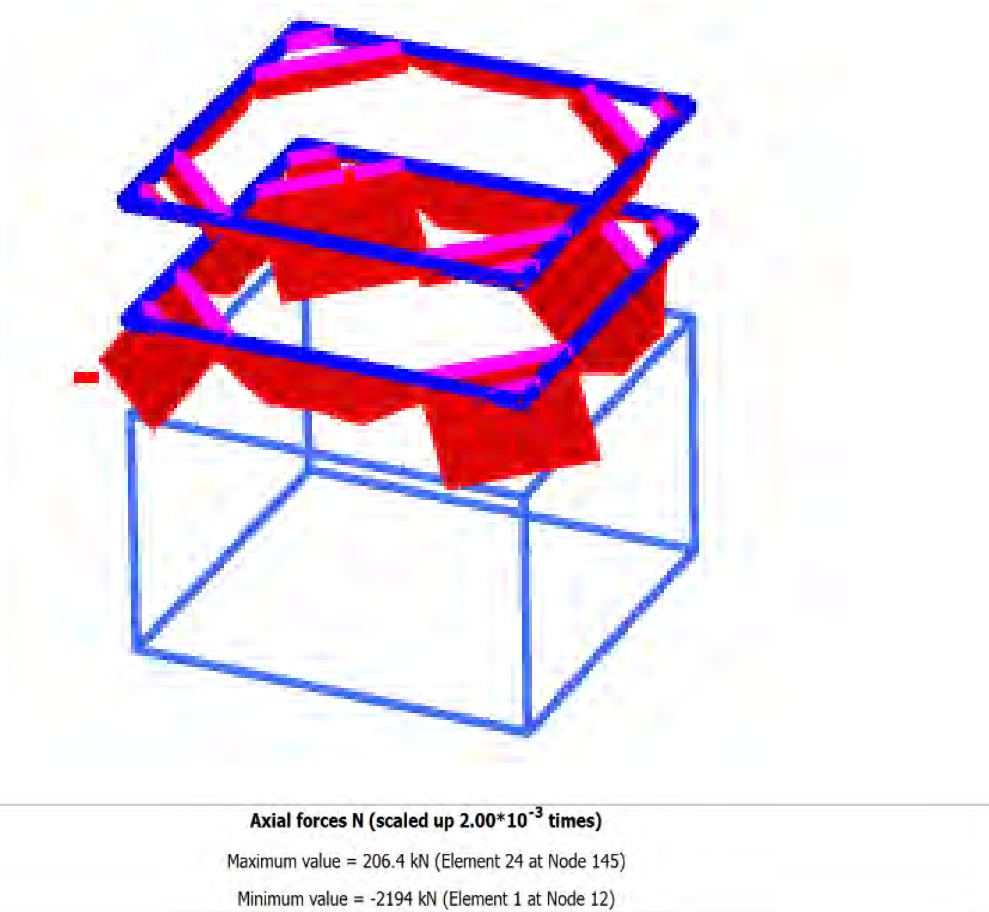


Fig. 3.15 Axial forces acting on the struts

The field data obtained from the strain gauge reading installed in the struts is shown in Fig. 3.16.

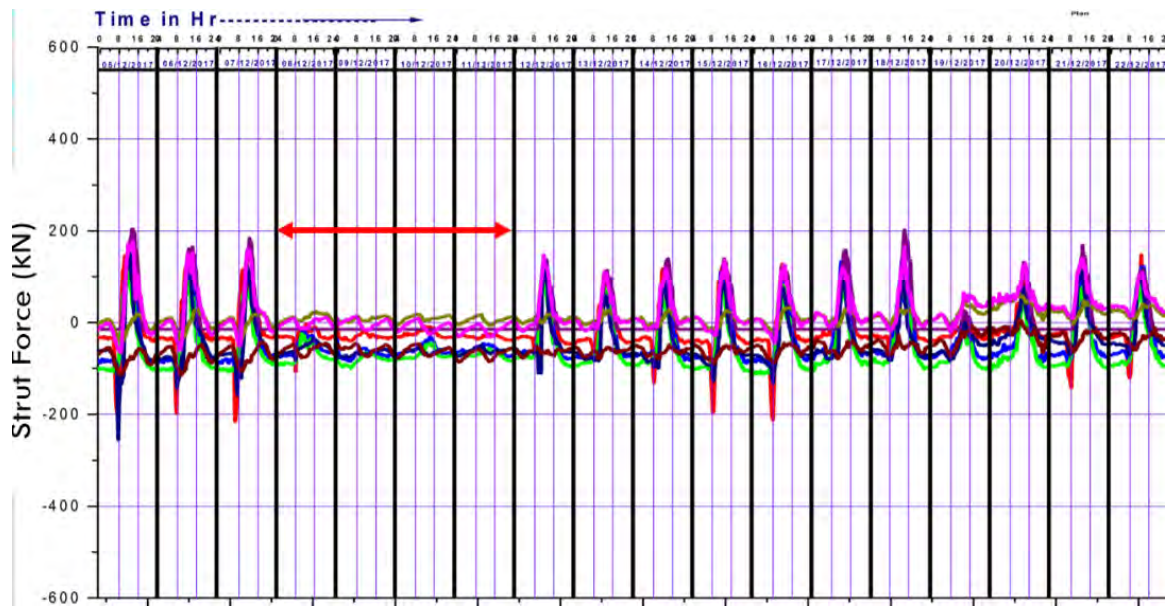


Fig. 3.16 Field instrumented data obtained for strut force (kN)

It has been observed from the field instrumented data for strut force is that maximum force acting on the strut is approximately 202 kN whereas maximum force obtained for strut force using PLAXIS 3D is 206 kN. The difference between the results is around 2%. In this particular case, it may be concluded that the model is validated.

3.8 PLAXIS 3D model versus data from the available literature

In this study, a validation of the model is done by following a case study of Siam Motor Machine Building in Bangkok which was conducted by Chhunla Chheng and Suched Likitlersuang (2017). The underground excavation depth was about 7.2 m below ground and the excavation area was a rectangle with 58.7 m long and 32.8 m wide as shown in Fig. 3.17. Two inclinometers installed at long and short sides of the sheet pile wall to monitor the field data.

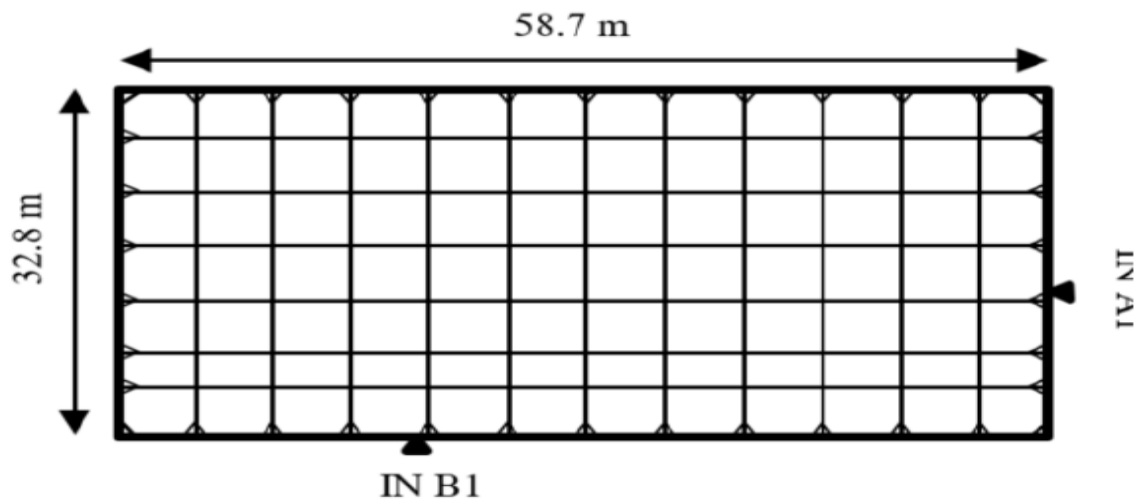


Fig. 3.17 Layout of Siam Machine Motor Building (Chhunla Chheng and Suched Likitlersuang, 2017)

According to the geology of the project area, the soil layers are generally divided into 7 different layers including Made Ground (MG), Bangkok Soft Clay (BSC), Medium Clay (MC), First Stiff Clay (1st SC), Clayey Sand (CS), Second Stiff Clay (2nd SC) and Hard Clay (HC). The constitutive modeling for soils used in this study was Hardening soil model (HSM) which is an advanced soil model for describing both soft and stiff soils. Different soil parameters used to model the soil is shown in Table 3.8 and the parameters used to model the structural components are shown in Table 3.9.

Table 3.8 Soil parameters used to model the soil (Chhunla Chheng and Suched Likitlersuang, 2017)

Parameters	Unit	Soil Type			
		Made Ground (MG)	Bangkok Soft Clay (BSC)	First Stiff Clay (1 st SC)	Clayey Sand (CS)
Unit Weight (γ)	kN/m ³	18	16.5	19.5	19
Cohesion, c'	kPa	1	1	25	1
Angle of friction, ϕ	Degree	25	23	26	27
Dilatancy angle, ψ	Degree	0	0	0	0
Secant Modulus, E_{50}	MPa	45.6	0.8	8.5	38
Oedometer Modulus, E_{oed}	MPa	45.6	0.85	9	38
Unloading-reloading modulus, E_{ur}	MPa	136.8	8	30	115
Poisson's ratio for unloading and reloading, ν_{ur}		0.2	0.2	0.2	0.2
Power, m		1	1	1	0.5
K_o value for normally consolidated soil, K_{onc}		0.58	0.7	0.5	0.55
Failure ratio, R_f		0.9	0.9	0.9	0.9
Interface factor, R_{int}		0.7	0.7	0.7	0.7

Table 3.9 Parameters used to model the structural component (Chhunla Chheng and Suched Likitlersuang, 2017)

Parameters	Unit	Sheet pile wall	Steel struts	Steel wallings
Area	m ²	-	0.012	0.029
Thickness	m	0.17	-	-
Unit Weight	kN/m ³	4.48	78.5	78.5
Modulus of Elasticity	kPa	-	200x10 ⁶	200x10 ⁶

Moreover, 10 kN/m² and 5kN/m² surcharge has been applied in the long side and short side of the excavation zone respectively. Coarse mesh setting was used to mesh the model, and 0.25 was used as a coarseness factor. Meshing Connectivity plot of the excavation zone is shown in Fig. 3.18.

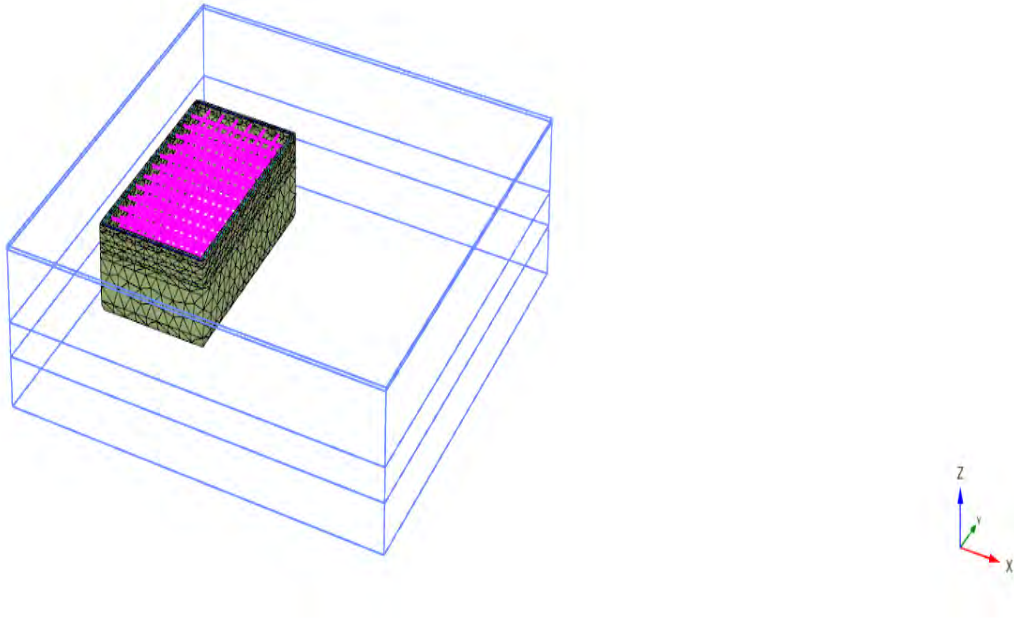


Fig. 3.18 Connectivity plot of the excavation zone.

Calculation was done by maintaining the staged construction procedure. The construction sequences are shown in Table 3.10.

Table 3.10 Construction Sequences

Stage	Construction Activities
1	Placement of Sheet pile wall and excavation to -1.50m
2	Installation of 1st level struts and wailings and excavation to -3.90 m
3	Installation of 2nd level struts and wailings and excavation to -5.80 m
4	Installation of 3rd level struts and wailings and excavation to -7.20 m

The output result of the displacement of the model is shown in Fig. 3.19.

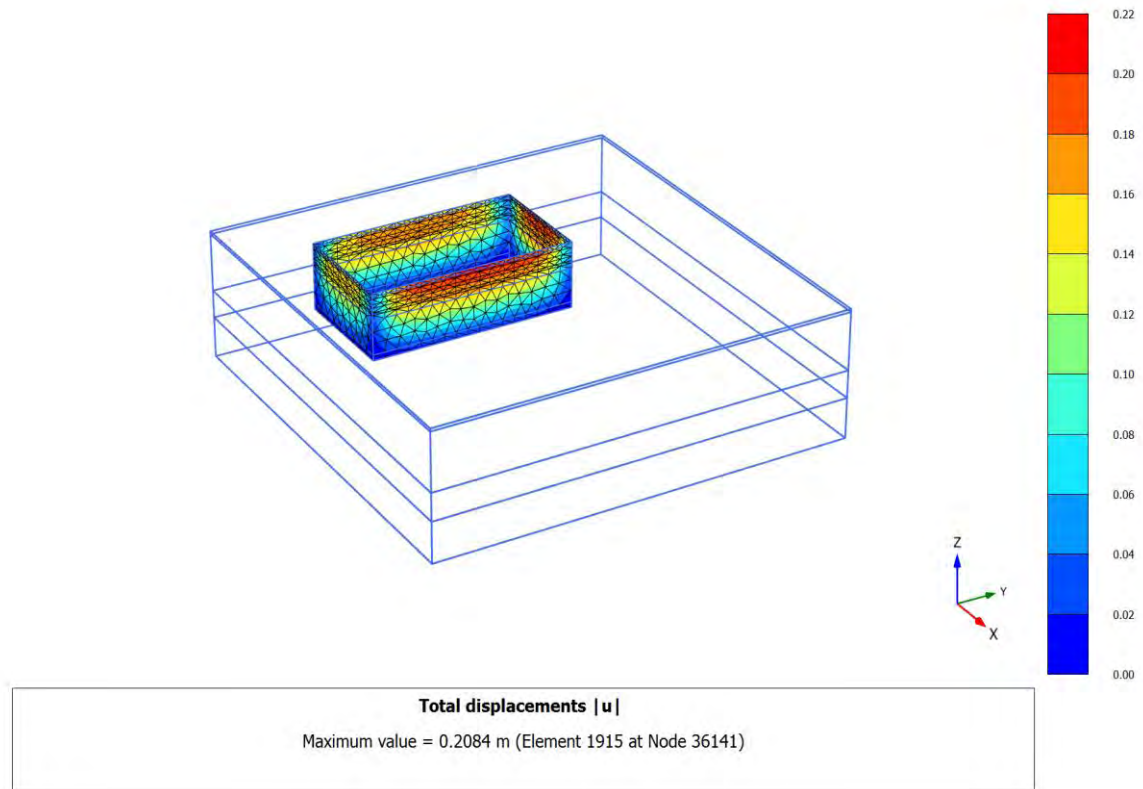


Fig. 3.19 Displacement of the Sheet pile wall

It is observed that maximum displacement occurs in the short side of the sheet pile wall where B1 inclinometer was used to measure the reading of displacement. The data for the displacement of the short side of the sheet pile wall obtained from the study of Chhunla Chheng and Suched Likitlersuang (2017) was 216mm and the same data appeared in the inclinometer was 222mm. In this study, the value obtained for the displacement of the same side of the sheet pile was 208.4mm. The discrepancy between the performed analysis with the review of Chhunla Chheng and Suched Likitlersuang is around 3.5% whereas the difference is about 6% with the inclinometer data. As the differences are within 10%, so it is recommended that the model is validated for this case.

3.9 Summary

The parametric studies in this chapter are intended to investigate the influence of several essential features in the modeling procedure of deep excavations. There may be several ambiguous questions before conducting the analysis, for example,

- (a) What kinds of features are needed to take into account in the analysis?
- (b) How significant is the influence of a certain type of features?
- (c) What is the difference if a particular feature is neglected?
- (d) Is it possible to consider all of the features in one analysis?
- (e) Which approach is recommended for practical use?

However, following the step-by-step detailed analyses, these questions are addressed appropriately. Some general conclusions are summarized below:

- Before the analysis, enough information should be collected for the modeling process, e.g., the geometry of the excavation, details of the retaining structures, construction sequences, and reliable material properties for both the soil and structures. Adequate constitutive models for the soil, structural components, and the soil/structure interface are required.
- Elements with reasonably coarser mesh in the analysis produce similar patterns in the computed deformations compared with corresponding elements with a finer mesh and take much less time to run. In the following part of the study to reduce calculation time for the complex model coarse meshing has been used.
- The soil-structure interface behavior is often neglected in the numerical analyses due to its complexity, but it is shown to have a significant influence on the excavation behavior in the parametric studies. Therefore, the soil-structure interface behavior needs to be considered appropriately in the analyses, and the interface properties need to be carefully selected. A reasonable interface factor has been studied in the following part of the study to incorporate soil-structure interface problem.
- To establish a validation is a must. In this study, two validations have been carried out one with field instrumentation data and another one with available literature.

CHAPTER 4

NUMERICAL MODELING

4.1 Introduction

This chapter will present the numerical modeling and derivation of geotechnical parameters for numerical analysis for commonly used finite element codes PLAXIS 3D. As described in Section 2.5, PLAXIS 3D has been chosen for the research study because it is mainly developed for excavation design, because of its popularity amongst practicing engineers, and because over the years a wealth of knowledge and experience available for reference has been accumulated.

In the following sections, the original base design using the Mohr-Coulomb (MC) model together with the design assumptions and modeling approach using idealization of various structural components of the retaining system will be reported. This is then followed by using advanced Hardening Soil (HS) model. Derivation of geotechnical parameters for the HS model based on available soil test results is also presented.

4.2 PLAXIS 3D Modeling

The following section describes modeling and design assumptions made for the numerical analysis. Soils were modeled by 10-noded elements. Undrained Method A was adopted for MC model and Undrained method D was adopted for HS model. Undrained behavior was chosen for low permeability cohesive soils. Initial groundwater was assumed to be 50 meters below the existing ground surface for the site in Dhaka and 0.9 meters below for the site in Chittagong and at excavation level during the progress of excavation in the Chittagong site. The pore pressure of soils below the excavation level was based on cluster interpolation. Reduced shear resistance was assumed with a standard reduction factor of 0.7 for steel sheet pile wall, contiguous pile wall and all soil interfaces and 0.5 for basement slab respectively.

The sheet pile wall was modeled as a plate element. Both the negative and positive interface was considered around the sheet pile wall to incorporate soil-structure interaction. The contiguous pile wall modeled as an embedded beam element. The

interaction between the pile and the surrounding soil at the pile shaft is described employing embedded interface elements. There is no need for mesh refinement around piles as the 3D mesh is not distorted by introducing embedded elements which make embedded piles very efficient and time-saving especially when a large group of piles is modeled (Engin and Brinkgreve 2009).

The internal strut, walling, king post, and raft foundation was modeled as beam element whereas bored piles were modeled as embedded beam. Piled-raft foundation system was considered as the type of foundation.

For advanced HS model, similar assumptions were used so that a direct comparison of performance could be made. Additional geotechnical parameters required for the input were added to those used in the MC model.

4.3 Derivation of soil stiffness parameters

Field test precisely consisting of standard penetration Test (SPT) which was conducted at the study area in Dhaka and Chittagong sites. Laboratory tests were conducted to determine the index properties and strength properties of Dhaka soil and Chittagong soil.

4.3.1 Derivation of soil parameters from field test

Field investigations have been performed in the form of SPT at all selected sites. Wash boring technique has been used for SPT. Disturbed samples were collected, and SPT N-value were recorded at every 1.5 m depth interval up to 39m in case of Dhaka site and 30m from existing ground level (EGL) in case of Chittagong site. The test procedure is described in ASTM D 1586 (ASTM, 1989).

4.3.2 Derivation of soil parameters from laboratory test

Disturbed and undisturbed samples were collected during SPT tests. Collected samples were tested in the Geotechnical Engineering Laboratory of Bangladesh University of Engineering and Technology (BUET). The tests were conducted according to ASTM

standards. Index and strength properties were determined to evaluate the sub-soil condition of the study area.

4.3.2.1 Tri-axial test

The test method covers the determination of strength and stress-strain relationships of a cylindrical specimen of an undisturbed or remolded saturated cohesive soil. Samples are isotropically consolidated and sheared in compression without drainage at a constant rate of axial deformation. For this research consolidated undrained test at two different effective stress were conducted for both the soil of Dhaka and Chittagong site according to ASTM D 4767 04. Experiments were carried out at undisturbed samples for both Dhaka and Chittagong sites. 50 kPa and 100 kPa effective confining stress were applied for both sites. The test was continued till failure or 20% axial strain of the specimen whichever occurred first. The results and graphs obtained from this test are shown in Appendix A.

4.4 Design Parameters

4.4.1 Introduction

A summary of input parameters for the Mohr-Coulomb model and Hardening Soil model will be presented in this section.

4.4.1.1 Parameters for Mohr Coulomb (MC) model

A summary of input parameters for Undrained Method B for Dhaka and Chittagong soil is presented in Table 4.1 and Table 4.2. In practice, it is common to assume the undrained modulus of elasticity to vary linearly with undrained shear strength because the undrained shear strength is also expected to vary proportionally with depth. And incremental factor for undrained shear strength is included to reflect this. The effective stiffness E' is derived from the undrained stiffness ratio related to undrained shear strength E_u/S_u using $E_u/E' = 3/2(1+\nu)$ and $\nu = 0.12-0.35$ (Worth and Houlsby 1985). When ν is taken as 0.3, the E_u/E' ratio reduces to 1.11. As for undrained shear strength, and the incremental factor is provided to reflect increases of E' with depth. Drained (ν') and undrained (ν_u) Poisson's ratio follows PLAXIS recommendation and so is the dilation angle ψ .

Table 4.1 A Summary of Input Parameters for MC Model for the site in Dhaka

Properties	Unit	Stiff Silty Clay	Medium Dense Fine Sand	Very Dense Silty Fine Sand
Unsaturated Unit Weight, γ_{unsat}	kN/m ³	18	16	17
Saturated Unit Weight, γ_{sat}	kN/m ³	20	18	20
Modulus of Elasticity, E	kN/m ²	26000	27000	28000
Poisson's ratio, ν		0.3	0.3	0.3
Shear Modulus, G	kN/m ²	10190	10385	10770
Cohesion, c'	kN/m ²	31	0	0
Angle of Friction, ϕ	Degree	14	31	33
Dilation Angle, Ψ	Degree	0	1	3
Interface factor, R_{int}		0.7	0.7	0.7

Table 4.2 A Summary of Input Parameters for MC Model for the site in Chittagong

Properties	Unit	Soft Clay	Medium Dense Fine Sand	Medium Stiff Silty Clay with Fine Sand
Unsaturated Unit Weight, γ_{unsat}	kN/m ³	16	17	15
Saturated Unit Weight, γ_{sat}	kN/m ³	17	20	17
Modulus of Elasticity, E	kN/m ²	27500	31000	31000
Poisson's ratio, ν		0.3	0.3	0.3
Shear Modulus, G	kN/m ²	10577	11924	11924
Cohesion, c'	kN/m ²	5	0	0
Angle of Friction, ϕ	Degree	30	34	31
Dilation Angle, Ψ	Degree	0	4	1
Interface factor, R_{int}		0.7	0.7	0.7

4.4.1.2 Parameters for Hardening Soil (HS) model.

The stiffness parameters for the Dhaka and Chittagong sites were derived from the results of triaxial test and consolidation test. K_{0nc} values were derived as per PLAXIS recommendation using Jacky's formula. Moreover, v_{ur} and R_f are as per PLAXIS recommendations. A summary of the soil parameters for HS model for Dhaka and Chittagong sites is shown in Table 4.3 and Table 4.4 respectively.

Table 4.3 A Summary of Input Parameters for HS Model for the site in Dhaka

Properties	Unit	Stiff Silty Clay	Medium Dense Fine Sand	Very Dense Silty Fine Sand
Unsaturated Unit Weight, γ_{unsat}	kN/m ³	18	16	17
Saturated Unit Weight, γ_{sat}	kN/m ³	20	18	20
Secant Modulus of Elasticity, E_{50}	kN/m ²	35000	43000	35000
Oedometer Modulus of Elasticity, E_{oed}	kN/m ²	33000	22000	35000
Unloading/ Reloading Modulus of Elasticity, E_{ur}	kN/m ²	105000	129000	105000
Poisson's ratio, ν		0.3	0.3	0.3
Cohesion, c'	kN/m ²	31	0	0
Angle of Friction, ϕ	Degree	14	31	33
Dilation Angle, Ψ	Degree	0	1	3
Unloading Reloading Poisson's Ratio, ν_{ur}		0.2	0.2	0.3
K_0 value for normally consolidated soil, K_{0nc}		0.640	0.4408	0.4554
Interface factor, R_{int}		0.7	0.7	0.7

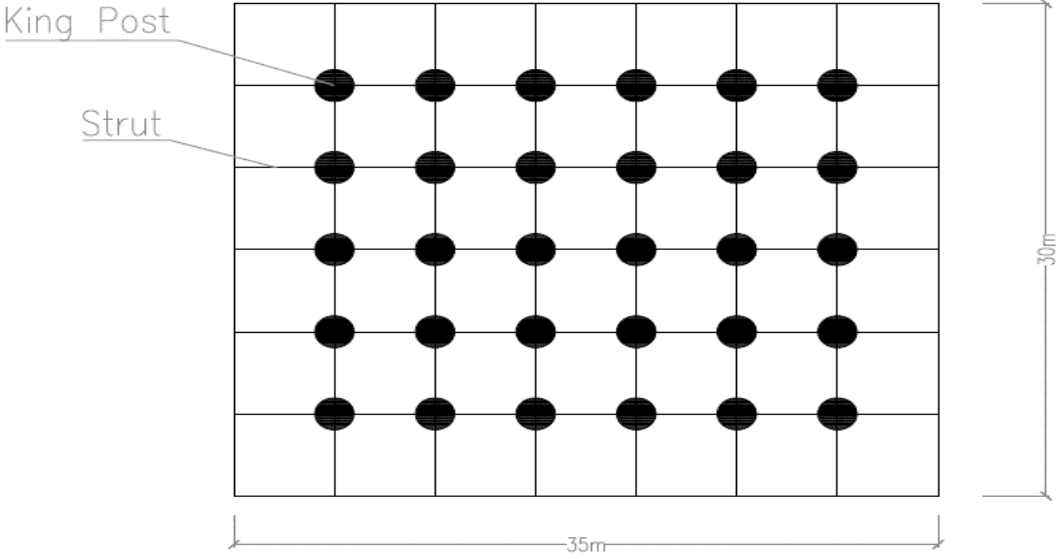
Table 4.4 A Summary of Input Parameters for HS Model for the site in Chittagong

Properties	Unit	Soft Clay	Medium Dense Fine Sand	Medium Stiff Silty Clay with Fine Sand
Unsaturated Unit Weight, γ_{unsat}	kN/m ³	16	17	15
Saturated Unit Weight, γ_{sat}	kN/m ³	17	20	17
Secant Modulus of Elasticity, E_{50}	kN/m ²	21000	43000	43000
Oedometer Modulus of Elasticity, E_{oed}	kN/m ²	21000	43000	43000
Unloading/Reloading Modulus of Elasticity, E_{ur}	kN/m ²	63000	129000	129000
Poisson's ratio, ν		0.3	0.3	0.3
Cohesion, c'	kN/m ²	5	0	0
Angle of Friction, ϕ	Degree	30	34	31
Dilation Angle, Ψ	Degree	0	4	1
Unloading Reloading Poisson's Ratio, ν_{ur}		0.2	0.2	0.3
K_0 value for normally consolidated soil, $K_0 \text{ nc}$		0.500	0.500	0.500
Interface factor, R_{int}		0.7	0.7	0.7

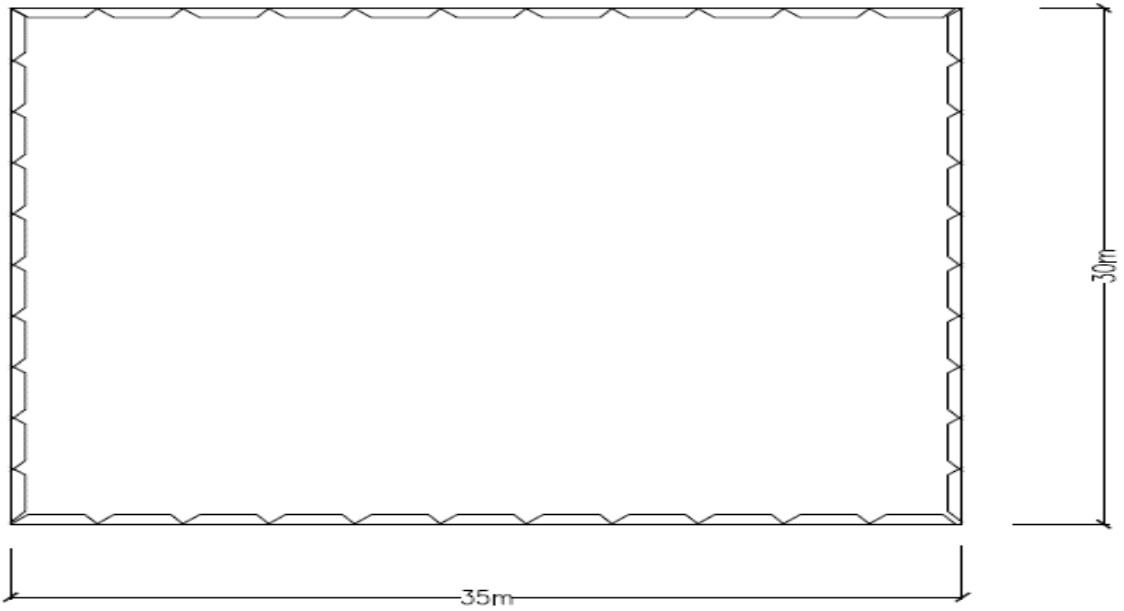
4.5 Numerical Analysis

A cross section of the excavation zone has been presented in Fig. 4.1. The section is approximately 35 m across between the sheet pile walls as well as for contiguous pile walls, and the excavation is 3m, 6m, and 9m respectively for single, double and three basement system deep. This section is considered comparatively further away from adjacent structures and corners, and thus possible interference from the nearby construction and corner effects can be avoided. The cross-section strutting levels, king posts, including bored piles are depicted in the following Fig. 4.2 for different basement system for sheet pile wall and Fig. 4.3 for contiguous pile wall. The finite element model

connectivity plot after the base slab being cast for the sheet pile and contiguous pile is presented in Fig. 4.4 and Fig. 4.5 respectively.



(a)

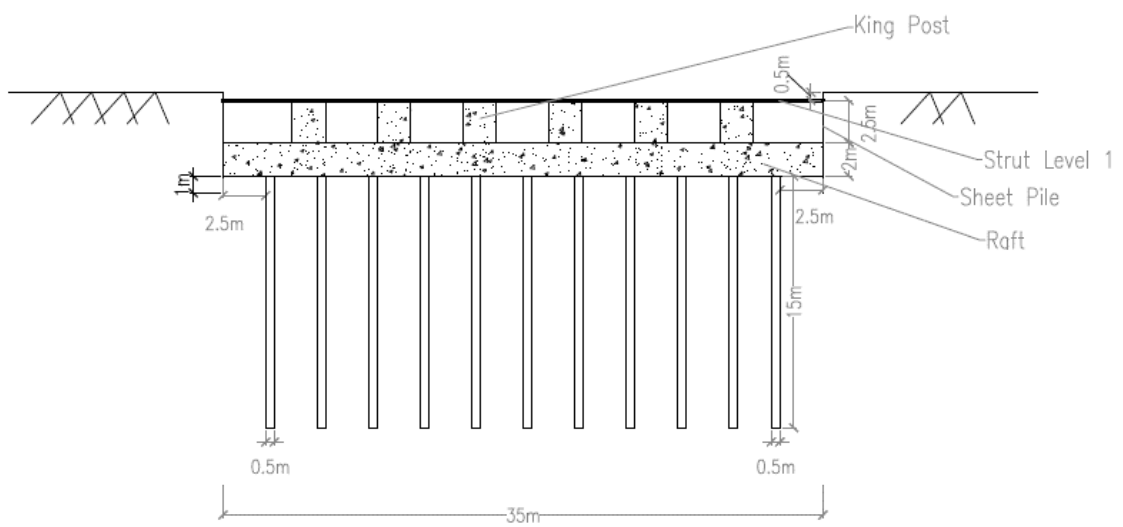


(b)

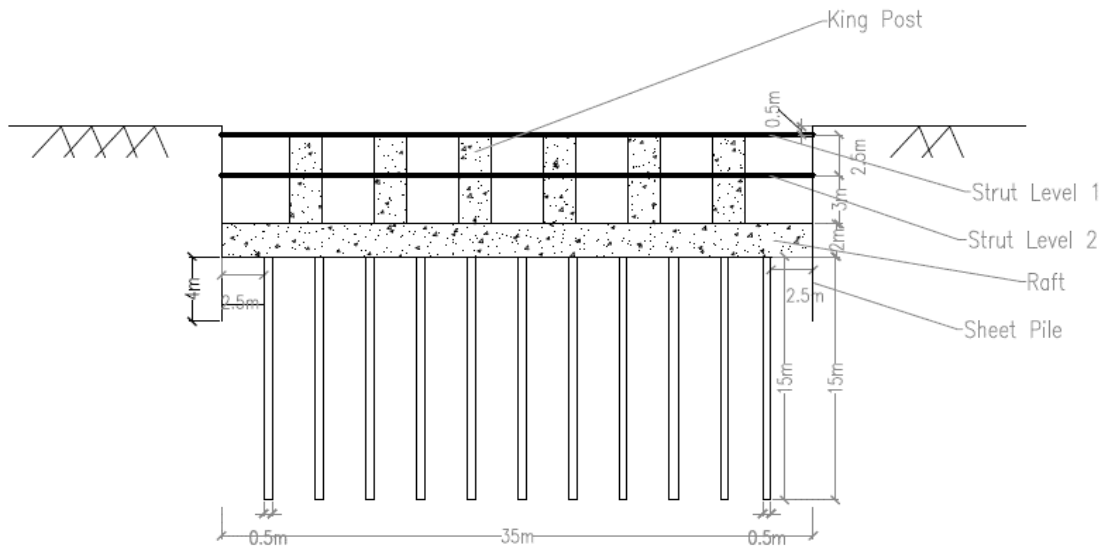


(c)

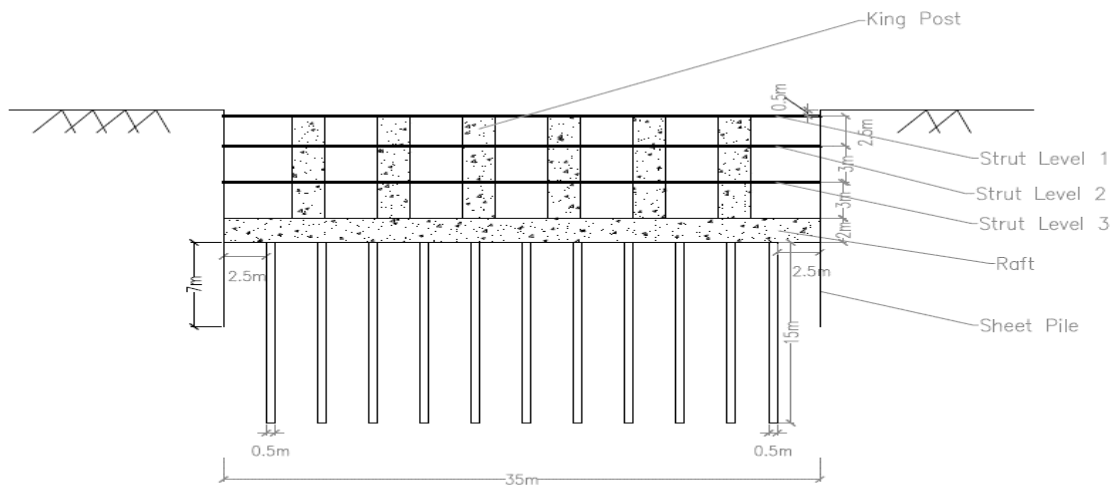
Fig. 4.1 Plan layout of a) Excavation zone b) Placement of Sheet pile wall c) Placement of Contiguous pile wall



(a)

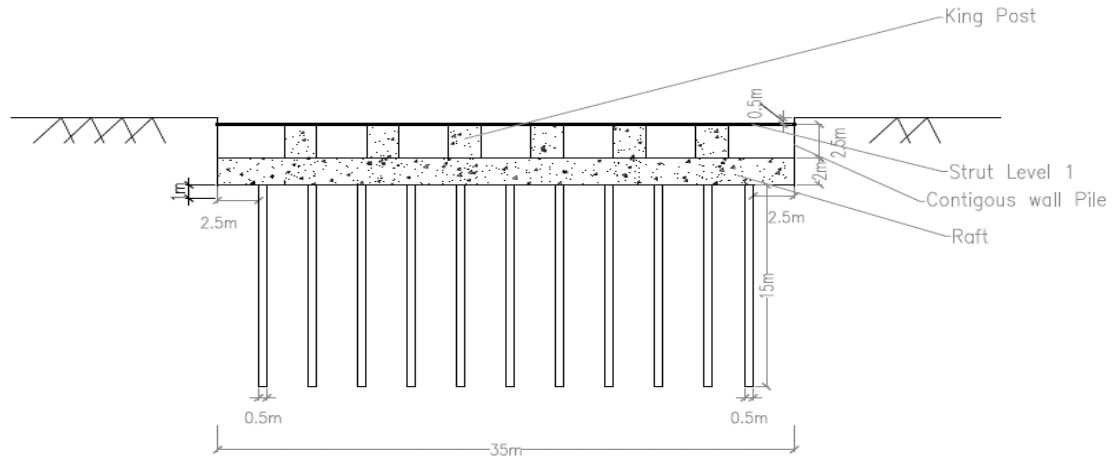


(b)

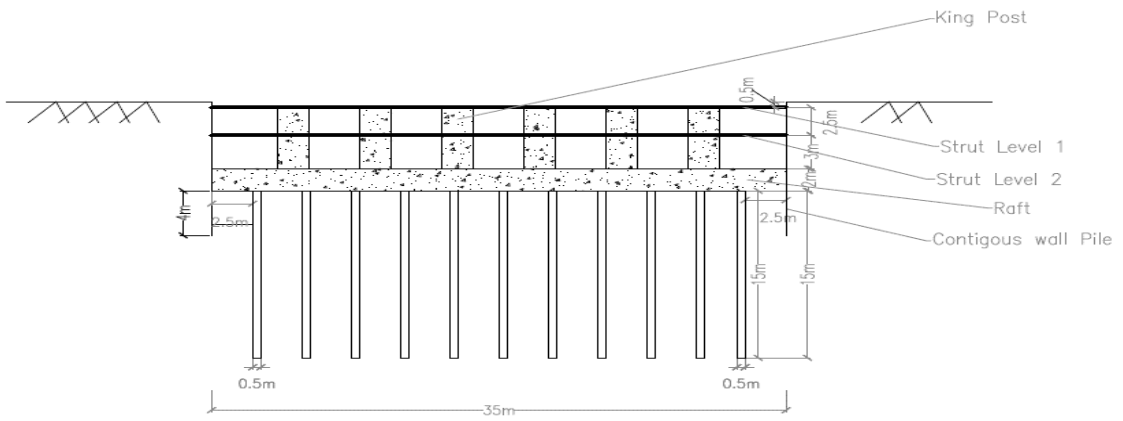


(c)

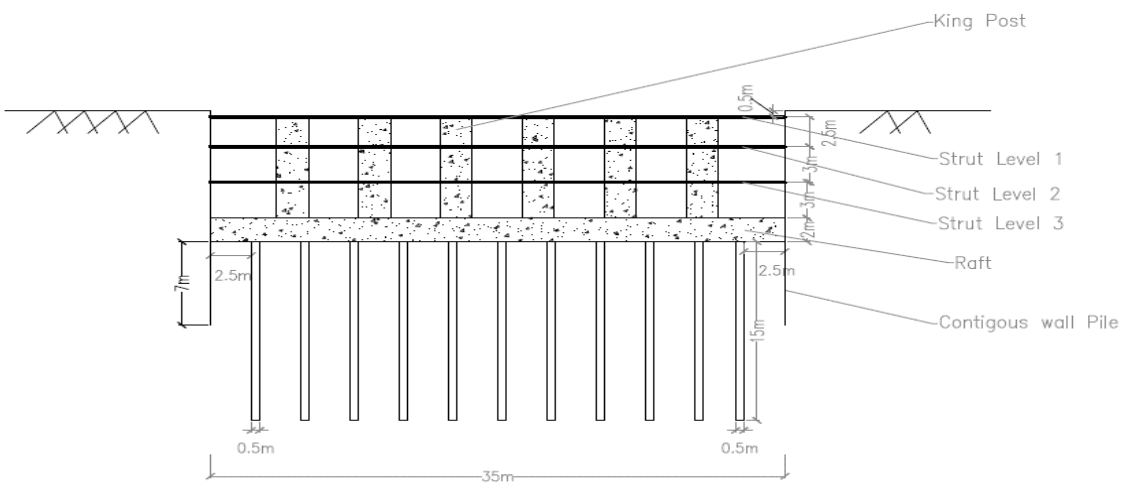
Fig. 4.2 Cross-sectional view of sheet pile wall retaining pile system a) Single basement b) Double basement c) Triple basement.



(a)



(b)



(c)

Fig. 4.3 Cross-sectional view of Contiguous pile wall retaining pile system a) Single basement b) Double basement c) Triple basement.

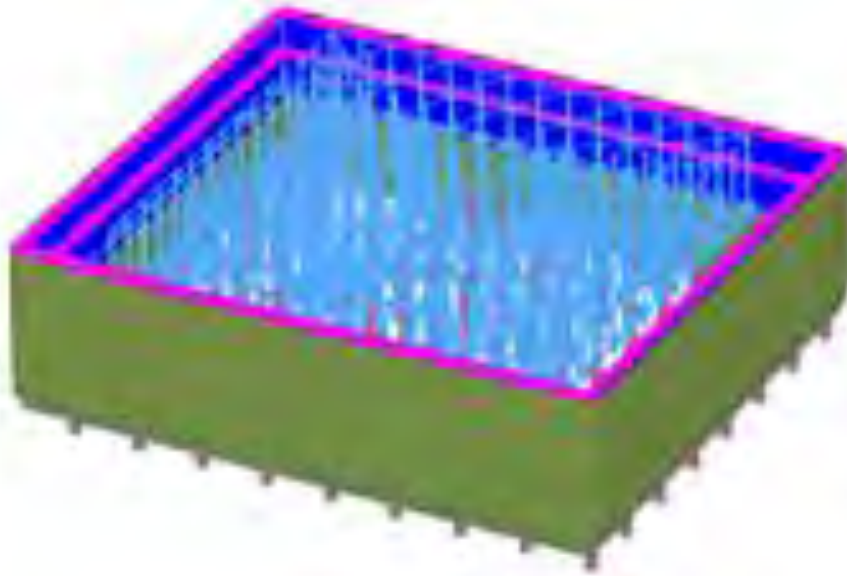


Fig. 4.4 Connectivity plot of finite element model containing sheet pile wall retaining system

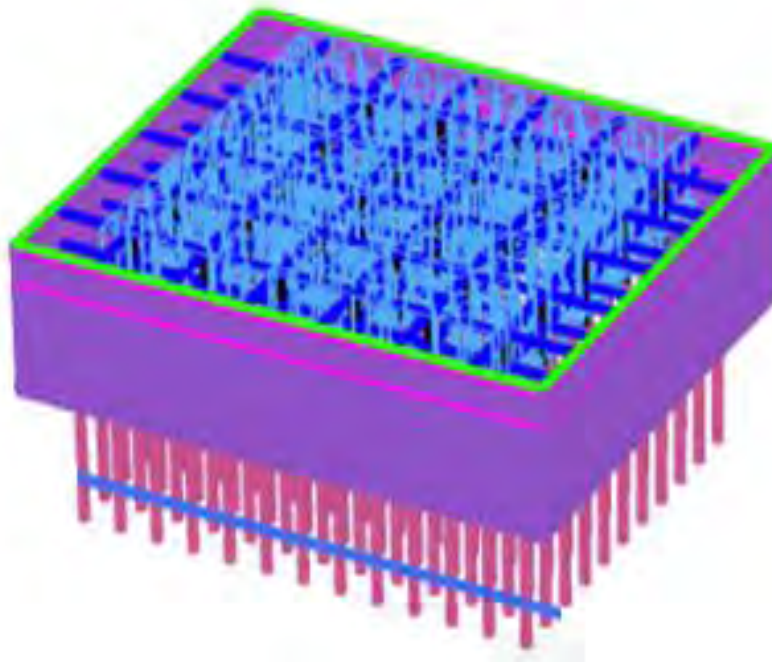


Fig. 4.5 Connectivity plot of finite element model containing contiguous pile wall retaining system

4.6 Modeling

The section describes numerical modeling of the excavation process.

4.6.1 Modeling of Soils and Excavation Sequences

A comparative study using the MC model and HS model will be carried with the parameters given in the previous section. Undrained Method A will be used for both MC and HS models.

The initial water level is assumed to be at 0.9 m below the existing ground level in case of Chittagong site and 40m below for the Dhaka site. Excavation is to be carried out to 0.5 m below each strutting level. The struts are installed. The water level will be drawn down at each stage of excavation to the excavation level. No drawdown outside of the excavation has been assumed. Moreover, no traffic loads or material stockpiles are behind the walls. Also, it has been assumed that the adjacent buildings are supported with piles.

Construction stage in PLAXIS 3D has been modeled based on the actual construction sequences outlined in Table 4.5.

Table 4.5 Stage Construction- Various phases in PLAXIS modeling

Retaining System	Basement Type	Phase	Activity
Sheet Pile Wall	Single	1	Install Sheet pile wall and king posts
		2	Excavate soil to -0.5m and install first level struts and wallings
		3	Excavate soil to -5m
		4	Install all the bored piles and cast base slab in place
		5	Activate all the surface load in the base slab
	Double	1	Install Sheet pile wall and king posts
		2	Excavate soil to -0.5m and install first level struts and wallings
		3	Excavate soil to -3m and install second level struts and wallings
		4	Excavate soil to -8m
		5	Install all the bored piles and cast base slab in place
		6	Activate all the surface load in the base slab
	Triple	1	Install Sheet pile wall and king posts
		2	Excavate soil to -0.5m and install first level struts and wallings
		3	Excavate soil to -3m and install second level struts and wallings
		4	Excavate soil to -6m and install third level struts and wallings
		5	Excavate soil to -11m
		6	Install all the bored piles and cast base slab in place
7		Activate all the surface load in the base slab	

Retaining System	Basement Type	Phase	Activity
Contiguous Pile Wall	Single	1	Install Contiguous pile wall and king posts
		2	Excavate soil to -0.5m and install Cap beam and first level struts and wallings
		3	Excavate soil to -5m
		4	Install all the bored piles and cast base slab in place
		5	Activate all the surface load in the base slab
Contiguous Pile Wall	Double	1	Install Contiguous pile wall and king posts
		2	Excavate soil to -0.5m and install Cap beam and first level struts and wallings
		3	Excavate soil to -3m and install second level struts and wallings
		4	Excavate soil to 8m
		5	Install all the bored piles and cast base slab in place
		6	Activate all the surface load in the base slab
	Triple	1	Install Contiguous pile wall and king posts
		2	Excavate soil to -0.5m and install first level struts and wallings
		3	Excavate soil to -3m and install second level struts and wallings
		4	Excavate soil to -6m and install third level struts and wallings
		5	Excavate soil to -11m
		6	Install all the bored piles and cast base slab in place
		7	Activate all the surface load in the base slab

4.6.2 Modeling of Structural Elements

The idealization of various structural components of the temporary ground support is described in the following paragraphs.

Sheet pile wall was modeled as plate elements. The equivalent thickness of the sheet pile was 0.427 m. Positive and Negative interface was considered around the sheet pile wall to incorporate soil-structure interaction. Temporary steel struts were modeled as beam elements with pin-connection at each end. King posts and cap beam were modeled as beam elements. Contiguous pile wall and bored piles were considered as embedded beam elements. The diameter of the contiguous pile was 0.5m and the spacing between contiguous pile was 0.15 m. Raft slab was modeled as a soil layer considering the linearly elastic model. A summary of structural elements properties are given in the following Table 4.6.

Table 4.6 Summary of Structural Elements Properties

Properties	Unit	Sheet pile wall	Steel Strut	Steel Walling	King Post	Cap Beam	Contiguous Pile	Pile below raft
Unit Weight, γ	kN/m ³	2.550	78.5	78.5	24	24	24	24
Area, A	m ²	-	0.00736	0.00862	0.4900	0.700		
Thickness, d	m	0.013	-		-	-		
Modulus of Elasticity, E	kN/m ²	14.6 x10 ⁶	210 x10 ⁶	210 x10 ⁶	30 x10 ⁶	30 x10 ⁶	30 x10 ⁶	30 x10 ⁶
Diameter	m	-	-	-	-	-	0.5	0.5
Element Type		Plate	Beam	Beam	Beam	Beam	Embedded Beam	Embedded Beam

4.7 Summary

- Reliable material models and input parameters are crucial to reproduce the observed performance in the field. The soil is a nonlinear and history-dependent material and has a sophisticated stress-strain-strength relationship. For practical applications, a realistic soil constitutive model needs to consider the essential features such as small-strain stiffness nonlinearity of the soil, and have a moderate level of complexity. Similarly, the model for structural components also needs to address adequately. When the particular material models are chosen for the soil and structures, the input parameters need to be carefully calibrated to represent the real material behavior. Chapter 4 presents the derivation of input soil parameters, numerical modeling, and structural elements.
- In general, PLAXIS recommended input parameters were adopted in cases where the parameters could not be established confidently from the laboratory, in-situ or empirical correlations. This is to keep the numerical calculations consistent.
- Modeling of structural elements was explained. 10-node elements were used to model soils. Stage-by-stage actual construction sequences were used, and surcharge was removed to reflect actual ground surface loading conditions. The initial water level was assumed to be 0.9 meters below the existing ground surface for Chittagong soil and 40 meter below for Dhaka soil. The water level outside of the excavation area remained constant throughout the excavation while it was at excavation level for every stage-excavation.

CHAPTER 5

RESULTS AND DISCUSSIONS

5.1 Introduction

Performance of deep excavation is related to both stability and deformation. The sheet pile walls and contiguous pile walls penetrated at least 3 m, 6m, and 9m for single, double and triple basement system respectively below the final excavation level to provide hydraulic cut-off. Moreover, the ratio of wall depth to an excavation depth of 2 for every basement system to provide a comfortable margin of safety against wall instability and excessive base heave. With the strengthening of retaining structure in place, the aspects of interest in the performance of deep excavation at hand reduced to wall deflection and ground surface settlement.

This chapter exhibits the results of numerical modeling of the excavation using the Mohr-Coulomb (MC) and Hardening Soil (HS) models for two sites in Dhaka and Chittagong using sheet pile wall retaining system and contiguous pile wall retaining system, and compare with the different conventional method. Finally, a comparative discussion will be done in between the sheet pile wall and contiguous pile wall considering several factors in the perspective of Bangladesh.

5.2 Retaining wall deflections

This section will exhibit wall deflections estimated using both MC and HS models and correlate them to the various conventional procedures followed by a discussion of the results.

Note that the while drawing different graphs sheet pile/ contiguous pile is set at the origin point of the graph and extends up to pre-defined depth for different cases in the Y-axis of the graph. In this study, the U_x value obtained from the PLAXIS output results of wall displacement depicts the lateral movement for the short side of the retaining wall in this study while the U_y value renders the lateral displacement value of the long side of the retaining wall. Moreover, the positive value of U_x indicates that the wall may be pushed into the soil retained and negative value of U_x represent the wall may tile away from the

soil retained for this particular study. Again, the positive value of U_y shows that the wall move away from the soil retained and the negative value of U_y indicates the wall may be pushed into the soil retained. The displacement in the X, Y, Z direction, as well as the total displacement, are also depicted in the graph to have a general idea of wall deflections for a particular case.

5.2.1 Sheet pile wall and contiguous pile wall deflections for Dhaka site for single basement system

The sheet pile wall and contiguous pile wall deflections for Dhaka site for single basement system for both the long side and short side of the sheet pile wall and contiguous pile wall obtained by applying MC model is shown in Fig. 5.1 and Fig. 5.2 and the sheet pile wall and contiguous pile wall deflections for Dhaka site for single basement system for both the long side and short side of the sheet pile wall and contiguous pile wall obtained by applying HS model is shown in Fig. 5.3 and Fig. 5.4.

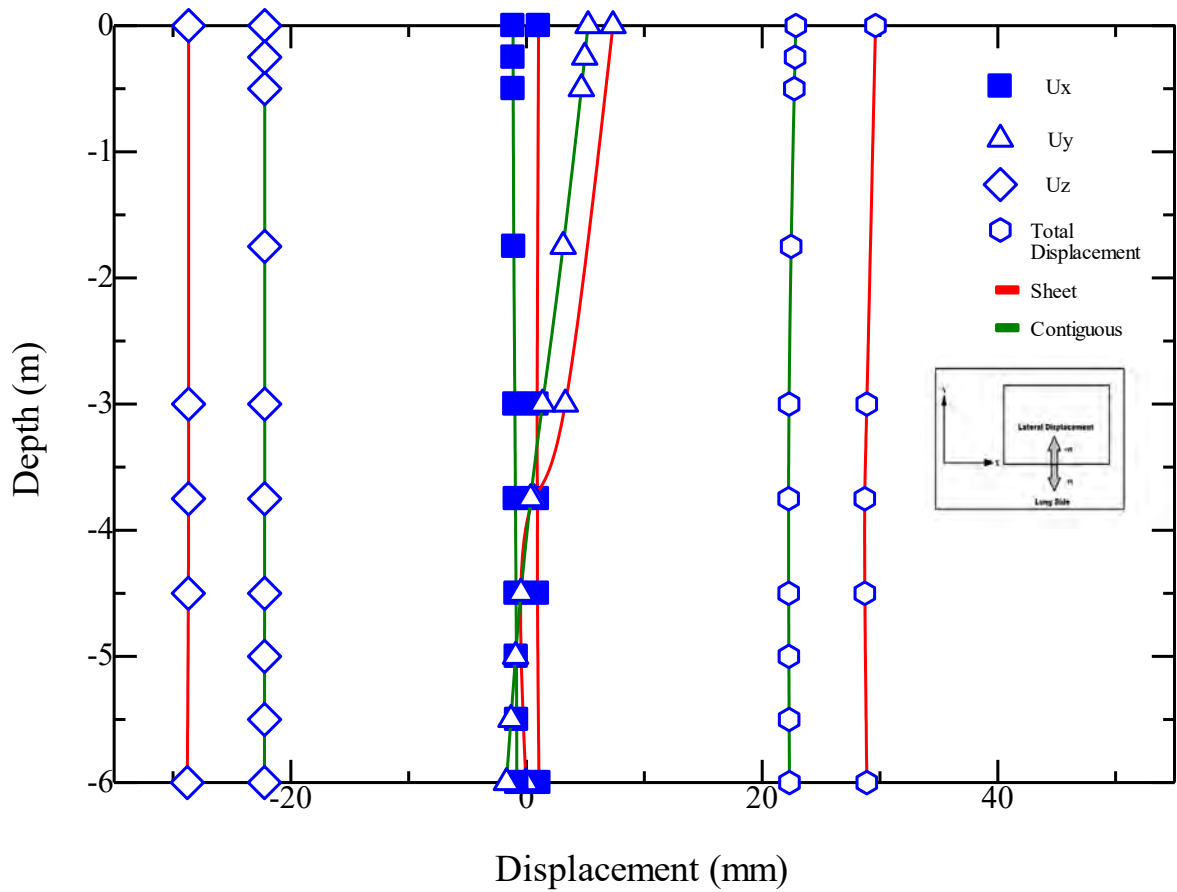


Fig. 5.1 Sheet pile wall and Contiguous pile wall displacement of Dhaka site having single basement system in the long side –MC model

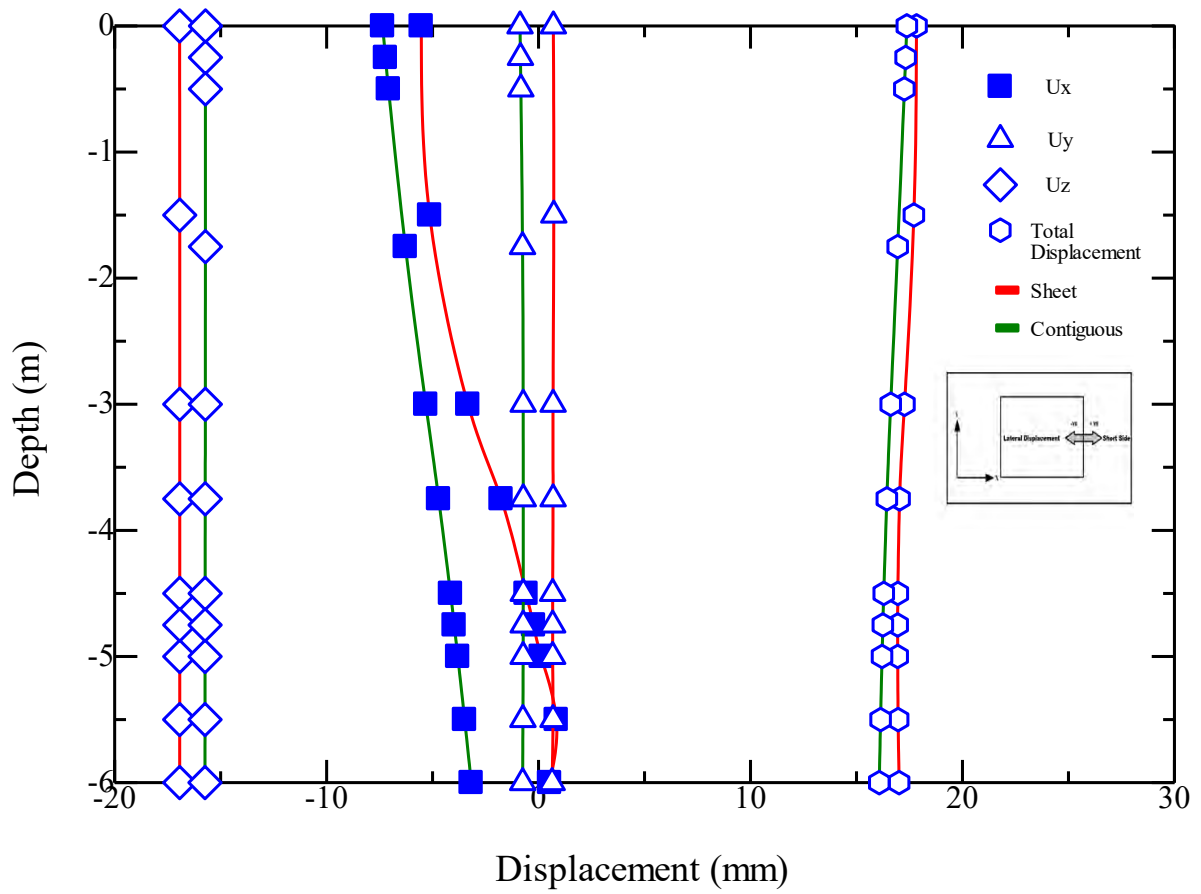


Fig. 5.2 Sheet pile wall and Contiguous pile wall displacement of Dhaka site having single basement system in the short side –MC model

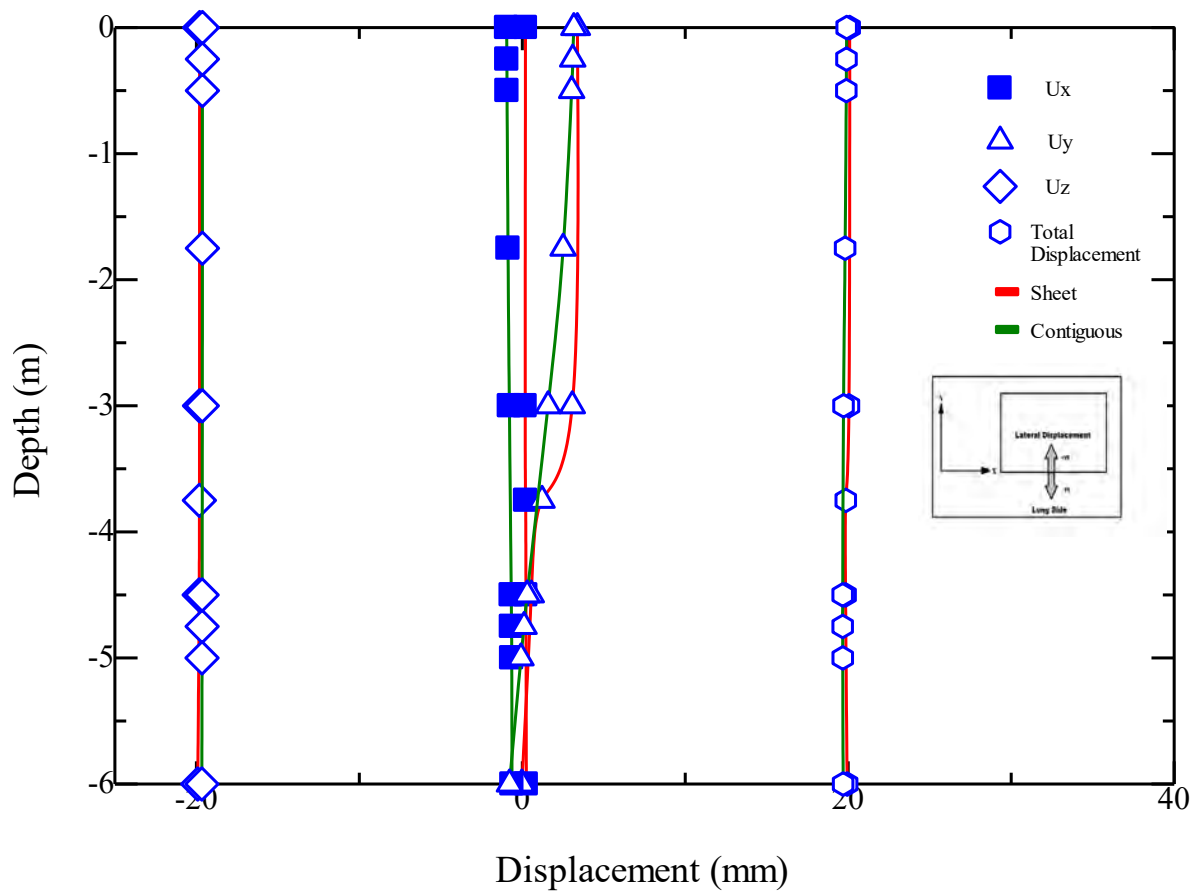


Fig. 5.3 Sheet pile wall and Contiguous pile wall displacement of Dhaka site having single basement system in the long side –HS model

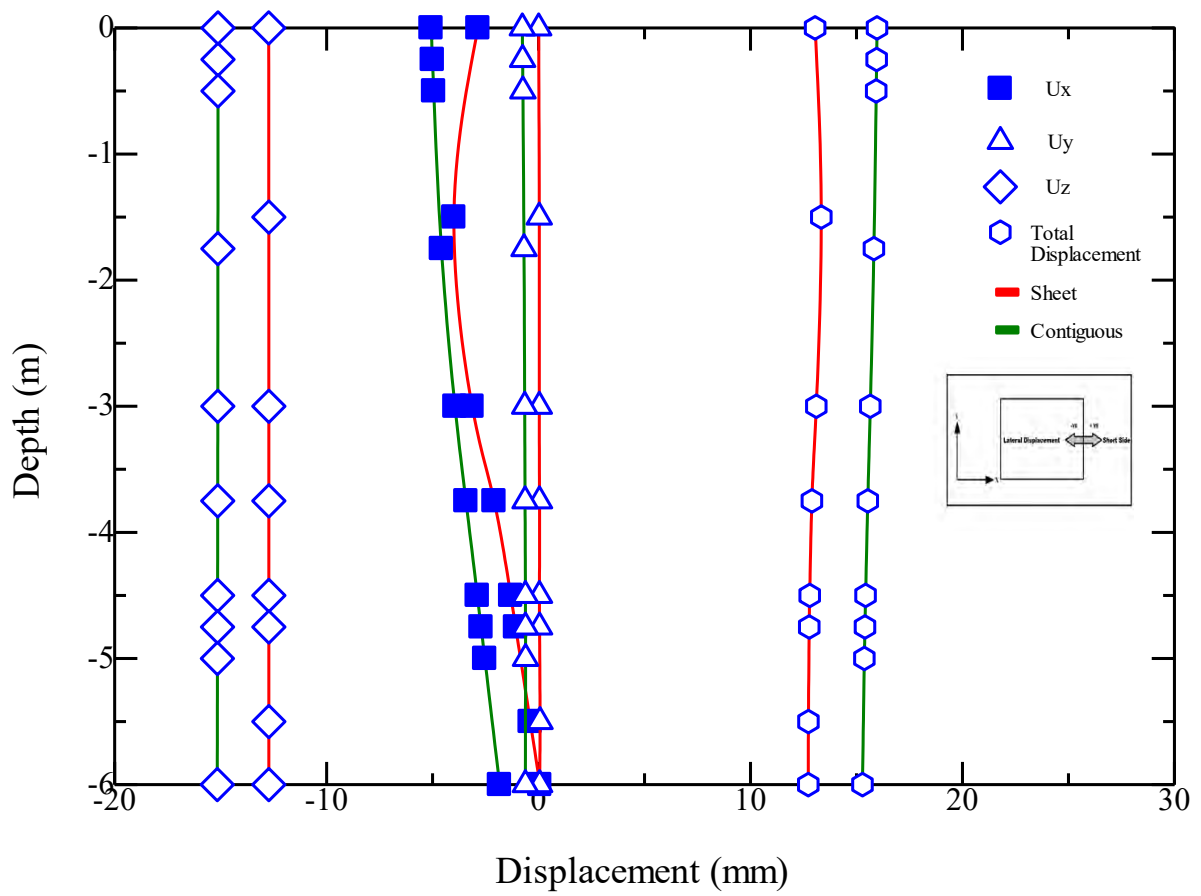


Fig. 5.4 Sheet pile wall and Contiguous pile wall displacement of Dhaka site having single basement system in the short side –HS model

It can be seen from the output result of MC model is that maximum lateral displacement is found out to be around 7mm in the long side of the sheet pile wall and 5mm in the long side of contiguous pile wall. Moreover, the maximum lateral displacement is 5.5 mm in the short side of sheet pile wall and 8mm in the short side of contiguous pile wall. The maximum displacement is occurred at the top portion of the wall in the both case. The maximum lateral displacement is on the positive side in the long side and on the negative side in the short side of sheet pile wall and contiguous pile wall which indicates that the sheet pile wall and contiguous pile wall move away from the retained soil. The reason for the case is due to the presence of strut at the top level. The displacement is almost restrained at the bottom of the wall. The effect of raft slab to control the wall movement is evident. The maximum total displacement obtains from this case is approximately 28mm in the long side of sheet pile wall and 22mm in the long side of contiguous pile. Again, the result of total displacement is 18mm in the short side of sheet pile wall and 16mm in the short side of contiguous pile wall.

It is evident that the HS model generally under-predicted wall deflections than the MC model because soil stiffness is defined much more accurately by using three different input stiffnesses: the tri-axial stiffness E_{50} , the tri-axial unloading stiffness E_{ur} and the oedometer loading stiffness E_{oed} . In contrast to the Mohr-Coulomb model, the Hardening Soil model also accounts for stress-dependency of stiffness moduli. This means that all stiffnesses increase with pressure. The maximum lateral displacement is 3mm which is found at the top of the wall in the long side of the sheet pile wall and 4mm in the short side of sheet pile wall which is located at 1.5m below the ground surface. On the other hand, the maximum lateral displacement is 3mm which is found at the top of the wall in the long side of the contiguous pile wall and 5mm in the short side of sheet pile wall which is also found at the top of the wall. Both of the displacement occurs in such a way that it indicates that the wall tilt away from the retained soil. The effect of raft slab to restrain wall movements is obvious. The maximum predicted total displacement is 20 mm in the long side and 13 mm in the short side of the sheet pile wall whereas it is 19mm in the long side and 16mm in the short side of contiguous pile wall.

It is observed from the output results that the contiguous pile wall shows better performance than the sheet pile wall. The contiguous pile wall experiences almost 27% less total wall displacement in the long side and 11% less total wall displacement in the

short side than the sheet pile wall in case of MC model. In case of HS model, the result of total displacement reduces in contiguous pile wall than the sheet pile wall by 5% in the long side and 19% in the short side. Moreover, the bulging of deflection curves above the raft slab is more visible in case of sheet pile wall than the contiguous pile wall. Furthermore, the lateral displacement curve is almost linear in case of contiguous pile wall due to fixity. In addition, it is also observed that the ground settlement of the sheet pile wall is also more than the contiguous pile wall.

A comparison of both the MC model and HS model for sheet pile wall and contiguous pile wall is shown in Table 5.1 and Table 5.2.

Table 5.1 A comparison between MC model and HS model for sheet pile displacement of Dhaka site having single basement system

Model	Long Side			Short Side	
	Depth (m)	Maximum Lateral Displacement (mm)	Direction from the retained soil	Maximum Lateral displacement (mm)	Direction from the retained soil
MC	0	7	outward	5.5	outward
HS	0	3	outward	3	outward
MC	3	3.29	outward	3.33	outward
HS	3	3.06	outward	3.13	outward

Table 5.2 A comparison between MC model and HS model for contiguous pile displacement of Dhaka site having single basement system

Model	Long Side			Short Side	
	Depth (m)	Maximum Lateral Displacement (mm)	Direction from the retained soil	Maximum Lateral displacement (mm)	Direction from the retained soil
MC	0	5	outward	8	outward
HS	0	3	outward	5	outward
MC	3	1	outward	5	outward
HS	3	0.5	outward	4	outward

A comparison of the output result with the available conventional method is shown in Table 5.3 and Table 5.4. In this study, three color codes are used to show the harmony with the available research. The green color is used to indicate a good match of the current result with the available research (result is within acceptable limit or the deviation is within 10%), Yellow is used to represent that the variation is within 20% and red color is used to describe the worst condition.

Table 5.3 A comparison of output result with available literature for the displacement of sheet pile wall and contiguous pile wall for Dhaka site having single basement system for MC model.











Researcher/ Research group	Basis of the comparison	Result from the literature	Result from sheet pile model	Result from contiguous pile model	Color code to show the Matching Condition
Clough and O'Rourke (1990)	Lateral Displacement	6 mm	7mm	8mm	Sheet pile wall  Contiguous pile wall 
Clough and O'Rourke (1990)	Lateral Displacement	18mm	7mm	8mm	Sheet pile wall  Contiguous pile wall 
Yandzio (1998)	Lateral Displacement	Bottom of the wall assumed not to displace	Matched	Matched	Sheet pile wall  Contiguous pile wall 
National Engineering Handbook (2007)	Maximum total displacement	25mm- 75mm	28mm	22mm	Sheet pile wall  Contiguous pile wall 
Kung (2009)	Lateral Displacement	6mm	7mm	8mm	Sheet pile wall  Contiguous pile wall 

Table 5.4 A comparison of output result with available literature for the displacement of sheet pile wall and contiguous pile wall for Dhaka site having single basement system for HS model.

Researcher/ Research group	Basis of the comparison	Result from the literature	Result from the sheet pile wall model	Result from the contiguous pile wall model	Color code to show the Matching Condition
Clough and O'Rourke (1990)	Lateral Displacement	6 mm	4mm	5mm	Sheet pile wall  Contiguous pile wall 
Clough and O'Rourke (1990)	Lateral Displacement	18mm	4mm	5mm	Sheet pile wall  Contiguous pile wall 
Yandzio (1998)	Lateral Displacement	Bottom of the wall assumed not to displace	Matched	Matched	Sheet pile wall  Contiguous pile wall 
National Engineering Handbook (2007)	Maximum total displacement		20mm	19mm	Sheet pile wall  Contiguous pile wall 
Kung (2009)	Lateral Displacement	6mm	4mm	5mm	Sheet pile wall  Contiguous pile wall 

5.2.2 Sheet pile wall deflections in Dhaka soil for double basement system

The sheet pile wall deflections for Dhaka site for double basement system for both the long side and short side of the sheet pile wall obtained by applying MC model is shown in Fig. 5.5 and Fig. 5.6 and HS model is shown in Fig. 5.7 and Fig. 5.8.

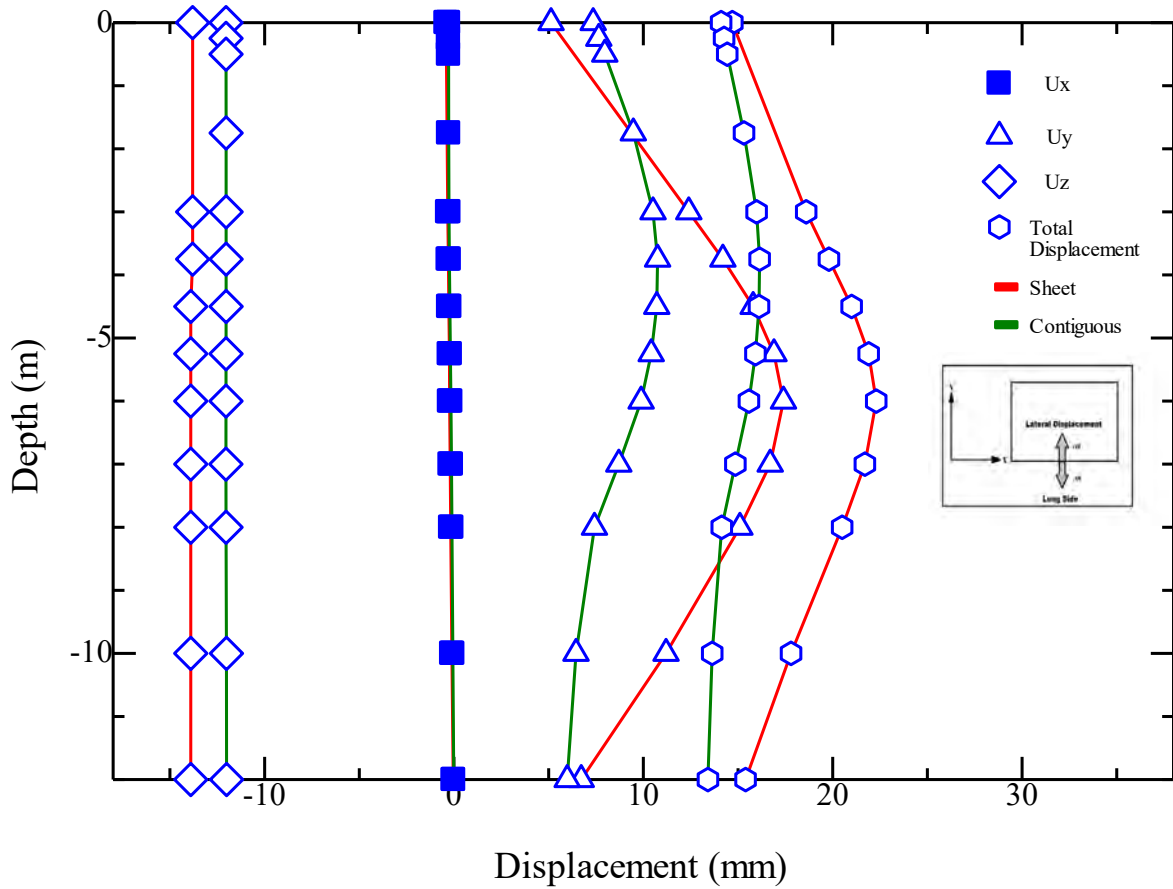


Fig. 5.5 Sheet pile wall and Contiguous pile wall displacement of Dhaka site having double basement system in the long side -MC model

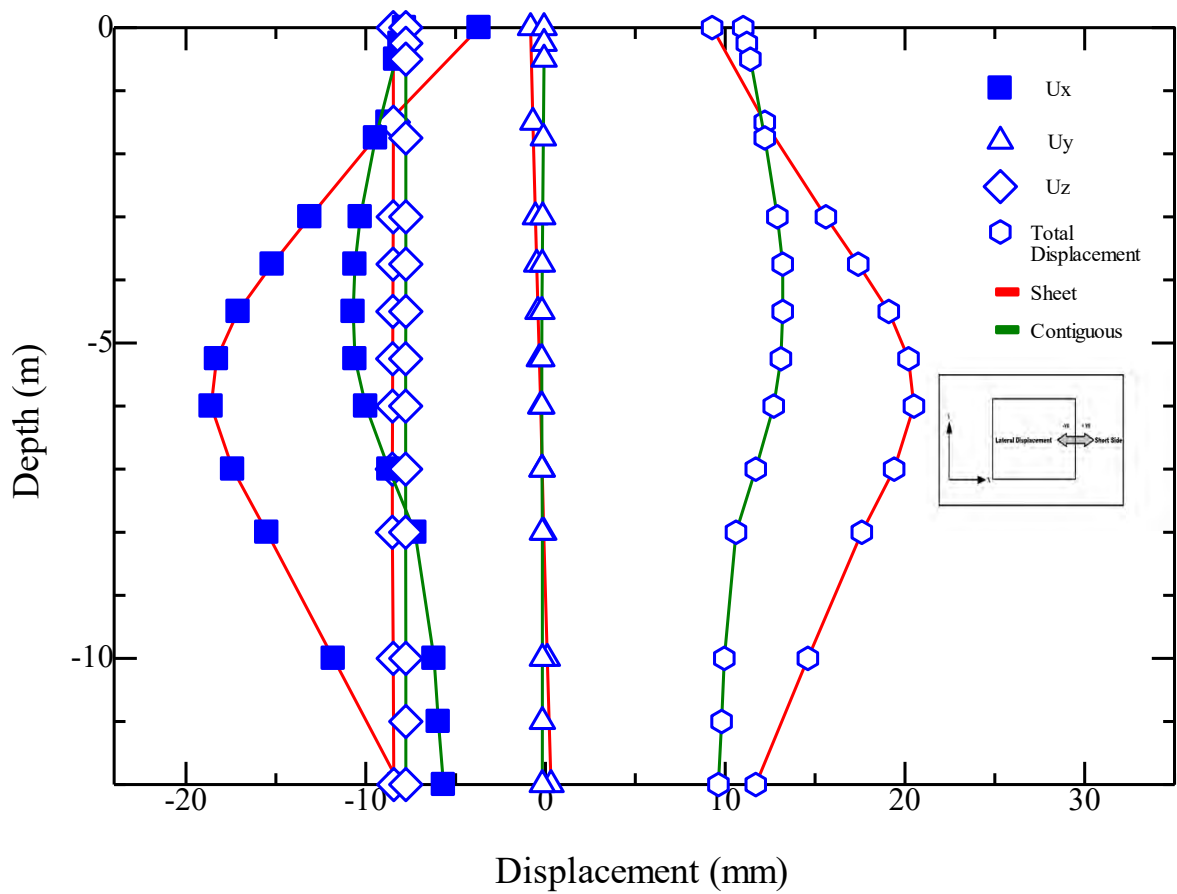


Fig. 5.6 Sheet pile wall and Contiguous pile wall displacement of Dhaka site having double basement system in the short side -MC model

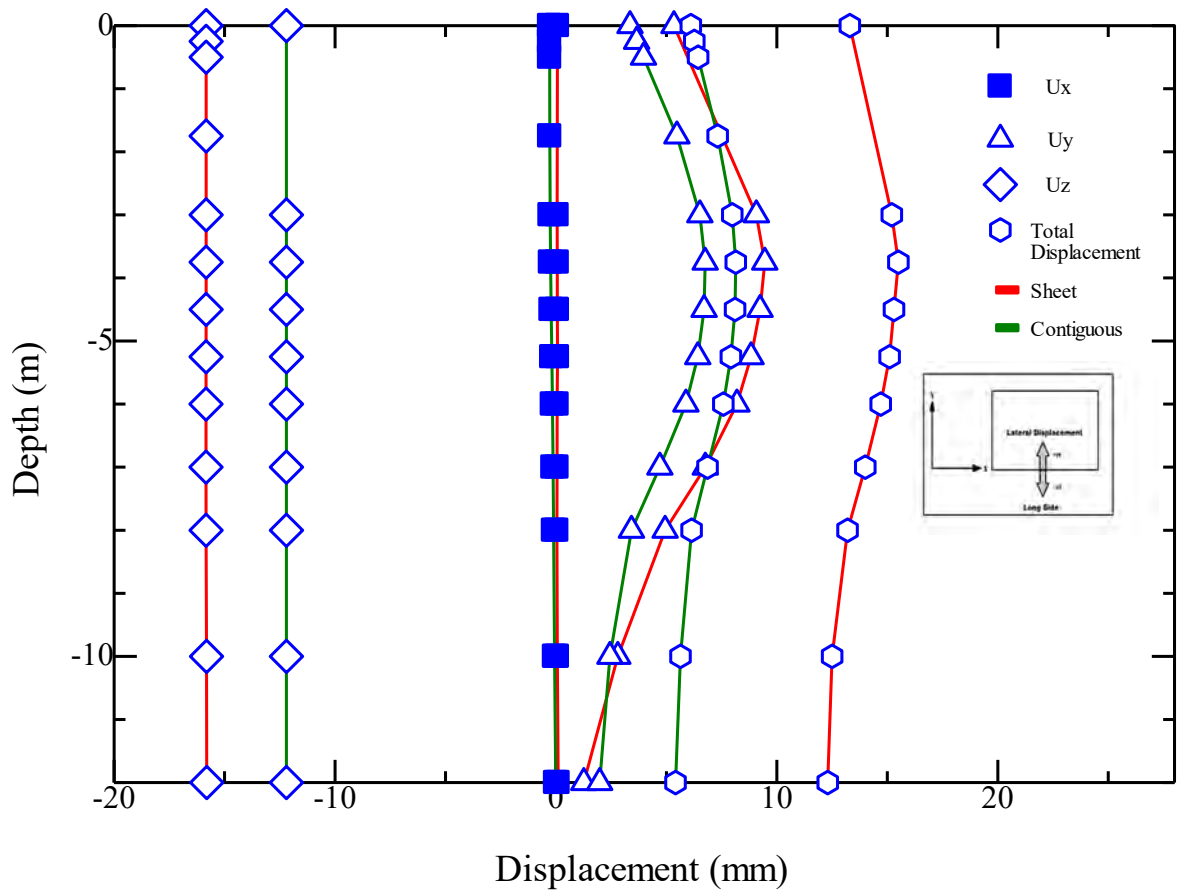


Fig. 5.7 Sheet pile wall and Contiguous pile wall displacement of Dhaka site having double basement system in the long side –HS model

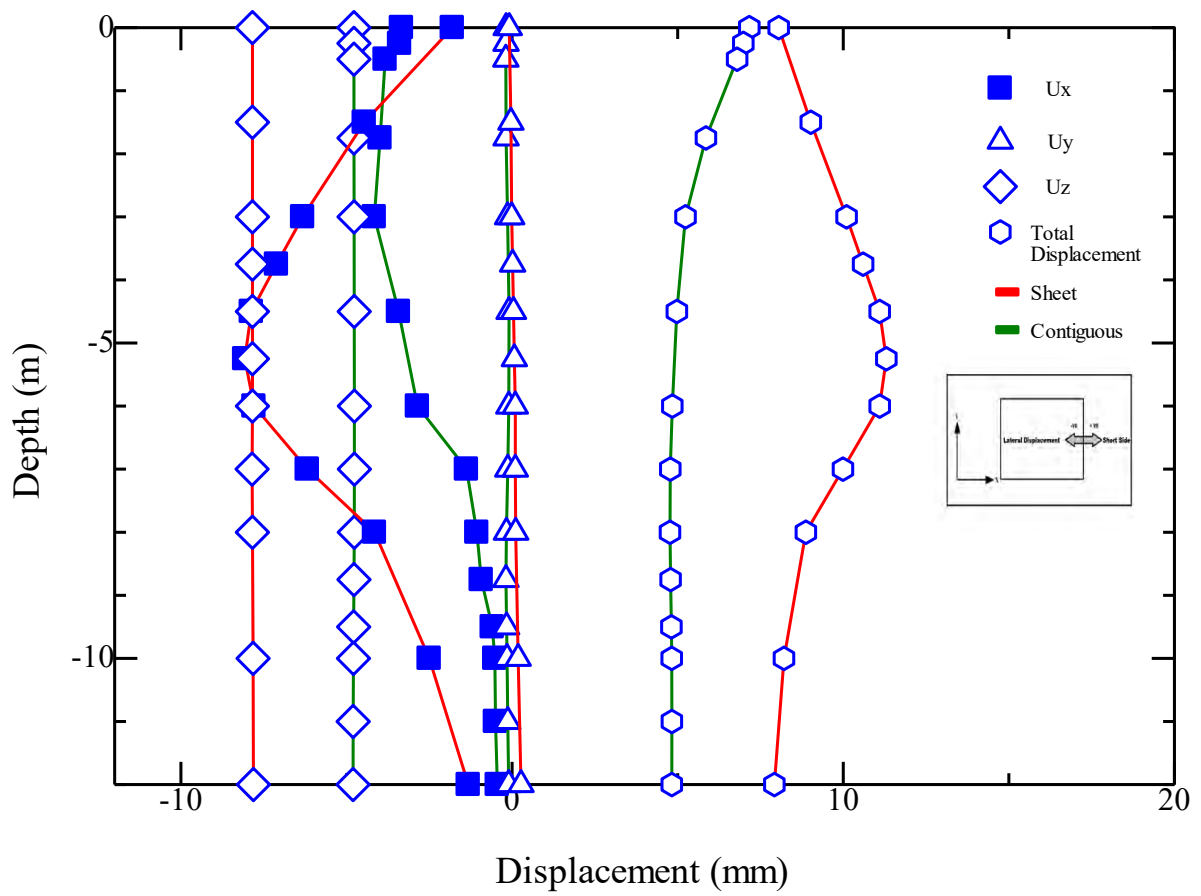


Fig. 5.8 Sheet pile wall and Contiguous pile wall displacement of Dhaka site having double basement system in the short side –HS model

It can be observed from the output result of MC model is that maximum lateral displacement is found out to be around 16mm in the long side of the sheet pile wall and 12mm in the long side of contiguous pile wall. Moreover, the maximum lateral displacement is 19 mm in the short side of sheet pile wall and 13mm in the short side of contiguous pile wall. The maximum displacement is found at almost near the bottom of the excavation (6m below the ground surface) in the both case. The maximum lateral displacement is on the positive side in the long side and on the negative side in the short side of sheet pile wall and contiguous pile wall which indicates that the sheet pile wall and contiguous pile wall move away from the retained soil. Movement of the wall is noticed at the bottom of the wall. The maximum total displacement obtained from this case is approximately 23mm in the long side of sheet pile wall and 16mm in the long side of contiguous pile. Again, the result of total displacement is 20mm in the short side of sheet pile wall and 18mm in the short side of contiguous pile wall.

It is evident that the HS model predicted lower wall deflections than the MC model. The maximum lateral displacement is 8mm in the long side of the sheet pile wall and 5mm in the long side of contiguous pile wall both of which is noticed at 3m below the ground surface. On the other hand, the maximum lateral displacement is 7mm and 4mm in the short side of sheet pile wall and contiguous pile wall respectively. The location of maximum lateral displacement is found at the same level of both the retaining system which is 6m below the ground surface. Both of the displacement occurs in such a way that it indicates that the wall move away from the retained soil. The effect of raft slab to restrain wall movements is obvious. It is also observed that movement at the bottom of the wall is almost restrained. The maximum predicted total displacement is 15mm in the long side and 11mm in the short side of the sheet pile wall whereas it is 7mm in the both side of contiguous pile wall.

It is observed from the output results that the contiguous pile wall shows better performance than the sheet pile wall. The contiguous pile wall experiences almost 50% less total wall displacement in the long side and 32% less total wall displacement in the short side than the sheet pile wall in case of MC model. In case of HS model, the result of total displacement reduces in contiguous pile wall than the sheet pile wall by 37.5% in the long side and 42% in the short side. Moreover, the bulging of deflection curves above the raft slab is more visible in case of sheet pile wall than the contiguous pile wall. In addition,

it is also observed that the ground settlement of the sheet pile wall is also more than the contiguous pile wall.

A comparison of both the MC model and HS model for sheet pile wall and contiguous pile wall is shown in Table 5.5 and Table 5.6.

Table 5.5 A comparison between MC model and HS model for sheet pile displacement of Dhaka site having double basement system

Model	Long Side			Short Side	
	Depth (m)	Maximum Lateral Displacement (mm)	Direction from the retained soil	Maximum Lateral displacement (mm)	Direction from the retained soil
MC	0	5	outward	3	outward
HS	0	4	outward	2	outward
MC	6	17	outward	18	outward
HS	6	7	outward	6	outward

Table 5.6 A comparison between MC model and HS model for contiguous pile displacement of Dhaka site having double basement system

Model	Long Side			Short Side	
	Depth (m)	Maximum Lateral Displacement (mm)	Direction from the retained soil	Maximum Lateral displacement (mm)	Direction from the retained soil
MC	0	8	outward	8	outward
HS	0	3	outward	5	outward
MC	6	9	outward	10	outward
HS	6	7	outward	2	outward

A comparison of the output result with the available conventional method is shown in Table 5.7 and Table 5.8.

Table 5.7 A comparison of output result with available literature for the displacement of sheet pile wall and contiguous pile wall for Dhaka site having double basement system for MC model.


















Researcher/ Research group	Basis of the comparison	Result from the literature	Result from sheet pile model	Result from contiguous pile model	Color code to show the Matching Condition
Clough and O'Rourke (1990)	Lateral Displacement	12mm	19mm	13mm	Sheet pile wall  Contiguous pile wall 
Clough and O'Rourke (1990)	Lateral Displacement	18mm	19mm	13mm	Sheet pile wall  Contiguous pile wall 
Yandzio (1998)	Lateral Displacement	Bottom of the wall assumed not to displace	Not matched	Not matched	Sheet pile wall  Contiguous pile wall 
National Engineering Handbook (2007)	Maximum total displacement	25mm- 75mm	20mm	18mm	Sheet pile wall  Contiguous pile wall 
Kung (2009)	Lateral Displacement	12mm	19mm	13mm	Sheet pile wall  Contiguous pile wall 

Table 5.8 A comparison of output result with available literature for the displacement of sheet pile wall and contiguous pile wall for Dhaka site having double basement system for HS model.

Researcher/ Research group	Basis of the comparison	Result from the literature	Result from the sheet pile wall model	Result from the contiguous pile wall model	Color code to show the Matching Condition
Clough and O'Rourke (1990)	Lateral Displacement	12mm	8mm	5mm	Sheet pile wall  Contiguous pile wall 
Clough and O'Rourke (1990)	Lateral Displacement	18mm	8mm	5mm	Sheet pile wall  Contiguous pile wall 
Yandzio (1998)	Lateral Displacement	Bottom of the wall assumed not to displace	Not matched	Matched	Sheet pile wall  Contiguous pile wall 
National Engineering Handbook (2007)	Maximum total displacement	25mm- 75mm	15mm	7mm	Sheet pile wall  Contiguous pile wall 
Kung (2009)	Lateral Displacement	12mm	8mm	5mm	Sheet pile wall  Contiguous pile wall 

5.2.3 Sheet pile wall and contiguous pile wall deflections for Dhaka site for triple basement system

The sheet pile wall and contiguous pile wall deflections for Dhaka site for triple basement system for both the long side and short side of the sheet pile wall and contiguous pile wall obtained by applying MC model is shown in Fig. 5.9 and Fig. 5.10 and the sheet pile wall and contiguous pile wall deflections for Dhaka site for single basement system for both the long side and short side of the sheet pile wall and contiguous pile wall obtained by applying HS model is shown in Fig. 5.11 and Fig. 5.12.

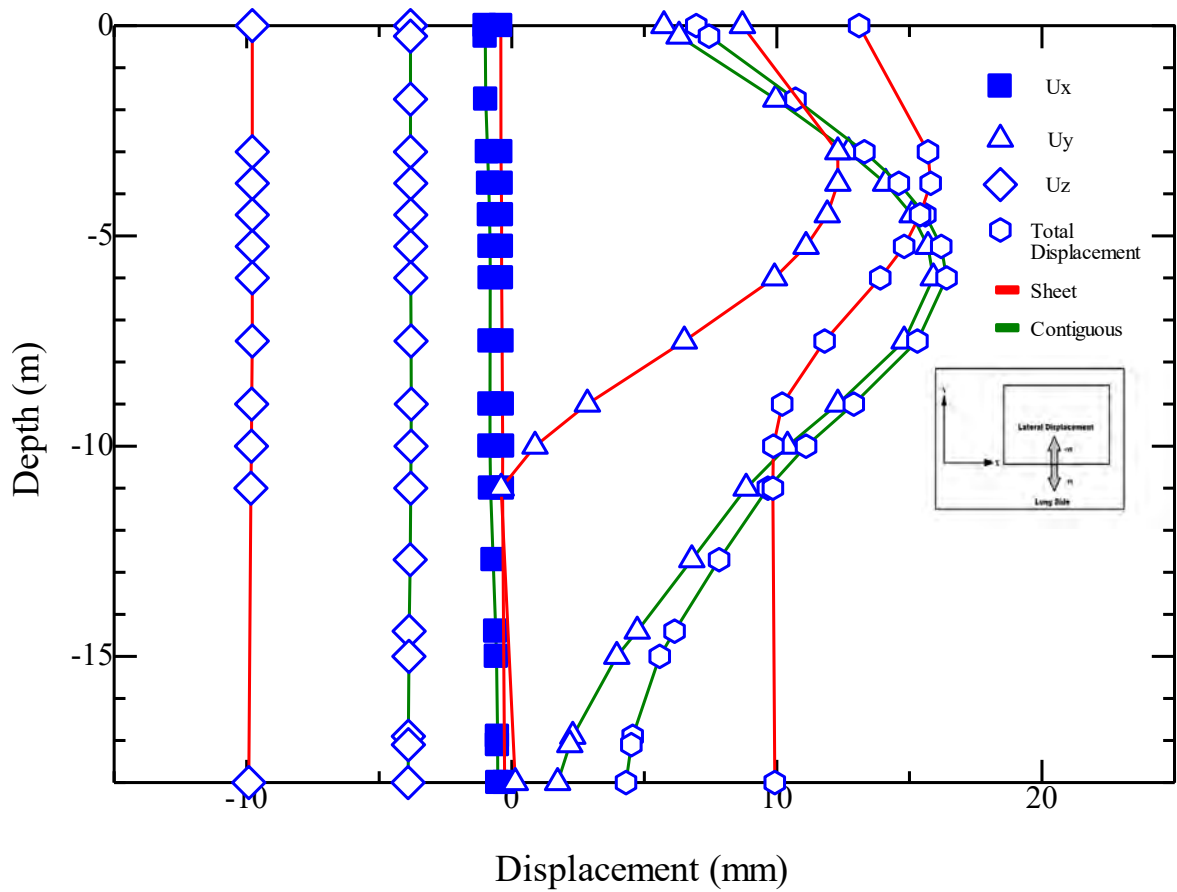


Fig. 5.9 Sheet pile wall and Contiguous pile wall displacement of Dhaka site having triple basement system in the long side –MC model

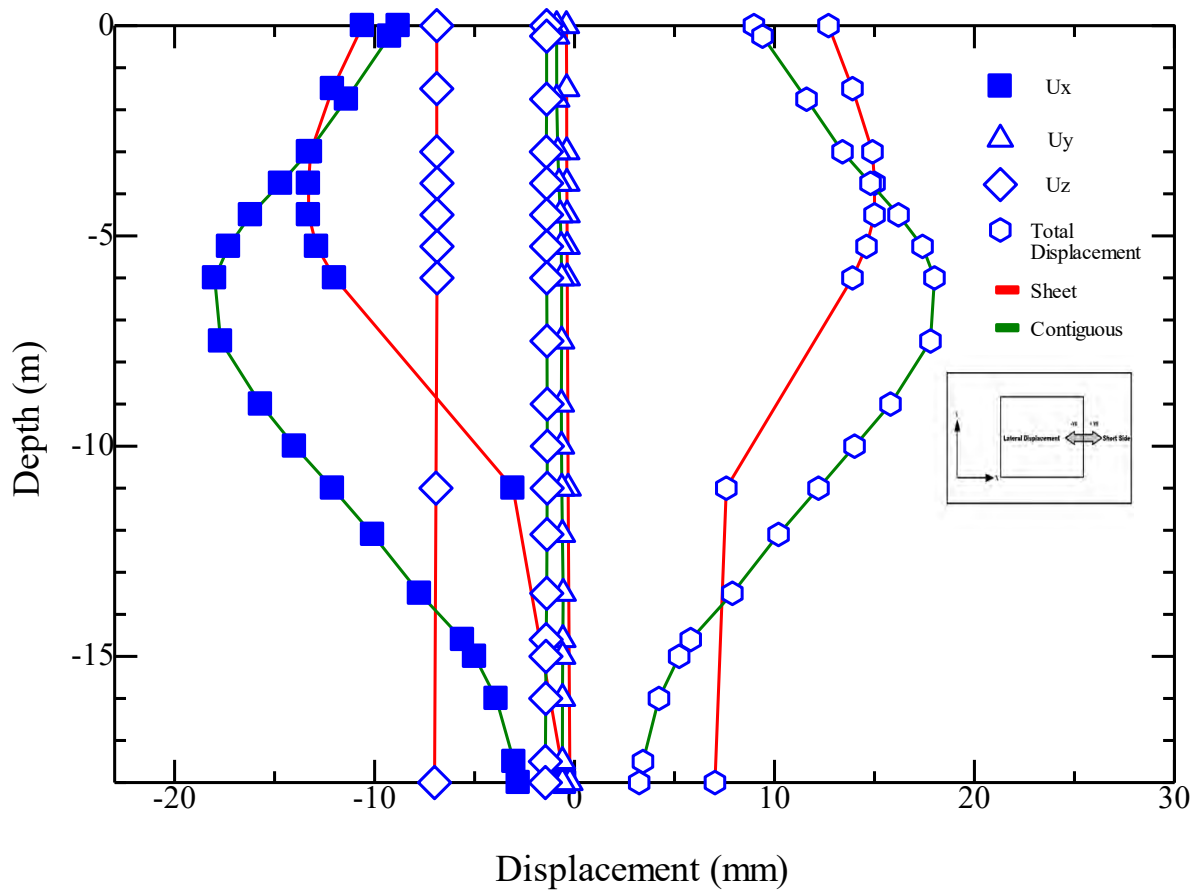


Fig. 5.10 Sheet pile wall and Contiguous pile wall displacement of Dhaka site having triple basement system in the short side –MC model

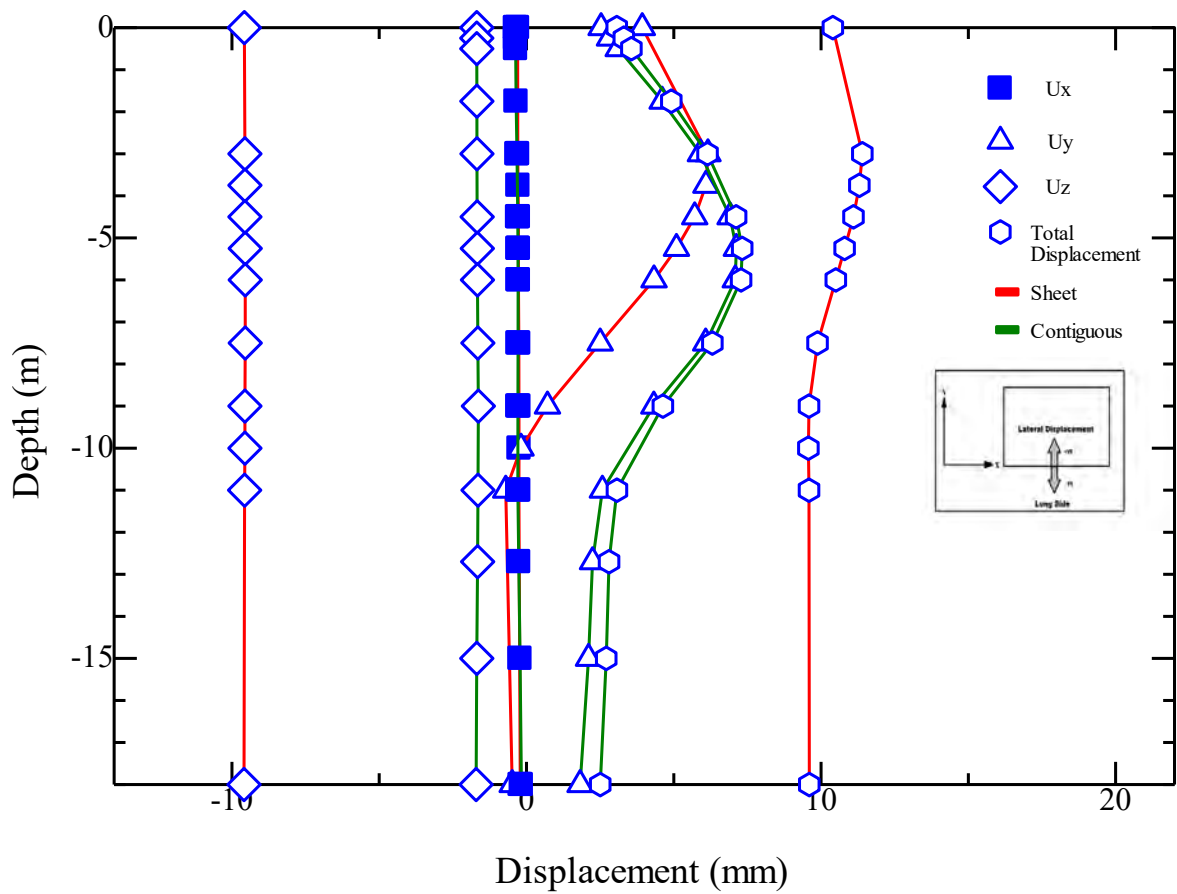


Fig. 5.11 Sheet pile wall and Contiguous pile wall displacement of Dhaka site having triple basement system in the long side –HS model

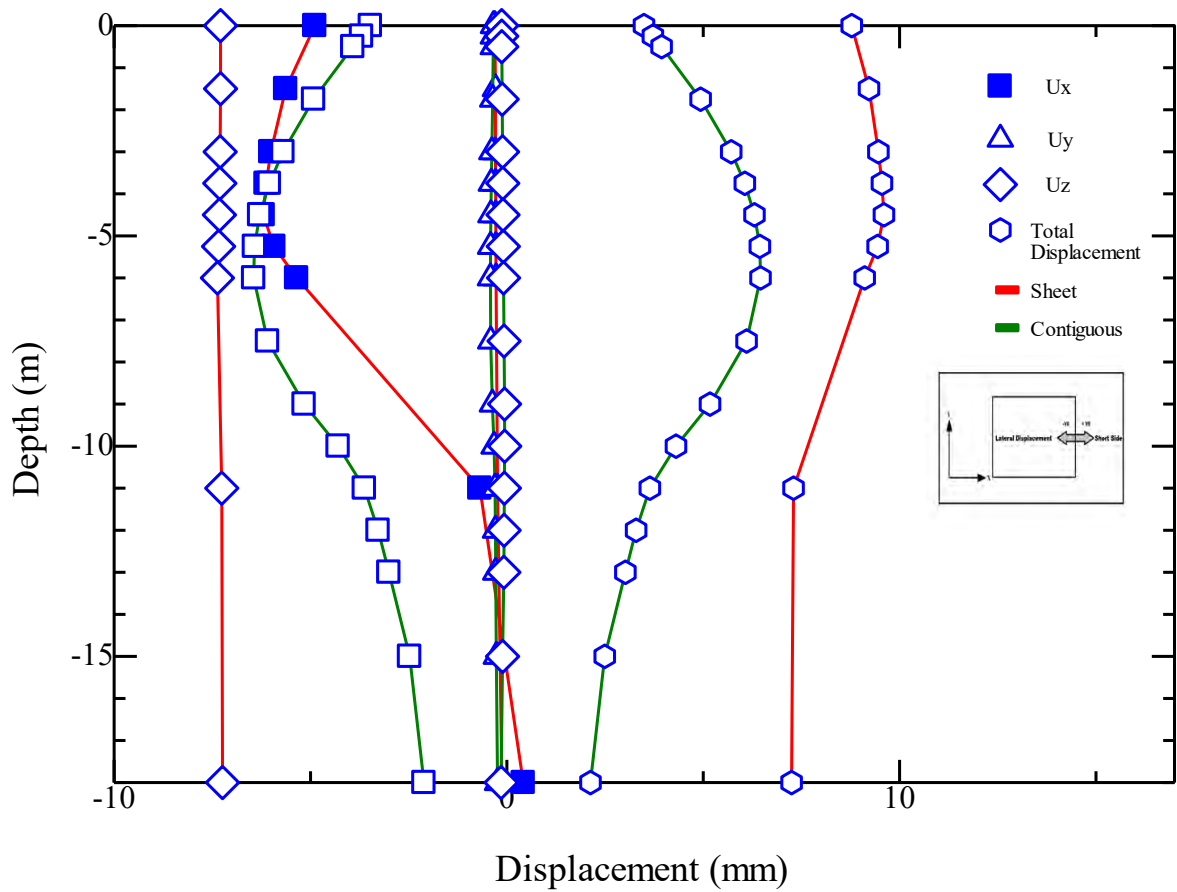


Fig. 5.12 Sheet pile wall and Contiguous pile wall displacement of Dhaka site having triple basement system in the short side –HS model

It can be noticed from the output result of MC model is that maximum lateral displacement is found out to be around 12mm in the long side of the sheet pile wall and 16mm in the long side of contiguous pile wall. Moreover, the maximum lateral displacement is 14 mm in the short side of sheet pile wall and 17mm in the short side of contiguous pile wall. The maximum displacement is found at the 6m below the ground surface of the wall in the both case. The maximum lateral displacement is on the positive side in the long side and on the negative side in the short side of sheet pile wall and contiguous pile wall which indicates that the sheet pile wall and contiguous pile wall move away from the retained soil. The displacement is almost restrained at the bottom of the wall. The effect of raft slab to control the wall movement is evident. The maximum total displacement obtained from this case is approximately 14mm in the long side of sheet pile wall and 15.5 mm in the long side of contiguous pile. Again, the result of total displacement is 15mm in the short side of sheet pile wall and 17mm in the short side of contiguous pile wall.

It is evident that the HS model generally predicts lower wall deflections than the MC model. The maximum lateral displacement is 7mm in the long side of the sheet pile wall and 6mm in the short side of sheet pile wall which is found at 3m below the ground surface for sheet pile wall. On the other hand, the maximum lateral displacement is 7mm in the long side of contiguous pile wall and 6mm in the short side of contiguous pile wall which is found at the 6m below the ground surface. Both of the displacement occurs in such a way that it indicates that the wall tilt away from the retained soil. The effect of raft slab to restrain wall movements is obvious. The maximum predicted total displacement is 11 mm in the long side and 8mm in the short side of the sheet pile wall whereas it is 10mm in the long side and 6mm in the short side of contiguous pile wall.

It is observed from the output results that the contiguous pile wall shows better performance than the sheet pile wall in this case only for HS model whereas sheet pile shows better performance than the contiguous pile wall than the contiguous pile wall in case of the MC model. The contiguous pile wall experiences almost 9% less total wall displacement in the long side and 25% less total wall displacement in the short side than the sheet pile wall in case of HS model. However, sheet pile wall experienced less displacement than the contiguous pile wall in case of MC model. The result of total displacement reduces in sheet pile wall than the contiguous pile wall by 10% in the long

side and 10% in the short side. Moreover, the bulging of deflection curves above the raft slab is more visible in both cases but the bulging is more in case of sheet pile wall than the contiguous pile wall. In addition, it is also observed that the ground settlement of the sheet pile wall is also more than the contiguous pile wall and the vertical displacement in the short side of contiguous pile wall is almost zero.

A comparison of both the MC model and HS model for sheet pile wall and contiguous pile wall is shown in Table 5.9 and Table 5.10.

Table 5.9 A comparison between MC model and HS model for sheet pile displacement of Dhaka site having triple basement system

Model	Long Side			Short Side	
	Depth (m)	Maximum Lateral Displacement (mm)	Direction from the retained soil	Maximum Lateral displacement (mm)	Direction from the retained soil
MC	0	8	Outward	11	outward
HS	0	4	Outward	5	outward
MC	9	2	Outward	6	outward
HS	9	1	Outward	2	outward

Table 5.10 A comparison between MC model and HS model for contiguous pile displacement of Dhaka site having triple basement system

Model	Long Side			Short Side	
	Depth (m)	Maximum Lateral Displacement (mm)	Direction from the retained soil	Maximum Lateral displacement (mm)	Direction from the retained soil
MC	0	6	outward	9	outward
HS	0	2.5	outward	3.5	outward
MC	9	11	outward	15	outward
HS	9	4.5	outward	5	outward

A comparison of the output result with the available conventional method is shown in Table 5.11 and Table 5.12. In this study, three color codes are used to show the harmony with the available research.

Table 5.11 A comparison of output result with available literature for the displacement of sheet pile wall and contiguous pile wall for Dhaka site having triple basement system for MC model.

















Researcher/ Research group	Basis of the comparison	Result from the literature	Result from sheet pile model	Result from contiguous pile model	Color code to show the Matching Condition
Clough and O'Rourke (1990)	Lateral Displacement	18mm	12mm	17mm	Sheet pile wall  Contiguous pile wall 
Clough and O'Rourke (1990)	Lateral Displacement	18mm	12mm	17mm	Sheet pile wall  Contiguous pile wall 
Yandzio (1998)	Lateral Displacement	Bottom of the wall assumed not to displace	Matched	Matched	Sheet pile wall  Contiguous pile wall 
National Engineering Handbook (2007)	Maximum total displacement	25mm- 75mm	14mm	16mm	Sheet pile wall  Contiguous pile wall 
Kung (2009)	Lateral Displacement	18mm	12mm	17mm	Sheet pile wall  Contiguous pile wall 

Table 5.12 A comparison of output result with available literature for the displacement of sheet pile wall and contiguous pile wall for Dhaka site having triple basement system for HS model.

Researcher/ Research group	Basis of the comparison	Result from the literature	Result from the sheet pile wall model	Result from the contiguous pile wall model	Color code to show the Matching Condition
Clough and O'Rourke (1990)	Lateral Displacement	18mm	6mm	7mm	Sheet pile wall  Contiguous pile wall 
Clough and O'Rourke (1990)	Lateral Displacement	18mm	6mm	7mm	Sheet pile wall  Contiguous pile wall 
Yandzio (1998)	Lateral Displacement	Bottom of the wall assumed not to displace	Matched	Matched	Sheet pile wall  Contiguous pile wall 
National Engineering Handbook (2007)	Maximum total displacement	25mm- 75mm	11mm	7mm	Sheet pile wall  Contiguous pile wall 
Kung (2009)	Lateral Displacement	18mm	6mm	7mm	Sheet pile wall  Contiguous pile wall 

5.2.4 Sheet pile wall and contiguous pile wall displacement for Chittagong site having single, double and triple basement

Due to a large amount of data, the sheet pile and contiguous pile wall's displacement result for Chittagong site will be discussed in this single section. The sheet pile and contiguous pile wall displacement of Chittagong site having single, double and triple basement system in the long side and short side of sheet pile and contiguous pile wall obtained by using MC model are shown in Fig. 5.13-5.18.

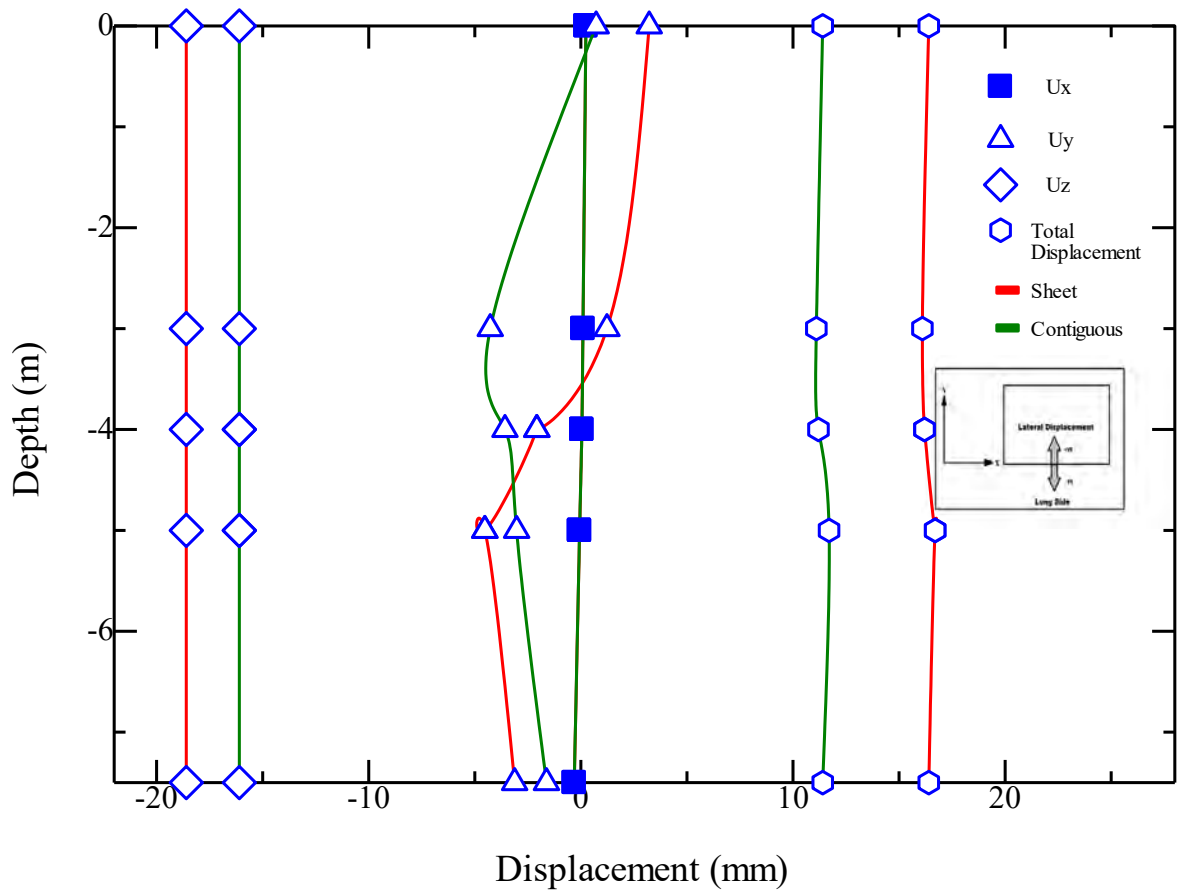


Fig. 5.13 Sheet pile wall and Contiguous pile wall displacement of Chittagong site having single basement system in the long side –MC model

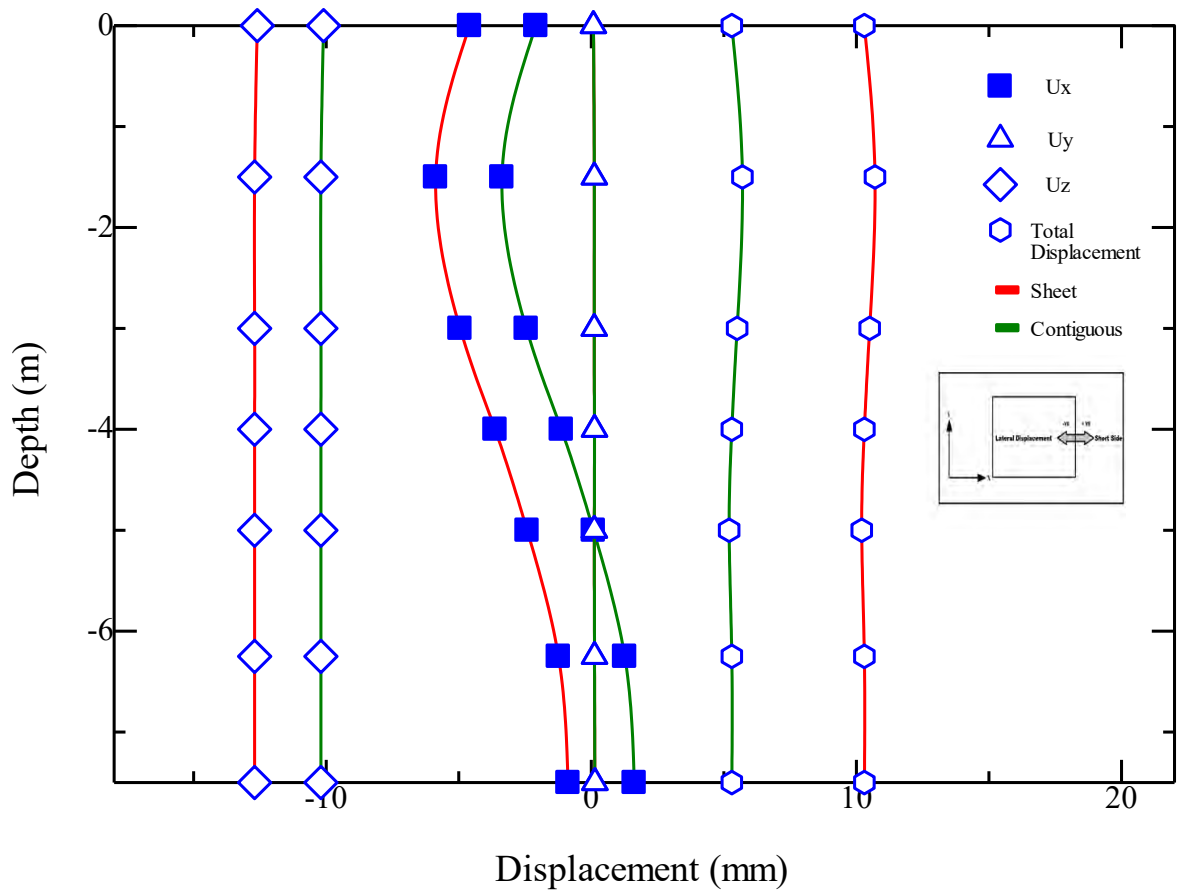


Fig. 5.14 Sheet pile wall and Contiguous pile wall displacement of Chittagong site having single basement system in the short side –MC model

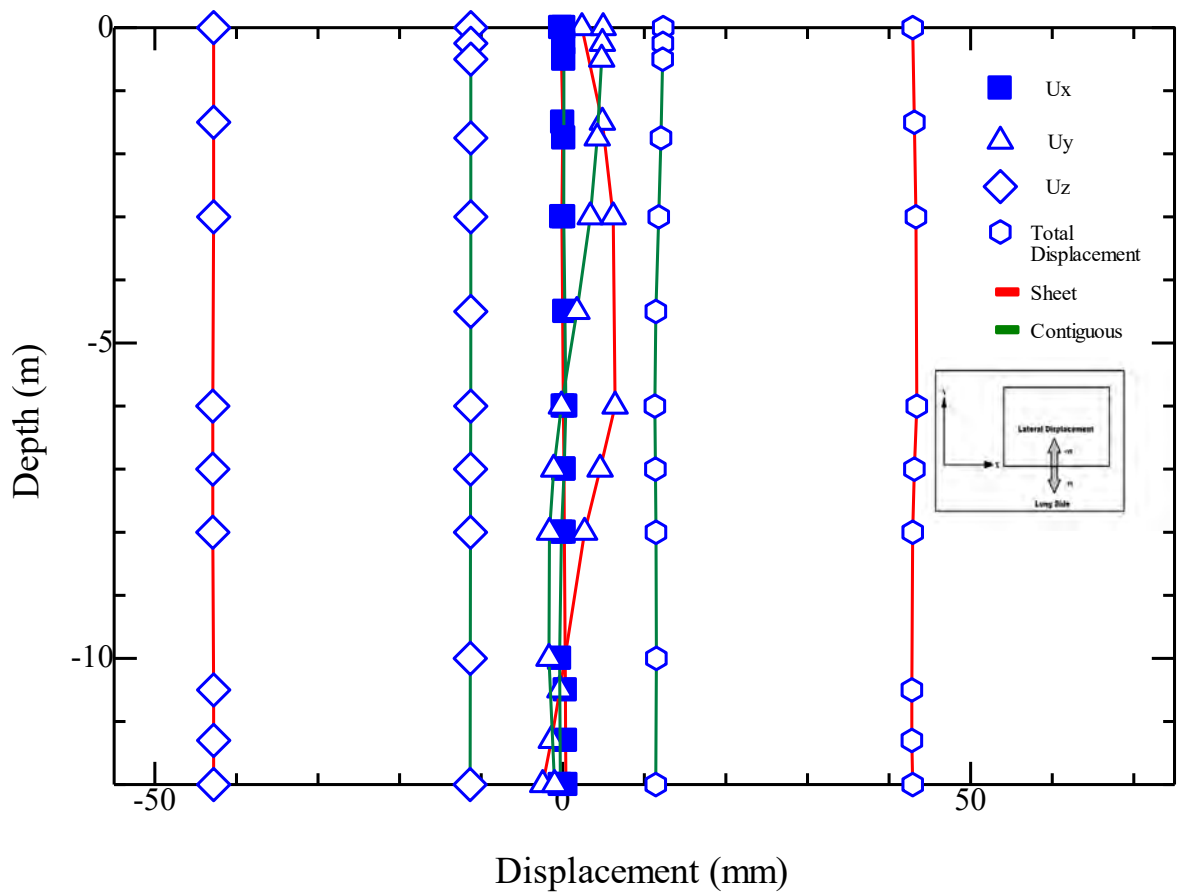


Fig. 5.15 Sheet pile wall and Contiguous pile wall displacement of Chittagong site having double basement system in the long side –MC model

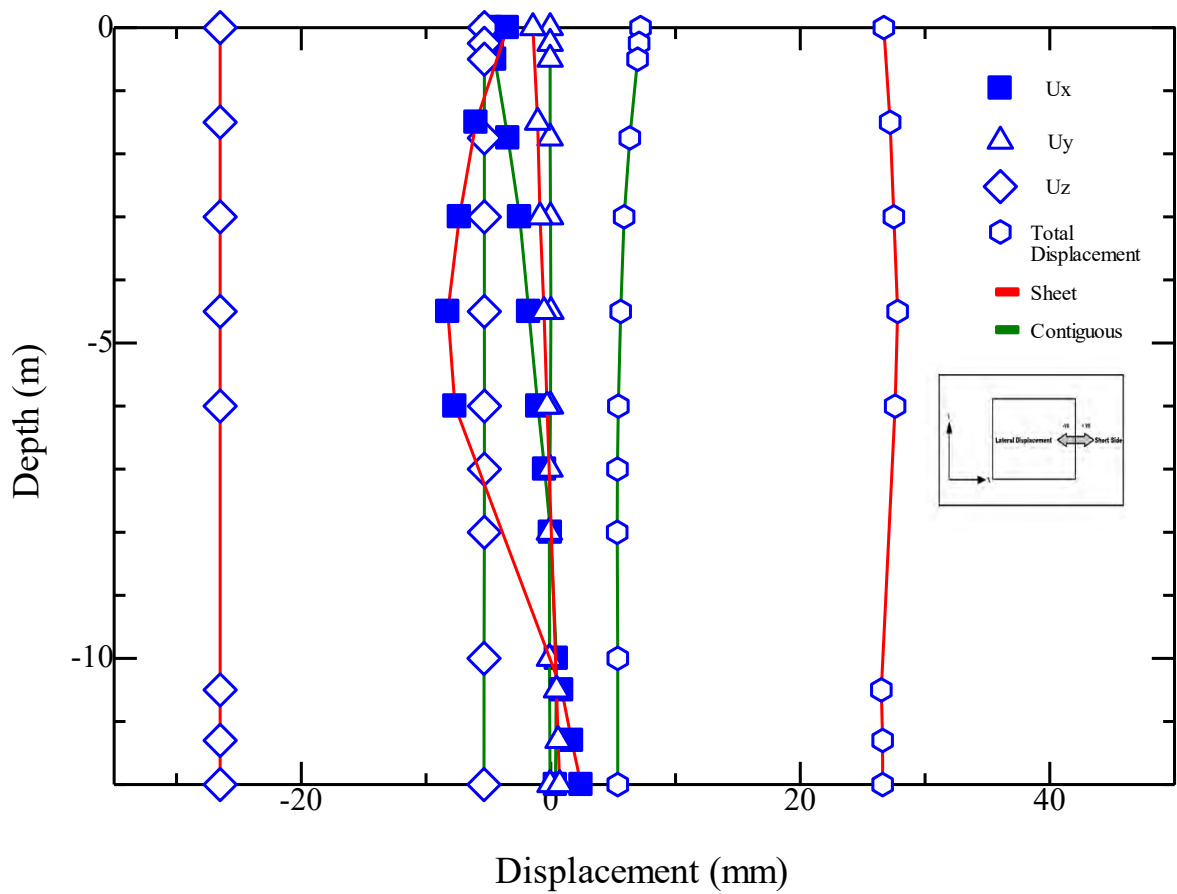


Fig. 5.16 Sheet pile wall and Contiguous pile wall displacement of Chittagong site having double basement system in the short side –MC model

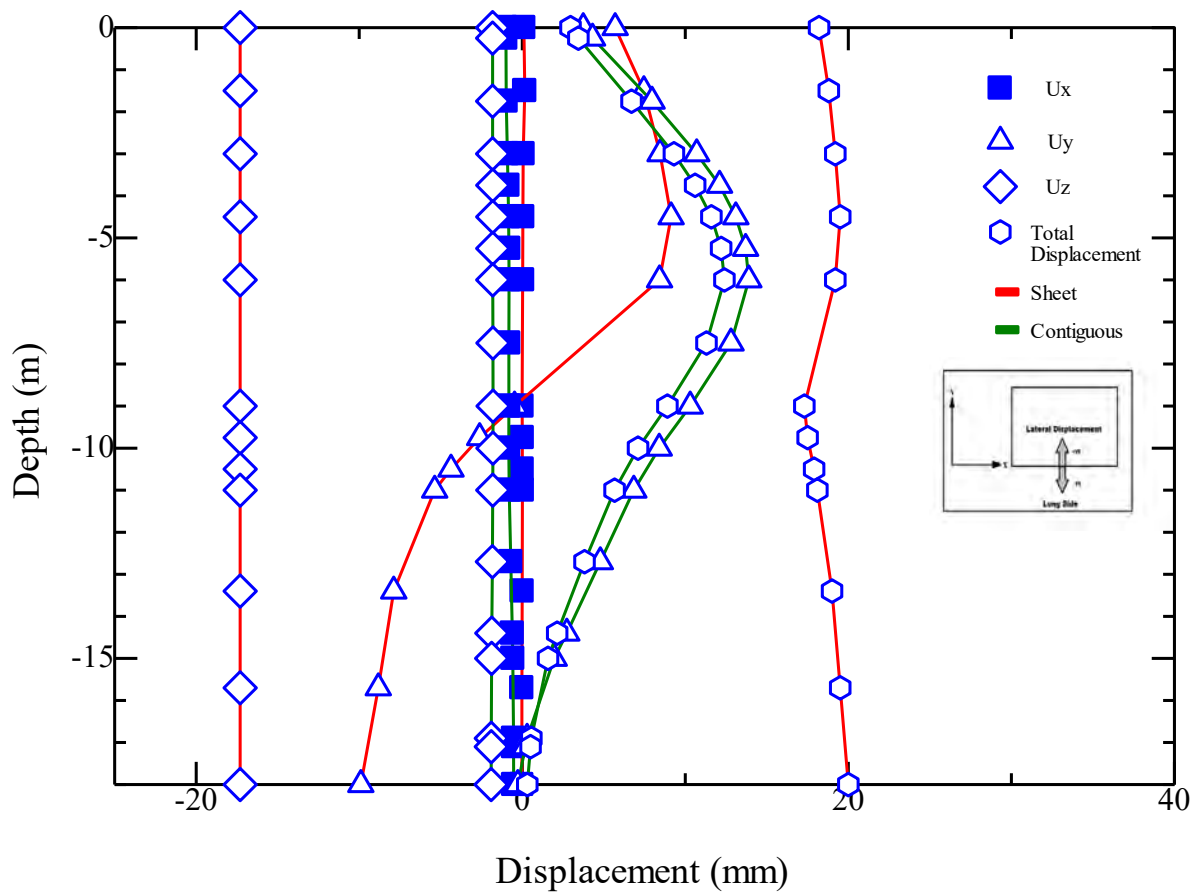


Fig. 5.17 Sheet pile wall and Contiguous pile wall displacement of Chittagong site having triple basement system in the long side –MC model

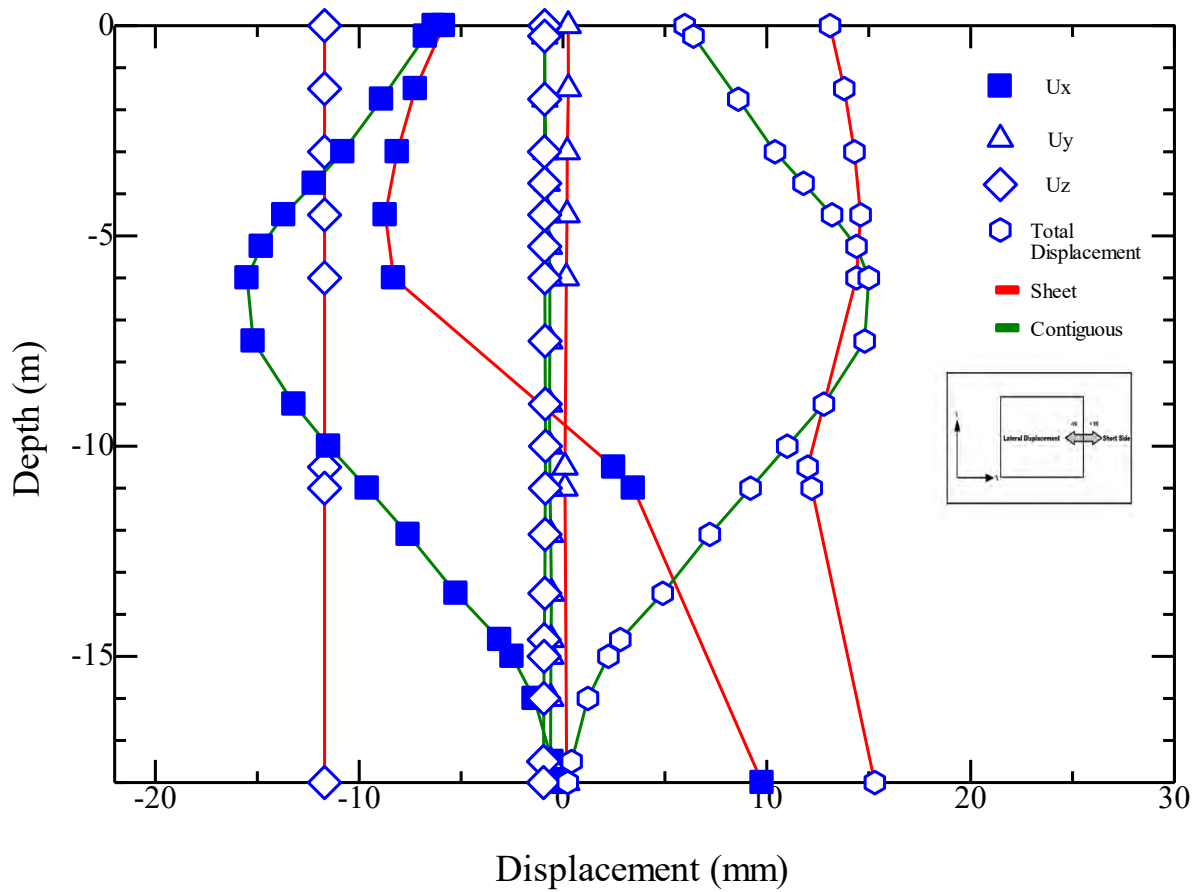


Fig. 5.18 Sheet pile wall and Contiguous pile wall displacement of Chittagong site having triple basement system in the short side –MC model

The sheet pile wall and contiguous pile wall displacement of Chittagong site having single, double and triple basement system in the long side and short side of sheet pile and contiguous pile obtained by HS model are shown in Fig. 5.19-5.24.

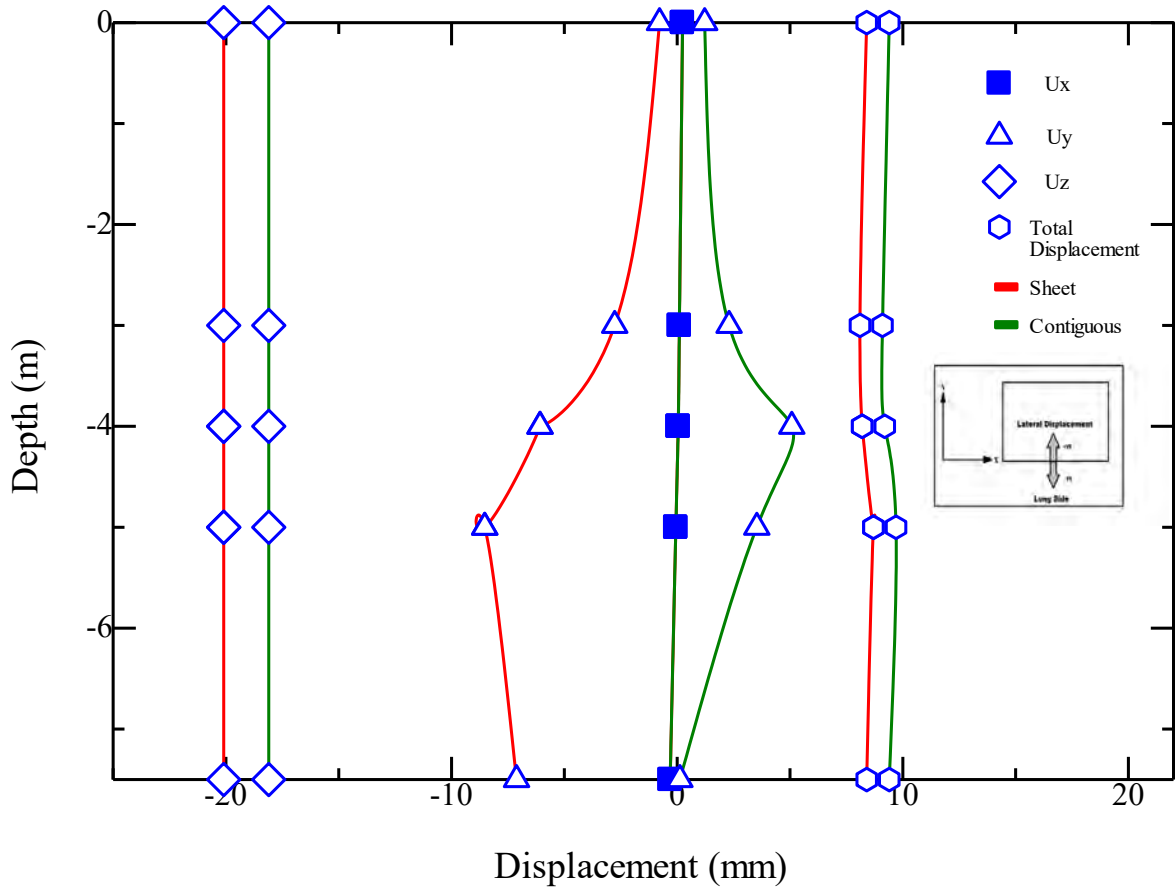


Fig. 5.19 Sheet pile wall and Contiguous pile wall displacement of Chittagong site having single basement system in the long side –HS model

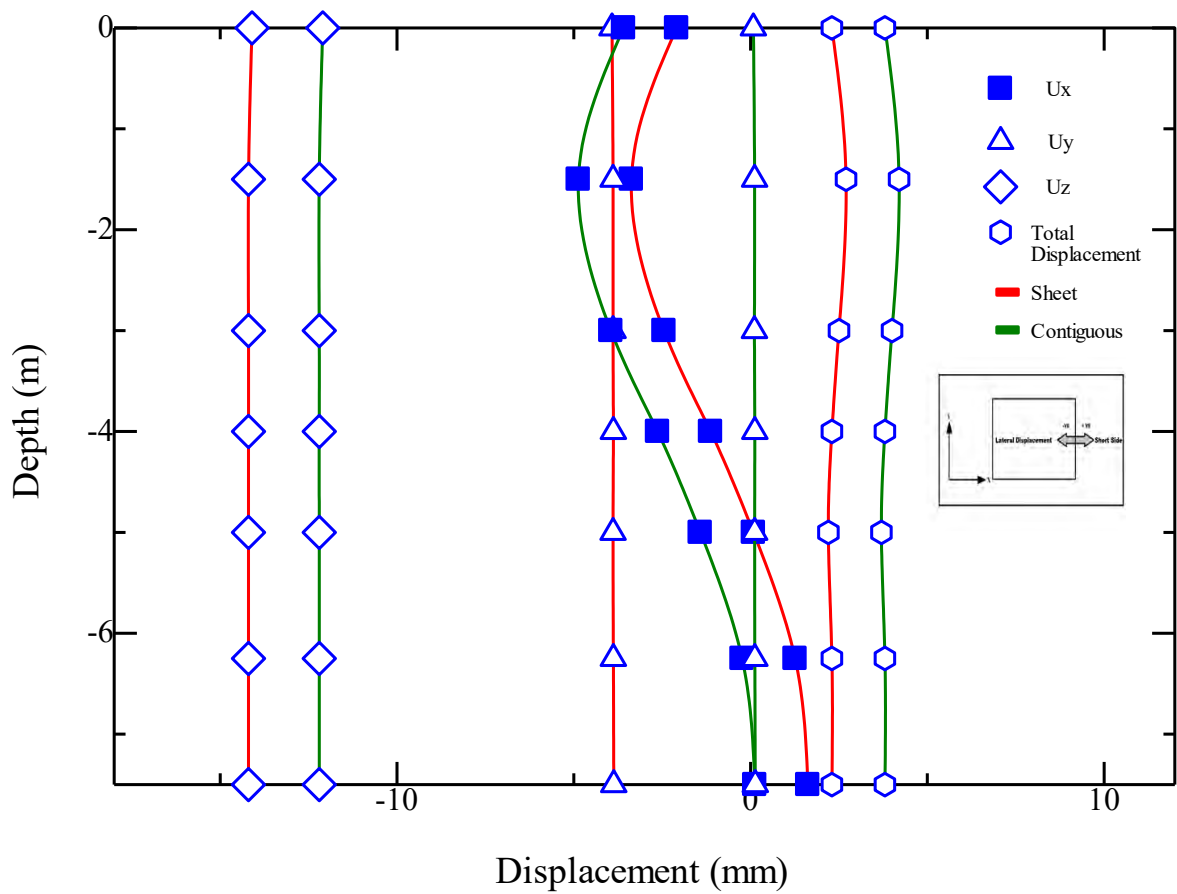


Fig. 5.20 Sheet pile wall and Contiguous pile wall displacement of Chittagong site having single basement system in the short side -HS model

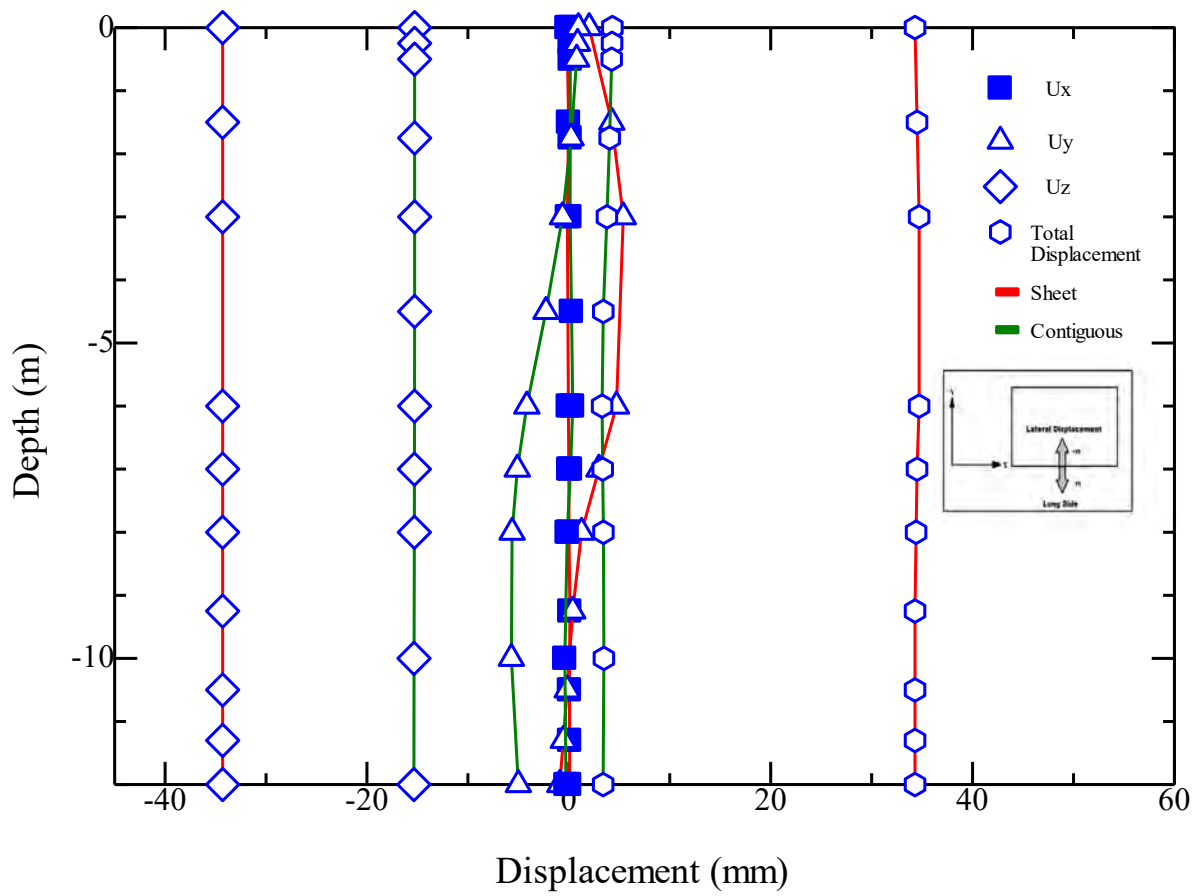


Fig. 5.21 Sheet pile wall and Contiguous pile wall displacement of Chittagong site having double basement system in the long side –HS model

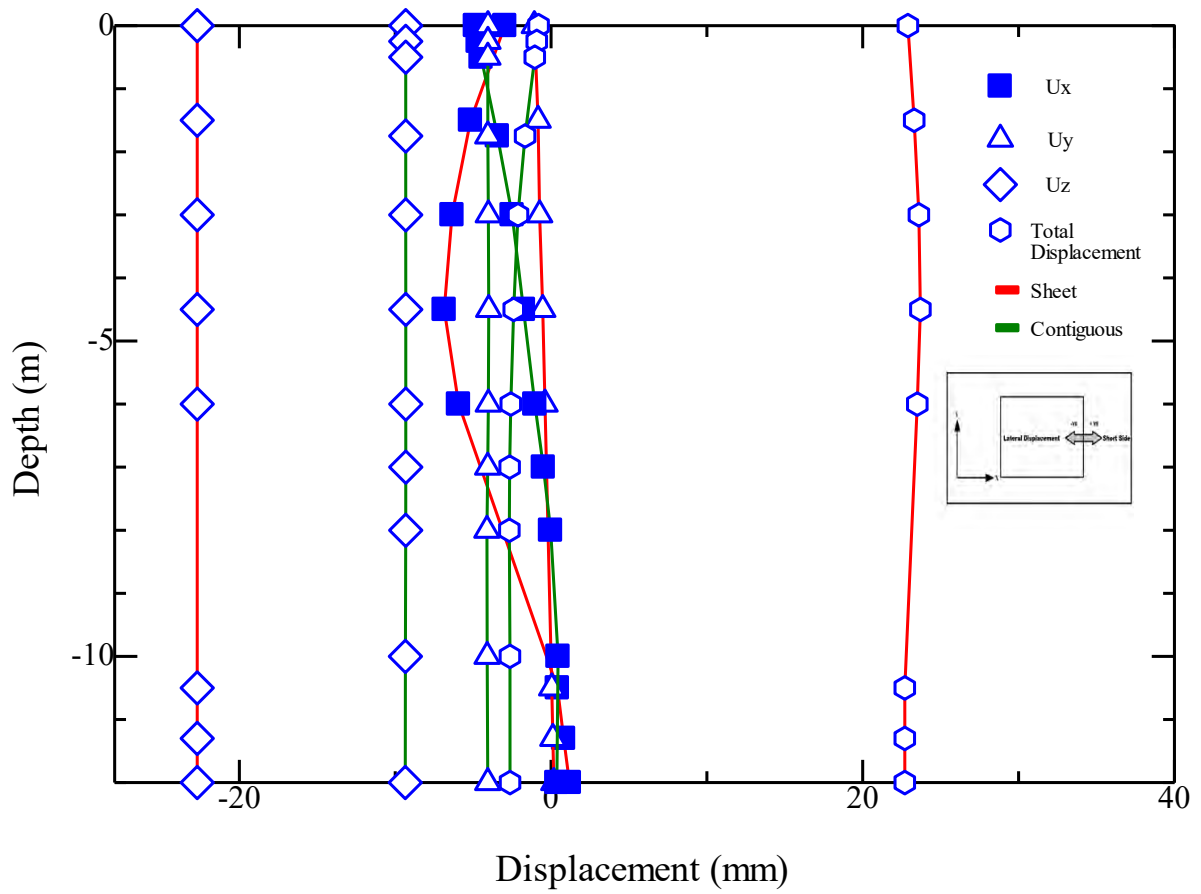


Fig. 5.22 Sheet pile wall and Contiguous pile wall displacement of Chittagong site having double basement system in the short side –HS model

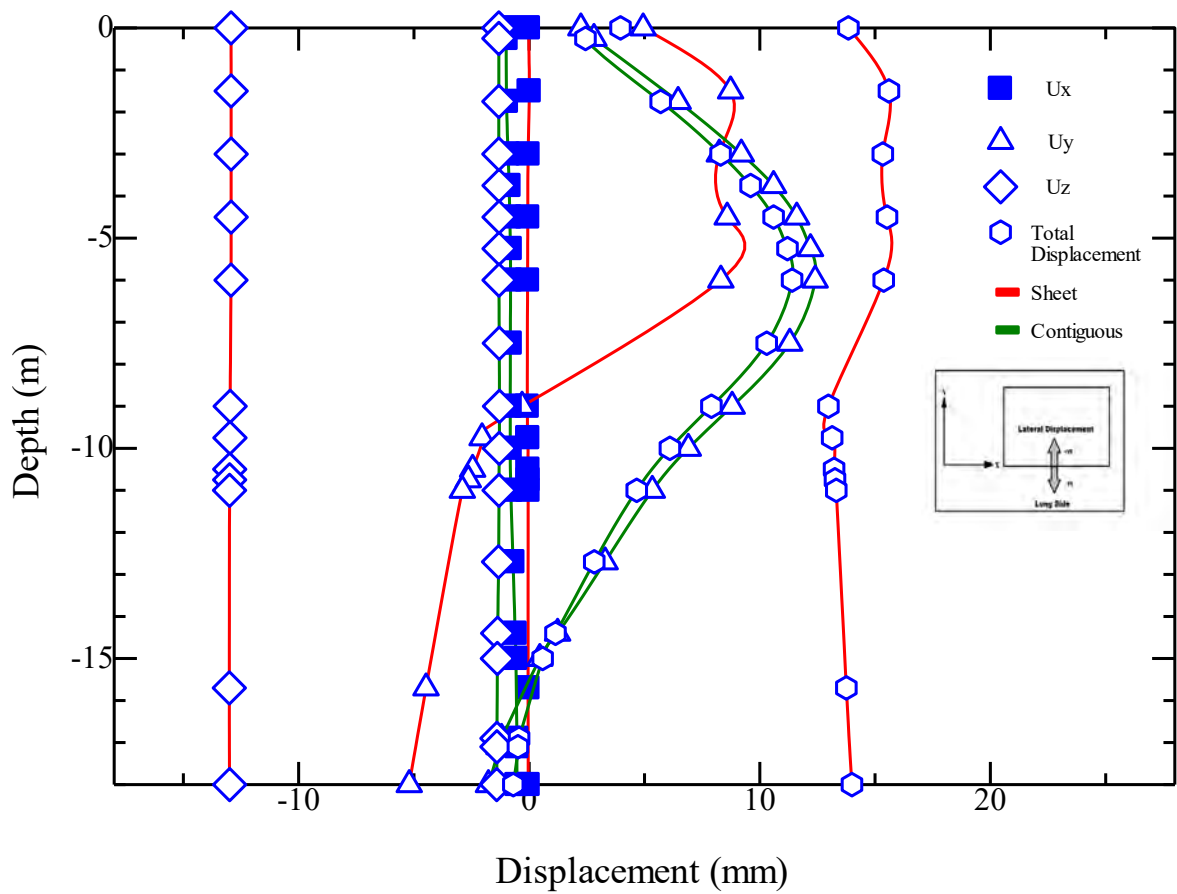


Fig. 5.23 Sheet pile wall and Contiguous pile wall displacement of Chittagong site having triple basement system in the long side –HS model

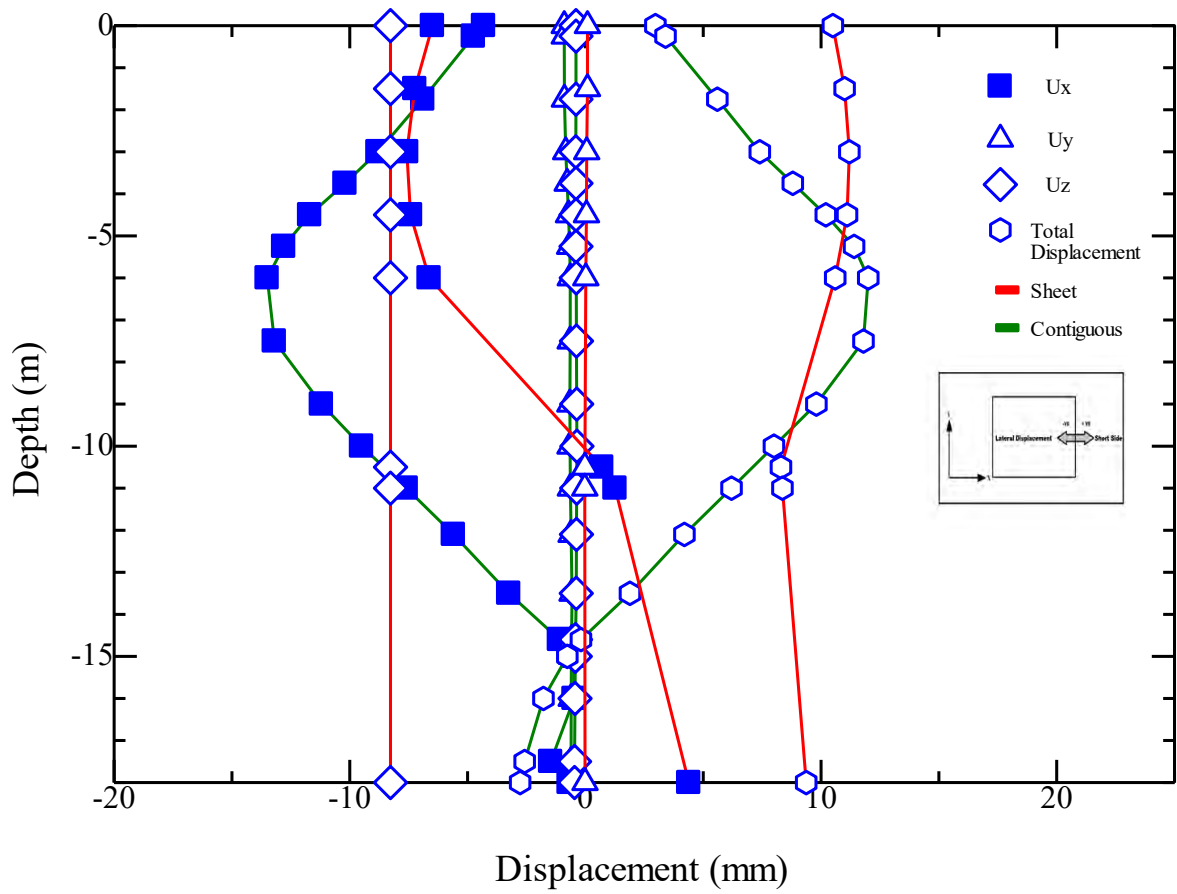


Fig. 5.24 Sheet pile wall and Contiguous pile wall displacement of Chittagong site having triple basement system in the short side –HS model

In this study, it is noticed that the sheet pile wall and contiguous pile wall experience a greater amount of displacement in case of single basement system when the penetration depth of the sheet pile wall and contiguous pile wall is double than the excavation depth. Although, they can be used as a temporary structure but cannot be used permanently like other scenarios of this study. However, it is observed that the sheet pile wall and contiguous pile wall displacement could be reduced by increasing the wall penetration depth and makes them usable like other scenarios. According to the study of Amer (2013), wall displacement can be reduced by increasing the penetration depth. It is also proved in this case by increasing the penetration depth by almost 50%. The result obtains for sheet pile wall and contiguous pile wall displacement of Chittagong site having single basement system shows that sheet pile wall faces 20% more wall movement in the long side and 66% in the short side of the contiguous pile wall in case of MC model. The result of HS model shows that sheet pile wall move towards the retained soil in the long side whereas the contiguous pile wall moves away from the retained soil. The walls move towards the retained soil in the short side of both walls. However, total displacement of contiguous pile is less than the sheet pile wall. Moreover, vertical displacement of contiguous pile wall is lower than the sheet pile wall.

In double basement system, the total displacement of the sheet pile wall is almost 3 times higher than the contiguous pile wall in case of MC model and 8 times in case of HS model. Anchor might be used to reduce the wall displacement in case of sheet pile wall. Moreover, bulging and vertical displacement is also higher in sheet pile wall than the contiguous pile wall.

In triple basement system, the total displacement of sheet pile wall is 35% higher than the contiguous pile wall in case of MC model and 7% in case of HS model. The contiguous pile wall shows better performance than the sheet pile wall in the consideration of vertical displacement.

It is noticed that the HS model predicted lower than the MC model due to the incorporation of three stiffness moduli. Moreover, it is found that sheet pile wall displacement experienced both inward and outward movement from the retained soil in case of the single basement system and triple basement system due to the presence of soft clay. It is recommend to use anchor system to reduce the wall displacement of Chittagong

site while using the sheet pile wall as retention system. Again, multiple struts level helps to reduce the movement according to the study of Bilgin and Erten (2009) which is also noticed in this case for the basement system having the same ratio of penetration depth. The result obtained for sheet pile wall and contiguous pile wall displacement of Chittagong site having single, double and triple basement system is outlined in Table 5.13 and Table 5.14.

Table 5.13 Sheet pile wall displacement of Chittagong site having single, double and triple basement system

Basement System	Soil model	Side of the wall	Maximum Lateral Displacement (mm)	Location of Maximum lateral displacement	Maximum Total Displacement (mm)
Single	MC	Long	4	5m below the ground surface	18
	HS	Long	9	5m below the ground surface	9
	MC	Short	3.5	2m below the ground surface	11
	HS	Short	4	2m below the ground surface	3
Double	MC	Long	8	1.5m below the ground surface	42
	HS	Long	8	1.5m below the ground surface	33
	MC	Short	10	6m below the ground surface	27
	HS	Short	7	6m below the ground surface	21
Triple	MC	Long	10	7m below the ground surface	20
	HS	Long	9	7m below the ground surface	15
	MC	Short	10	5m below the ground surface	14
	HS	Short	9	5m below the ground surface	12

Table 5.14 Contiguous pile wall displacement of Chittagong site having single, double and triple basement system

Basement System	Soil model	Side of the wall	Maximum Lateral Displacement (mm)	Location of Maximum lateral displacement	Maximum Total Displacement (mm)
Single	MC	Long	5	3m below the ground surface	11
	HS	Long	5	3m below the ground surface	9
	MC	Short	6	1.5m below the ground surface	6
	HS	Short	5	1.5m below the ground surface	4
Double	MC	Long	5	top of the wall	12
	HS	Long	6	top of the wall	4
	MC	Short	5	top of the wall	13
	HS	Short	5	top of the wall	4
Triple	MC	Long	13	6m below the ground surface	14
	HS	Long	11	6m below the ground surface	13
	MC	Short	15	6m below the ground surface	15
	HS	Short	13	6m below the ground surface	14

The comparisons of the output result with the available conventional method are shown in Table 5.15 to Table 5.20.

Table 5.15 A comparison of output result with available literature for the displacement of sheet pile wall and contiguous pile wall for Chittagong site having single basement system for MC model.











Researcher/ Research group	Basis of the comparison	Result from the literature	Result from sheet pile model	Result from contiguous pile model	Color code to show the Matching Condition
Clough and O'Rourke (1990)	Lateral Displacement	6 mm	4mm	3mm	Sheet pile wall  Contiguous pile wall 
Clough and O'Rourke (1990)	Lateral Displacement	18mm	4mm	3mm	Sheet pile wall  Contiguous pile wall 
Yandzio (1998)	Lateral Displacement	Bottom of the wall assumed not to displace	Not matched	Matched	Sheet pile wall  Contiguous pile wall 
National Engineering Handbook (2007)	Maximum total displacement	25mm- 75mm	18mm	11mm	Sheet pile wall  Contiguous pile wall 
Kung (2009)	Lateral Displacement	6mm	4mm	3mm	Sheet pile wall  Contiguous pile wall 

Table 5.16 A comparison of output result with available literature for the displacement of sheet pile wall and contiguous pile wall for Chittagong site having single basement system for HS model.











Researcher/ Research group	Basis of the comparison	Result from the literature	Result from the sheet pile wall model	Result from the contiguous pile wall model	Color code to show the Matching Condition
Clough and O'Rourke (1990)	Lateral Displacement	6 mm	9mm	5mm	Sheet pile wall  Contiguous pile wall 
Clough and O'Rourke (1990)	Lateral Displacement	18mm	9mm	5mm	Sheet pile wall  Contiguous pile wall 
Yandzio (1998)	Lateral Displacement	Bottom of the wall assumed not to displace	Not matched	Matched	Sheet pile wall  Contiguous pile wall 
National Engineering Handbook (2007)	Maximum total displacement		9mm	9mm	Sheet pile wall  Contiguous pile wall 
Kung (2009)	Lateral Displacement	6mm	9mm	5mm	Sheet pile wall  Contiguous pile wall 

Table 5.17 A comparison of output result with available literature for the displacement of sheet pile wall and contiguous pile wall for Chittagong site having double basement system for MC model.











Researcher/ Research group	Basis of the comparison	Result from the literature	Result from sheet pile model	Result from contiguous pile model	Color code to show the Matching Condition
Clough and O'Rourke (1990)	Lateral Displacement	12mm	10mm	5mm	Sheet pile wall  Contiguous pile wall 
Clough and O'Rourke (1990)	Lateral Displacement	18mm	10mm	5mm	Sheet pile wall  Contiguous pile wall 
Yandzio (1998)	Lateral Displacement	Bottom of the wall assumed not to displace	Matched	Matched	Sheet pile wall  Contiguous pile wall 
National Engineering Handbook (2007)	Maximum total displacement	25mm- 75mm	42mm	13mm	Sheet pile wall  Contiguous pile wall 
Kung (2009)	Lateral Displacement	12mm	10mm	5mm	Sheet pile wall  Contiguous pile wall 

Table 5.18 A comparison of output result with available literature for the displacement of sheet pile wall and contiguous pile wall for Chittagong site having double basement system for HS model.



Researcher/ Research group	Basis of the comparison	Result from the literature	Result from the sheet pile wall model	Result from the contiguous pile wall model	Color code to show the Matching Condition
Clough and O'Rourke (1990)	Lateral Displacement	12mm	8mm	6mm	Sheet pile wall  Contiguous pile wall 
Clough and O'Rourke (1990)	Lateral Displacement	18mm	8mm	mm	Sheet pile wall  Contiguous pile wall 
Yandzio (1998)	Lateral Displacement	Bottom of the wall assumed not to displace	Matched	Matched	Sheet pile wall  Contiguous pile wall 
National Engineering Handbook (2007)	Maximum total displacement	25mm- 75mm	33mm	4mm	Sheet pile wall  Contiguous pile wall 
Kung (2009)	Lateral Displacement	12mm	8mm	6mm	Sheet pile wall  Contiguous pile wall 

Table 5.19 A comparison of output result with available literature for the displacement of sheet pile wall and contiguous pile wall for Chittagong site having triple basement system for MC model.





















Researcher/ Research group	Basis of the comparison	Result from the literature	Result from sheet pile model	Result from contiguous pile model	Color code to show the Matching Condition
Clough and O'Rourke (1990)	Lateral Displacement	18mm	10mm	15mm	Sheet pile wall  Contiguous pile wall 
Clough and O'Rourke (1990)	Lateral Displacement	18mm	10mm	15mm	Sheet pile wall  Contiguous pile wall 
Yandzio (1998)	Lateral Displacement	Bottom of the wall assumed not to displace	Not matched	Matched	Sheet pile wall  Contiguous pile wall 
National Engineering Handbook (2007)	Maximum total displacement	25mm- 75mm	20mm	15mm	Sheet pile wall  Contiguous pile wall 
Kung (2009)	Lateral Displacement	18mm	10mm	15mm	Sheet pile wall  Contiguous pile wall 

Table 5.20 A comparison of output result with available literature for the displacement of sheet pile wall and contiguous pile wall for Chittagong site having triple basement system for HS model.

Researcher/ Research group	Basis of the comparison	Result from the literature	Result from the sheet pile wall model	Result from the contiguous pile wall model	Color code to show the Matching Condition
Clough and O'Rourke (1990)	Lateral Displacement	18mm	9mm	13mm	Sheet pile wall  Contiguous pile wall 
Clough and O'Rourke (1990)	Lateral Displacement	18mm	9mm	13mm	Sheet pile wall  Contiguous pile wall 
Yandzio (1998)	Lateral Displacement	Bottom of the wall assumed not to displace	Not matched	Matched	Sheet pile wall  Contiguous pile wall 
National Engineering Handbook (2007)	Maximum total displacement	25mm- 75mm	15mm	14mm	Sheet pile wall  Contiguous pile wall 
Kung (2009)	Lateral Displacement	18mm	9mm	13mm	Sheet pile wall  Contiguous pile wall 

5.2.5 Comparison between the sheet pile wall and the contiguous pile wall

The comparison between sheet pile wall and contiguous pile wall for both Dhaka soil and Chittagong soil having different basement system is shown in Table 5.21.

Table 5.21 Comparison between Sheet pile wall and contiguous pile wall

Site	Basement system	Soil model	Maximum displacement for sheet pile wall (mm)	Maximum displacement for contiguous pile wall (mm)	Best option based on the resisting wall movement
Dhaka Site	Single	MC	28	22	Contiguous pile wall
		HS	20	19	Contiguous pile wall
	Double	MC	20	18	Contiguous pile wall
		HS	15	8	Contiguous pile wall
	Triple	MC	14	16	Sheet pile wall
		HS	11	7	Contiguous pile wall
Chittagong Site	Single	MC	18	11	Contiguous pile wall
		HS	9	9	Both
	Double	MC	42	13	Contiguous pile wall
		HS	33	4	Contiguous pile wall
	Triple	MC	20	15	Contiguous pile wall
		HS	15	14	Contiguous pile wall

In most cases, it is evident that the contiguous pile wall shows better performance than the sheet pile wall to reduce the wall movement. The contiguous pile wall movement is in average 20% lower than the sheet pile wall movement in case of Dhaka site, and the percentage is more in case of Chittagong site. So, it is evident that the contiguous pile wall performs better in the ground comprised of soft clay such as Chittagong soil. It is recommended that contiguous pile wall is more viable than the sheet pile wall in case of countering wall movement.

5.3 Internal forces of retaining wall

This section investigates the internal forces, namely axial, shear and moments of sheet pile wall and contiguous pile wall associated with the excavation work. The differences between the sheet pile wall and contiguous pile wall and the MC model and the HS from the original design are presented here for comparison. Due to the availability of large amount of data, output results are shown in **APPENDIX B** and the summarized results are shown in Table 5.22 to Table 5.27.

Table 5.22 Axial force of retaining wall in Dhaka soil having different basement system

Retaining System	Site	Basement System	Soil Model	Side of the Retaining system	Maximum Positive axial force (kN)	Maximum Negative axial force (kN)
Sheet Pile Wall	Dhaka Site	Single	MC	Long	320	180
			MC	Short	25	12
			HS	Long	70	110
			HS	Short	13	7
Sheet Pile Wall	Dhaka Site	Double	MC	Long	80	160
			MC	Short	40	75
			HS	Long	60	150
			HS	Short	35	70
Sheet Pile Wall	Dhaka Site	Triple	MC	Long	105	60
			MC	Short	105	15
			HS	Long	180	190
			HS	Short	170	190
Contiguous Pile Wall	Dhaka Site	Single	MC	Long	55	10
			MC	Short	43	0
			HS	Long	90	10
			HS	Short	60	2
Contiguous Pile Wall	Dhaka Site	Double	MC	Long	40	70
			MC	Short	30	30
			HS	Long	38	65
			HS	Short	30	28
Contiguous Pile Wall	Dhaka Site	Triple	MC	Long	140	25
			MC	Short	11	5
			HS	Long	100	55
			HS	Short	110	50

Table 5.23 Axial force of retaining wall in Chittagong Site having different basement system

Retaining System	Site	Basement System	Soil Model	Side of the Retaining system	Maximum Positive axial force (kN)	Maximum Negative axial force (kN)
Sheet Pile Wall	Chittagong Site	Single	MC	Long	28	5
			MC	Short	28	5
			HS	Long	27	5
			HS	Short	27	5
Sheet Pile Wall	Chittagong Site	Double	MC	Long	230	150
			MC	Short	120	70
			HS	Long	110	140
			HS	Short	90	50
Sheet Pile Wall	Chittagong Site	Triple	MC	Long	110	40
			MC	Short	60	110
			HS	Long	60	60
			HS	Short	20	35
Contiguous Pile Wall	Chittagong Site	Single	MC	Long	26	5
			MC	Short	25	5
			HS	Long	24	5
			HS	Short	24	6
Contiguous Pile Wall	Chittagong Site	Double	MC	Long	100	0
			MC	Short	52	8
			HS	Long	95	0
			HS	Short	50	8
Contiguous Pile Wall	Chittagong Site	Triple	MC	Long	100	45
			MC	Short	50	100
			HS	Long	50	55
			HS	Short	18	35

Table 5.24 Shear force of retaining wall in Dhaka Site having different basement system

Retaining System	Site Type	Basement System	Soil Model	Side of the Retaining system	Maximum Positive shear force (kN)	Maximum Negative shear force (kN)
Sheet Pile Wall	Dhaka Site	Single	MC	Long	40	30
			MC	Short	12	35
			HS	Long	45	35
			HS	Short	10	35
Sheet Pile Wall	Dhaka Site	Double	MC	Long	220	80
			MC	Short	30	120
			HS	Long	200	80
			HS	Short	25	120
Sheet Pile Wall	Dhaka Site	Triple	MC	Long	40	35
			MC	Short	12	35
			HS	Long	55	30
			HS	Short	10	55
Contiguous Pile Wall	Dhaka Site	Single	MC	Long	40	50
			MC	Short	8	8
			HS	Long	75	40
			HS	Short	4	6.5
Contiguous Pile Wall	Dhaka Site	Double	MC	Long	60	150
			MC	Short	7	7
			HS	Long	55	140
			HS	Short	6	6
Contiguous Pile Wall	Dhaka Site	Triple	MC	Long	50	110
			MC	Short	55	60
			HS	Long	65	55
			HS	Short	8.5	4.5

Table 5.25 Shear force of retaining wall in Chittagong Site having different basement system

Retaining System	Site Type	Basement System	Soil Model	Side of the Retaining system	Maximum Positive shear force (kN)	Maximum Negative shear force (kN)
Sheet Pile Wall	Chittagong Site	Single	MC	Long	20	7
			MC	Short	20	8
			HS	Long	20	6
			HS	Short	20	6
Sheet Pile Wall	Chittagong Site	Double	MC	Long	35	50
			MC	Short	40	42
			HS	Long	75	75
			HS	Short	40	45
Sheet Pile Wall	Chittagong Site	Triple	MC	Long	55	20
			MC	Short	25	38
			HS	Long	40	20
			HS	Short	10	28
Contiguous Pile Wall	Chittagong Site	Single	MC	Long	20	6
			MC	Short	18	6
			HS	Long	17	5
			HS	Short	17	5
Contiguous Pile Wall	Chittagong Site	Double	MC	Long	35	60
			MC	Short	4	12
			HS	Long	25	55
			HS	Short	4	11
Contiguous Pile Wall	Chittagong Site	Triple	MC	Long	50	20
			MC	Short	22	34
			HS	Long	35	18
			HS	Short	8	24

Table 5.26 Bending moment of retaining wall in Dhaka Site having different basement system

Retaining System	Site Type	Basement System	Soil Model	Side of the Retaining system	Maximum Positive bending moment (kN-m)	Maximum Negative bending moment (kN-m)
Sheet Pile Wall	Dhaka Site	Single	MC	Long	11	10
			MC	Short	5.5	5.5
			HS	Long	10	8
			HS	Short	6.5	5
Sheet Pile Wall	Dhaka Site	Double	MC	Long	60	30
			MC	Short	40	30
			HS	Long	58	35
			HS	Short	40	30
Sheet Pile Wall	Dhaka Site	Triple	MC	Long	18	14
			MC	Short	11	10
			HS	Long	20	12
			HS	Short	15	18
Contiguous Pile Wall	Dhaka Site	Single	MC	Long	18	25
			MC	Short	4.5	1.5
			HS	Long	30	33
			HS	Short	3.5	1
Contiguous Pile Wall	Dhaka Site	Double	MC	Long	50	85
			MC	Short	4.5	2
			HS	Long	45	85
			HS	Short	4.5	2
Contiguous Pile Wall	Dhaka Site	Triple	MC	Long	80	50
			MC	Short	5	5
			HS	Long	50	58
			HS	Short	2	2

Table 5.27 Bending moment of retaining wall in Chittagong Site having different basement system

Retaining System	Site Type	Basement System	Soil Model	Side of the Retaining system	Maximum Positive bending moment (kN-m)	Maximum Negative bending moment (kN-m)
Sheet Pile Wall	Chittagong Site	Single	MC	Long	6	8
			MC	Short	6	8.5
			HS	Long	6	7
			HS	Short	6	7
Sheet Pile Wall	Chittagong Site	Double	MC	Long	5	8
			MC	Short	10	10
			HS	Long	6	8.5
			HS	Short	6	8
Sheet Pile Wall	Chittagong Site	Triple	MC	Long	14	12
			MC	Short	14	14
			HS	Long	13	8
			HS	Short	7	6
Contiguous Pile Wall	Chittagong Site	Single	MC	Long	6	7
			MC	Short	6	7
			HS	Long	6	7
			HS	Short	6	6
Contiguous Pile Wall	Chittagong Site	Double	MC	Long	25	48
			MC	Short	3	3.8
			HS	Long	25	42
			HS	Short	2.3	3.5
Contiguous Pile Wall	Chittagong Site	Triple	MC	Long	11	11
			MC	Short	13	11
			HS	Long	11	10
			HS	Short	6.5	6

The followings are the conclusions drawn from the results:

It is observed that larger wall deflections induced larger axial, shear and moment. In the MC model, the tensile force is higher in case of sheet pile wall retaining single, double and triple basement system both for Dhaka and Chittagong site than the HS model. However, in the case of contiguous pile wall compressive force is higher for Dhaka site having single and triple basement system and for other cases, tensile force is higher than the results obtained by the HS model.

The shear force is higher in case of MC model for sheet pile wall retaining Dhaka site having single and double basement system and for Chittagong site having single and triple basement system. Also, the shear force is more significant in the case MC model for contiguous pile wall retaining Dhaka site having single and triple basement system and Chittagong site having single, double and triple basement system. In general, the positive and negative moments are more significant in the case of MC model than the HS model for both sheet pile wall and contiguous pile wall, and also sheet pile wall experienced larger moment than the contiguous pile wall. Moreover, the increase in soil stiffness reduced shear in the retaining wall.

5.4 Effect of adjacent structure near to the excavation zone

In this study, the effect of the adjacent structure on the model has been investigated. Dhaka site having a double basement system have been chosen to analyze the impact of adjacent structure. It has been considered that in total 8 six -storied buildings are around the excavation area. The surcharge load that has been imposed by each building is assumed as 86kN/m^2 . The capability of both the retaining system has been checked. The displacement of the model using both the retaining system is shown in Fig. 5.21-5.22.

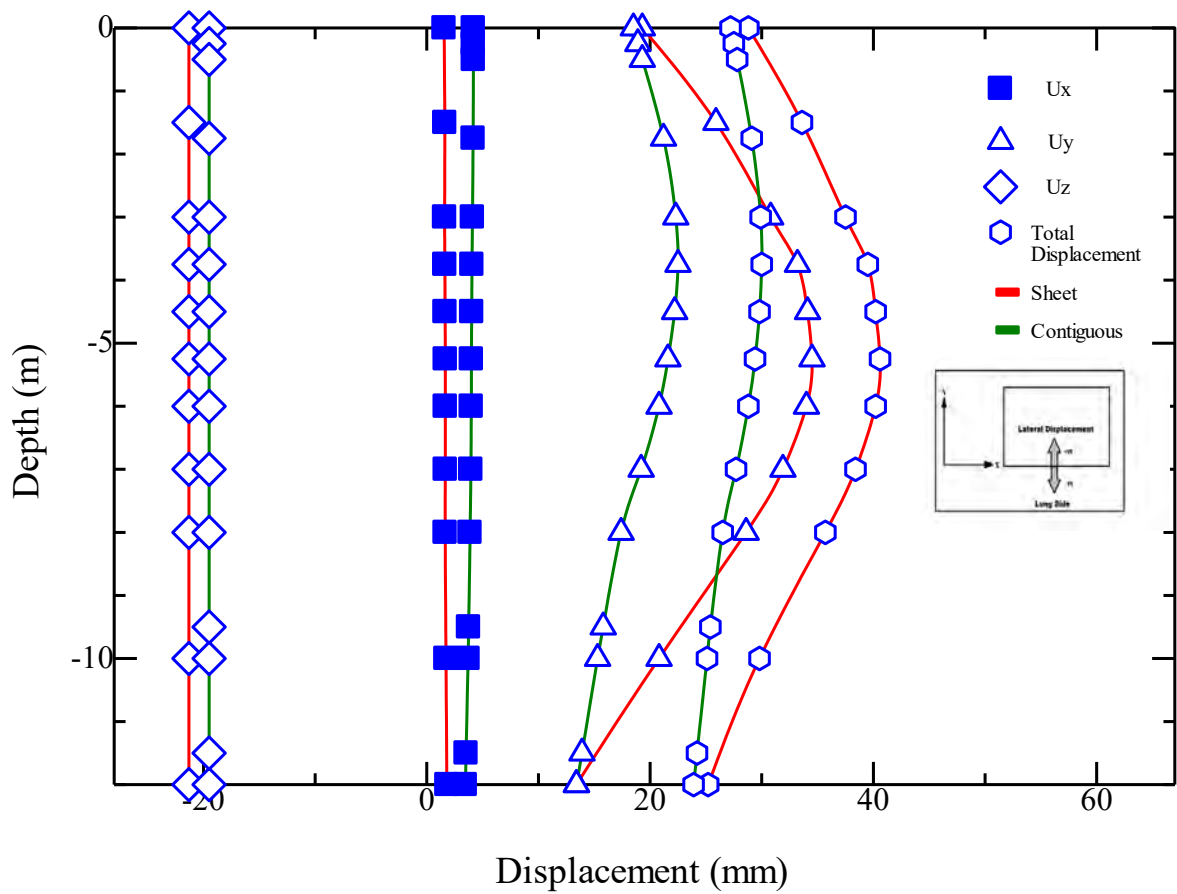


Fig. 5.21 Sheet pile wall and contiguous pile wall displacement in the long side of Dhaka site having double basement system - with presence of adjacent structure

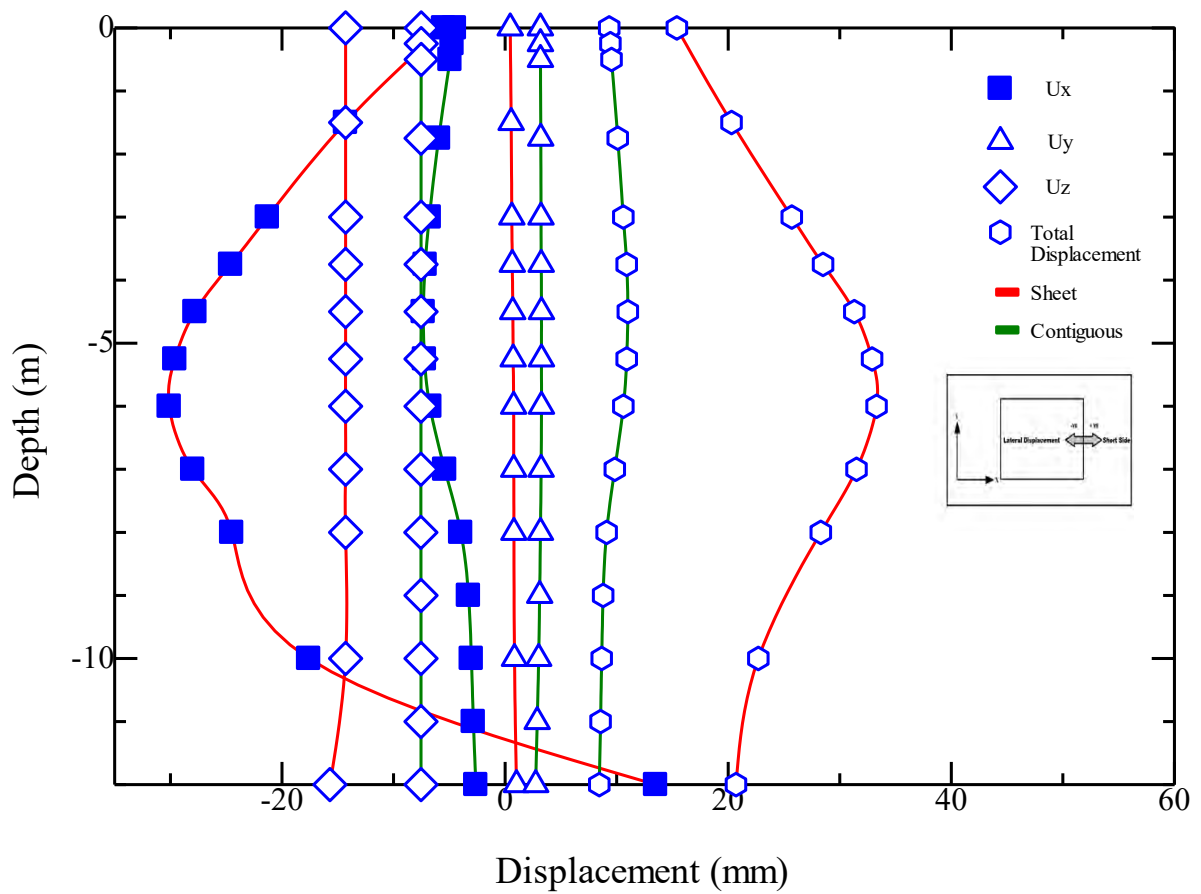


Fig. 5.22 Sheet pile wall and contiguous pile wall displacement in the short side of Dhaka site having double basement system - with presence of adjacent structure

The effect of the adjacent structure on the model is visible. It is observed from section 5.2.2 that the maximum lateral displacement is found 16mm in the long side and 21mm in the short side of the sheet pile wall without the presence of any adjacent structures. On the other hand, the maximum lateral displacement is 25mm and 27 mm respectively for the long side and short side of sheet pile wall in the presence of adjacent structures. The total movement is 23mm and 22mm for the long side, and short side of sheet pile wall without the presence of adjoining structures respectively whereas the value is 41mm and 33mm for the long side and short side of sheet pile wall in the presence of nearby structures.

The maximum lateral displacement is found 11mm in the long side and 12mm in the short side of the contiguous pile wall without the presence of any adjacent structures whereas the value is 21mm and 9mm in the long side and short side respectively in the presence of nearby structures. The total movement is 16mm and 13mm for the long side, and short side of contiguous pile wall without the presence of adjoining structures respectively whereas the value is 28mm and 13mm for the long side and short side of the contiguous pile wall in the presence of nearby structures.

It is noticed from the above discussion that the contiguous pile wall is more susceptible than the sheet pile in case of resisting wall movement with the presence of adjoining structures near the excavated area. The contiguous pile wall resist 47% less wall movement than sheet pile wall in the long side and 2.5 times less wall movement than the sheet pile wall in the short side in present of adjacent structure. In complicated urban settings, contiguous pile wall can be deployed successfully.

5.5 Effect of the number of struts in each bracing level

In this study, the influence of the number of the struts in each bracing level has been analyzed. In the actual model, six struts are used in the X direction keeping 5m spacing, and five struts are used in the Y direction maintaining the same spacing like X direction. The influence of the number of struts has been investigated by reducing the number of struts in both the direction. The struts are reduced to four struts in the X direction by maintaining 7m spacing and two struts in the Y direction by keeping 10m spacing. In this study, the influence of the number of struts in Dhaka site having a double basement system is chosen for the comparison between the sheet pile wall and the contiguous pile

wall. The wall displacements of both the sheet pile wall and contiguous pile wall are shown in Fig. 5.23-5.24.

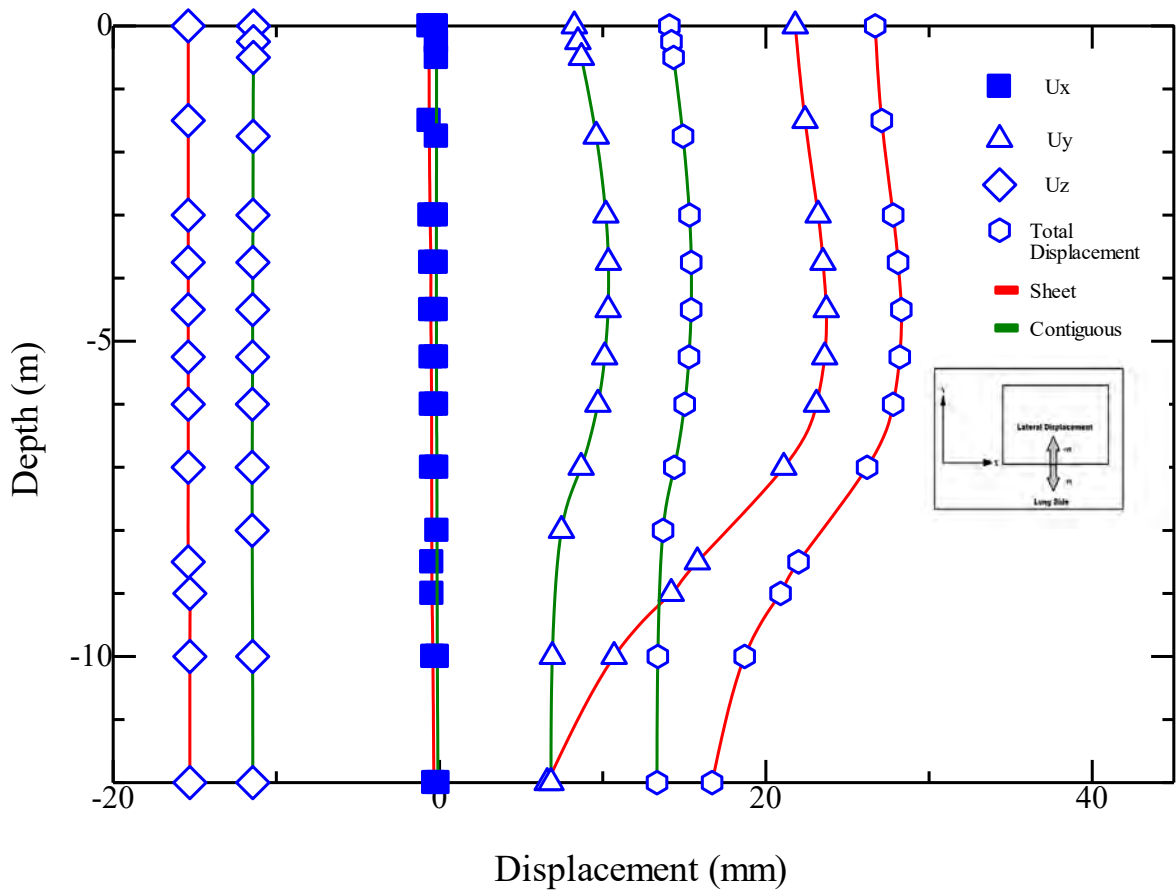


Fig. 5.23 Sheet pile and contiguous pile wall displacement of Dhaka site having double basement system in the long side – reducing the number of struts in both X and Y direction in each bracing level.

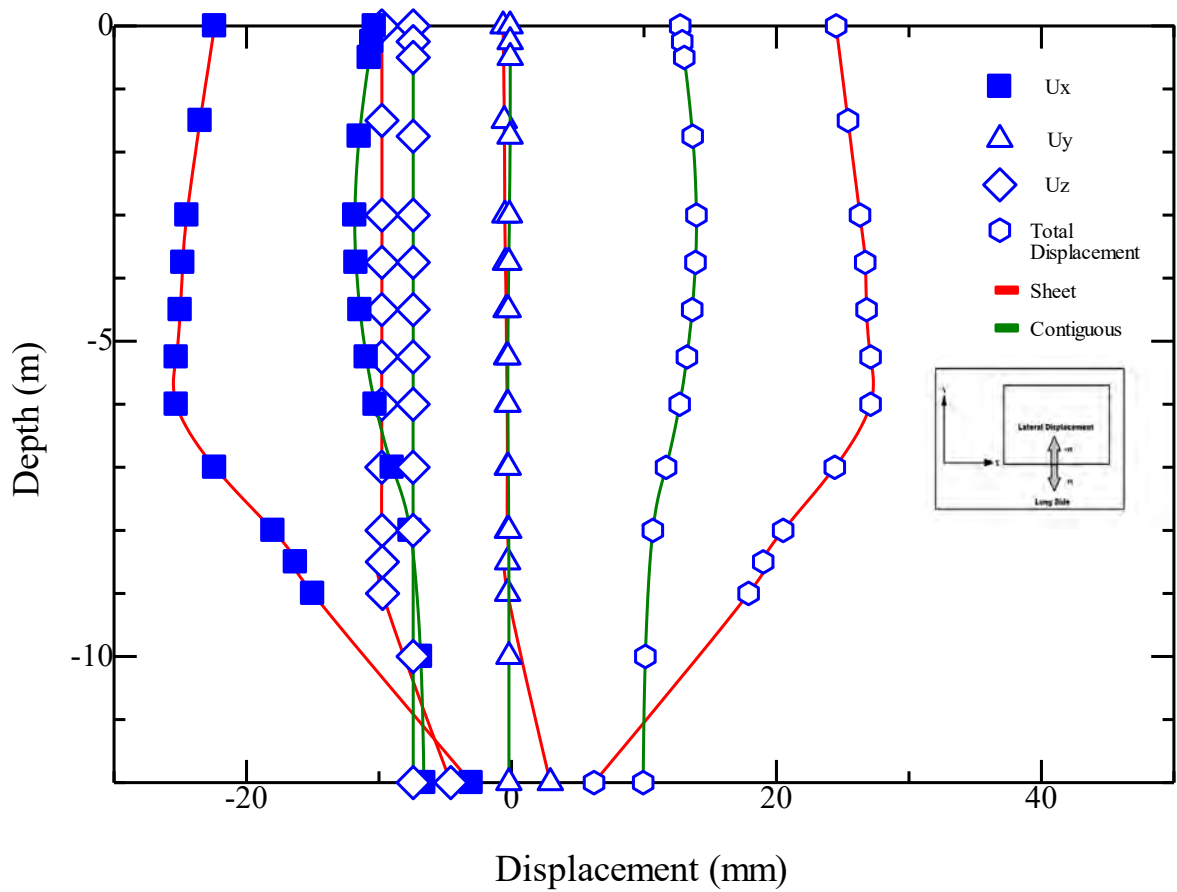


Fig. 5.24 Sheet pile and contiguous pile wall displacement of Dhaka site having double basement system in the short side – reducing the number of struts in both X and Y direction in each bracing level.

The effect of the reduction of the number of struts on the model is evident. It is discerned that the maximum lateral displacement is found from section 5.2.2 as 16mm in the long side and 21mm in the short side of the sheet pile wall containing six struts in the X direction and five struts in the Y direction of each bracing level. On the other hand, the maximum lateral displacement was 23mm and 27 mm respectively for the long side and short side of sheet pile wall while reducing the number of struts to four struts in the X direction and two struts in the Y direction. The total movement is increased by 5mm and 7mm for the long side, and short side of the sheet pile wall respectively by reducing the number of struts in each bracing system.

The maximum lateral displacement is found 11mm in the long side and 12mm in the short side of the contiguous pile wall from the section 5.2.2 whereas the value is found 11mm and 13mm in the long side and short side respectively while reducing the number of the struts. The total movement is found 16mm and 13mm for the long side, and short side of contiguous pile wall respectively from section 5.2.2 whereas the value is 16mm and 14mm for the long side and short side of the contiguous pile wall get by reducing the number of struts. The change occurs in case of contiguous pile wall due to the minimization of struts in each bracing level is quite negligible. The number of struts can be reduced the cost.

It is testified from the above discussion is that the contiguous pile wall is more capable than the sheet pile wall in case of resisting wall movement while reducing the number of struts in each bracing level in the excavated area. Again, Chowdhury et al. (2013) showed that increasing the number of struts would decrease the wall movements in case of a sheet pile wall. It is also proved in the present study in case of the sheet pile wall, and also it is concluded in the current study that in the case of the contiguous pile wall the scenario is quite negligible.

5.6 Ground settlement

Due to a large amount of data from the numerical analysis in this study, Dhaka site having a double basement system is chosen to investigate the ground settlement due to the insertion of the retaining wall. Ground surface settlement profiles of Dhaka site having a double basement system at the final stage of excavation are presented in the section.

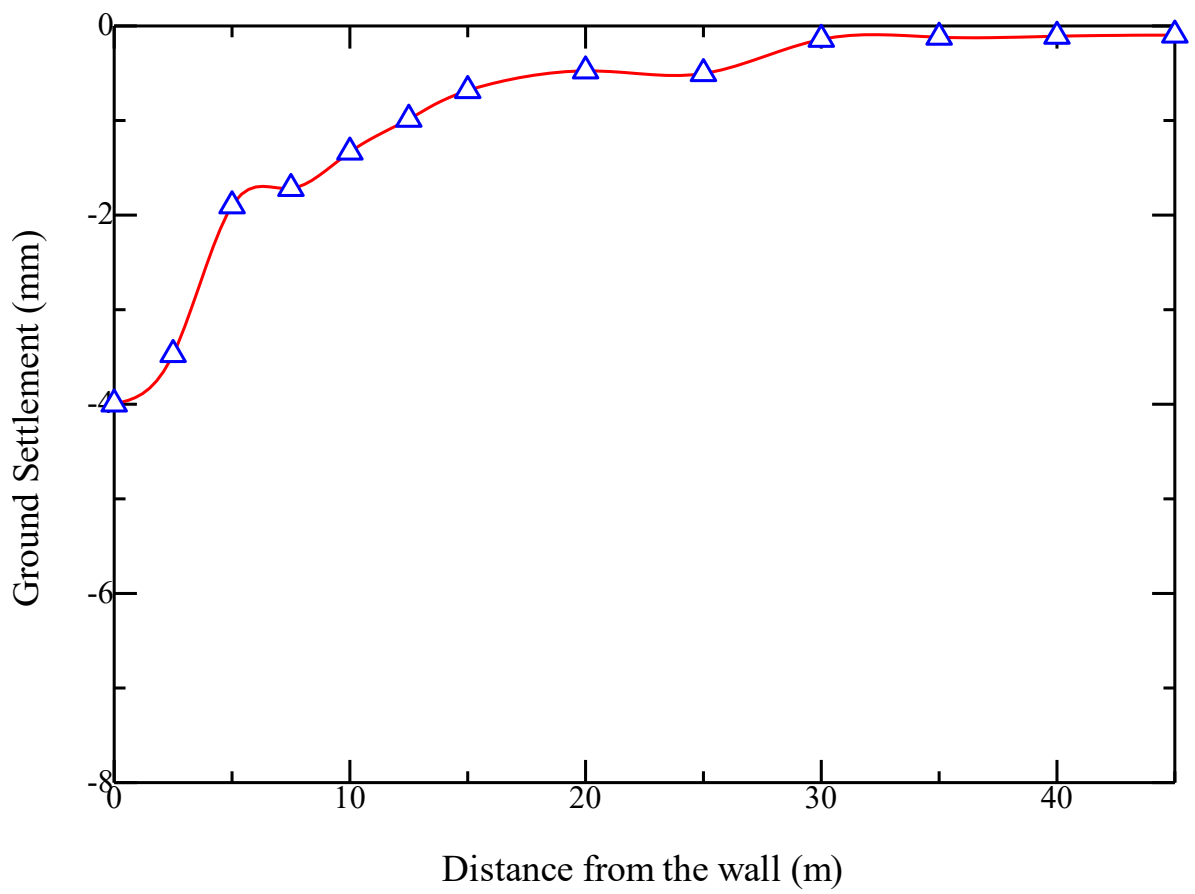




Fig. 5.25 Ground surface settlement profiles of Dhaka site having a double basement system

It is noticed from the Fig. 5.25 that the ground settlement decreased with the increase of distance from the retaining wall. Moreover, the settlement decreased up to a certain distance from the wall, and then the settlement curve became horizontal. The range to which settlement reduces with distance from the wall is termed as primary influence zone. In this study, the maximum ground settlement is found as 4mm, and the primary influence zone is extended up to 27m. A comparison is shown in the Table 5.28 with the conventional procedure available from different literature.

Table 5.28 Comparison of ground settlement of the current study with the conventional methods

Researcher	Basis of the comparison	Result from the literature	Result from the current study	Color code to represent the matching condition
Peck (1969)	Ground Settlement	Primary influence zone should be upto 25m	27m	
Clough and O'Rourke (1990)	Ground Settlement	9mm	4mm	

5.7 Basal Heave

Basal-heave failure in a braced excavation in clay may be induced by insufficient shear strength, which supports the weight of soil within the critical zone around the excavation. During an excavation, the soil outside the excavation zone moves downward and inward because of its own weight and surcharge; this tends to cause soil inside the excavation zone to heave up. The collapse of the bracing system may occur if the amount of basal-heave movement is excessive. The basal heave of Dhaka site having double basement system is shown in Fig. 5.26.

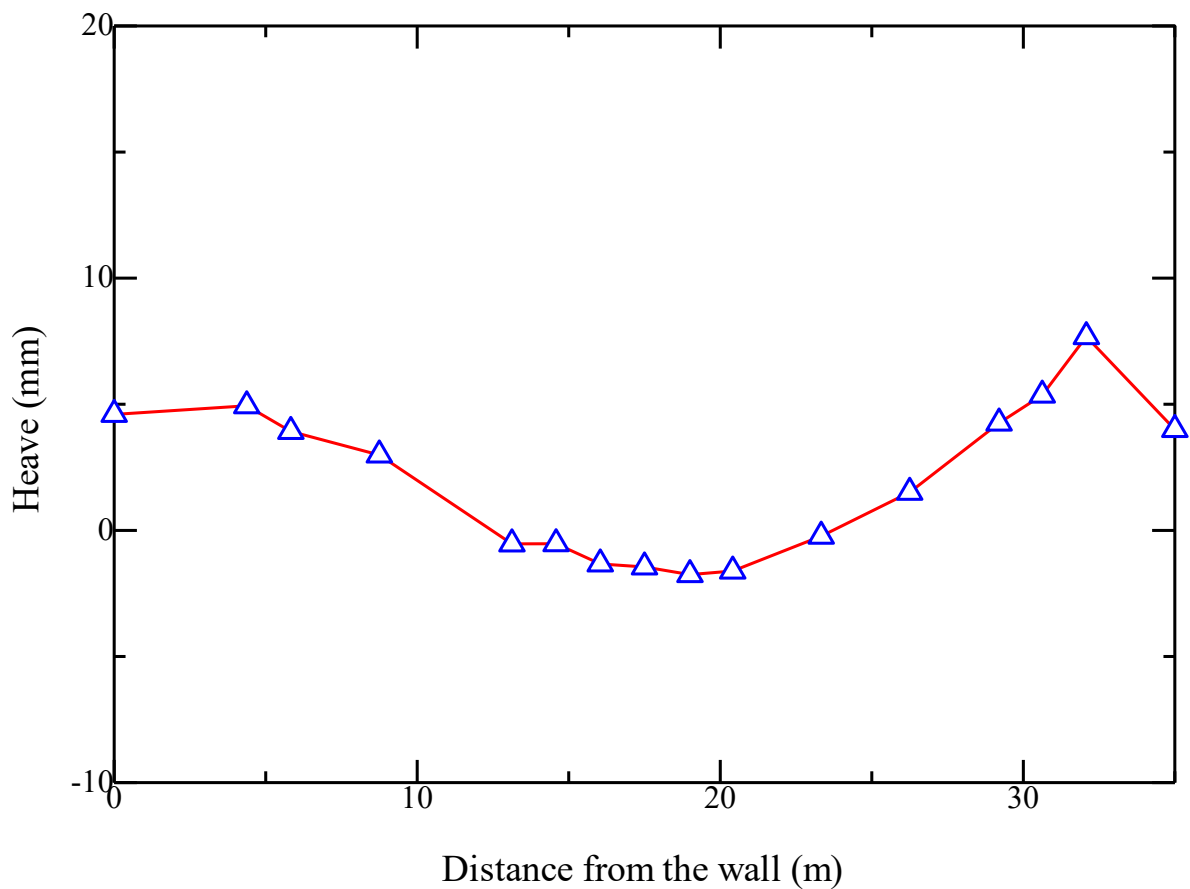


Fig. 5.26 The basal heave of Dhaka soil having double basement system

According to Peck et al. (1974) if the $\frac{\gamma H}{c} \leq 6$ then the effect of basal heave will be negligible. In this study, the fraction is nearly 3.5, so the possibility of basal heave failure is less. Moreover, the maximum heave obtains from the study is nearly 8mm. In this study after conducting safety analysis it is observed that factor of safety against basal heave failure is almost 1.7. A matching condition is shown in the following Table 5.29.

Table 5.29 Factor of safety against basal heave compared with available literature

Researcher	Basis of the comparison	Result obtained from the literature	Result obtained from the current study
Clough and O'Rourke (1990)	Basal Heave	1.5	1.7
Terzaghi (1943)	Basal Heave	1.2	1.7
Bjerrum& Eide	Basal Heave	1.4	1.7
Goh	Basal Heave	1.6	1.7

5.8 Cost comparison of steel sheet pile wall and contiguous pile wall in the context of Bangladesh

Time and cost - both factors are essential for taking decision for any construction project. A comparison of both the retaining structure in the context of Bangladesh is discussed in this section.

Sheet pile retaining system is widely used throughout the world as an option for retaining structure as it offers rapid construction. However, In Bangladesh the use of sheet pile wall is minimal. The contiguous pile wall is the accessible retaining structure in Bangladesh as it offers reduced cost than the steel sheet pile wall. A cost comparison is shown between the contiguous pile wall and steel sheet pile for a double basement system in this study.

The number of contiguous piles required for a double basement system covering an area of 35mx30m is around 200. To carry out the excavation process using contiguous pile wall retaining system it is calculated that around 4 crore BDT is required.

In the current study, information has been taken from different steel sheet pile importer of Bangladesh to calculate the cost required for using a steel sheet pile wall as a retaining structure. It is verified through cross information is that the cost needed for the steel sheet pile wall is BDT 90000 per Ton. The formula used to calculate the weight of the sheet pile is:

$$\text{Weight of Sheet pile wall} = 7.85 \times \text{Length of sheet pile wall (m)} \times \text{Width of sheet pile wall (m)} \times \text{Thickness of sheet pile wall (mm)}$$

According to the formula, the total weight of the sheet pile wall is around 160 Ton, and the total cost required for sheet pile wall is approximately 14.32 crore BDT which is much almost 3.5 times higher than the contiguous pile wall.

CHAPTER 6

CONCLUSIONS AND RECOMMENDATIONS

6.1 Conclusions

This research compares the effect of the sheet pile wall and the contiguous pile wall for deep foundations in the context of Bangladesh using numerical analysis. Moreover, this research has investigated the ground response as well as sheet pile wall and contiguous pile wall horizontal deflections for deep excavations. Initially, MC model has been used in the finite element code PLAXIS 3D. Later, an attempt has been made to see if it is possible to obtain better predictions using a more advanced HS model based.

The previous chapters have investigated the performance of deep excavations and the influence of various critical aspects through parametric studies on a simplified excavation and detailed analyses of two more case histories for validation of the model. These studies provide insight into this complex soil-structure interaction problem, and have practical implications on the design and analysis of deep excavations. Each chapter has given detailed discussions and conclusions separately. These conclusions are synthesized in this chapter to give a more comprehensive summary:

- Finite element analysis is an effective way to investigate the performance of deep excavations, in which detailed geotechnical and structural aspects such as (i) the geometry of the excavation, (ii) structural components of the retaining system, (iii) ground conditions, (iv) sophisticated soil behavior, and (v) actual construction sequence, can be accounted for adequately. The standard procedure of advanced finite element analysis of deep excavations is described in Chapter 4, which includes modeling (i) the soil and structural components (both geometry and material properties), (ii) the soil-structure interface behavior, (iii) boundary conditions, and (iv) the construction sequence. Some critical issues in regard to the modeling process of deep excavations are discussed in Chapter 3, such as (i) selection of element types for the soil and structure (ii) the soil-structure interface behavior, (iii) variation of stiffness and strength properties of the soil, and (iv) reliability of the simplified and improved analysis.

- Research and practice have shown that accurate prediction of the performance of deep excavations, especially the ground movement, requires a realistic soil model that can consider the small-strain stiffness nonlinearity of the soil, which is confirmed again in this thesis. Also, the soil model adopted needs to be calibrated with soil properties corresponding to geotechnical conditions in the construction site. Essential features in the retaining structure, e.g., construction joints in the retaining wall have a significant influence on the excavation behavior, and they can also be considered in the constitutive model for the structure. Moreover, a realistic contact model at the soil-structure interface is required to take into account the influence of the interface behavior.
- Detailed parametric studies, based on a simplified model which includes essential features of deep excavations, are necessary to understand the influence of various essential aspects in deep excavations, and should be conducted before more sophisticated case studies. There are several advantages of this process, (i) it is easier to build up the model and less time-consuming to run the calculation, (ii) more details can be looked into, (iii) certain aspects which are difficult to account for in complex case studies, e.g. soil/wall contact and soil/pile contact, can be investigated more easily, (iv) numerical problems can be identified and solved more conveniently, and (v) skills and experiences learned in this process are useful preparation for the more complex case history studies.
- The parametric studies in Chapter 3 suggest that elements with reasonably coarser mesh in the analysis produce similar patterns in the computed deformations compared with corresponding elements with a finer mesh and take much less time to run. In the following part of the study to reduce calculation time for the complex model coarse meshing has been used.
- It is also suggested that the computed ground deformations and wall deflections are sensitive to the soil-structure interface and the strength and stiffness properties of soil. Neglecting any of these effects may affect the accuracy of the analysis, but considering all of them in one analysis may not be practical to use. Engineers need to decide which aspects are more critical in a specific problem and address these issues in the analysis with a moderate level of complexity.

- In general, the contiguous pile wall experienced fewer wall movements than the sheet pile wall on the Dhaka and Chittagong site. The lateral displacements of the sheet pile wall for Dhaka site are lower than the lateral displacement of sheet pile wall for Chittagong site due to the presence of stiff soil in Dhaka site.
- In case of a single basement system, the contiguous pile wall shows 11% and 27% less wall movements in the short and long side than the sheet pile wall for Dhaka site in case of MC model and 19% and 5% less wall movement in short and long side than the sheet pile wall for Dhaka site in case of HS model. However, the penetration depths of the retaining wall have to increase in order to reduce wall movements in case of Chittagong site. The contiguous pile wall resists 20% less wall movements in the long side and 66% less wall movements in the short side than the sheet pile wall after the increment of penetration depth up to 2.5 times than the excavation depth.
- In double basement system, the contiguous pile wall shows effectiveness in countering wall displacements. The results of Dhaka site shows that the displacement of sheet pile wall is 32% higher in the long side and 53% higher in the short side than the sheet pile wall. On the other hand, the results of Chittagong site indicate that sheet pile wall experiences much higher displacements than the contiguous pile wall. In general, the result is 3 times higher in case of MC model and 8 times higher in case of HS model than the contiguous pile wall. It is recommended to increase the number of bracing components to reduce the wall displacement of sheet pile wall in the Chittagong site.
- In triple basement system, the contiguous pile wall resists more wall displacement than the sheet pile wall in the Chittagong site. The results indicates that contiguous pile wall resists 35% more wall displacement than the sheet pile wall in case of MC model and 7% more wall displacement than the sheet pile wall in case of HS model. However, sheet pile wall shows better result in the Dhaka site in case of MC model but the results of contiguous pile wall shows better performance in case of HS model.
- In general, it is noticed that the HS model predicts lower than the MC model both for the Sheet pile wall and contiguous pile wall. The reason behind this is due to the fact that the MC model does not consider the strain-dependent stiffness behavior or the small strain characteristics that involve high stiffness modulus at

small strain levels of soil. The MC model only uses a single Young's modulus and does not also distinguish between loading and unloading stiffness. In the HS model, soil stiffness is calculated much more accurately by using three different stiffnesses (triaxial loading secant stiffness, triaxial unloading/reloading stiffness and oedometer loading tangent stiffness). The MC model represents Young's modulus of soil in the in situ stress state. On the other hand, the HS model represents its three moduli at the reference pressure, and these moduli at the in situ stress state are automatically calculated as a function of the current stress state.

- It is observed in all the cases that the vertical settlement of sheet pile wall is much higher than the contiguous pile wall. The rigidity of contiguous pile wall allow the contiguous pile wall to settle less than the sheet pile wall.
- It is noticed that sheet pile wall shows more bulging than the contiguous pile wall. In single basement system, the lateral displacement curve of contiguous pile wall is almost linear. However, the linearity of the displacement curve shows more concavity with the increase of basement level. The bulging in contiguous pile wall is less due to fixity (Dunchan et al. 2005). The cap provided in the contiguous pile wall prevents the rotation and deflections.
- In this study, the results are compared with the available literatures and based on the comparison, different color codes are used to show the harmony of the results with the available literatures. Green color is used to show the best match (results are within limit or deviations are within 10%), Yellow color is used to show moderate match (deviations are within 10%-20%) and Red color denotes worst condition (deviations are more than 20%). In this study, in total 60 cases are compared with them. The number of green code in case of contiguous pile wall is much higher than the sheet pile wall. Contiguous pile wall shows best match of 57 cases out of 60 cases whereas the number is 47 for the case of sheet pile wall.
- The contiguous pile wall is more effective than the sheet pile wall in resisting wall displacement in the presence of nearby structures. The results indicates that the contiguous pile wall resists 0.5 times more wall displacement in the long side and 2.5 times more wall displacement in the short side than the sheet pile wall. It is recommended to use contiguous pile wall in the congested urban areas of Dhaka and Chittagong.

- Contiguous pile wall shows better performance while reducing the number of structural components in the bracing system. So the cost of structural components can be reduced by installing a contiguous pile wall as a shore protection system.
- The results of the Ground settlement and basal heave show that the finite element model is capable of resisting ground deformation problem and basal heave failure. The finite element model's prediction of factor of safety against basal heave failure shows harmony with the conventional method.
- Construction project management is like juggling three balls – time, cost and quality. The contiguous pile wall offers reduced cost as well as quality. So, it is recommended that the contiguous pile wall can be provided as a feasible option of shore protection system on the context of Bangladesh.

6.2 Recommendations for Future Work

In spite of the fact that the advancements available through cheap computer hardware and the improvement of modeling techniques have made numerically modeling a necessity for routine design. The advanced models such as the HS model remain unpopular due to lack of necessary advanced tests (at least the drained tri axial test), especially in the commercial environment where these tests are considered not only time-consuming but expensive. Besides, because of the lack of field calibration to obtain confidence in the method and especially the input soil stiffness, it is understandable that the simple MC model remains a popular choice.

It is recommended:

- Advanced tests (drained triaxial test) should be carried out, so that appropriate parameters are available for constitutive soil modeling. Recommendations based on experience and empirical correlations established elsewhere may be useful for preliminary study or for specific sites where the correlations found, but may not be necessarily suitable for the problems in hand. Laboratory tests or field tests do not necessarily provide the stiffness parameters that can lead to best match results.

- Stiffness parameters obtained from the laboratory or in-situ tests must be compared with the stiffness parameters obtained by calibration against actual field performance data. In complex soil profiles, it is challenging to derive representative stiffness parameters for each of the soil layers, but gross response stiffness parameters for the entire profiles can be obtained.
- Geotechnical instrumentation techniques are well-developed and are capable of providing necessary data for analysis. It is preferable that the instruments be installed at the right locations or inside the structural elements like a sheet pile wall to monitor actual wall deflections.
- It is understandable why the model remains a popular choice. The HS model which can predict better ground surface settlement, which is essential for adjacent building structures and utility damage assessment, should be encouraged to be used in the routine design. Alternatively, the HS model can be coupled with the MC model such that the HS model can be set for soil cluster near the surface while the rest of the soil clusters can use the MC model to archive better ground surface settlement prediction. Such a procedure may require field verification.
- Contiguous pile wall showed better performance than the sheet pile wall on the context of Bangladesh. However, the sheet pile wall is still useful for rapid construction and might be used as a temporary structure.

REFERENCES

- Ahmadpour, Behrouz, Masoud Amel Sakhi, and Mohsen Kamalian. "Study of Loose Soil Layer Effects on Excavations Supported by Steel Sheet Pile Walls—a Numerical Study." *Journal of Engineering Geology* 12, no. 5 (2019): 31-54.
- Allen-King, Richelle M, Hester Groenevelt, and Douglas M Mackay. "Analytical Method for the Sorption of Hydrophobic Organic Pollutants in Clay-Rich Materials." *Environmental science & technology* 29, no. 1 (1995): 148-53.
- Amrani, Dounia. "Numerical Modeling and Parametric Study of Flexible Wall Reinforced with Anchor System." In *Recent Advances in Geo-Environmental Engineering, Geomechanics and Geotechnics, and Geohazards*, 331-34: Springer, 2019.
- Arai, Yasushi, Osamu Kusakabe, Osamu Murata, and Shinji Konishi. "A Numerical Study on Ground Displacement and Stress During and after the Installation of Deep Circular Diaphragm Walls and Soil Excavation." *Computers and Geotechnics* 35, no. 5 (2008): 791-807.
- Athanasopoulos, GA, VS Vlachakis, and PC Pelekis. "Installation and Performance of a Steel Sheet Pile Wall for Supporting an Excavation in Urban Environment." In *Geo-Frontiers 2011: Advances in Geotechnical Engineering*, 3370-80, 2011.
- Atkinson, JH, and SE Stallebrass. "A Model for Recent Stress History and Non-Linearity in the Stress-Strain Behaviour of Overconsolidated Soil." Paper presented at the Proceedings of the 7th International Conference on Computer Methods and Advances in Geomechanics, Cairns, 1991.
- Azzam, WR, and AZ Elwakil. "Performance of Axially Loaded-Piled Retaining Wall: Experimental and Numerical Analysis." *International Journal of Geomechanics* 17, no. 2 (2016): 04016049.
- Benz, T. "Small-Strain Stiffness of Soils and Its Numerical Consequences, Mitteilung Des Instituts Für Geotechnik Der Universität Stuttgart." *Germany. Stuttgart* (2006).
- Bhatkar, T, D Barman, A Mandal, and A Usmani. "Prediction of Behaviour of a Deep Excavation in Soft Soil: A Case Study." *International Journal of Geotechnical Engineering* 11, no. 1 (2017): 10-19.
- Bilgin, Ömer, and M Bahadır Erten. "Analysis of Anchored Sheet Pile Wall Deformations." In *Contemporary Topics in Ground Modification, Problem Soils, and Geo-Support*, 137-44, 2009.

- Bishop, AW, and DW Hight. "The Value of Poisson's Ratio in Saturated Soils and Rocks Stressed under Undrained Conditions." *Geotechnique* 27, no. 3 (1977): 369-84.
- BJERRUM, L, and O EIDE. "Stability of Struttred Excavations in Clay." *Publikasjon-Norges Geotekniske Institutt* 200 (1997): 1-16.
- Bjerrum, Laurits, and Ove Eide. "Stability of Struttred Excavations in Clay." *Geotechnique* 6, no. 1 (1956): 32-47.
- Bolton, MD, and W Powrie. "Behaviour of Diaphragm Walls in Clay Prior to Collapse." *Géotechnique* 38, no. 2 (1988): 167-89.
- Bolton, M. D., and W. Powrie. "The Collapse of Diaphragm Walls Retaining Clay." *Geotechnique* 37, no. 3 (1987): 335-53.
- Bolton, MD, and DI Stewart. "The Effect on Propped Diaphragm Walls of Rising Groundwater in Stiff Clay." *Géotechnique* 44, no. 1 (1994): 111-27.
- Boonyarak, Thayanan, Kullapat Phisitkul, Charles WW Ng, Wanchai Teparaksa, and Zaw Zaw Aye. "Observed Ground and Pile Group Responses Due to Tunneling in Bangkok Stiff Clay." *Canadian Geotechnical Journal* 51, no. 5 (2014): 479-95.
- Bose, SK, and NN Som. "Parametric Study of a Braced Cut by Finite Element Method." *Computers and Geotechnics* 22, no. 2 (1998): 91-107.
- Brammer, Hugh. "The Geography of the Soils of Bangladesh." (1996).
- Brinkgreve, RBJ, E Engin, and WM Swolfs. "Plaxis 3d Material Models Manual." In Plaxis Bv, 2012.
- Brinkgreve, RBJ, and PA Vermeer. "Plaxis: Finite Element Code for Soil and Rock Analyses: Version 7." *Technical Manual. Rotterdam: AA Balkema* (1998).
- Burland, JB. "Movements around Excavations in London Clay." Paper presented at the Proc. 7th Eur. Conf. Soil Mech. and Fnd Engng, 1979.
- Caquot, Albert Irénée, and Jean Lehuérou Kérisel. *Tables for the Calculation of Passive Pressure, Active Pressure and Bearing Capacity of Foundations*. Gauthier-Villars, 1948.
- Chheng, Chhunla, and Suched Likitlersuang. "3d Finite Element Modelling of Sheet Pile Wall Excavation: A Case Study in Bangkok." *IPTEK Journal of Proceedings Series* 3, no. 6 (2017).
- Chowdhury, Subha Sankar, Kousik Deb, and Aniruddha Sengupta. "Estimation of Design Parameters for Braced Excavation: Numerical Study." *International Journal of Geomechanics* 13, no. 3 (2012): 234-47.

- Clarke, BG, and CP Wroth. "Analysis of Dunton Green Retaining Wall Based on Results of Pressuremeter Tests." *Geotechnique* 34, no. 4 (1984): 549-61.
- Clough, G Wayne. "Construction Induced Movements of in Situ Walls." *Design and performance of earth retaining structures* (1990): 439-70.
- Clough, G Wayne, and Lawrence A Hansen. "Clay Anisotropy and Braced Wall Behavior." *Journal of Geotechnical and Geoenvironmental Engineering* 107, no. ASCE 16391 (1981).
- Clough, G Wayne, Elizabeth M Smith, and Bryan P Sweeney. "Movement Control of Excavation Support Systems by Iterative Design." Paper presented at the Foundation engineering: current principles and practices, 1989.
- Clough, G Wayne, and Yuet Tsui. "Performance of Tied-Back Walls in Clay." *Journal of Geotechnical and Geoenvironmental Engineering* 100, no. Proc. Paper 11028 (1974).
- Corral, Gonzalo, and Andrew J Whittle. "Re-Analysis of Deep Excavation Collapse Using a Generalized Effective Stress Soil Model." Paper presented at the Earth Retention Conference 3, 2010.
- Coulomb, Charles Augustin. "Essai Sur Une Application Des Regles De Maximis Et Minimis a Quelques Problemes De Statique Relatifs a L'architecture (Essay on Maximums and Minimums of Rules to Some Static Problems Relating to Architecture)." (1973).
- Cuadrado Cabello, Agustín. "Análisis Tenso-Deformacional En Rotura Y Condiciones De Seguridad De Pantallas En Voladizo Y Ancladas. Comparación Con Métodos Clásicos." (2010).
- Day, RA. "Net Pressure Analysis of Cantilever Sheet Pile Walls." *Geotechnique* 49, no. 2 (1999): 231-45.
- Day, RA, and DM Potts. "Modelling Sheet Pile Retaining Walls." *Computers and Geotechnics* 15, no. 3 (1993): 125-43.
- De Moor, EK. "An Analysis of Bored Pile/Diaphragm Wall Installation Effects." *Géotechnique* 44, no. 2 (1994): 341-47.
- Dong, Y, H Burd, G Houlsby, and Y Hou. "Advanced Numerical Modelling of a Complex Deep Excavation Case History in Shanghai." (2013).
- Dong, Yuepeng, Harvey Burd, Guy Houlsby, and Zhonghua Xu. "3d Fem Modelling of a Deep Excavation Case Considering Small-Strain Stiffness of Soil and Thermal Shrinkage of Concrete." (2013).

- Duncan, James M, and Chin-Yung Chang. "Nonlinear Analysis of Stress and Strain in Soils." *Journal of Soil Mechanics & Foundations Div* (1970).
- Finno, Richard J, Dimitrios K Atmatzidis, and Scott B Perkins. "Observed Performance of a Deep Excavation in Clay." *Journal of Geotechnical Engineering* 115, no. 8 (1989): 1045-64.
- Finno, Richard J, J Tanner Blackburn, and Jill F Roboski. "Three-Dimensional Effects for Supported Excavations in Clay." *Journal of Geotechnical and Geoenvironmental Engineering* 133, no. 1 (2007): 30-36.
- Finno, Richard J, Indra S Harahap, and Paul J Sabatini. "Analysis of Braced Excavations with Coupled Finite Element Formulations." *Computers and Geotechnics* 12, no. 2 (1991): 91-114.
- Finno, Richard J, and Steven M Nerby. "Saturated Clay Response During Braced Cut Construction." *Journal of geotechnical engineering* 115, no. 8 (1989): 1065-84.
- Fourie, AB, and DM Potts. "Comparison of Finite Element and Limiting Equilibrium Analyses for an Embedded Cantilever Retaining Wall." *Geotechnique* 39, no. 2 (1989): 175-88.
- Goh, ATC, Fan Zhang, Wengang Zhang, Yanmei Zhang, and Hanlong Liu. "A Simple Estimation Model for 3d Braced Excavation Wall Deflection." *Computers and Geotechnics* 83 (2017): 106-13.
- Golait, YS, AH Padade, and T Cherian. "Prediction of Quantitative Response of under-Reamed Anchor Piles in Soft Clay Using Laboratory Model Study." *Journal of Testing and Evaluation* 46, no. 2 (2017).
- Gourvenec, SM, and W Powrie. "Three-Dimensional Finite-Element Analysis of Diaphragm Wall Installation." *Geotechnique* 49, no. 6 (1999): 801-23.
- GuhaRay, Anasua, and Dilip Kumar Baidya. "Reliability-Based Analysis of Cantilever Sheet Pile Walls Backfilled with Different Soil Types Using the Finite-Element Approach." *International Journal of Geomechanics* 15, no. 6 (2015): 06015001.
- Gunn, MJ, and CRI Clayton. "Installation Effects and Their Importance in the Design of Earth-Retaining Structures." *Geotechnique* 42, no. 1 (1992): 137-41.
- Hashash, Youssef MA, and Andrew J Whittle. "Ground Movement Prediction for Deep Excavations in Soft Clay." *Journal of geotechnical engineering* 122, no. 6 (1996): 474-86.

- Hashash, Youssef MA, and Andrew J Whittle. "Mechanisms of Load Transfer and Arching for Braced Excavations in Clay." *Journal of Geotechnical and Geoenvironmental Engineering* 128, no. 3 (2002): 187-97.
- Hossain, AT. "The Engineering Behaviour of the Tropical Clay Soils of Dhaka, Bangladesh." Durham University, 2001.
- HOSSAIN, ATM SHAKHAWAT, and DG Toll. "Geomechanical Aspects of Some Tropical Clay Soils from Dhaka, Bangladesh." *Engineering Geology for Tomorrow's Cities, Special publication 22* (2006).
- Hou, YM, JH Wang, and LL Zhang. "Finite-Element Modeling of a Complex Deep Excavation in Shanghai." *Acta Geotechnica* 4, no. 1 (2009): 7-16.
- Hsieh, PG. "Prediction of Ground Movements Caused by Deep Excavation in Clay." Ph. D. dissertation, Department of Construction Engineering, National Taiwan ..., 1999.
- Hsieh, Pio-Go, and Chang-Yu Ou. "Shape of Ground Surface Settlement Profiles Caused by Excavation." *Canadian geotechnical journal* 35, no. 6 (1998): 1004-17.
- Hsieh, Pio-Go, Chang-Yu Ou, and Yi-Lang Lin. "Three-Dimensional Numerical Analysis of Deep Excavations with Cross Walls." *Acta Geotechnica* 8, no. 1 (2013): 33-48.
- Huang, Maosong, Chenrong Zhang, and Zao Li. "A Simplified Analysis Method for the Influence of Tunneling on Grouped Piles." *Tunnelling and Underground Space Technology* 24, no. 4 (2009): 410-22.
- Hubbard, HW, DM Potts, David Miller, and JB Burland. "Design of the Retaining Walls for the M25 Cut and Cover Tunnel at Bell Common." *Geotechnique* 34, no. 4 (1984): 495-512.
- Jesmani, Mehrab, Ali Kasrania, and Mehrad Kamalzare. "Finite Element Modelling of Undrained Vertical Bearing Capacity of Piles Adjacent to Different Types of Clayey Slopes." *International Journal of Geotechnical Engineering* 12, no. 2 (2018): 147-54.
- Jimenez Salas, José Antonio. "Geotecnia Y Cimientos." (1980).
- Jongpradist, Pornkasem, Theerapong Kaewsri, Attasit Sawatparnich, Suchatvee Suwansawat, Sompote Youwai, Warat Kongkitkul, and Jutha Sunitsakul. "Development of Tunneling Influence Zones for Adjacent Pile Foundations by Numerical Analyses." *Tunnelling and Underground Space Technology* 34 (2013): 96-109.

- Kempfert, Hans-Georg, and Berhane Gebreselassie. *Excavations and Foundations in Soft Soils*. Springer Science & Business Media, 2006.
- Kitiyodom, Pastsakorn, Tatsunori Matsumoto, and Kanji Kawaguchi. "A Simplified Analysis Method for Piled Raft Foundations Subjected to Ground Movements Induced by Tunnelling." *International Journal for Numerical and Analytical Methods in Geomechanics* 29, no. 15 (2005): 1485-507.
- Kondner, Robert L. "A Hyperbolic Stress-Strain Formulation for Sands." Paper presented at the Proc. 2 nd Pan Am. Conf. on Soil Mech. and Found. Eng., Brazil, 1963, 1963.
- Kung, Gordon T, C Hsein Juang, Evan C Hsiao, and Youssef M Hashash. "Simplified Model for Wall Deflection and Ground-Surface Settlement Caused by Braced Excavation in Clays." *Journal of Geotechnical and Geoenvironmental Engineering* 133, no. 6 (2007): 731-47.
- Lee, CJ. "Three-Dimensional Numerical Analyses of the Response of a Single Pile and Pile Groups to Tunnelling in Weak Weathered Rock." *Tunnelling and Underground Space Technology* 32 (2012): 132-42.
- Lee, Fook-Hou, Sze-Han Hong, Qian Gu, and Pengjun Zhao. "Application of Large Three-Dimensional Finite-Element Analyses to Practical Problems." *International Journal of Geomechanics* 11, no. 6 (2010): 529-39.
- Lee, Fook-Hou, Kwet-Yew Yong, Kevin CN Quan, and Kum-Thong Chee. "Effect of Corners in Strutted Excavations: Field Monitoring and Case Histories." *Journal of Geotechnical and Geoenvironmental Engineering* 124, no. 4 (1998): 339-49.
- Lee, Yong-Joo, and Richard H Bassett. "Influence Zones for 2d Pile–Soil–Tunnelling Interaction Based on Model Test and Numerical Analysis." *Tunnelling and Underground Space Technology* 22, no. 3 (2007): 325-42.
- Lee, Yong-Joo, and Richard H Bassett. "A Model Test and Numerical Investigation on the Shear Deformation Patterns of Deep Wall–Soil–Tunnel Interaction." *Canadian geotechnical journal* 43, no. 12 (2006): 1306-23.
- Lentini, Valentina, and Francesco Castelli. "Numerical Modelling and Experimental Monitoring of a Full-Scale Diaphragm Wall." *International Journal of Civil Engineering* (2019): 1-14.
- Leung, Erin HY, and Charles WW Ng. "Wall and Ground Movements Associated with Deep Excavations Supported by Cast in Situ Wall in Mixed Ground Conditions."

- Journal of geotechnical and geoenvironmental engineering* 133, no. 2 (2007): 129-43.
- Liang, Rongzhu, Tangdai Xia, Maosong Huang, and Cungang Lin. "Simplified Analytical Method for Evaluating the Effects of Adjacent Excavation on Shield Tunnel Considering the Shearing Effect." *Computers and Geotechnics* 81 (2017): 167-87.
- Lim, Aswin, Chang-Yu Ou, and Pio-Go Hsieh. "Evaluation of Clay Constitutive Models for Analysis of Deep Excavation under Undrained Conditions." *Journal of GeoEngineering* 5, no. 1 (2010): 9-20.
- Liu, GB, Charles W Ng, and ZW Wang. "Observed Performance of a Deep Multistrutted Excavation in Shanghai Soft Clays." *Journal of Geotechnical and Geoenvironmental Engineering* 131, no. 8 (2005): 1004-13.
- Liu, Guo B, Rebecca J Jiang, Charles WW Ng, and Y Hong. "Deformation Characteristics of a 38 M Deep Excavation in Soft Clay." *Canadian Geotechnical Journal* 48, no. 12 (2011): 1817-28.
- Liu, HY, John C Small, and John P Carter. "Effects of Tunnelling on Existing Support Systems of Intersecting Tunnels in the Sydney Region." Paper presented at the Proceedings of the First Southern Hemisphere International Rock Mechanics Symposium (SHIRMS), held in Perth, Australia, 16-19 September 2008, 2008.
- Long, Michael. "Database for Retaining Wall and Ground Movements Due to Deep Excavations." *Journal of Geotechnical and Geoenvironmental Engineering* 127, no. 3 (2001): 203-24.
- Mair, RJ. "Developments in Geotechnical Engineering Research: Application to Tunnels and Deep Excavations." Paper presented at the Proceedings of Institution of Civil Engineers: Civil Engineering, 1993.
- Mana, Abdulaziz I, and G Wayne Clough. "Prediction of Movements for Braced Cuts in Clay." *Journal of Geotechnical and Geoenvironmental Engineering* 107, no. ASCE 16312 Proceeding (1981).
- McRostie, GC, KN Burn, and Robert J Mitchell. "The Performance of Tied-Back Sheet Piling in Clay." *Canadian Geotechnical Journal* 9, no. 2 (1972): 206-18.
- Mroueh, Hussein, and Isam Shahrour. "Three-Dimensional Finite Element Analysis of the Interaction between Tunneling and Pile Foundations." *International Journal for Numerical and Analytical Methods in Geomechanics* 26, no. 3 (2002): 217-30.
- Muir Wood, D. "Kinematic Hardening Model for Structured Soil." *Numerical Models in Geomechanics* (1995): 83-88.

- Nematollahi, Mojtaba, and Daniel Dias. "Three-Dimensional Numerical Simulation of Pile-Twin Tunnels Interaction—Case of the Shiraz Subway Line." *Tunnelling and Underground Space Technology* 86 (2019): 75-88.
- Ng, Charles WW. "Observed Performance of Multipropped Excavation in Stiff Clay." *Journal of Geotechnical and Geoenvironmental Engineering* 124, no. 9 (1998): 889-905.
- "Stress Paths in Relation to Deep Excavations." *Journal of geotechnical and geoenvironmental engineering* 125, no. 5 (1999): 357-63.
- Ng, CW, ML Lings, B Simpson, and DFT Nash. "An Approximate Analysis of the Three-Dimensional Effects of Diaphragm Wall Installation." *Geotechnique* 45, no. 3 (1995): 497-507.
- Ng, CWW, Y Hong, GB Liu, and T Liu. "Ground Deformations and Soil-Structure Interaction of a Multi-Propped Excavation in Shanghai Soft Clays." *Géotechnique* 62, no. 10 (2012): 907.
- Ng, CWW, H Lu, and SY Peng. "Three-Dimensional Centrifuge Modelling of the Effects of Twin Tunnelling on an Existing Pile." *Tunnelling and Underground Space Technology* 35 (2013): 189-99.
- Ng, CWW, and RWM Yan. "Three-Dimensional Modelling of a Diaphragm Wall Construction Sequence." *Geotechnique* 49, no. 6 (1999): 825-34.
- O'rouke, TD. "Base Stability and Ground Movement Prediction for Excavations in Soft Clay." Paper presented at the RETAINING STRUCTURES. PROCEEDINGS OF THE CONFERENCE ORGANIZED BY THE INSTITUTION OF CIVIL ENGINEERS AND HELD ON 20-23 JULY, 1992 AT ROBINSON COLLEGE, CAMBRIDGE, 1993.
- Orazalin, Zhandos Y, Andrew J Whittle, and Matthew B Olsen. "Three-Dimensional Analyses of Excavation Support System for the Stata Center Basement on the Mit Campus." *Journal of Geotechnical and Geoenvironmental Engineering* 141, no. 7 (2015): 05015001.
- Ou, Chang-Yu, Dar-Chang Chiou, and Tzong-Shiann Wu. "Three-Dimensional Finite Element Analysis of Deep Excavations." *Journal of Geotechnical Engineering* 122, no. 5 (1996): 337-45.
- Ou, Chang-Yu, Pio-Go Hsieh, and Dar-Chang Chiou. "Characteristics of Ground Surface Settlement During Excavation." *Canadian geotechnical journal* 30, no. 5 (1993): 758-67.

- Ou, Chang-Yu, Jui-Tang Liao, and Horn-Da Lin. "Performance of Diaphragm Wall Constructed Using Top-Down Method." *Journal of geotechnical and geoenvironmental engineering* 124, no. 9 (1998): 798-808.
- Ou, Chang-Yu, Bor-Yuan Shiau, and I-Wen Wang. "Three-Dimensional Deformation Behavior of the Taipei National Enterprise Center (Tnec) Excavation Case History." *Canadian Geotechnical Journal* 37, no. 2 (2000): 438-48.
- Ou, CY, YL Lin, and PG Hsieh. "Case Record of an Excavation with Cross Walls and Buttress Walls." *Journal of GeoEngineering* 1, no. 2 (2006): 79-87.
- Padfield, CJ, and RJ Mair. *Design of Retaining Walls Embedded in Stiff Clay*. 1984.
- Palmer, JH La Verne, and T Cameron Kenney. "Analytical Study of a Braced Excavation in Weak Clay." *Canadian Geotechnical Journal* 9, no. 2 (1972): 145-64.
- Peck, Ralph B. "Deep Excavations and Tunneling in Soft Ground." *Proc. 7th ICSMFE, 1969* (1969): 225-90.
- Phienweij, N. "Ground Movement in Station Excavations of Bangkok First Mrt." Paper presented at the Proceedings of the 6th International Symposium on Tunnelling for Urban Development (IS-Shanghai 2008), Shanghai, China, 2008.
- Poh, TY, and IH Wong. "Effects of Construction of Diaphragm Wall Panels on Adjacent Ground: Field Trial." *Journal of geotechnical and geoenvironmental engineering* 124, no. 8 (1998): 749-56.
- Potts, David. *Guidelines for the Use of Advanced Numerical Analysis*. Thomas Telford, 2002.
- Potts, DM, and AJ Bond. "Calculation of Structural Forces for Propped Retaining Walls." Paper presented at the Proceedings Of The International Conference On Soil Mechanics And Foundation Engineering-International Society For Soil Mechanics And Foundation Engineering, 1994.
- Powrie, W, and ESF Li. "Finite Element Analyses of an in Situ Wall Propped at Formation Level." *Geotechnique* 41, no. 4 (1991): 499-514.
- Rankine, William John Macquorn. "Ii. On the Stability of Loose Earth." *Philosophical transactions of the Royal Society of London*, no. 147 (1857): 9-27.
- Reimann, Klaus-Ulrich, and Karl Hiller. "Geology of Bangladesh." (1993).
- Richards, DJ, and W Powrie. "Centrifuge Model Tests on Doubly Propped Embedded Retaining Walls in Overconsolidated Kaolin Clay." *Géotechnique* 48, no. 6 (1998): 833-46.

- Roscoe, K_H, and JB Burland. "On the Generalized Stress-Strain Behaviour of Wet Clay." (1968).
- Sahajda, Krzysztof. "Ground Anchor Loads Measured on an Excavation Sheet Pile Wall." In *Tunneling and Underground Construction*, 974-83, 2014.
- SCHAFER, R, and Th Triantafyllidis. "Influence of the Construction Process on the Deformation of Diaphragm Walls in Soft Clayey Ground." Paper presented at the Tunnelling And Underground Space Technology. Underground Space For Sustainable Urban Development. Proceedings Of The 30th Ita-Aites World Tunnel Congress Singapore, 22-27 MAY 2004, 2004.
- Schanz, T. "Formulation and Verification of the Hardening-Soil Model." *RBJ Brinkgreve, Beyond 2000 in Computational Geotechnics* (1999): 281-90.
- Schweiger, HF. "Influence of Constitutive Model and Ec7 Design Approach in Fem Analysis of Deep Excavations." Paper presented at the Proceeding of ISSMGE International Seminar on Deep Excavations and Retaining Structures, Budapest, 2009.
- Selemetas, D, JR Standing, and RJ Mair. "The Response of Full-Scale Piles to Tunnelling." Paper presented at the Proc. of the Fifth Int. Symposium on Geotechnical Aspects of Underground Construction in Soft Ground, Amsterdam, 2005.
- Shi, Jiangwei, Zhongzhi Fu, and Wanli Guo. "Investigation of Geometric Effects on Three-Dimensional Tunnel Deformation Mechanisms Due to Basement Excavation." *Computers and Geotechnics* 106 (2019): 108-16.
- Shi, Jiangwei, Guobin Liu, Pei Huang, and CWW Ng. "Interaction between a Large-Scale Triangular Excavation and Adjacent Structures in Shanghai Soft Clay." *Tunnelling and Underground Space Technology* 50 (2015): 282-95.
- Shi, Jiangwei, CWW Ng, and Yonghui Chen. "Three-Dimensional Numerical Parametric Study of the Influence of Basement Excavation on Existing Tunnel." *Computers and Geotechnics* 63 (2015): 146-58.
- Simpson, B. "Retaining Structures: Displacement and Design." *Géotechnique* 42, no. 4 (1992): 541-76.
- Skempton, AW, and WH Ward. "Investigations Concerning a Deep Cofferdam in the Thames Estuary Clay at Shellhaven." *Geotechnique* 3, no. 3 (1952): 119-39.
- Škrabl, Stanislav. "Interactional Approach of Cantilever Pile Walls Analysis." *Acta Geotechnica Slovenica* 6, no. 4 (2006): 46-59.

- Surarak, Chanaton. "Geotechnical Aspects of the Bangkok Mrt Blue Line Project." Griffith University, 2011.
- Symons, I, and DR Carder. "Field Measurements on Embedded Retaining Walls." *Géotechnique* 42, no. 1 (1992): 117-26.
- Takemura, Jiro, Midori Kondoh, Taichi Esaki, Masayuki Kouda, and Osamu Kusakabe. "Centrifuge Model Tests on Double Propped Wall Excavation in Soft Clay." *Soils and Foundations* 39, no. 3 (1999): 75-87.
- Tan, Yong, and Dalong Wang. "Characteristics of a Large-Scale Deep Foundation Pit Excavated by the Central-Island Technique in Shanghai Soft Clay. I: Bottom-up Construction of the Central Cylindrical Shaft." *Journal of Geotechnical and Geoenvironmental Engineering* 139, no. 11 (2013): 1875-93.
- Terzaghi, Karl. "Theoretical Soil Mechanics. Johnwiley & Sons." *New York* (1943): 11-15.
- Terzaghi, Karl, Ralph B Peck, and G Mesri. "Soil Mechanics in Engineering Practice, John Wiley & Sons." *Inc., New York* (1967).
- Van Baars, Stefan. "Numerical Check of the Meyerhof Bearing Capacity Equation for Shallow Foundations." *Innovative Infrastructure Solutions* 3, no. 1 (2018): 9.
- Vermeer, PA. "A Double Hardening Model for Sand." *Geotechnique* 28, no. 4 (1978): 413-33.
- Vinoth, M, and SM Ghan. "Support of Deep Excavation Using Contiguous Pile—a Case Study." In *Geotechnical Applications*, 273-81: Springer, 2019.
- Wang, JH, ZH Xu, and WD Wang. "Wall and Ground Movements Due to Deep Excavations in Shanghai Soft Soils." *Journal of Geotechnical and Geoenvironmental Engineering* 136, no. 7 (2009): 985-94.
- Whittle, Andrew J, and Michael J Kavvadas. "Formulation of Mit-E3 Constitutive Model for Overconsolidated Clays." *Journal of Geotechnical Engineering* 120, no. 1 (1994): 173-98.
- Wong, IH, TY Poh, and HL Chuah. "Analysis of Case Histories from Construction of the Central Expressway in Singapore." *Canadian geotechnical journal* 33, no. 5 (1996): 732-46.
- Wong, Ing Hieng, Teoh Yaw Poh, and Han Leong Chuah. "Performance of Excavations for Depressed Expressway in Singapore." *Journal of geotechnical and geoenvironmental engineering* 123, no. 7 (1997): 617-25.

- Wong, Kai S, and Bengt B Broms. "Lateral Wall Deflections of Braced Excavations in Clay." *Journal of Geotechnical Engineering* 115, no. 6 (1989): 853-70.
- Wood, LA, and AJ Perrin. "Observations of a Struttred Diaphragm Wall in London Clay: A Preliminary Assessment." *Géotechnique* 34, no. 4 (1984): 563-79.
- Wu, Tien-Hsing, and Sidney Berman. "Earth Pressure Measurements in Open Cut: Contract D-8, Chicago Subway." *Géotechnique* 3, no. 6 (1953): 248-58.
- Xiang, Yanyong, and Shanqun Feng. "Theoretical Prediction of the Potential Plastic Zone of Shallow Tunneling in Vicinity of Pile Foundation in Soils." *Tunnelling and Underground Space Technology* 38 (2013): 115-21.
- Xu, ZH. "Deformation Behavior of Deep Excavations Supported by Permanent Structures in Shanghai Soft Deposit." *PhD, Shanghai Jiao Tong University, China* (2007).
- Yong, Choo C, and Erwin Oh. "Modelling Ground Response for Deep Excavation in Soft Ground." *International Journal* 11, no. 26 (2016): 2633-42.
- Zdravkovic, L, DM Potts, and HD St John. "Modelling of a 3d Excavation in Finite Element Analysis." Paper presented at the Stiff Sedimentary Clays: Genesis and Engineering Behaviour: Géotechnique Symposium, 2005.
- Zhang, Jie, Rui Xie, and Han Zhang. "Mechanical Response Analysis of the Buried Pipeline Due to Adjacent Foundation Pit Excavation." *Tunnelling and Underground Space Technology* 78 (2018): 135-45.

APPENDIX A

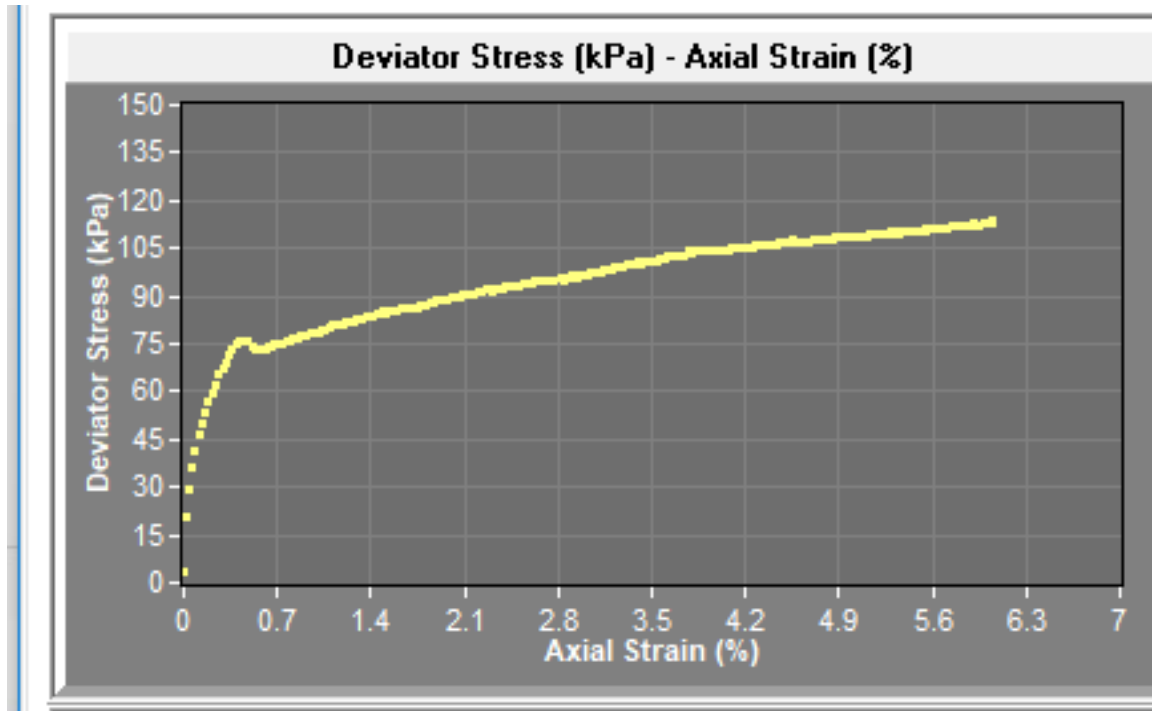


Fig. A-1 Deviator stress (kPa) vs axial strain (%) graph for soil sample of Dhaka site (Effective stress 50kPa)

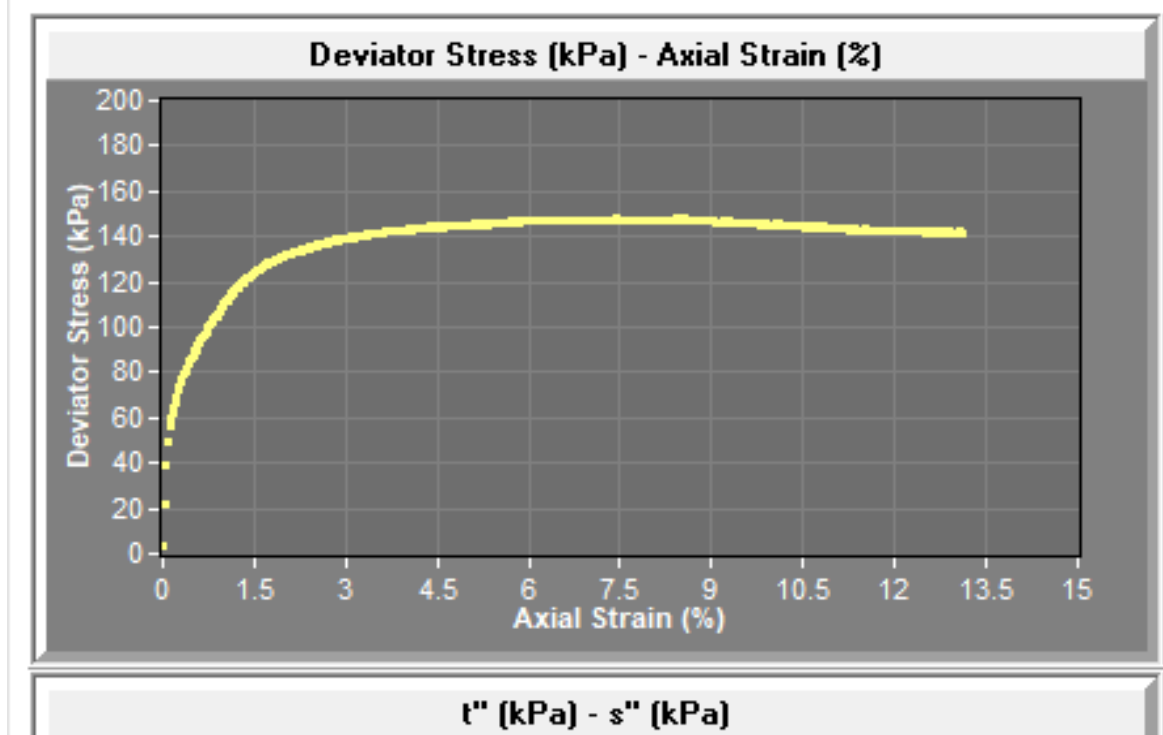


Fig. A-2 Deviator stress (kPa) vs axial strain (%) graph for soil sample of Dhaka site (Effective stress 100kPa)

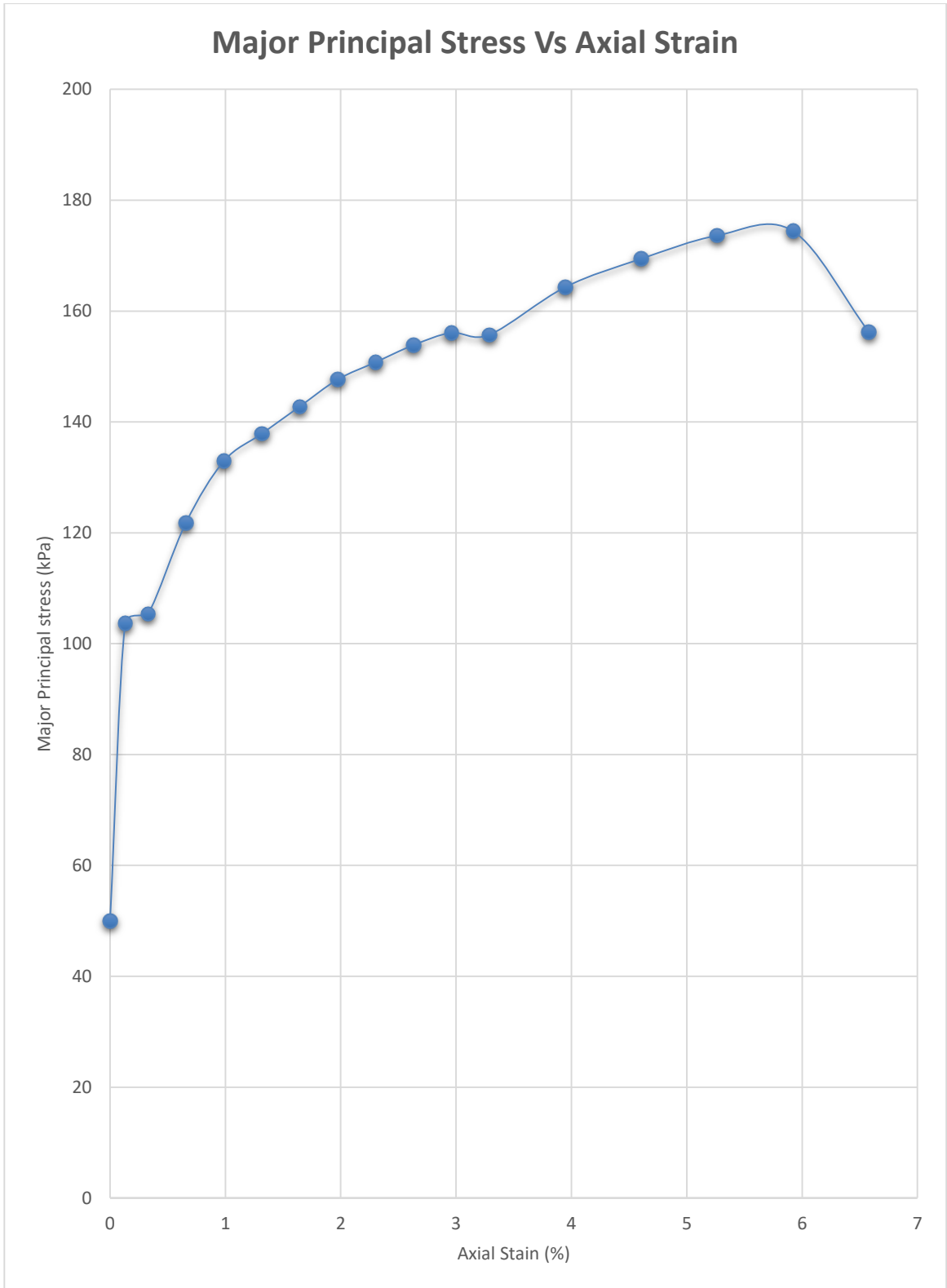


Fig. A-3 Major principal stress (kPa) vs axial strain (%) graph for soil sample of Chittagong site (Effective stress 50kPa)

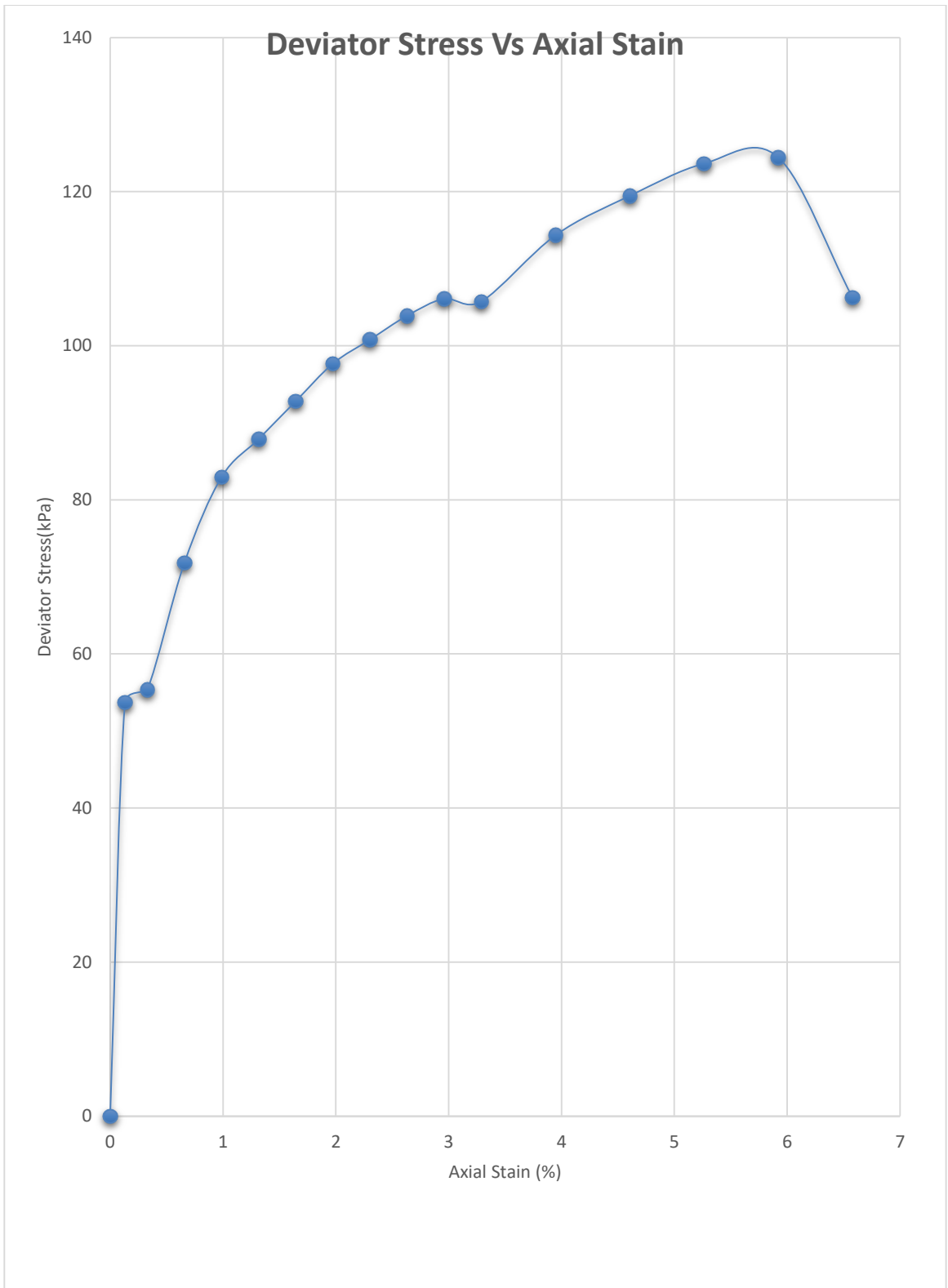


Fig. A-4 Deviator stress (kPa) vs axial strain (%) graph for soil sample of Chittagong site (Effective stress 50kPa)

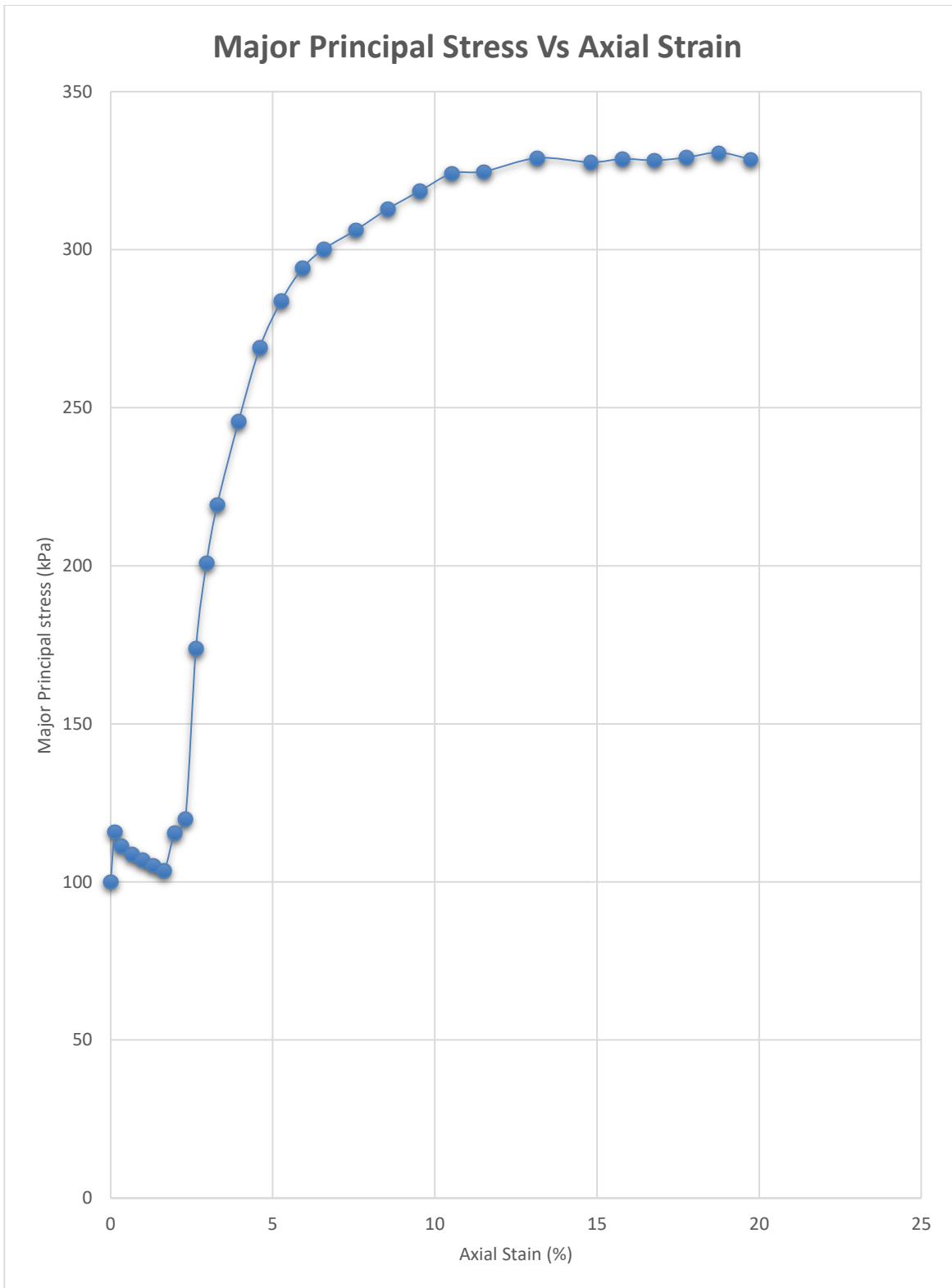


Fig. A-5 Major principal stress (kPa) vs axial strain (%) graph for soil sample of Chittagong site (Effective stress 100kPa)

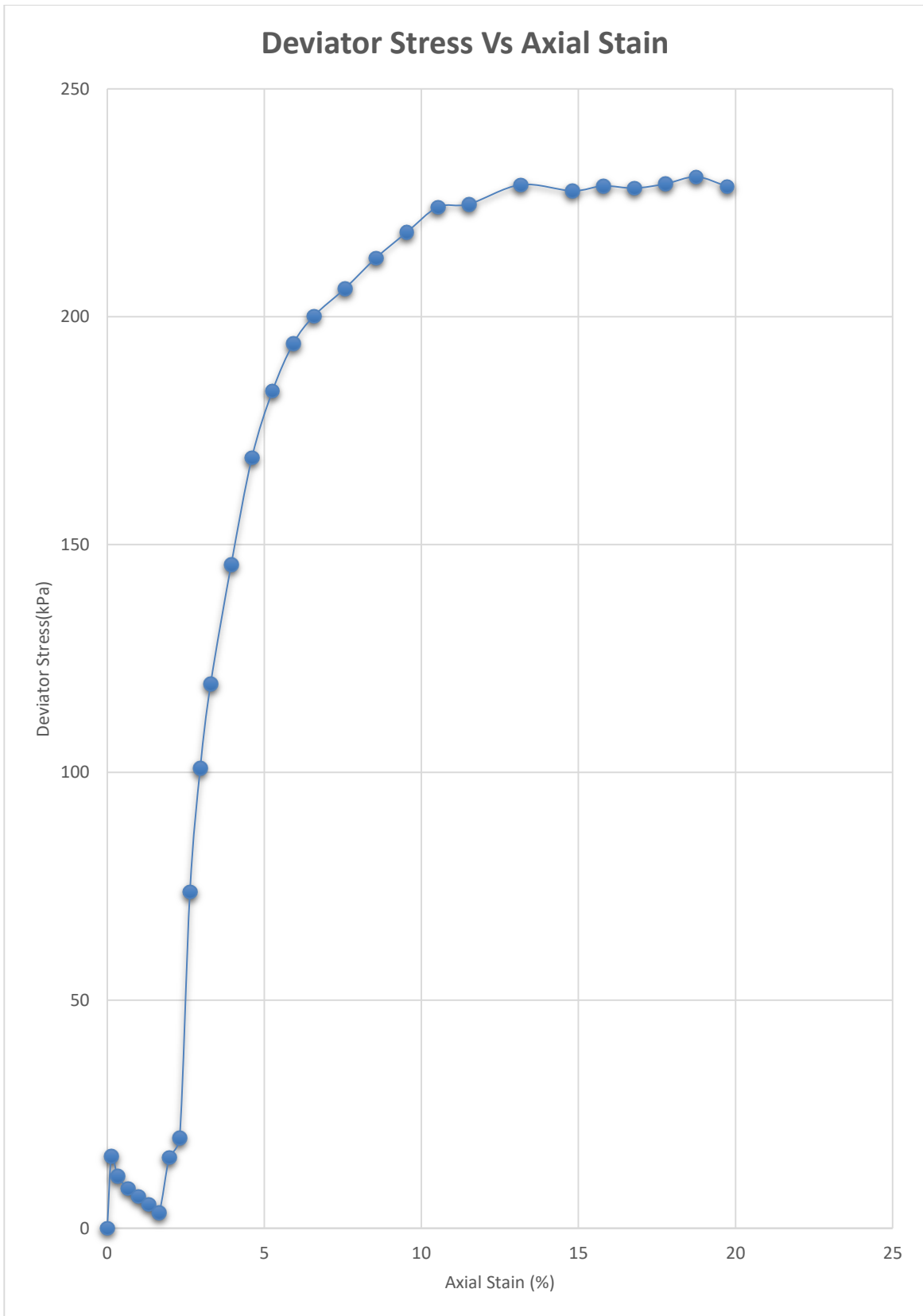


Fig. A-6 Deviator stress (kPa) vs axial strain (%) graph for soil sample of Chittagong site (Effective stress 100kPa)

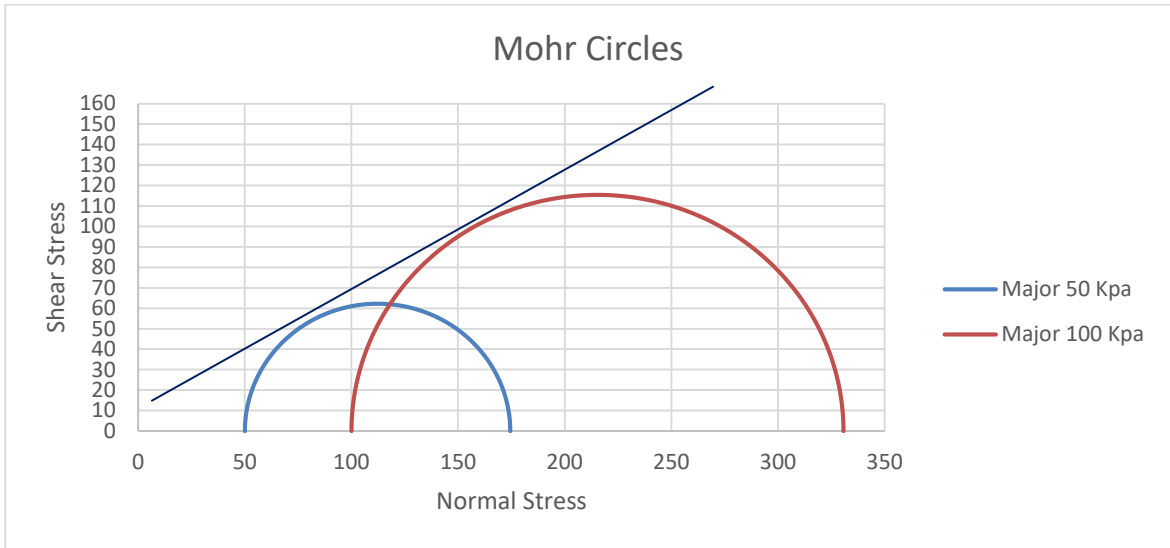


Fig. A-7 Mohr circles for Chittagong site

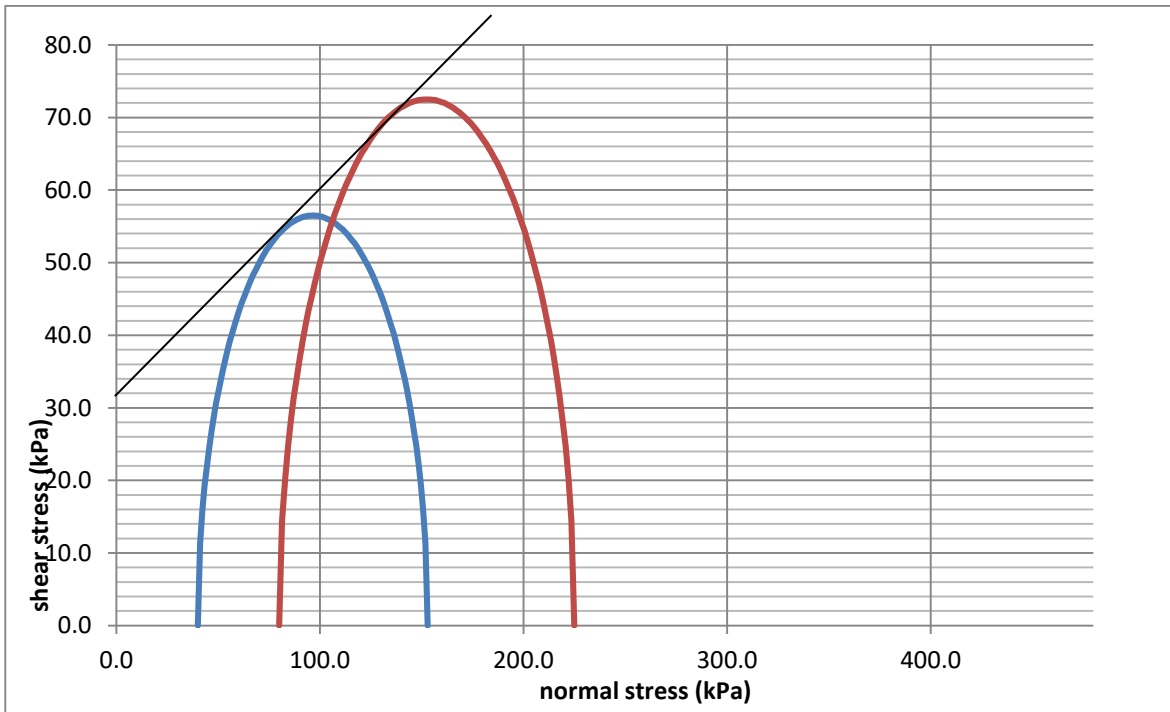
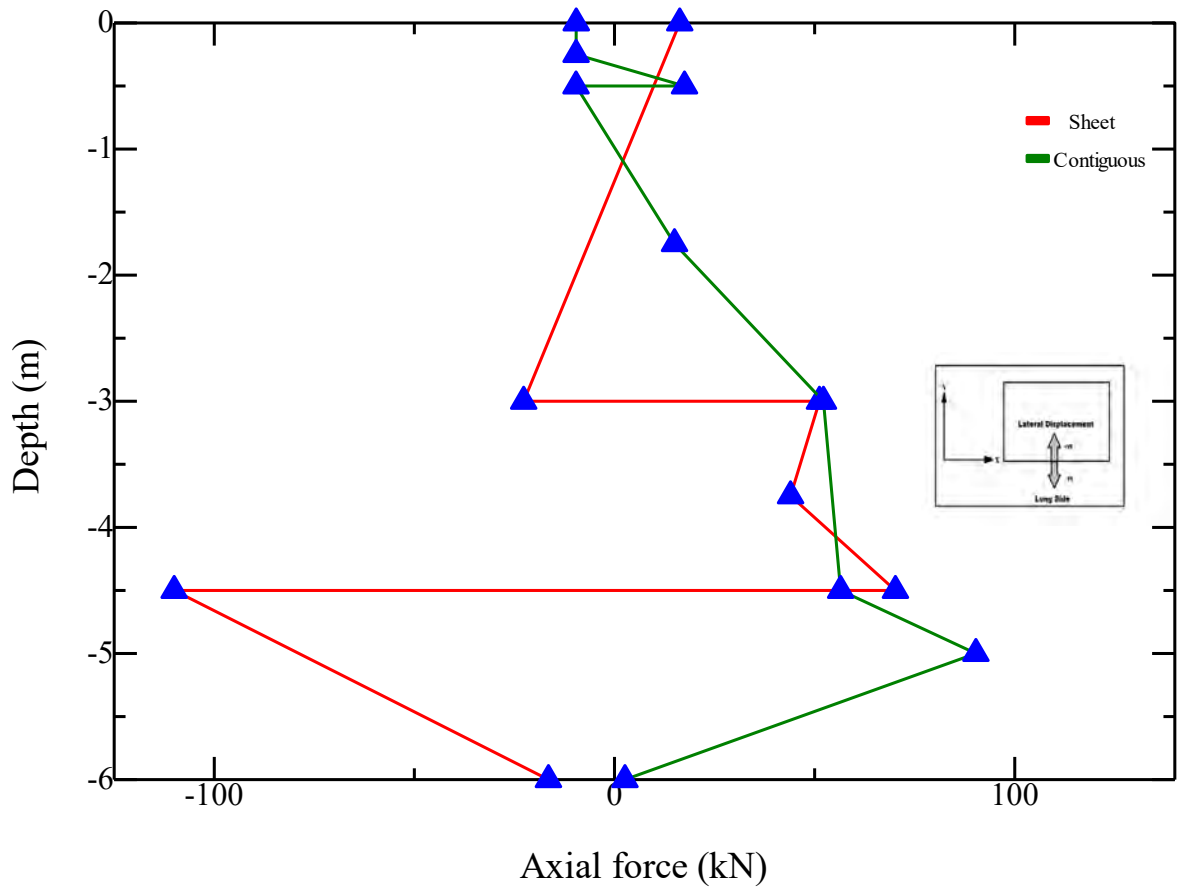
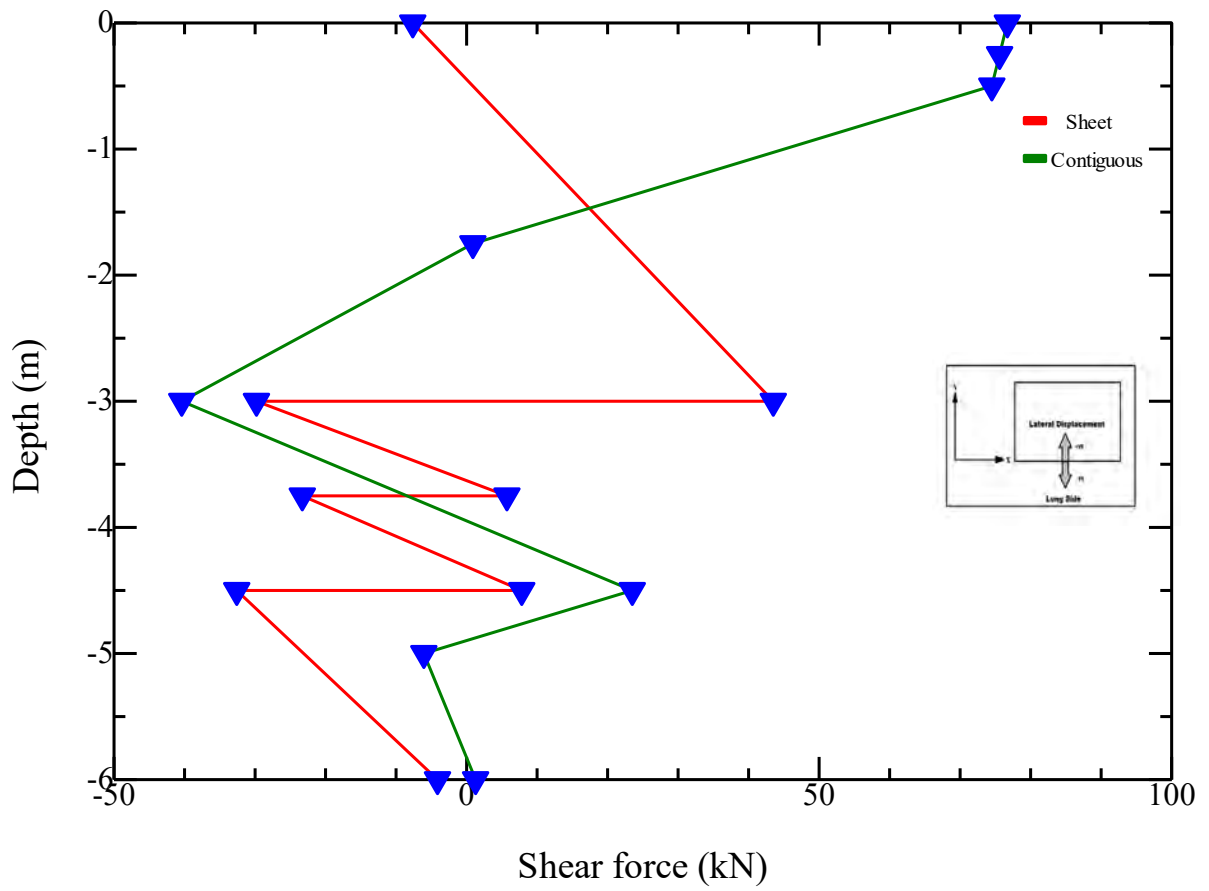


Fig. A-8 Mohr circles for Dhaka site

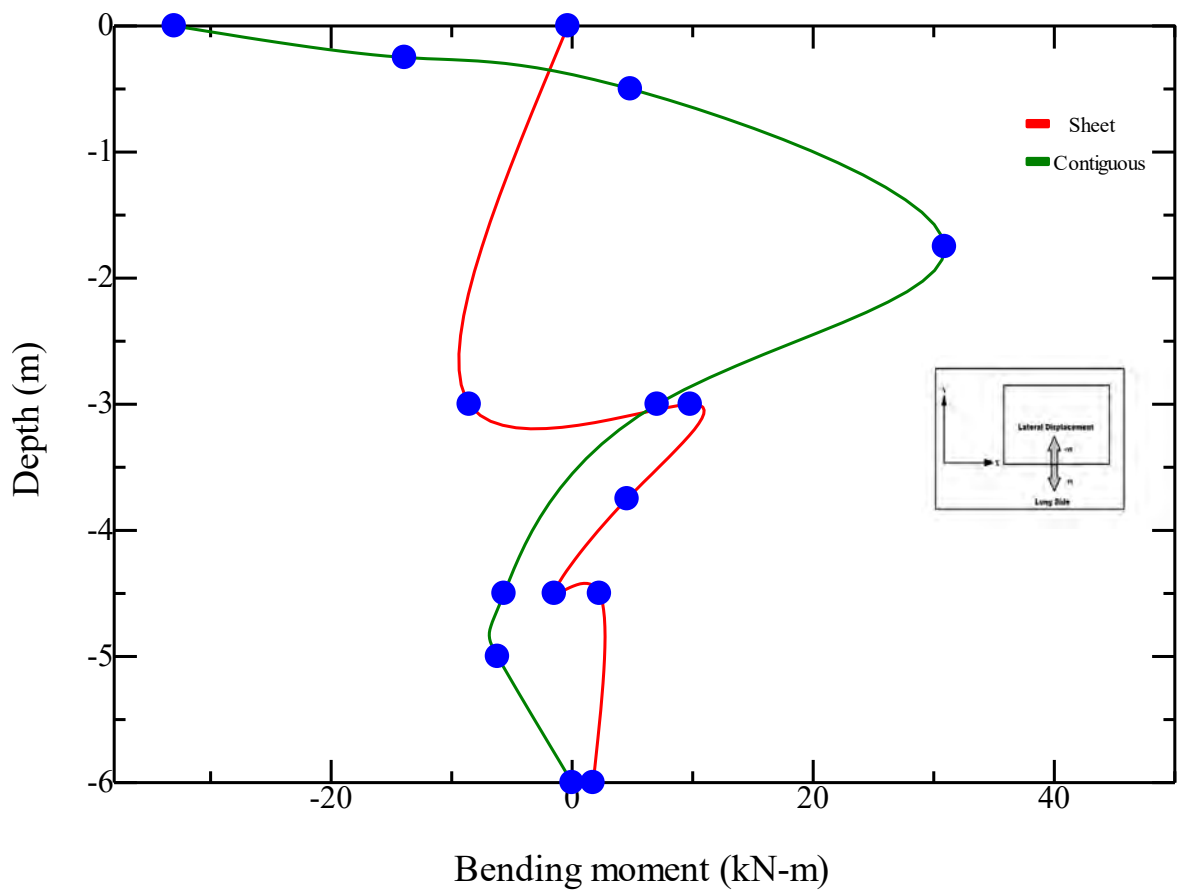
APPENDIX B



(a)

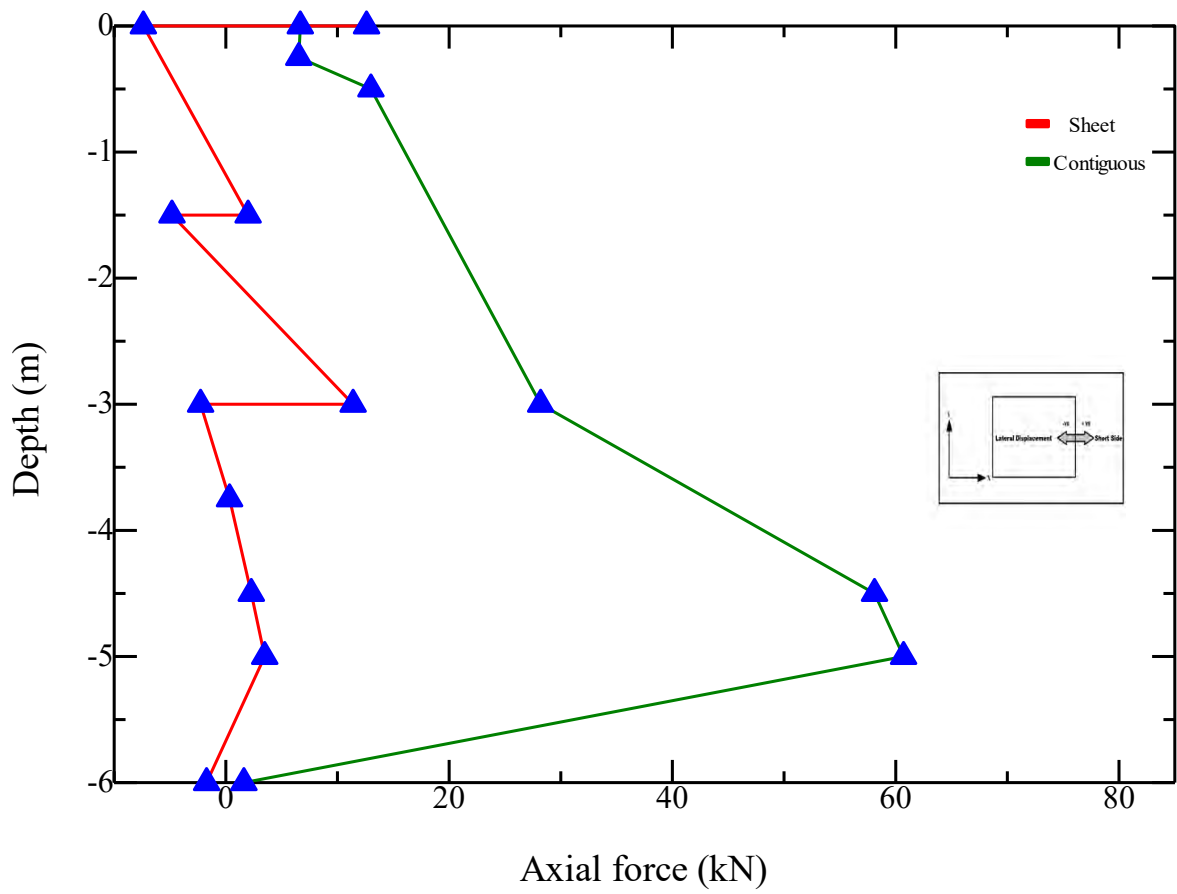


(b)

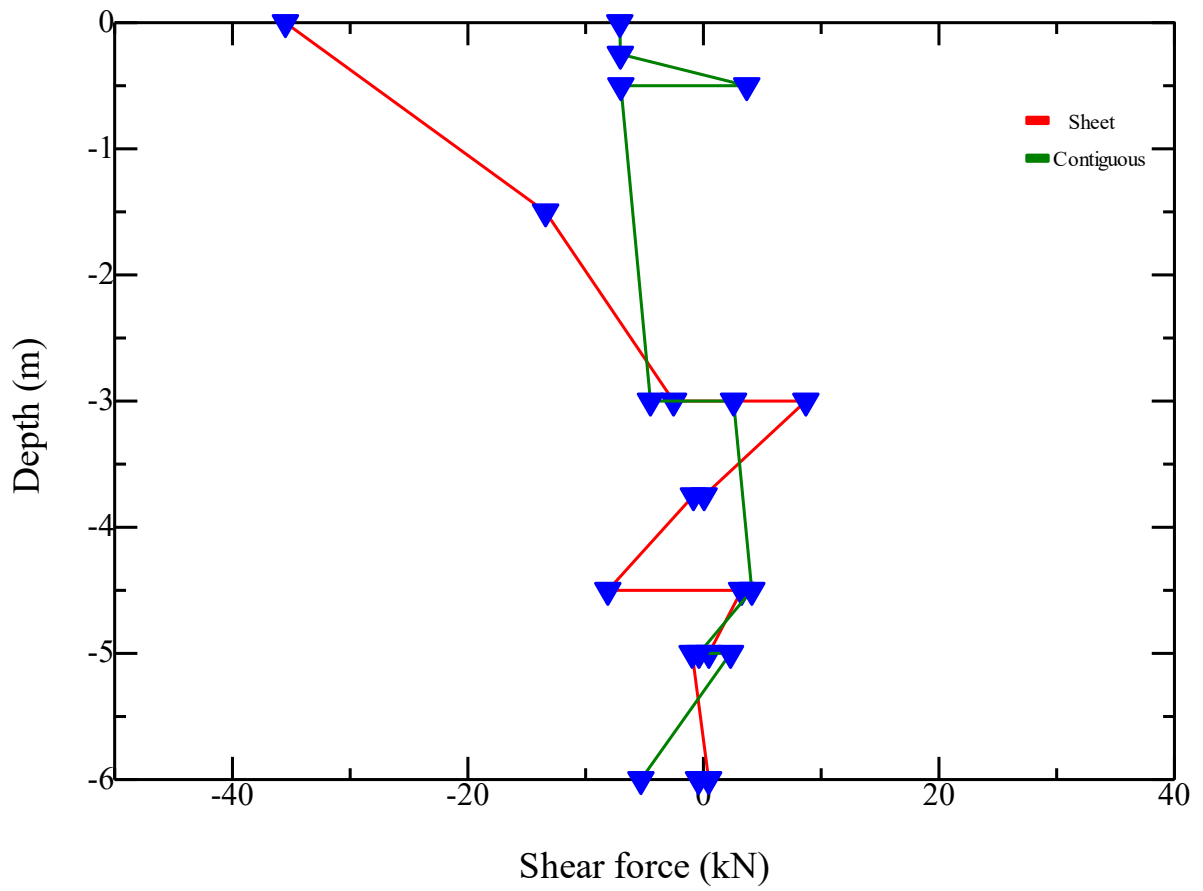


(c)

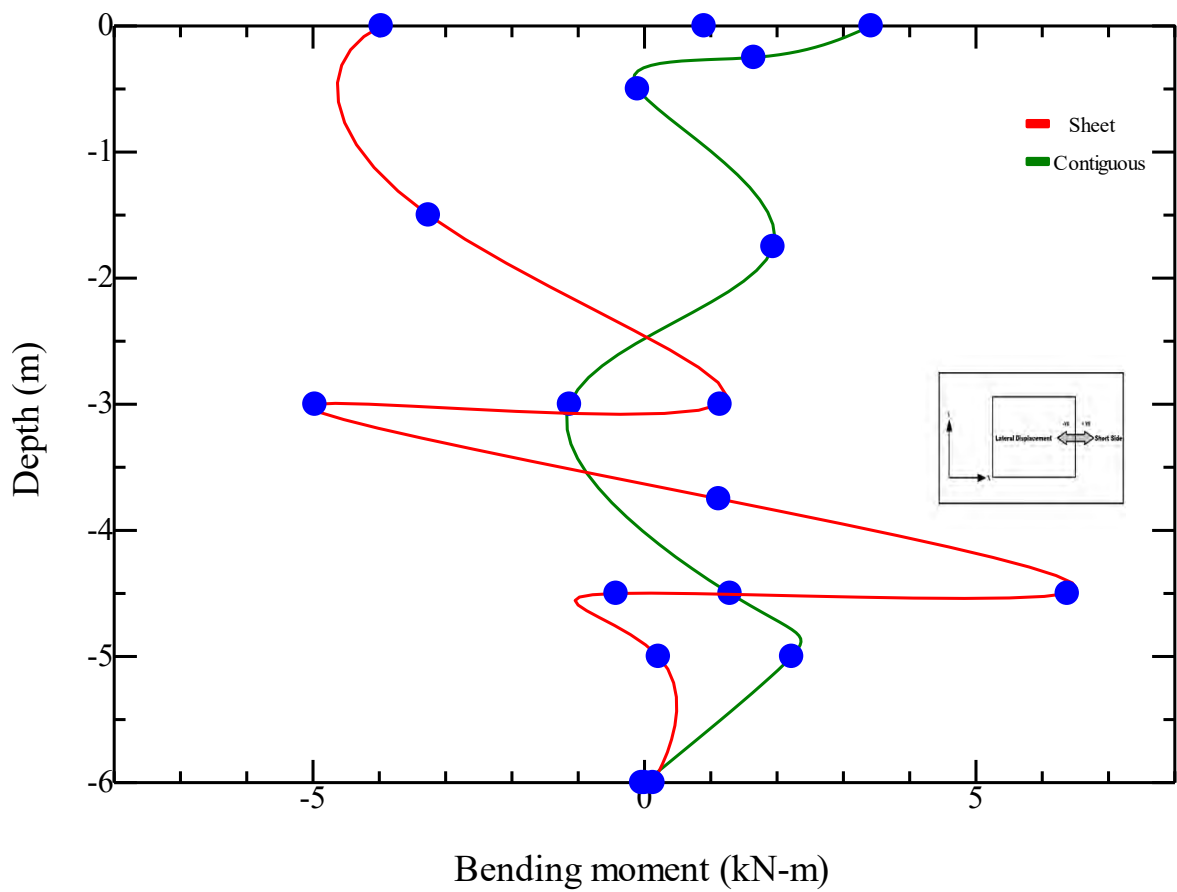
Fig. B-1 Internal forces in the long side of sheet pile and contiguous pile wall of Dhaka site having single basement system-(a) axial force (b) shear force (c) bending moment- HS model



(a)

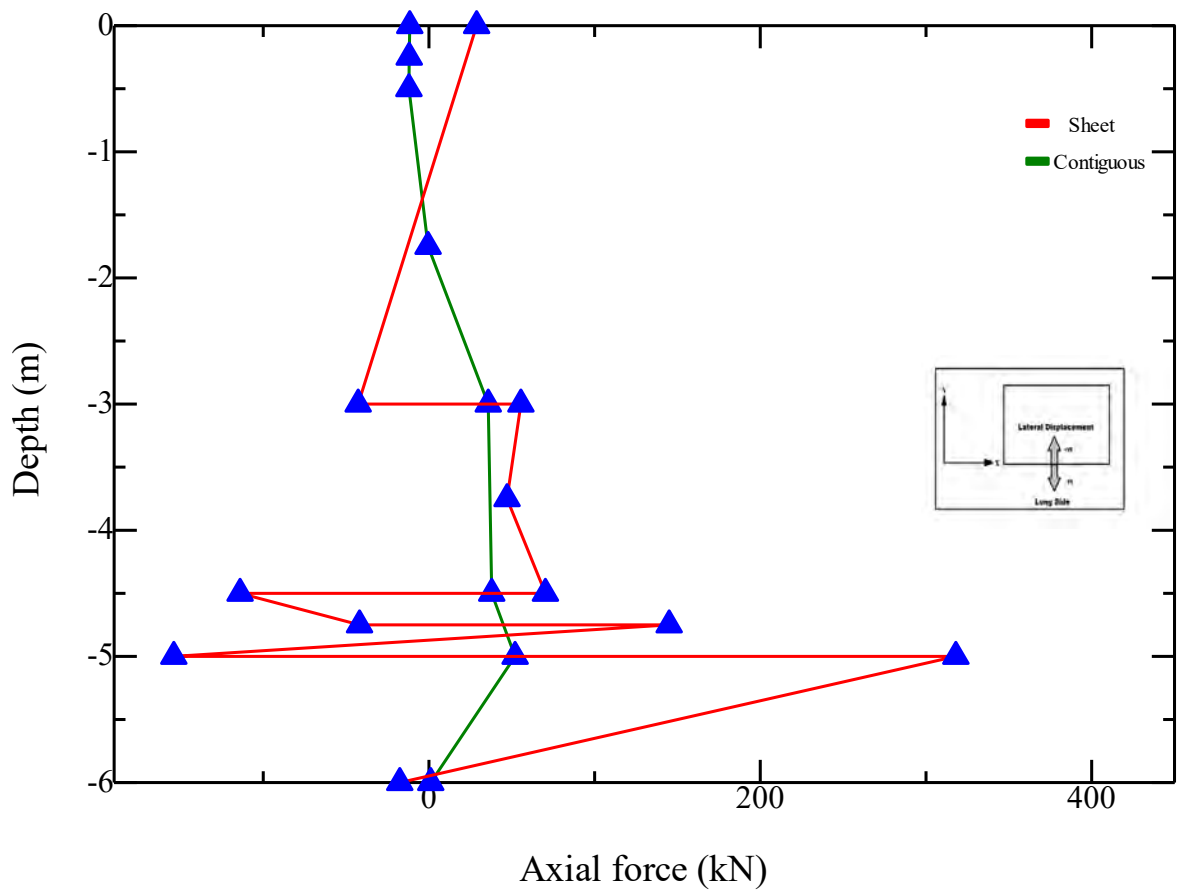


(b)

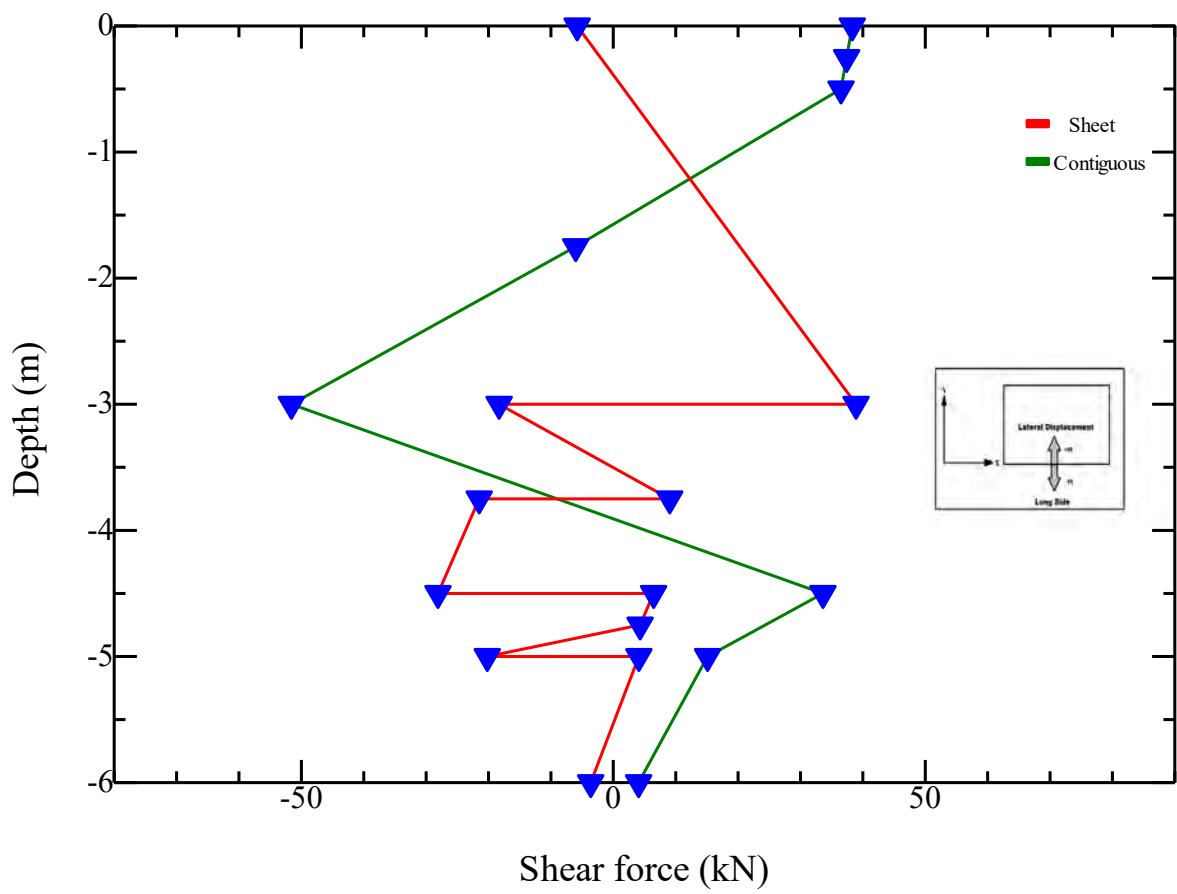


(c)

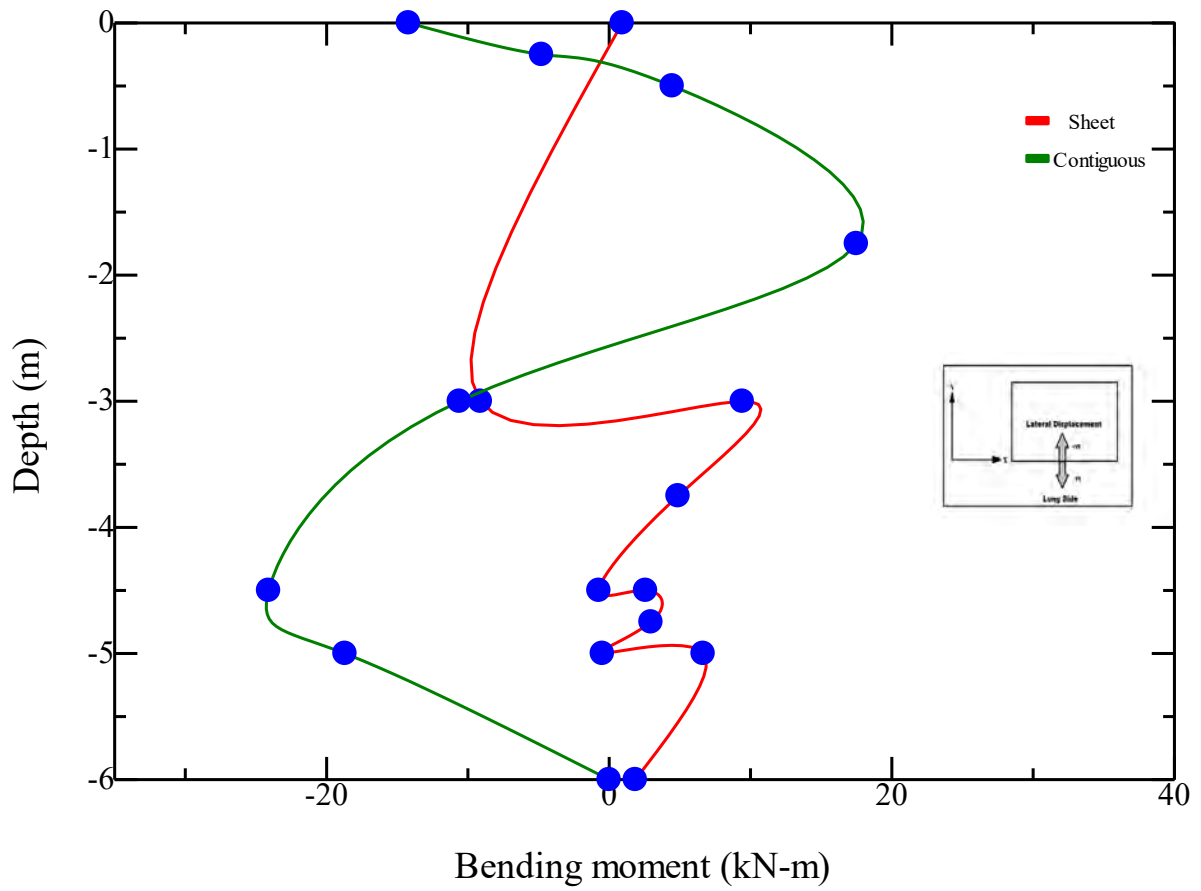
Fig. B-2 Internal forces in the short side of sheet pile and contiguous pile wall of Dhaka site having single basement system-(a) axial force (b) shear force (c) bending moment- HS model



(a)

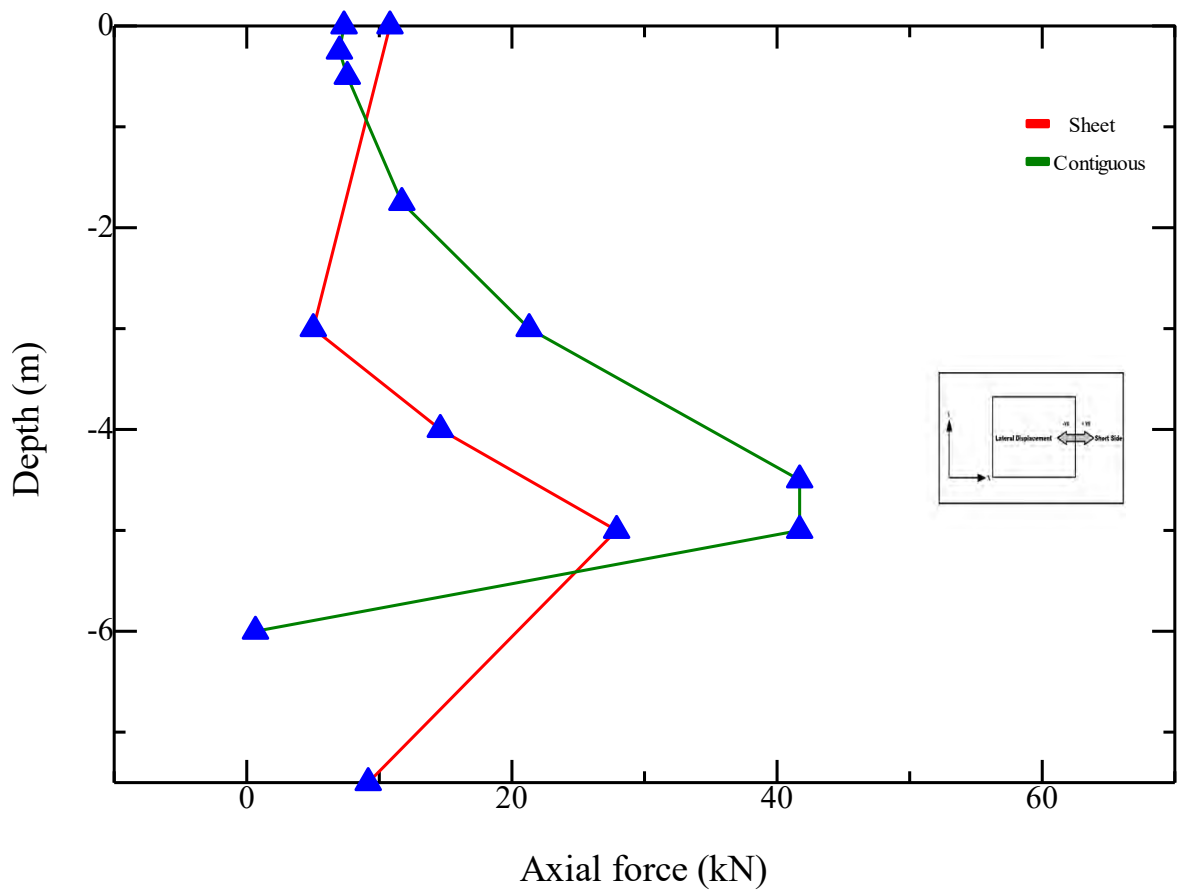


(b)

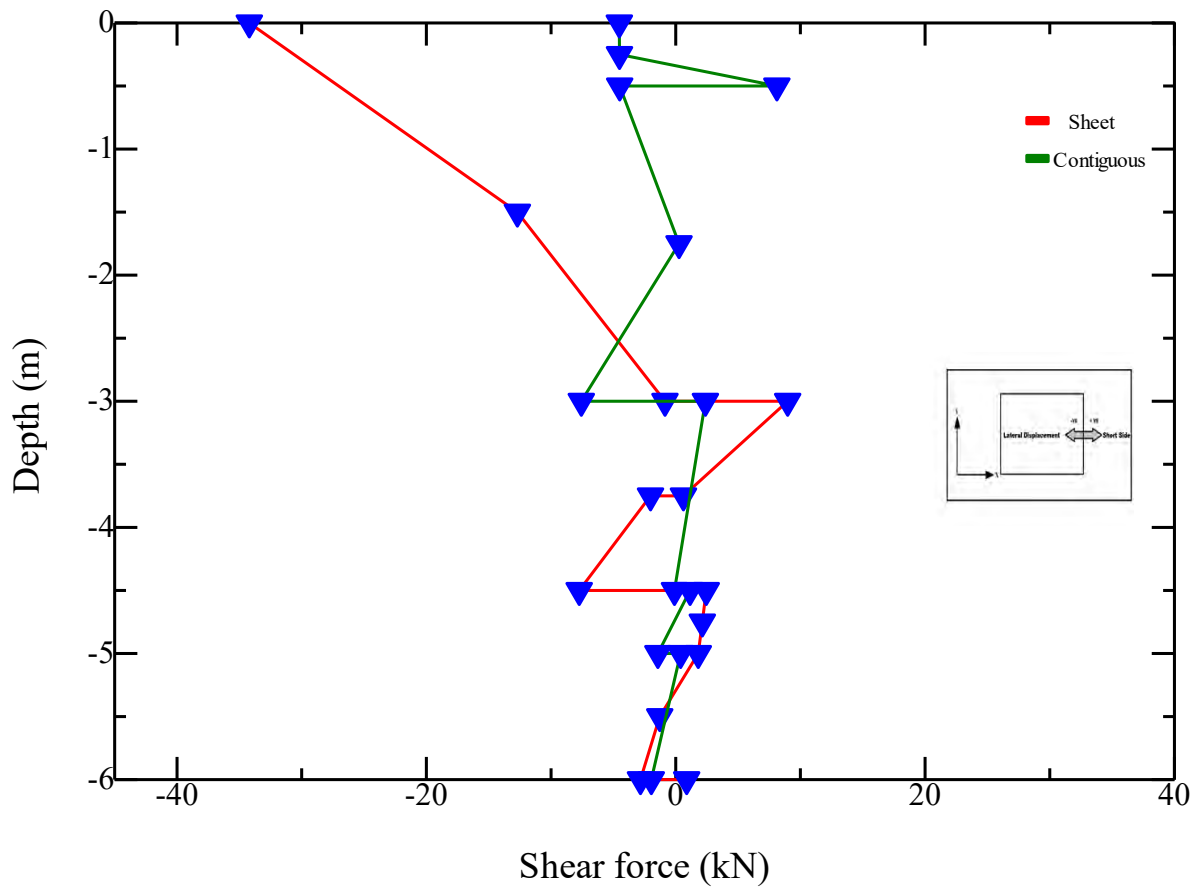


(c)

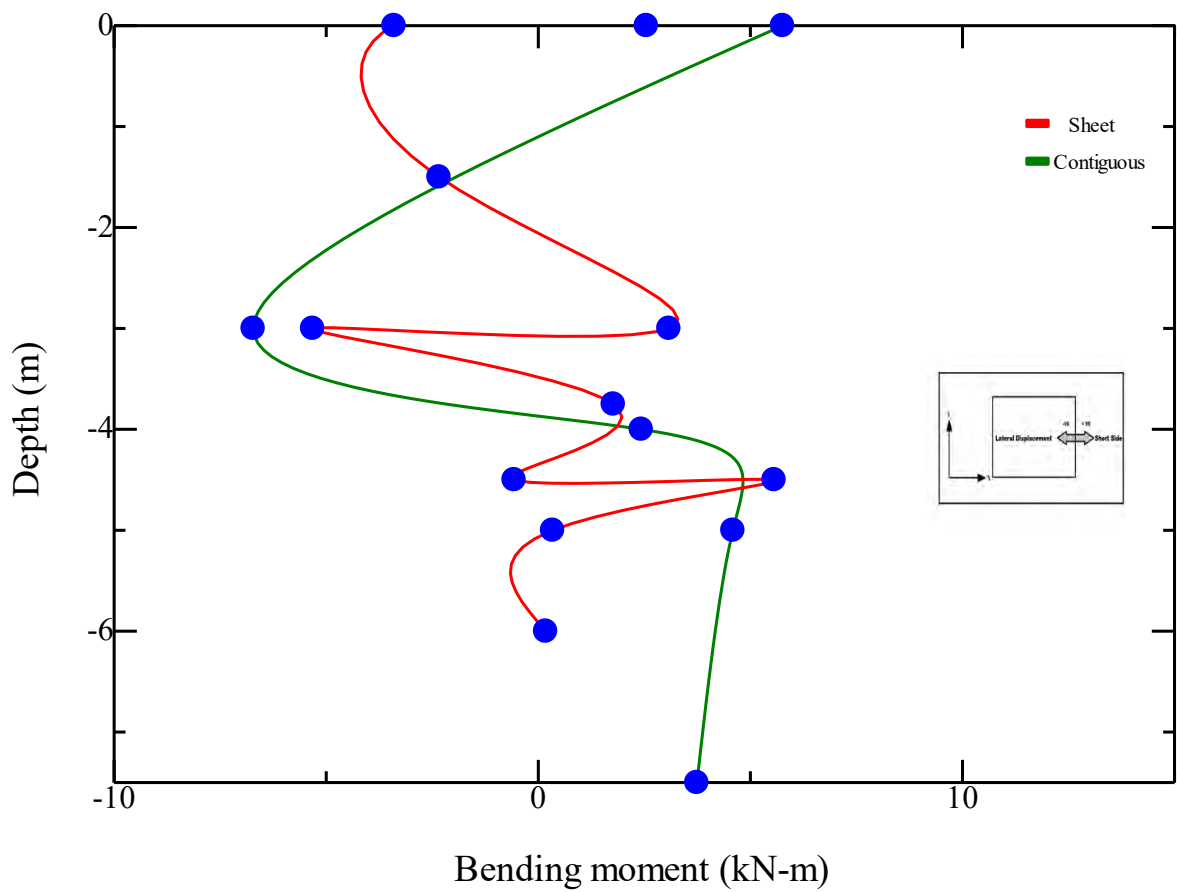
Fig. B-3 Internal forces in the long side of sheet pile and contiguous pile wall of Dhaka site having single basement system-(a) axial force (b) shear force (c) bending moment- MC model



(a)

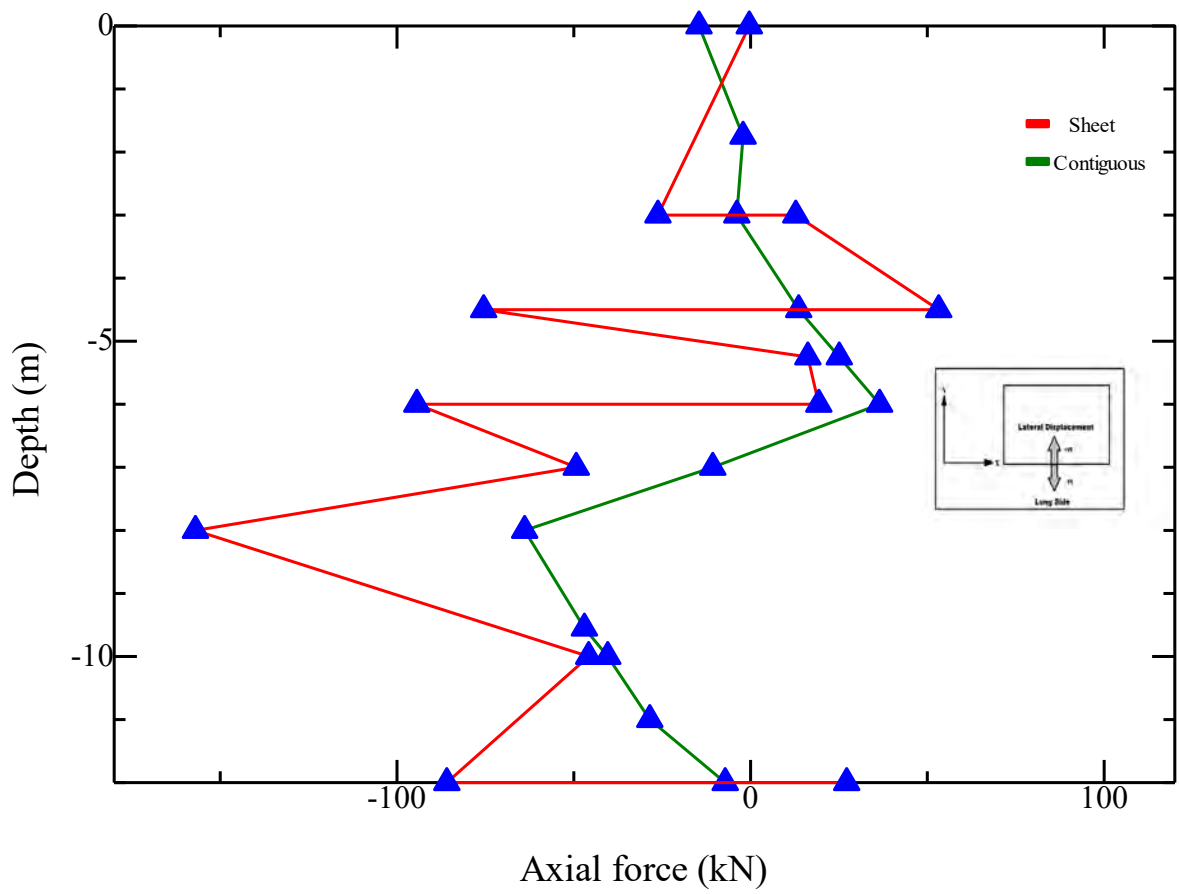


(b)

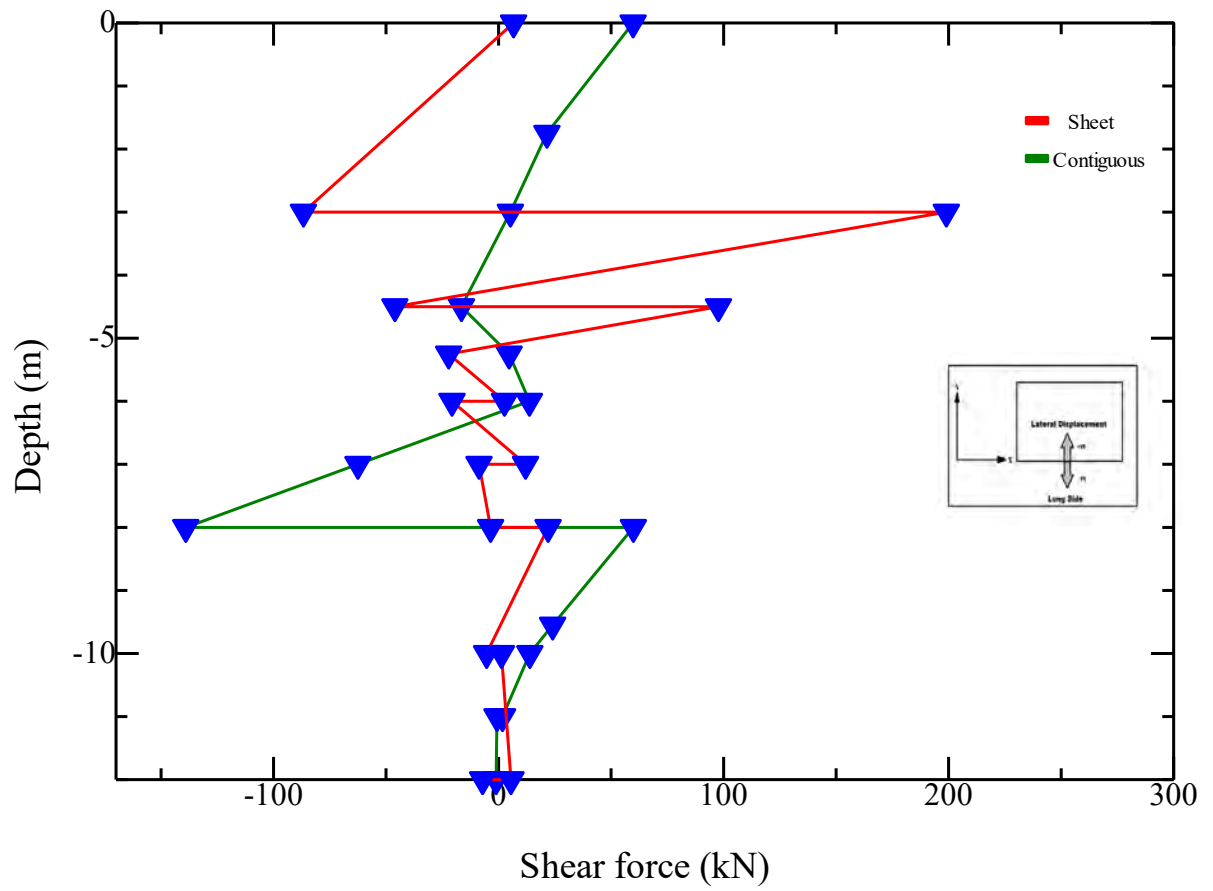


(c)

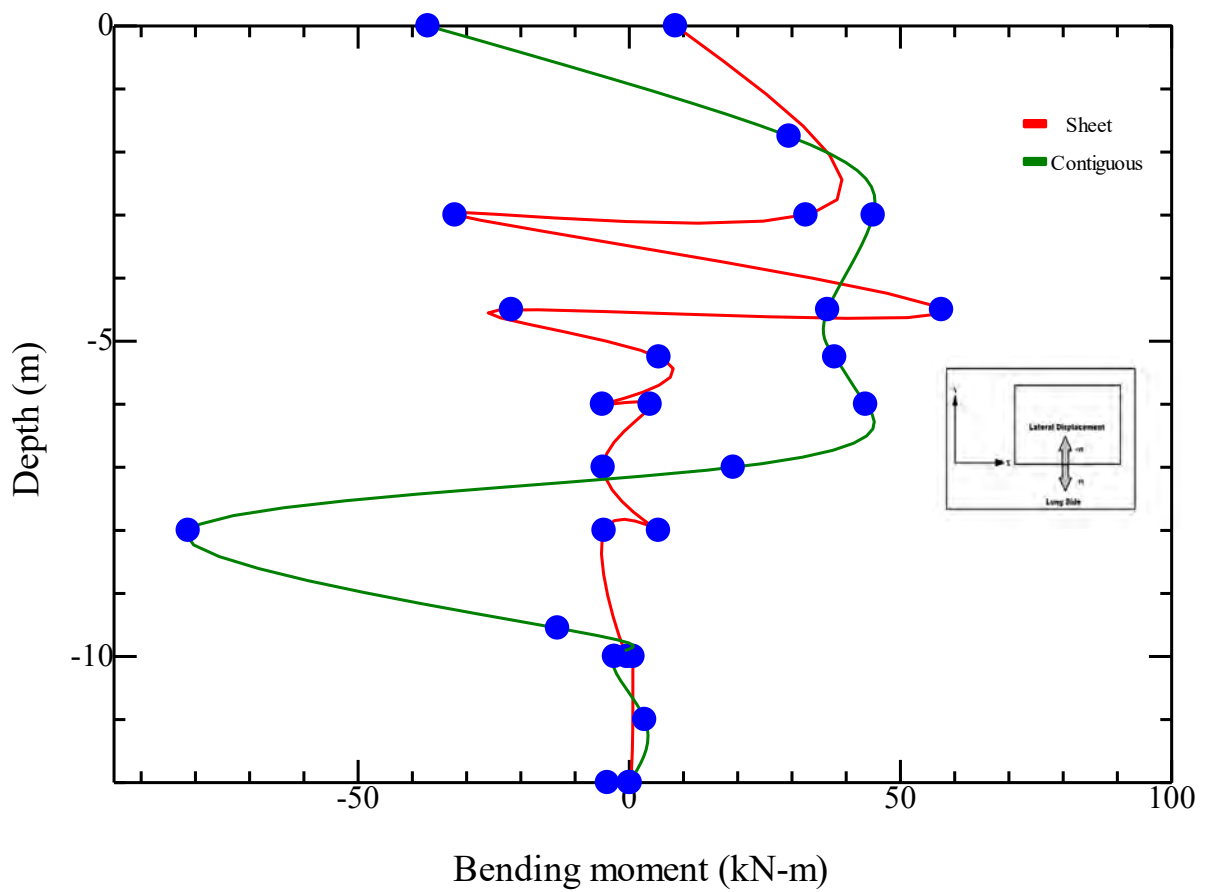
Fig. B-4 Internal forces in the short side of sheet pile and contiguous pile wall of Dhaka site having single basement system-(a) axial force (b) shear force (c) bending moment- MC model



(a)

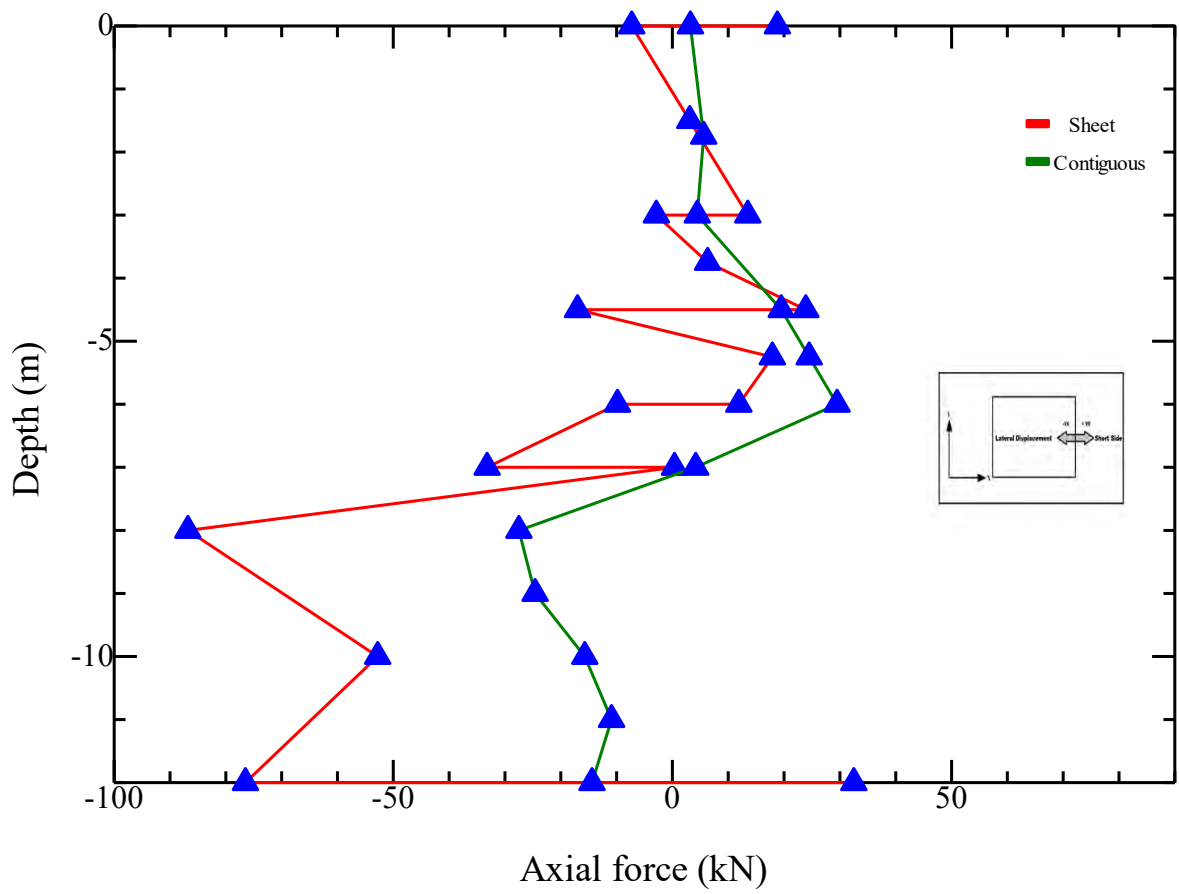


(b)

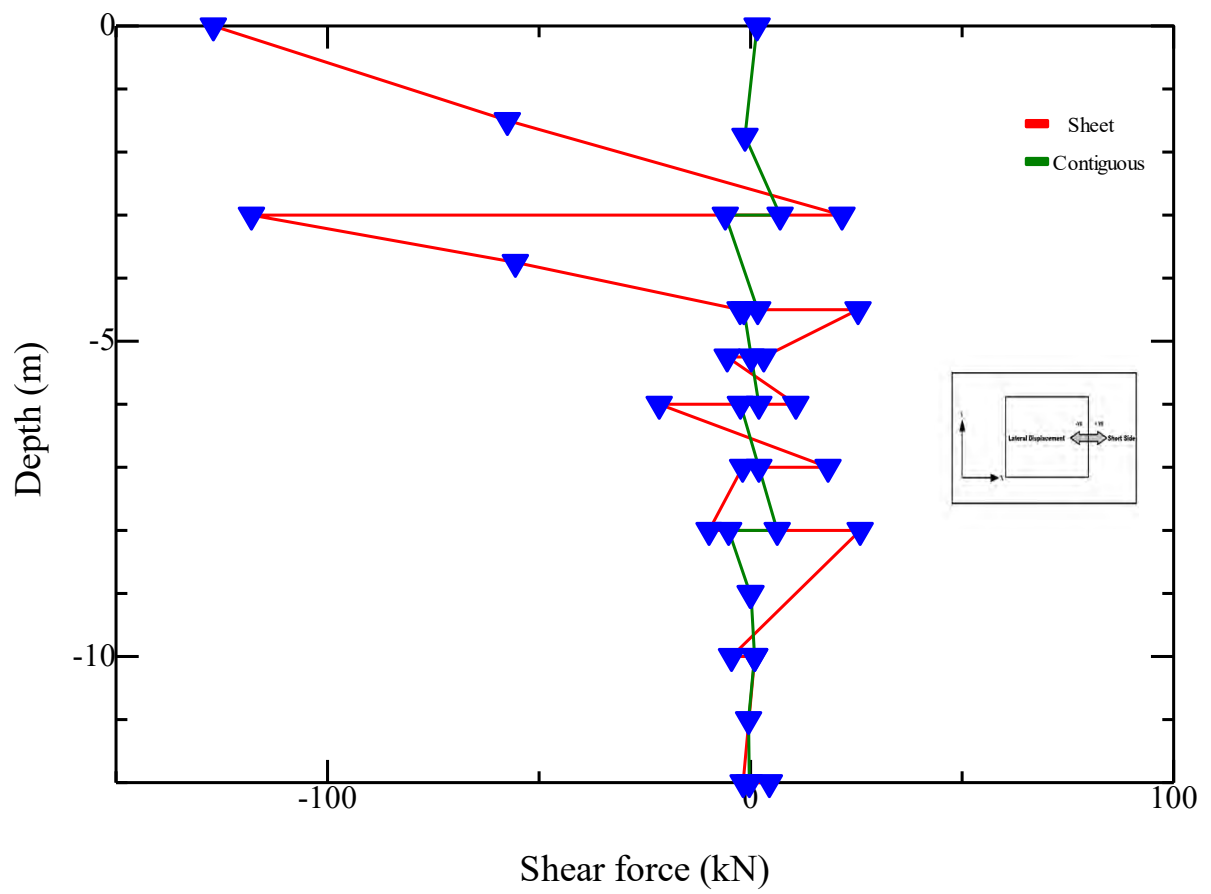


(c)

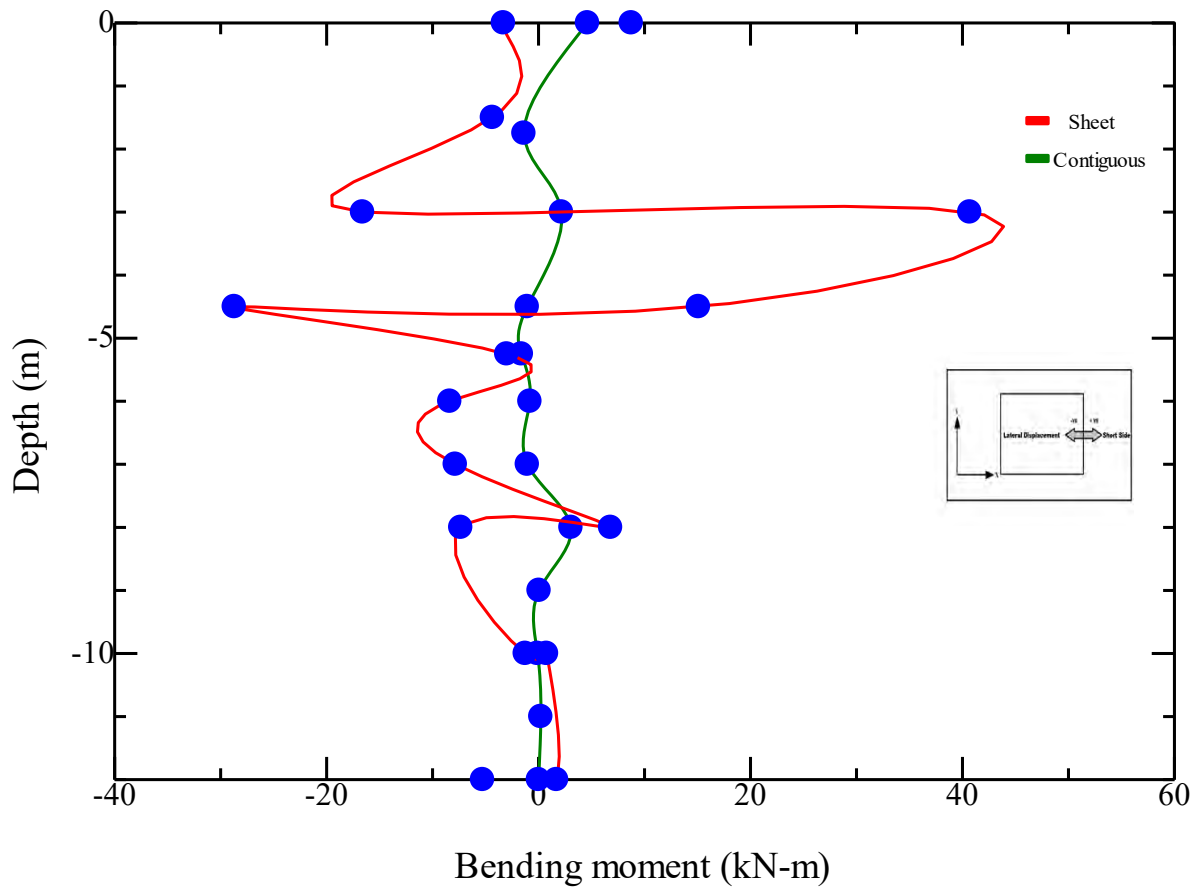
Fig. B-5 Internal forces in the long side of sheet pile and contiguous pile wall of Dhaka site having double basement system-(a) axial force (b) shear force (c) bending moment- HS model



(a)

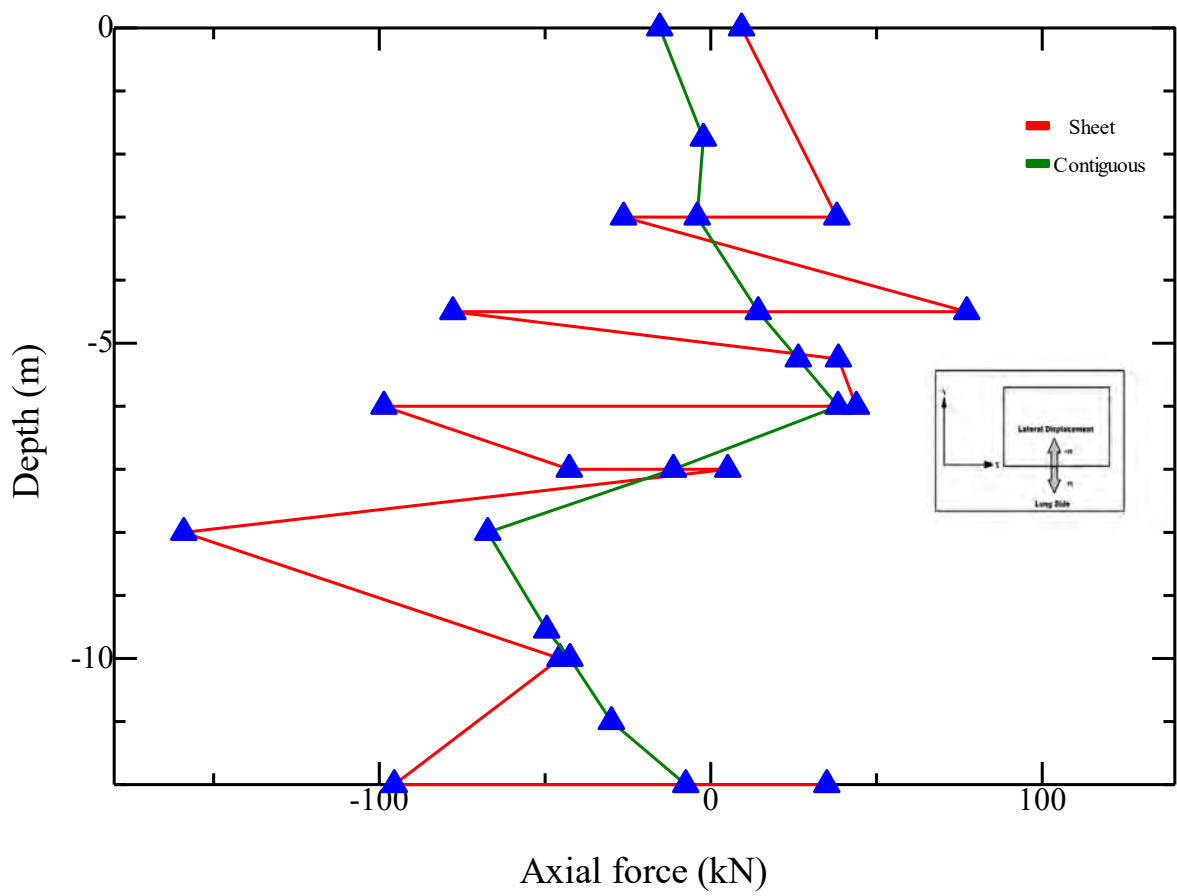


(b)

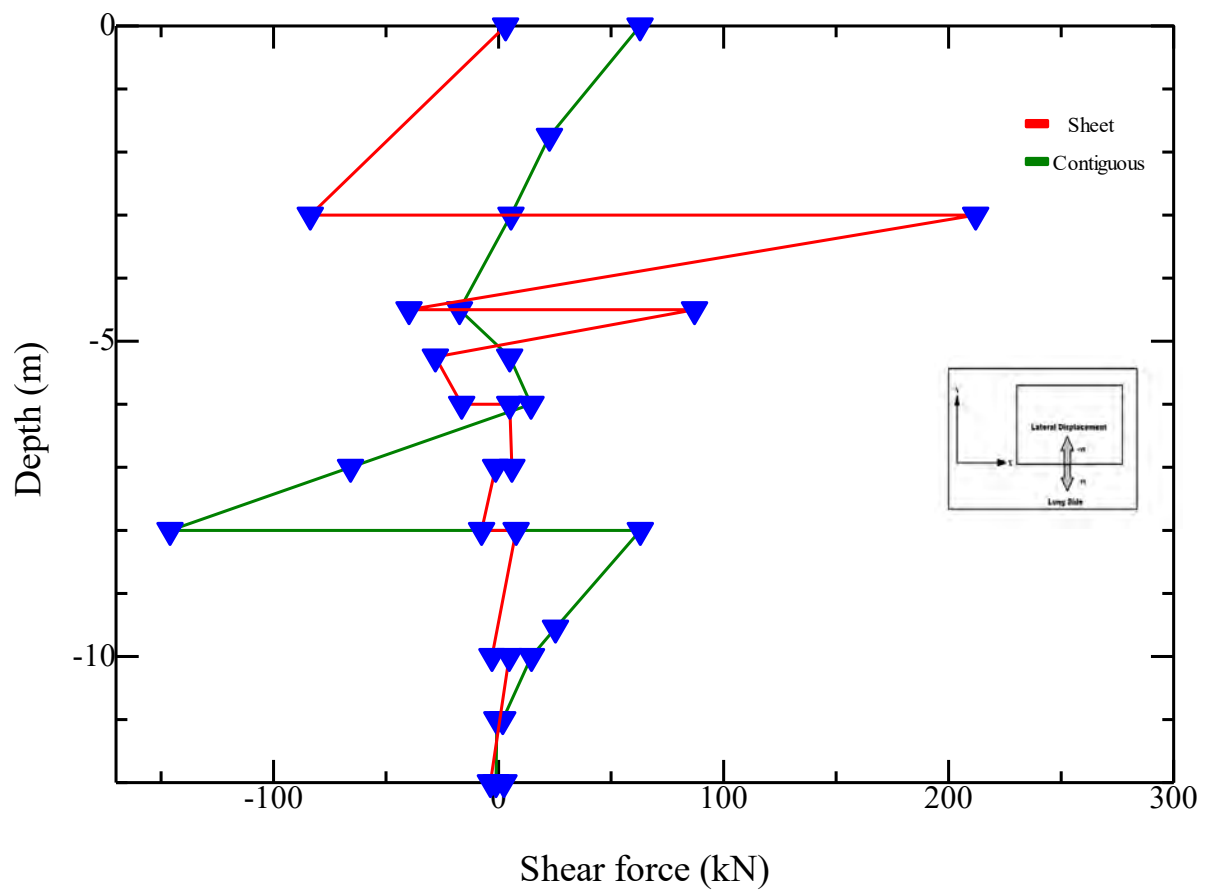


(c)

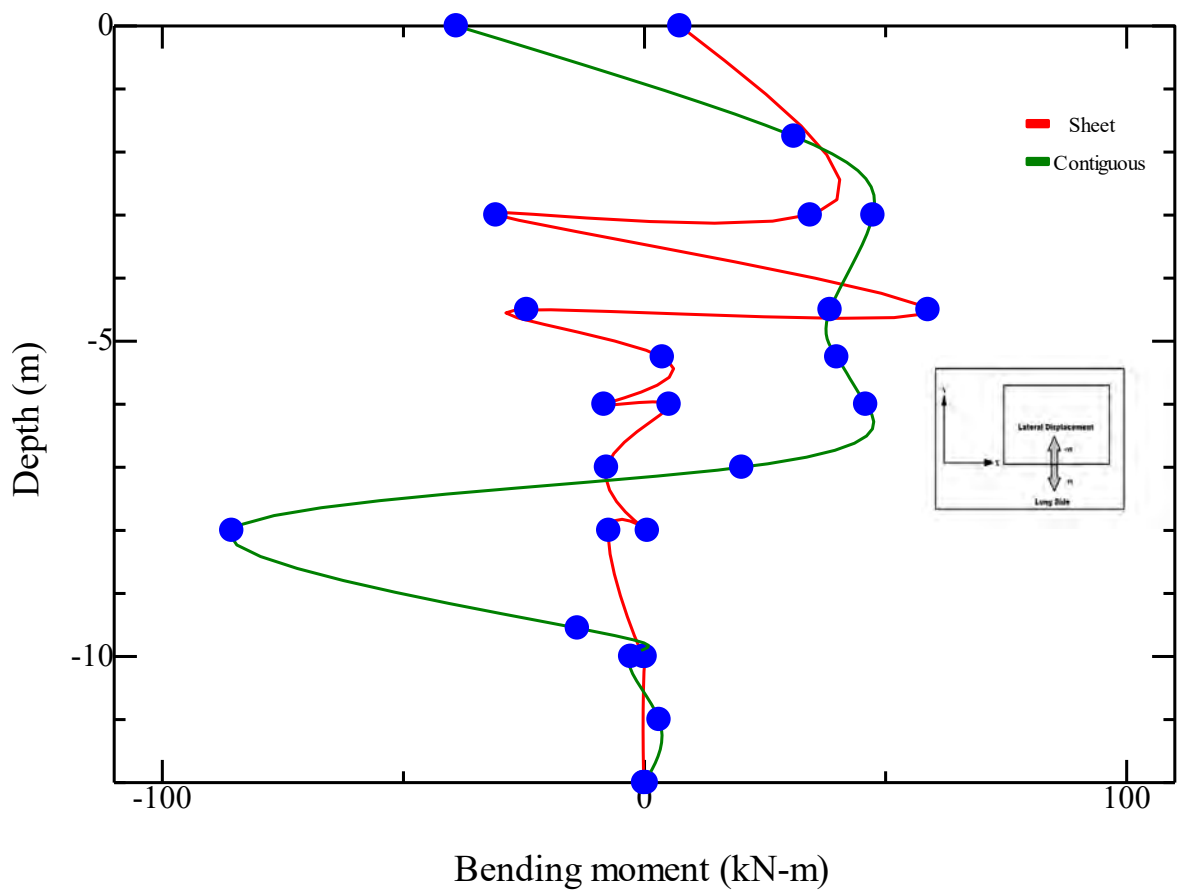
Fig. B-6 Internal forces in the short side of sheet pile and contiguous pile wall of Dhaka site having double basement system-(a) axial force (b) shear force (c) bending moment- HS model



(a)

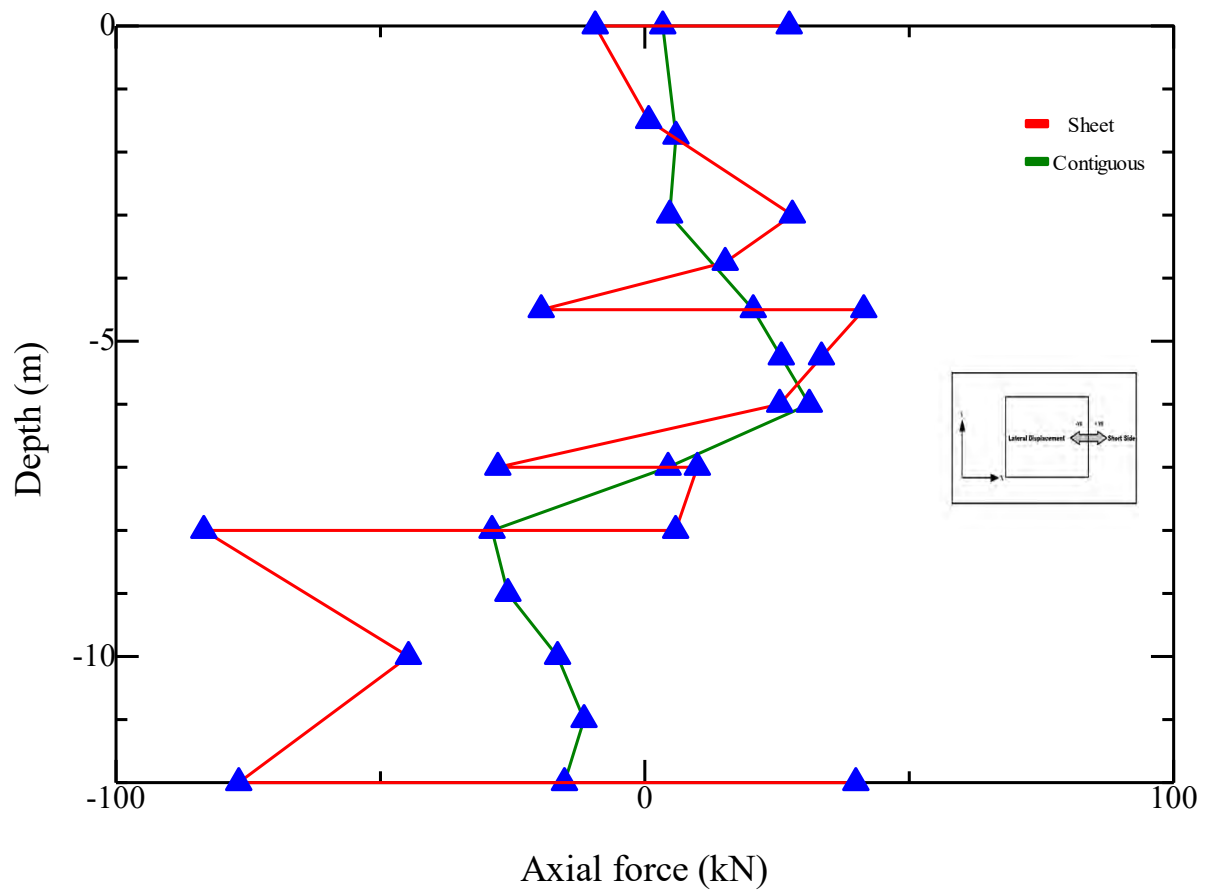


(b)

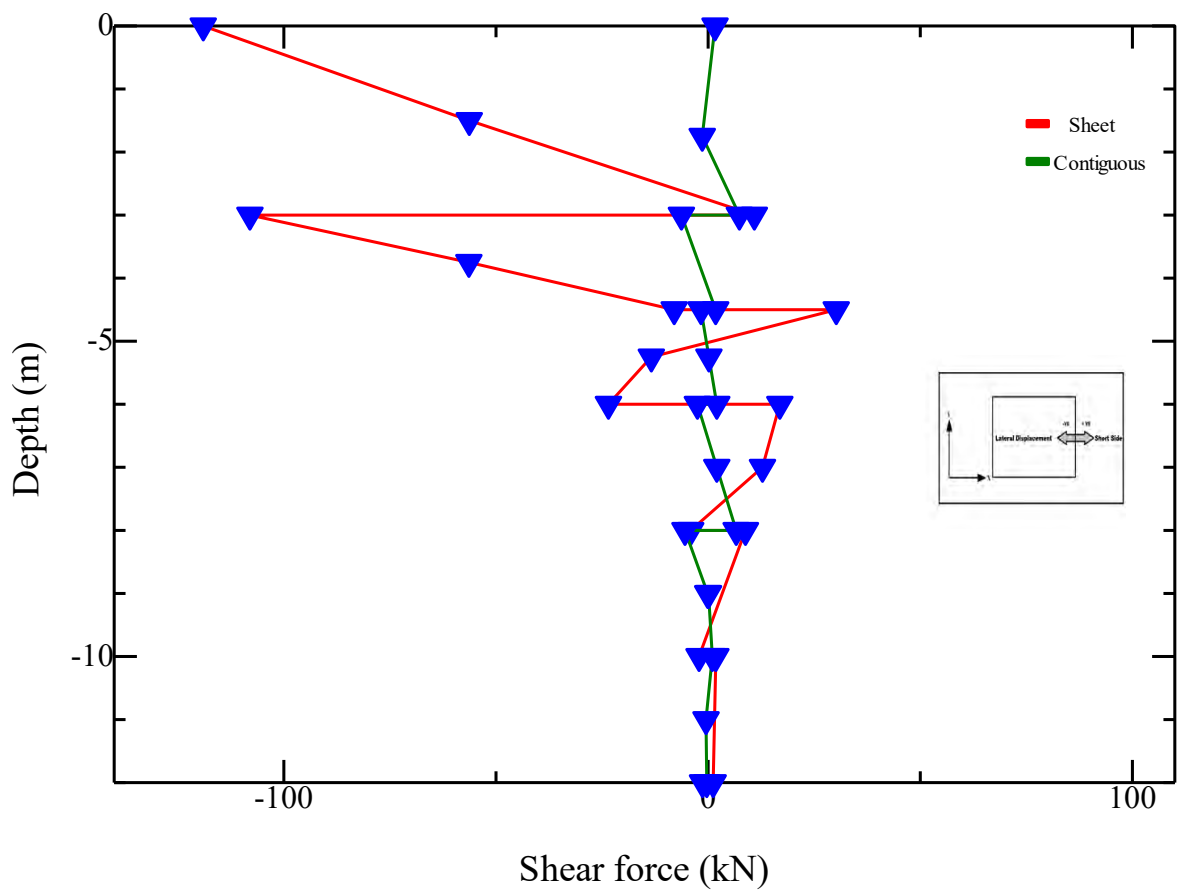


(c)

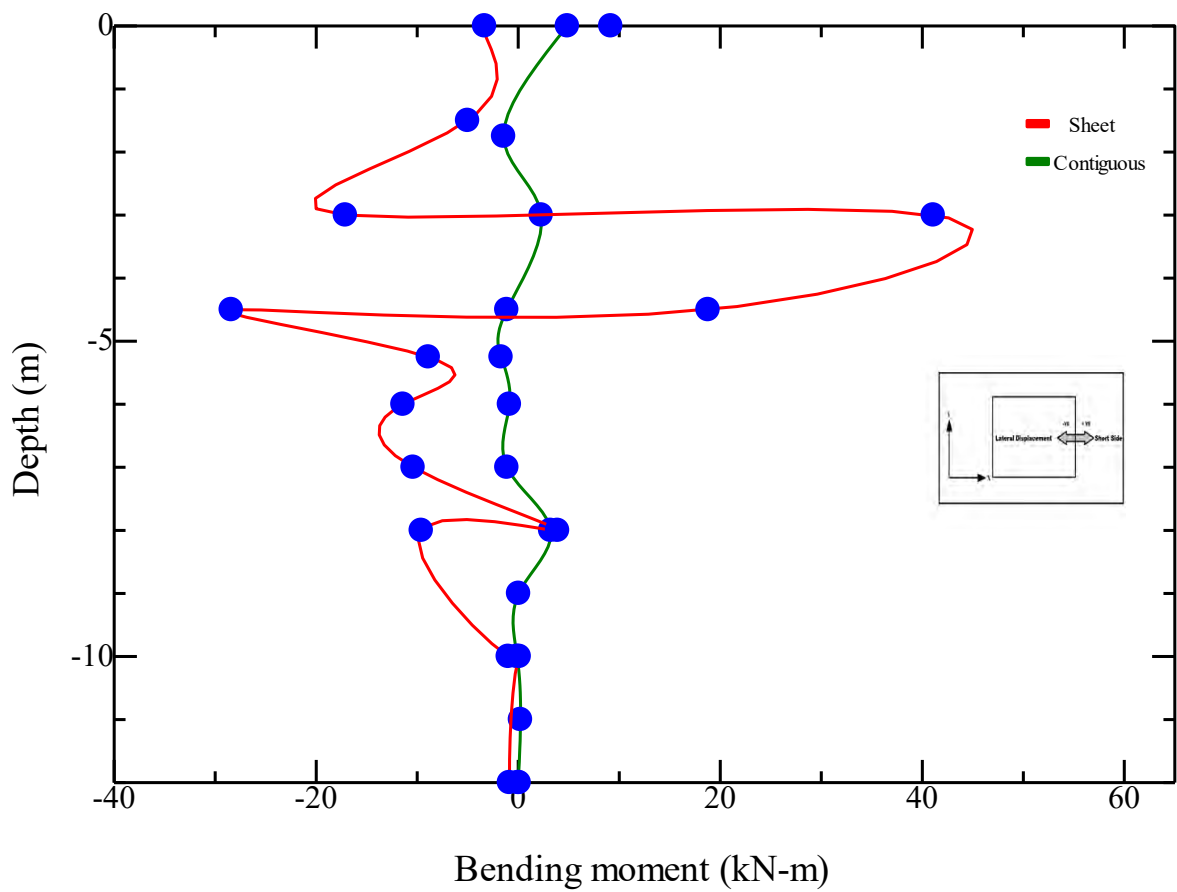
Fig. B-7 Internal forces in the long side of sheet pile and contiguous pile wall of Dhaka site having double basement system-(a) axial force (b) shear force (c) bending moment- MC model



(a)

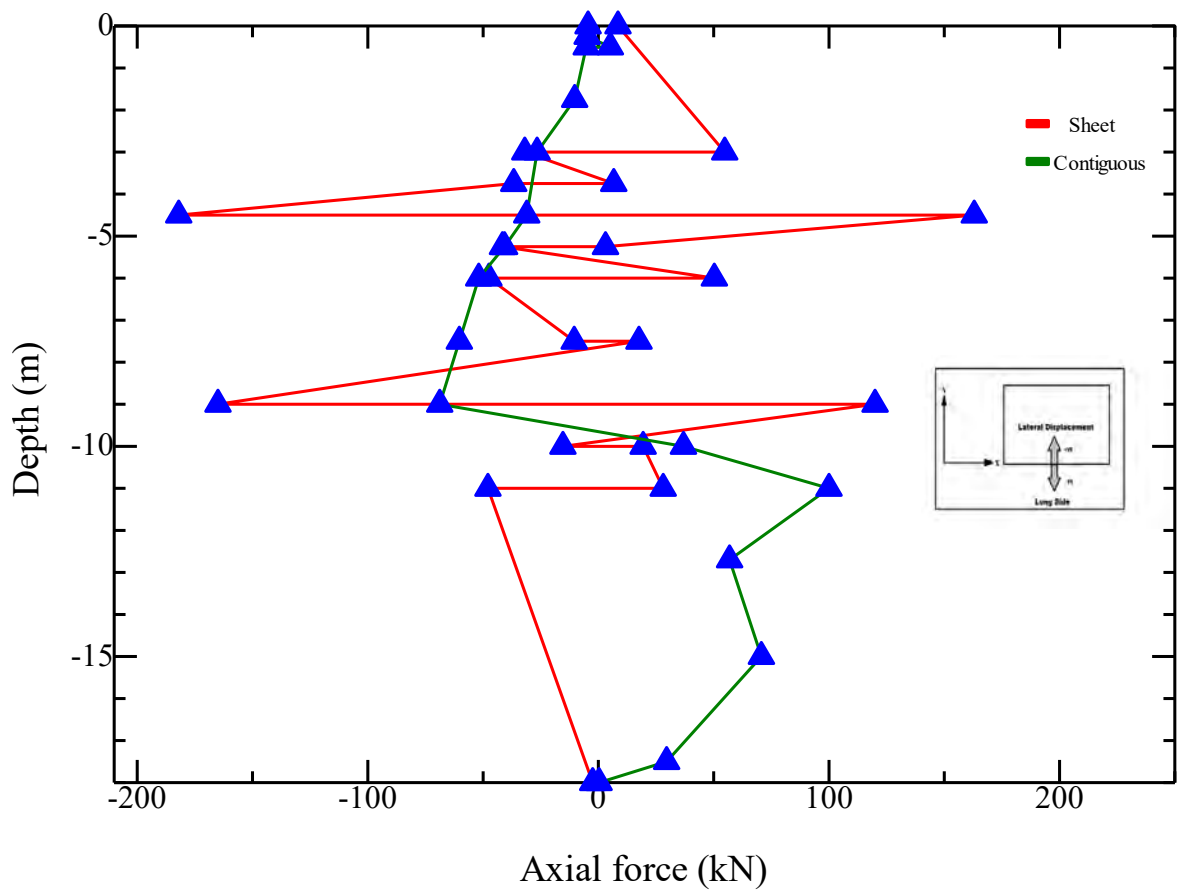


(b)

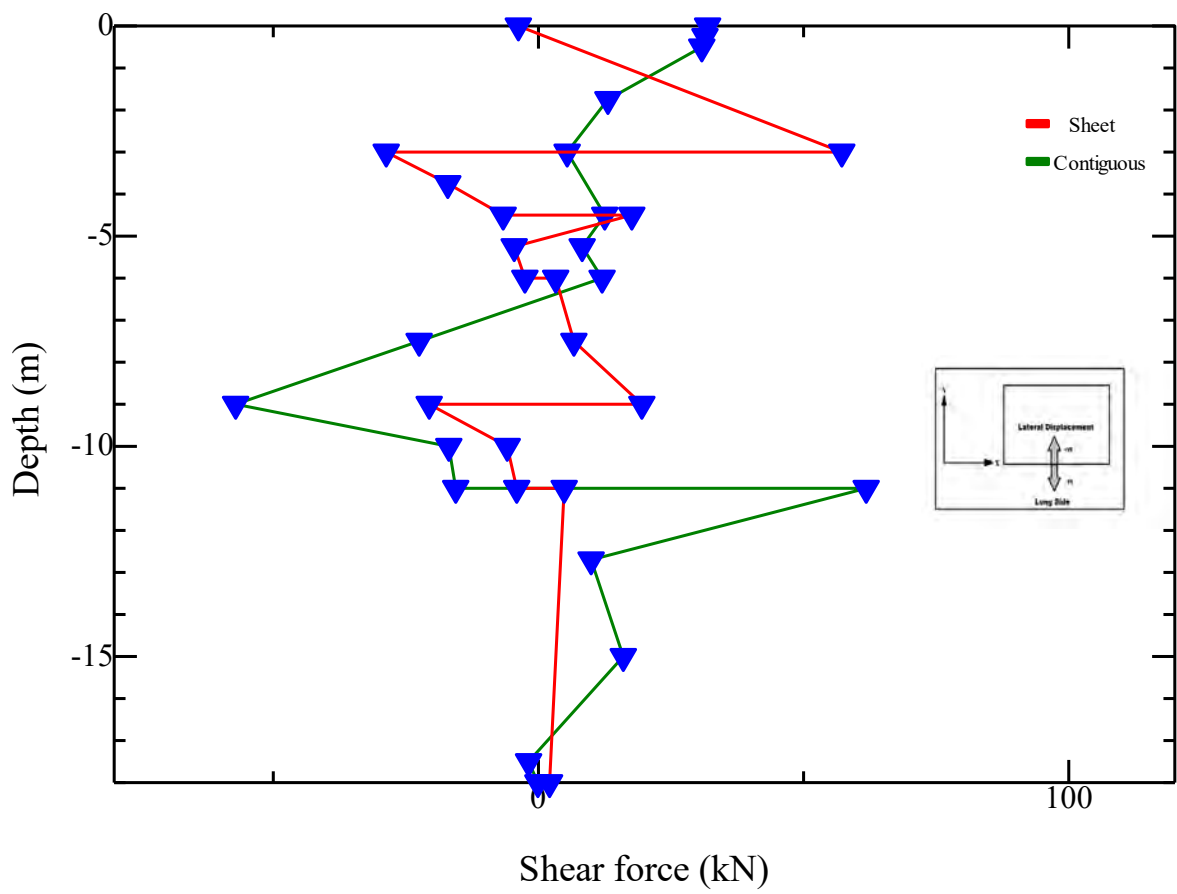


(c)

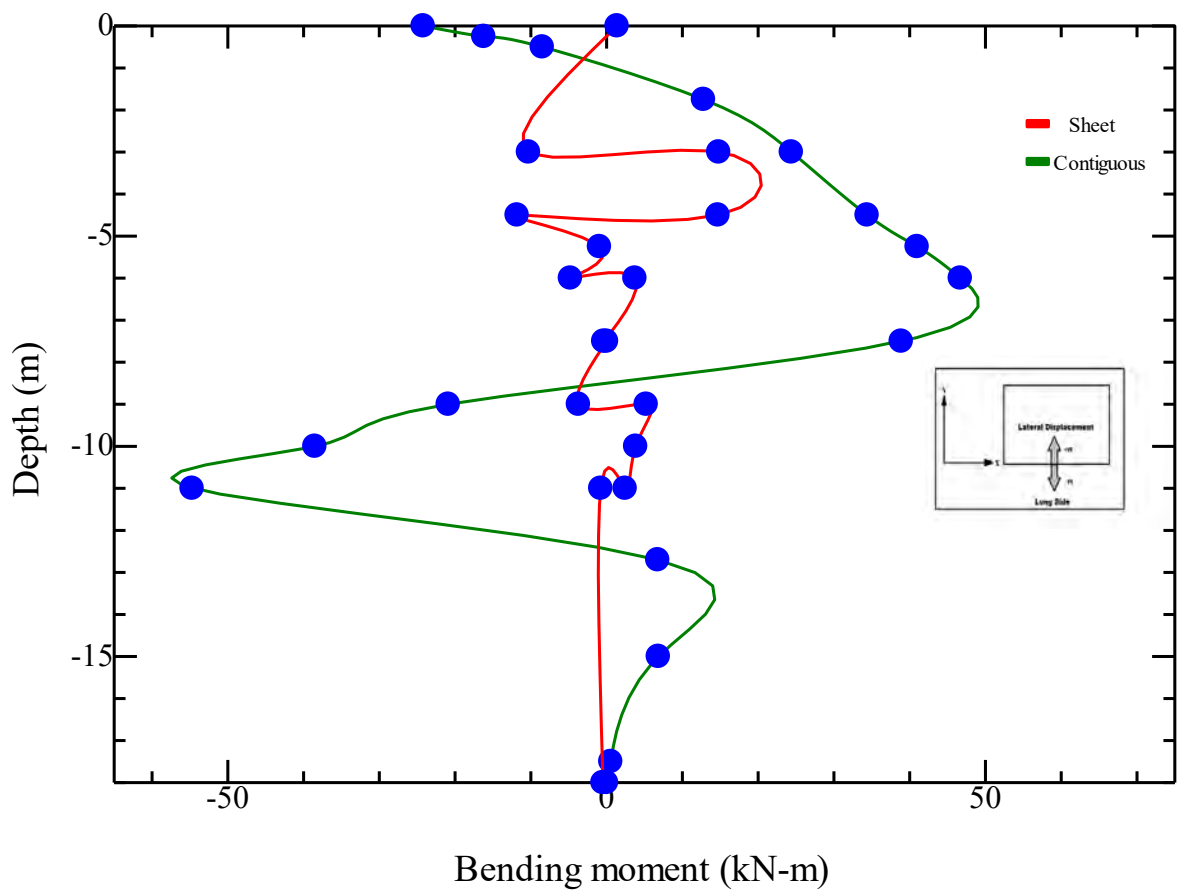
Fig. B-8 Internal forces in the short side of sheet pile and contiguous pile wall of Dhaka site having double basement system-(a) axial force (b) shear force (c) bending moment- MC model



(a)

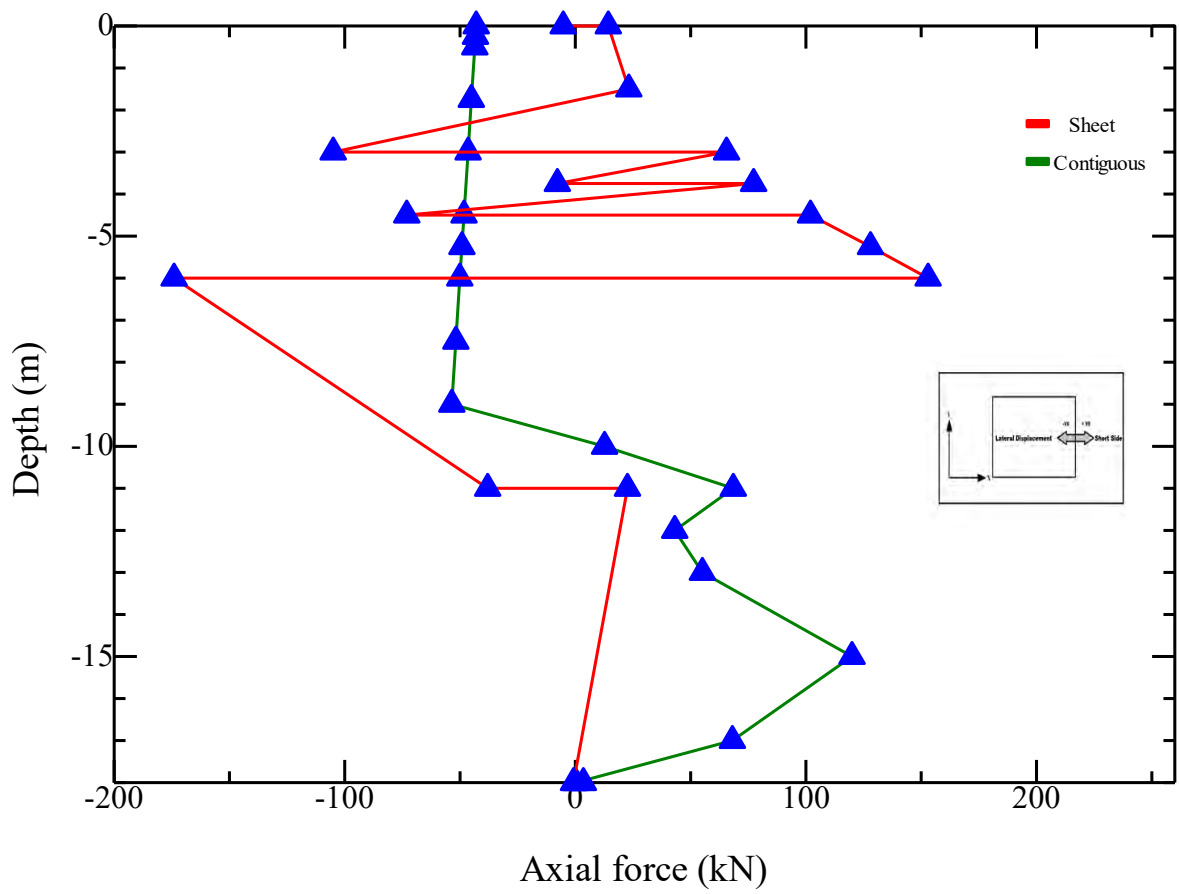


(b)

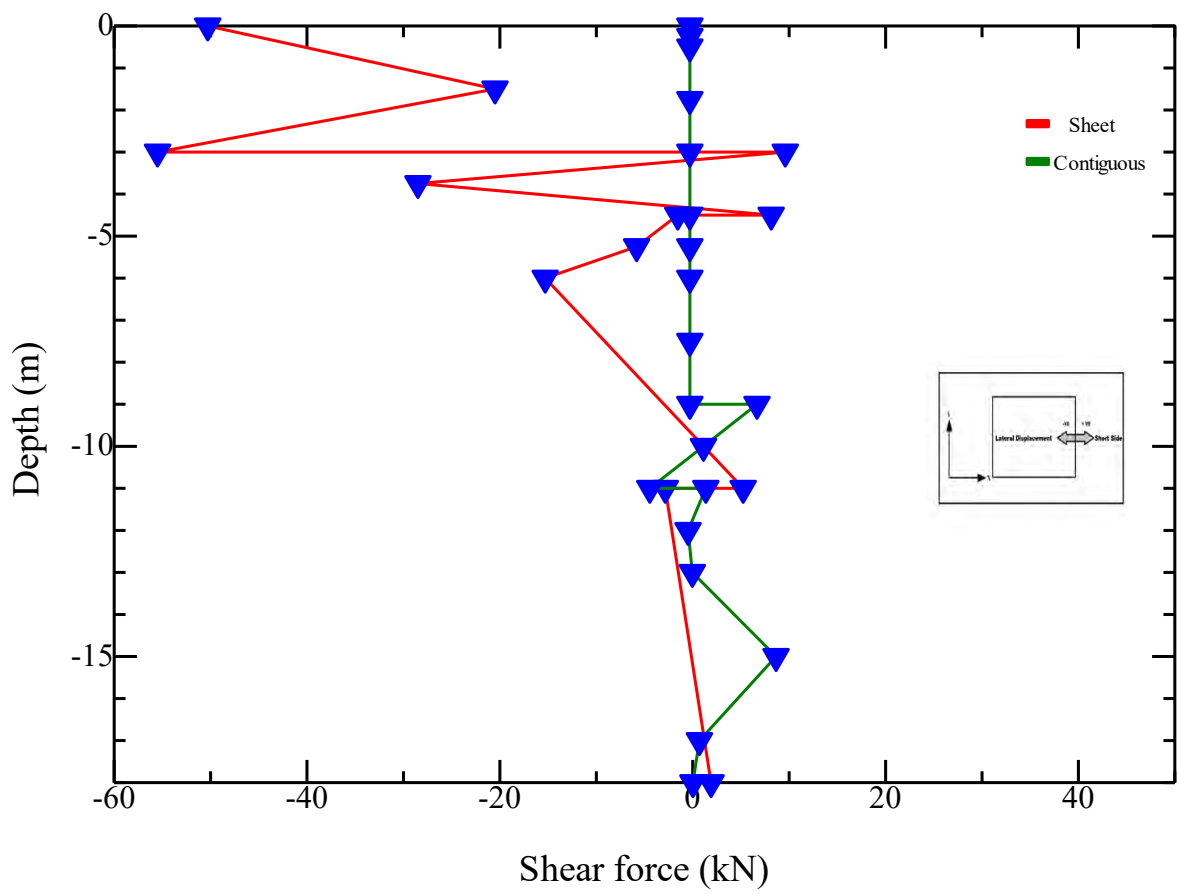


(c)

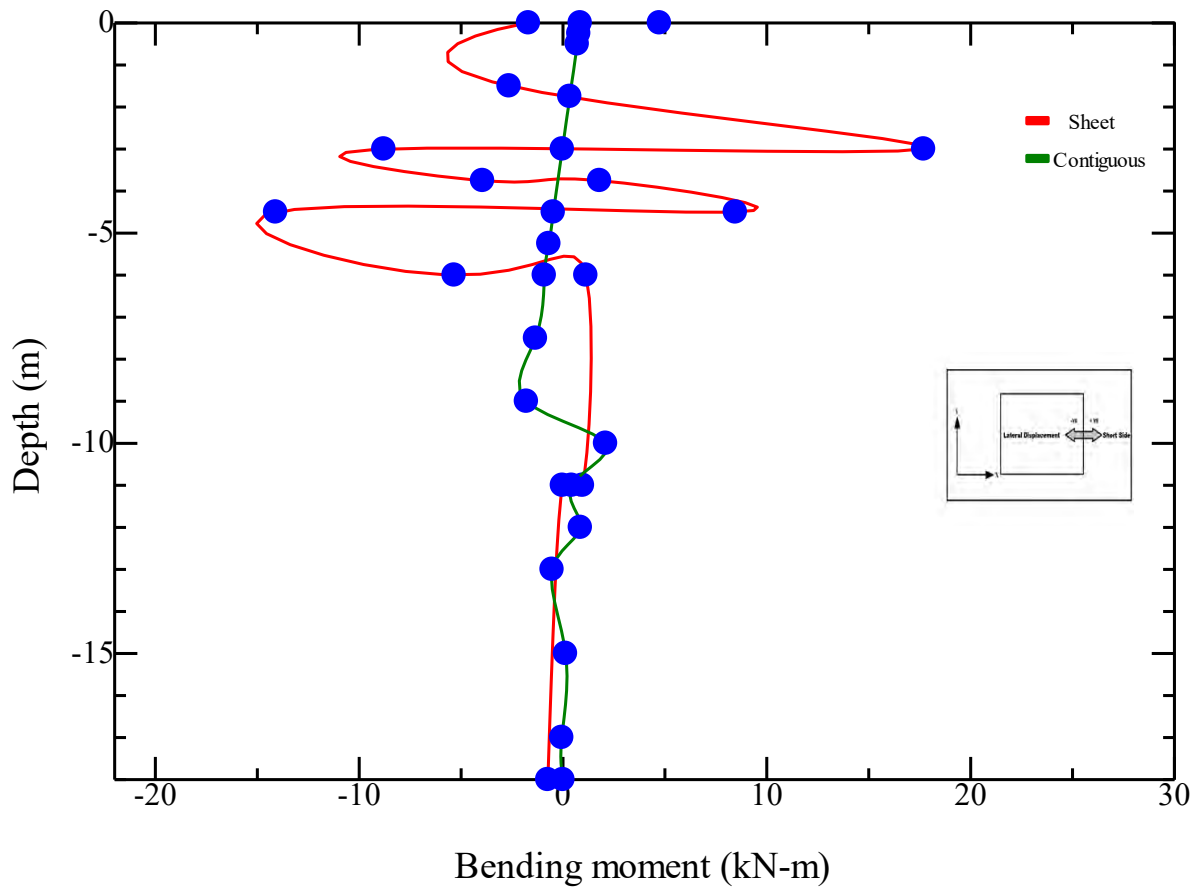
Fig. B-9 Internal forces in the long side of sheet pile and contiguous pile wall of Dhaka site having triple basement system-(a) axial force (b) shear force (c) bending moment- HS model



(a)

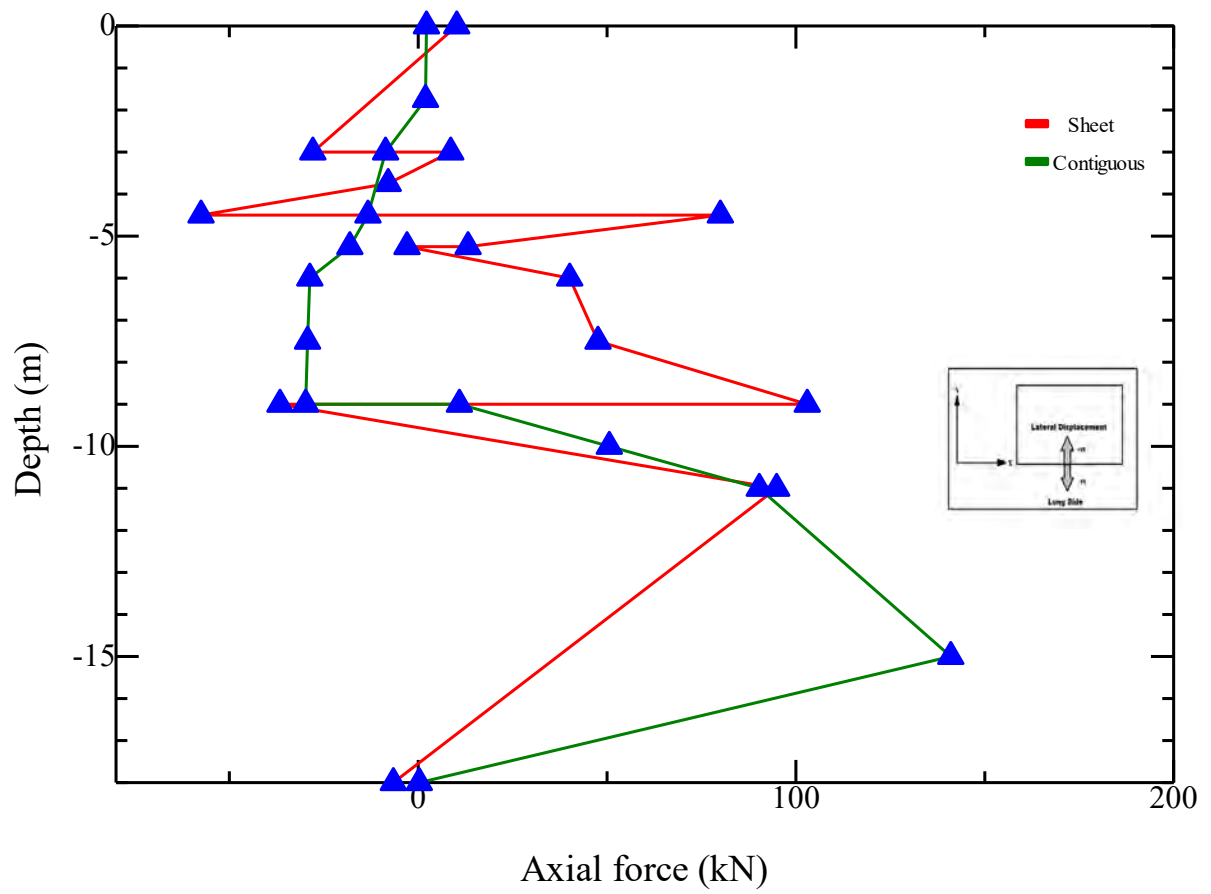


(b)

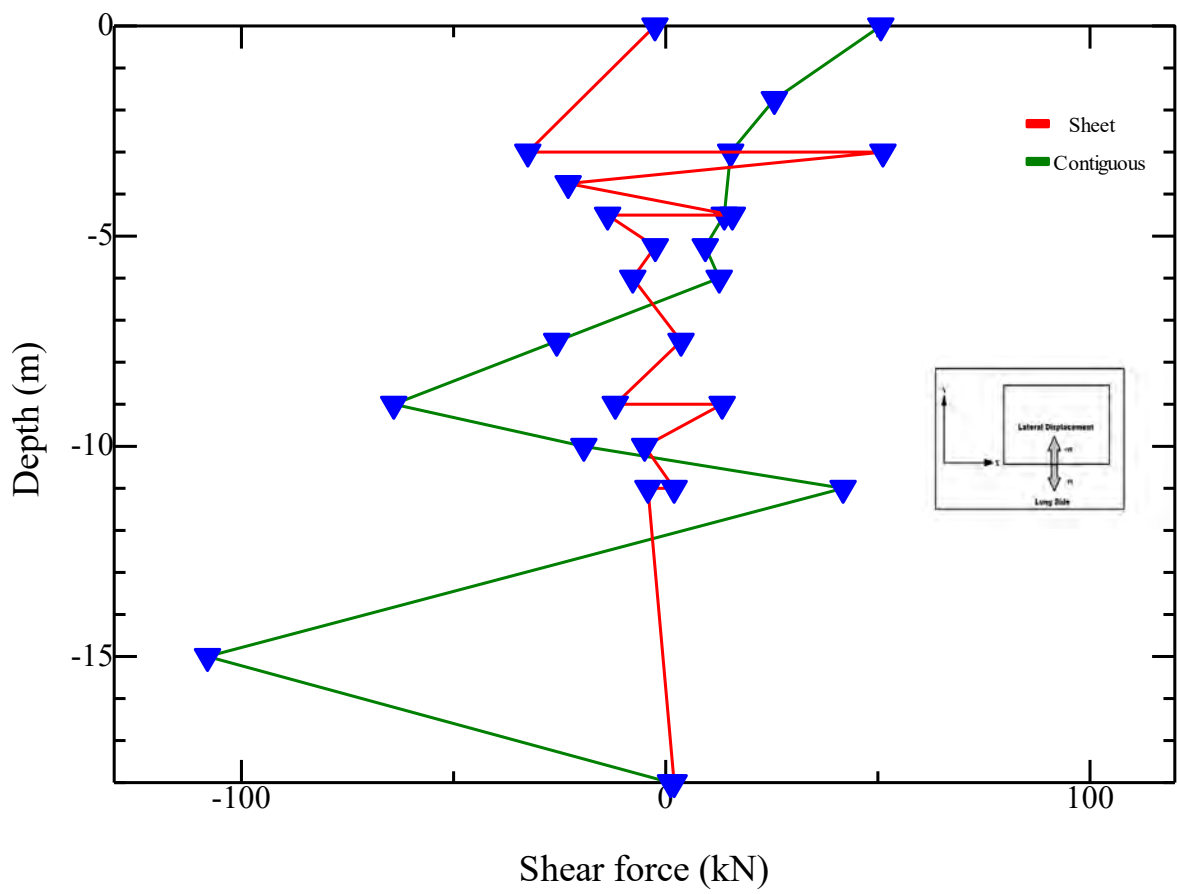


(c)

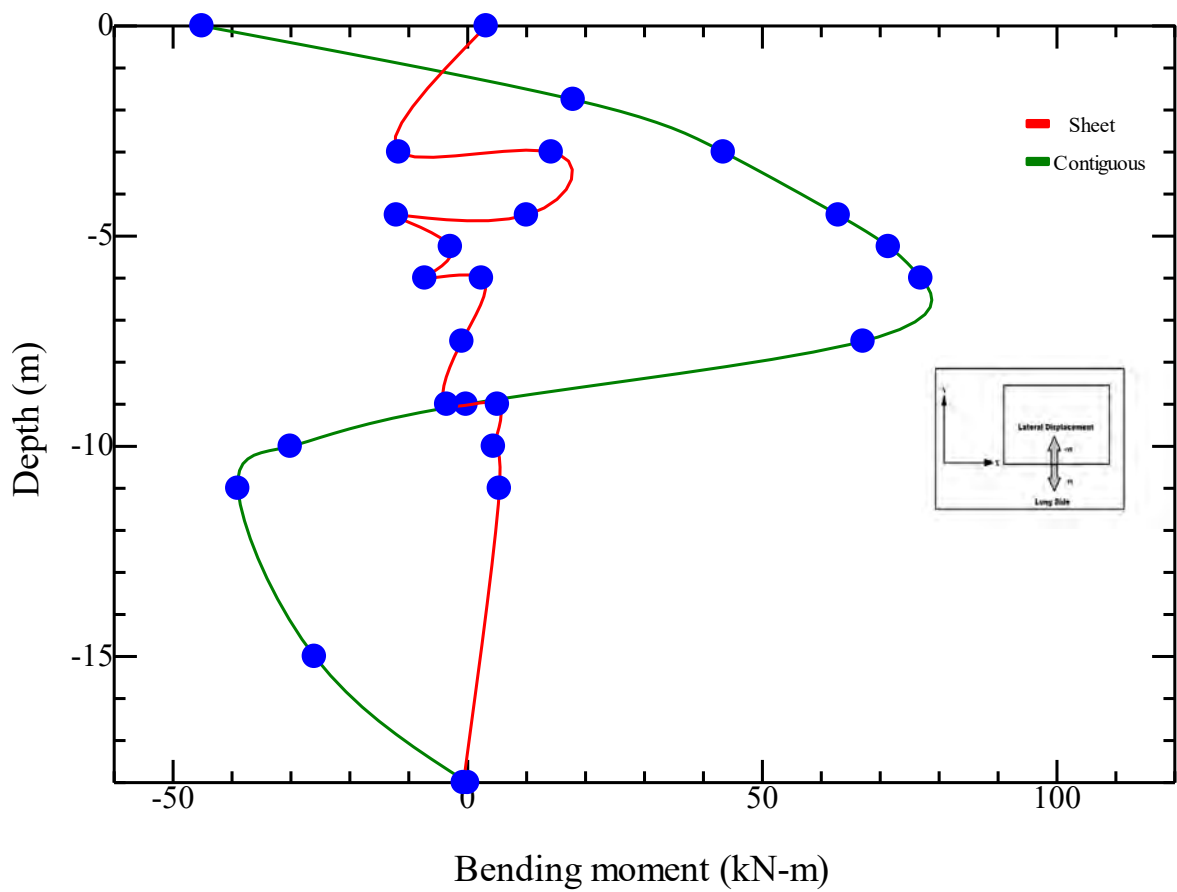
Fig. B-10 Internal forces in the short side of sheet pile and contiguous pile wall of Dhaka site having triple basement system-(a) axial force (b) shear force (c) bending moment- HS model



(a)

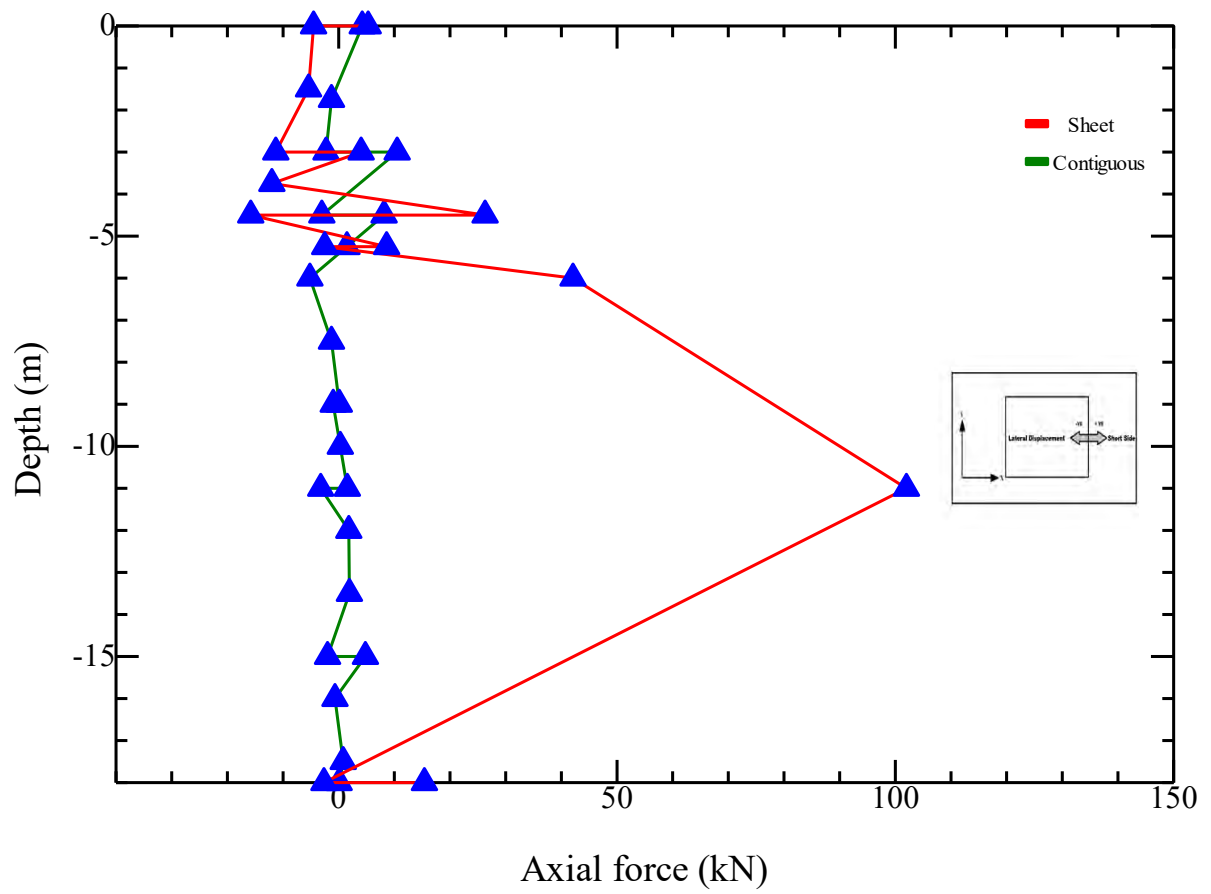


(b)

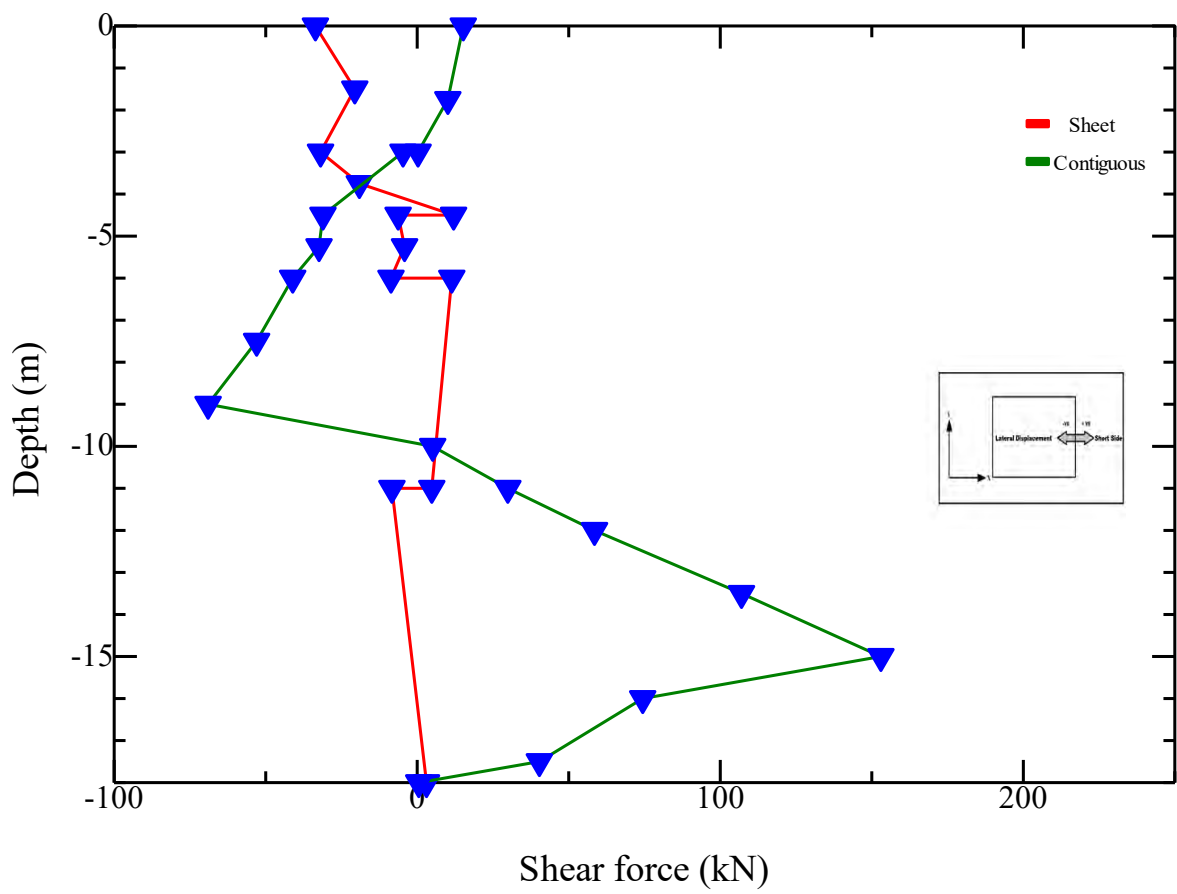


(c)

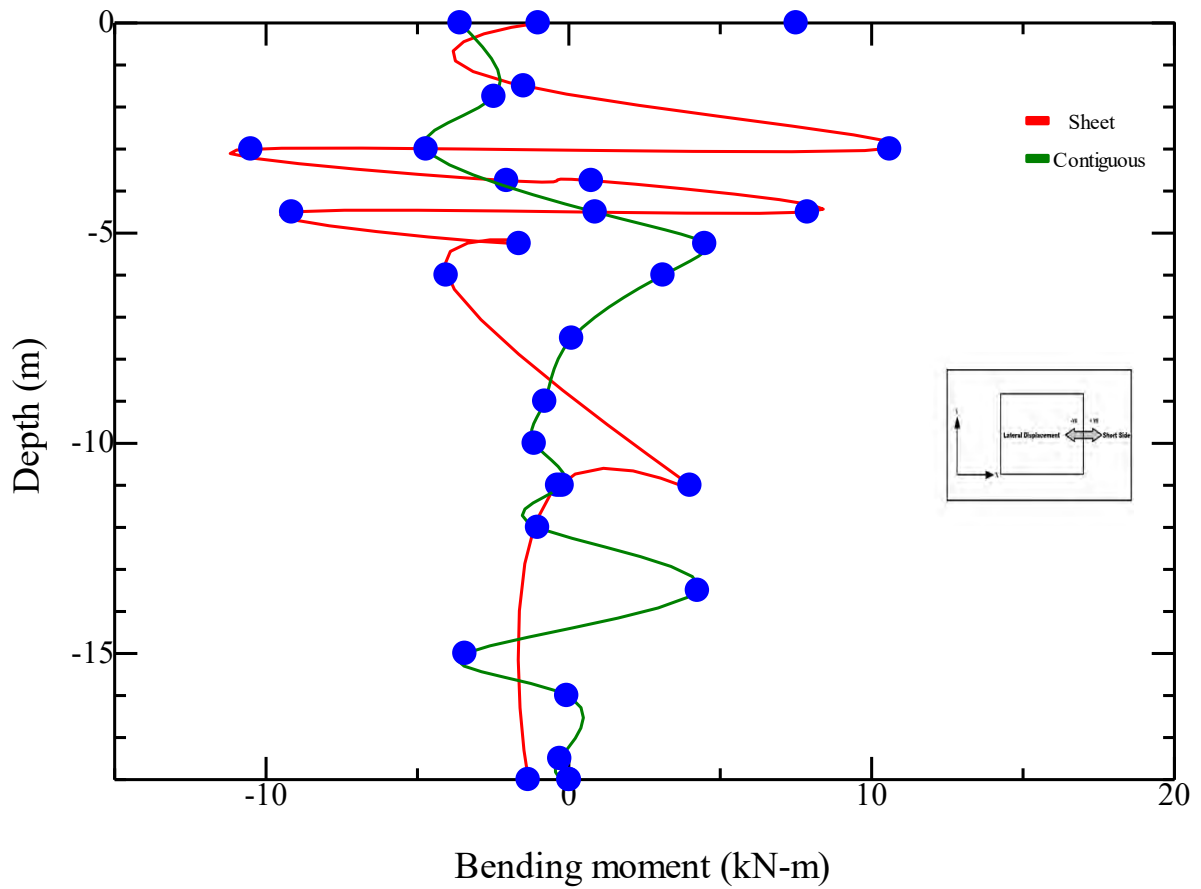
Fig. B-11 Internal forces in the long side of sheet pile and contiguous pile wall of Dhaka site having triple basement system-(a) axial force (b) shear force (c) bending moment- MC model



(a)

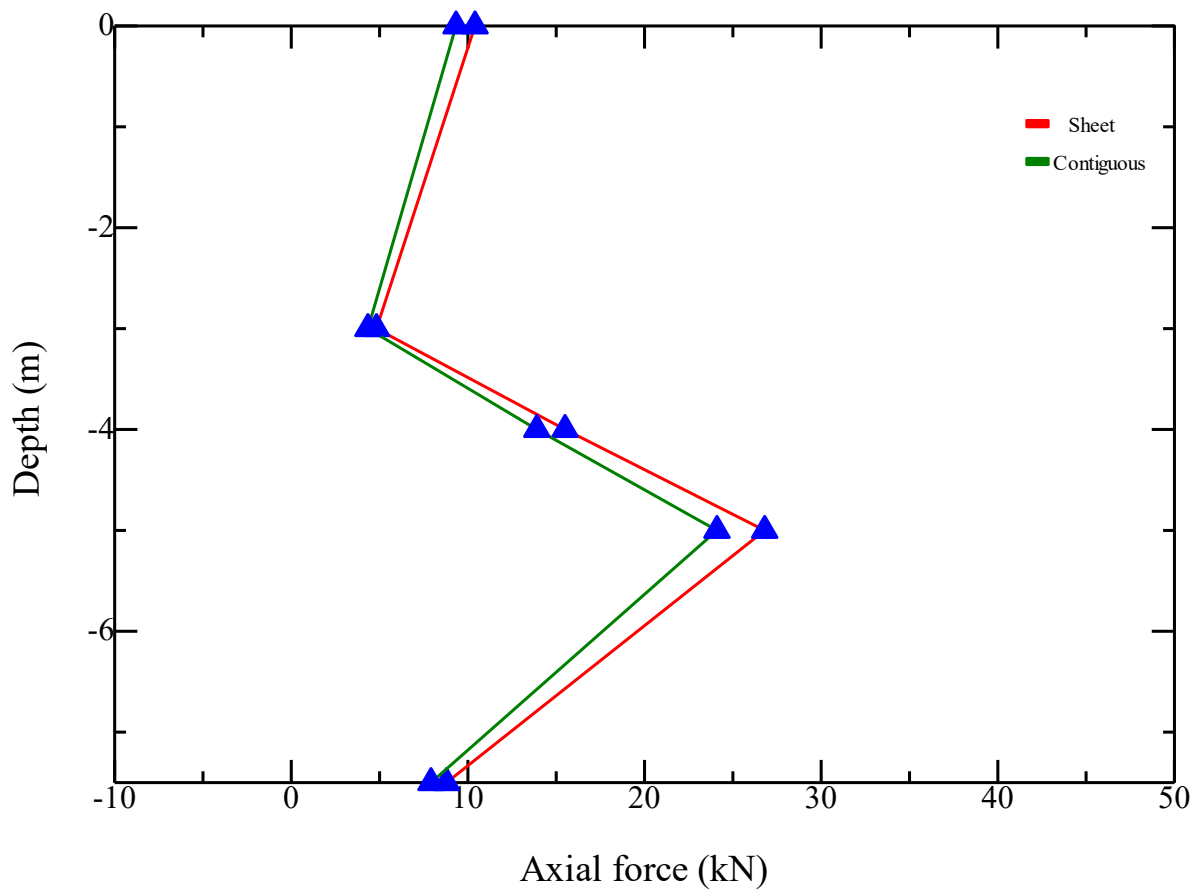


(b)

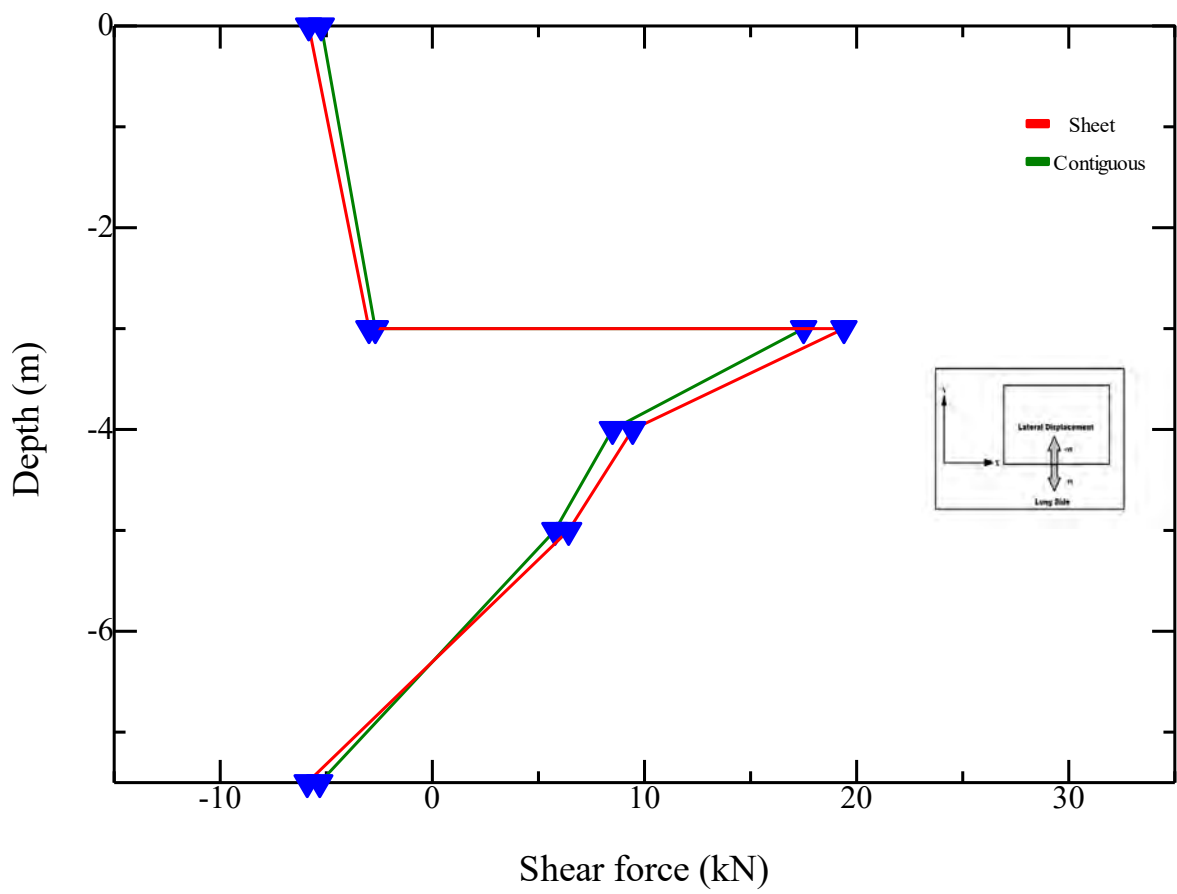


(c)

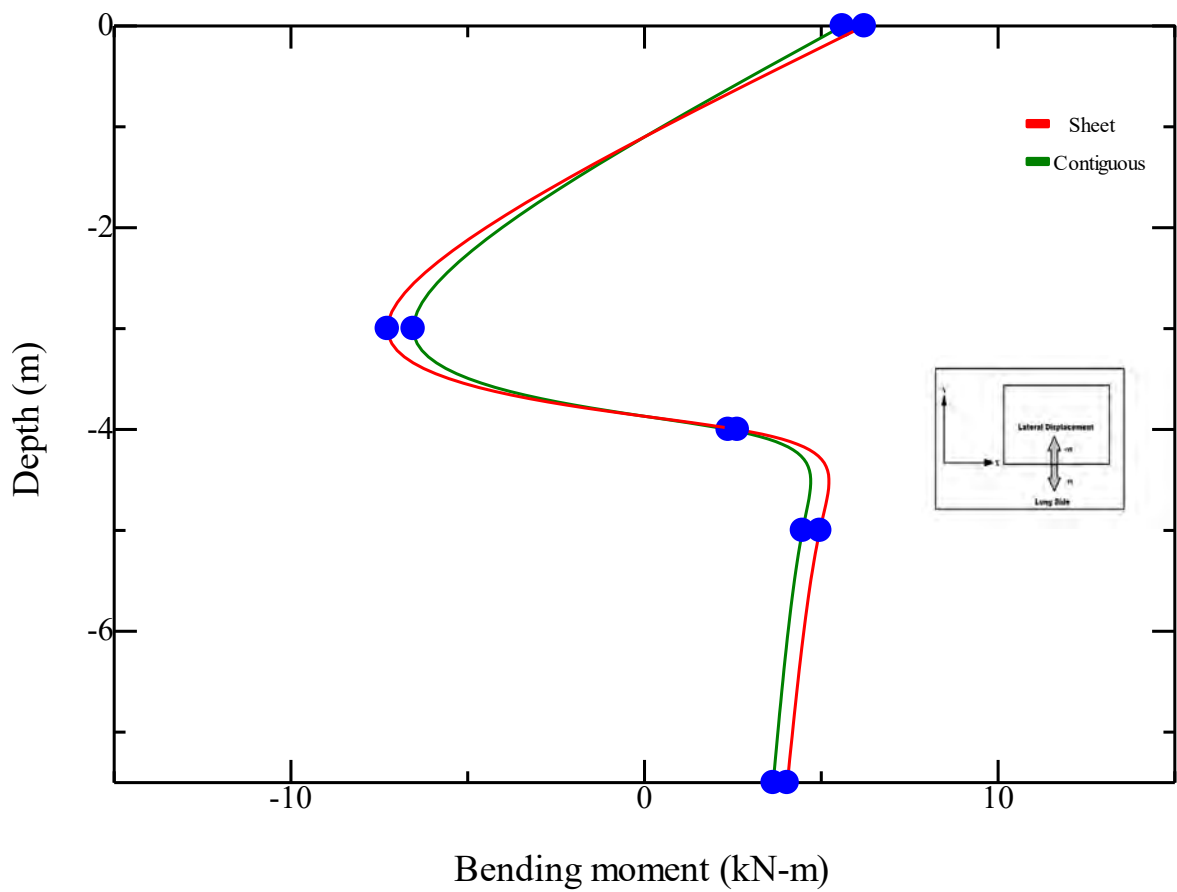
Fig. B-12 Internal forces in the short side of sheet pile and contiguous pile wall of Dhaka site having triple basement system-(a) axial force (b) shear force (c) bending moment- MC model



(a)

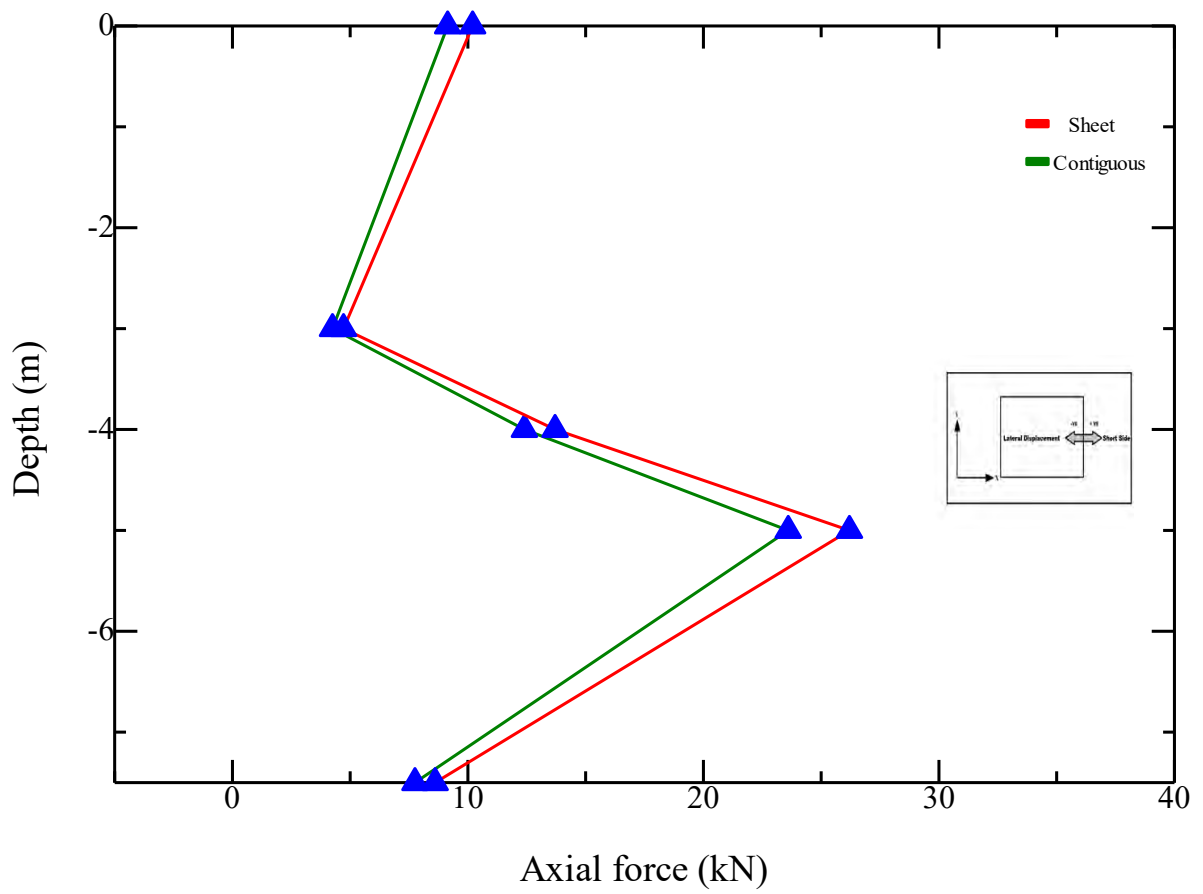


(b)

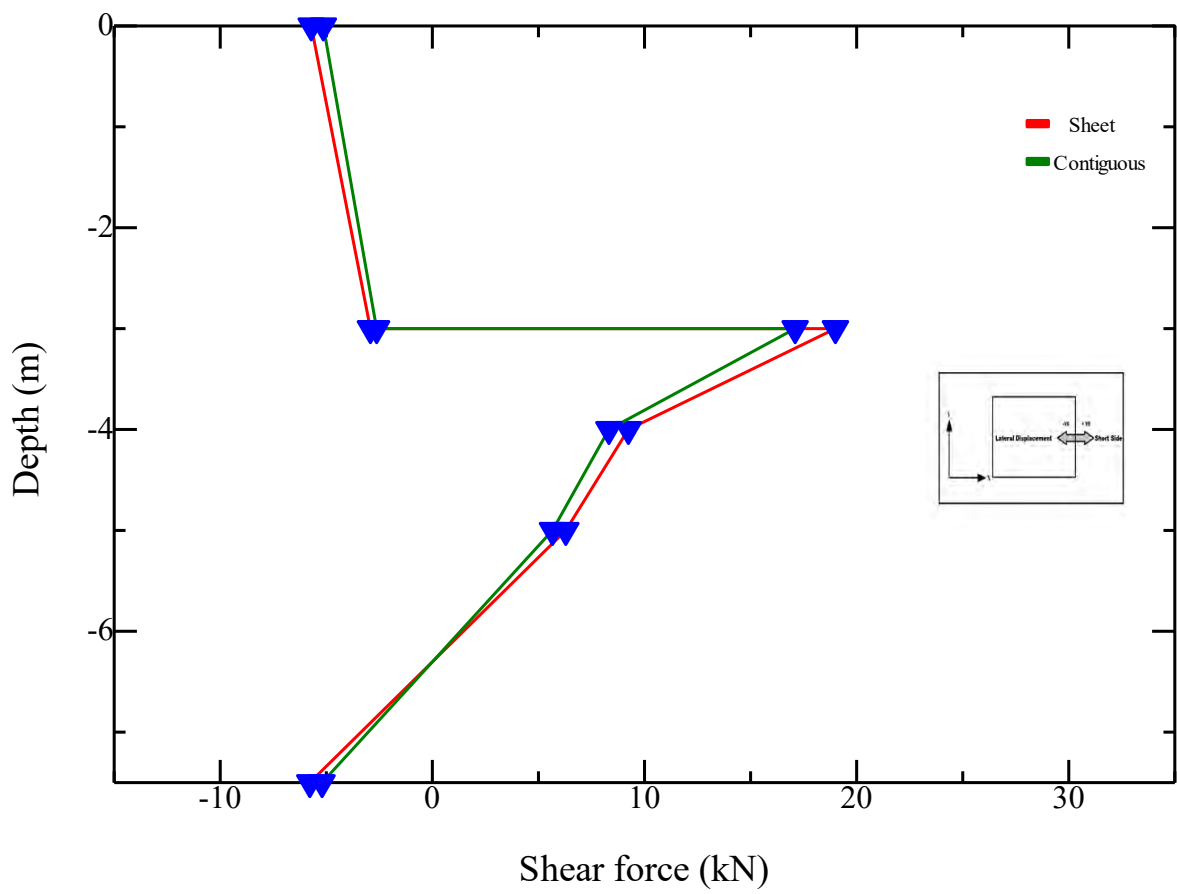


(c)

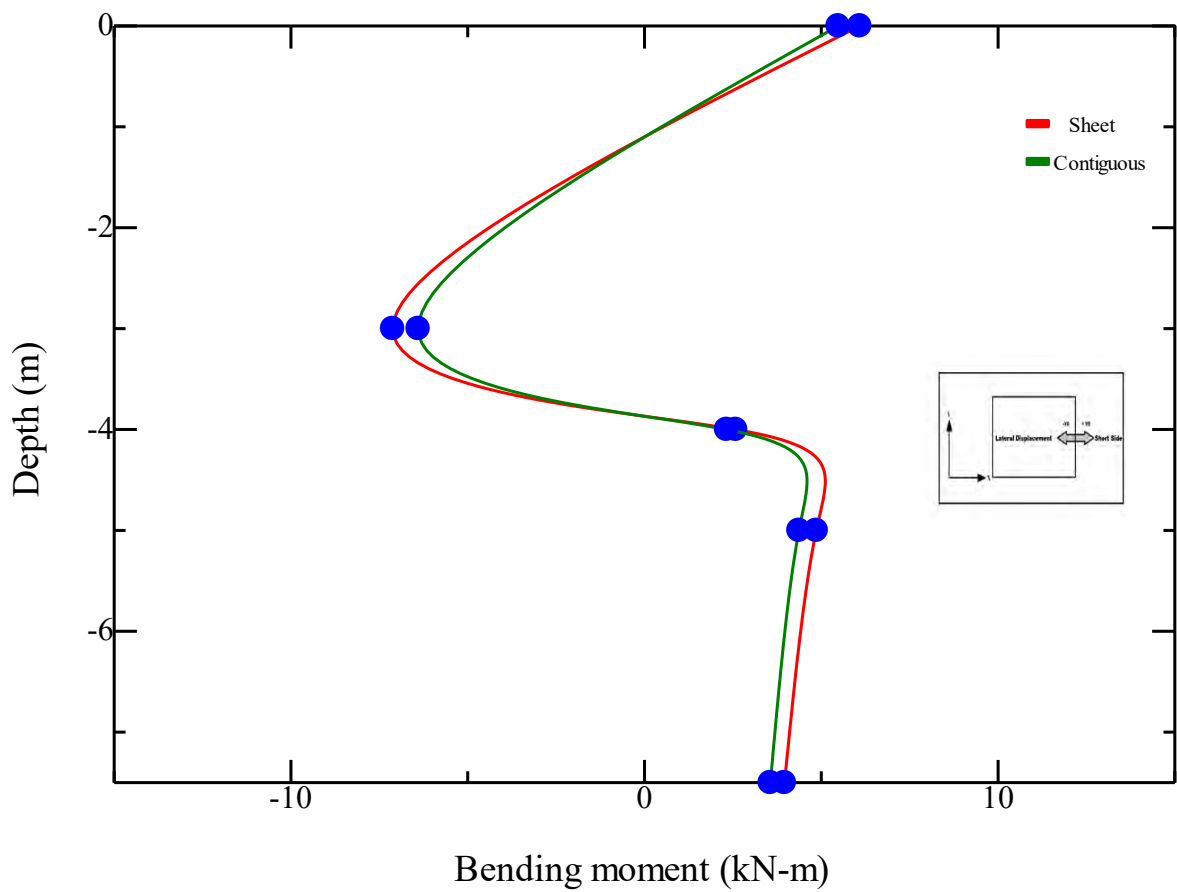
Fig. B-13 Internal forces in the long side of sheet pile and contiguous pile wall of Chittagong site having single basement system-(a) axial force (b) shear force (c) bending moment- HS model



(a)

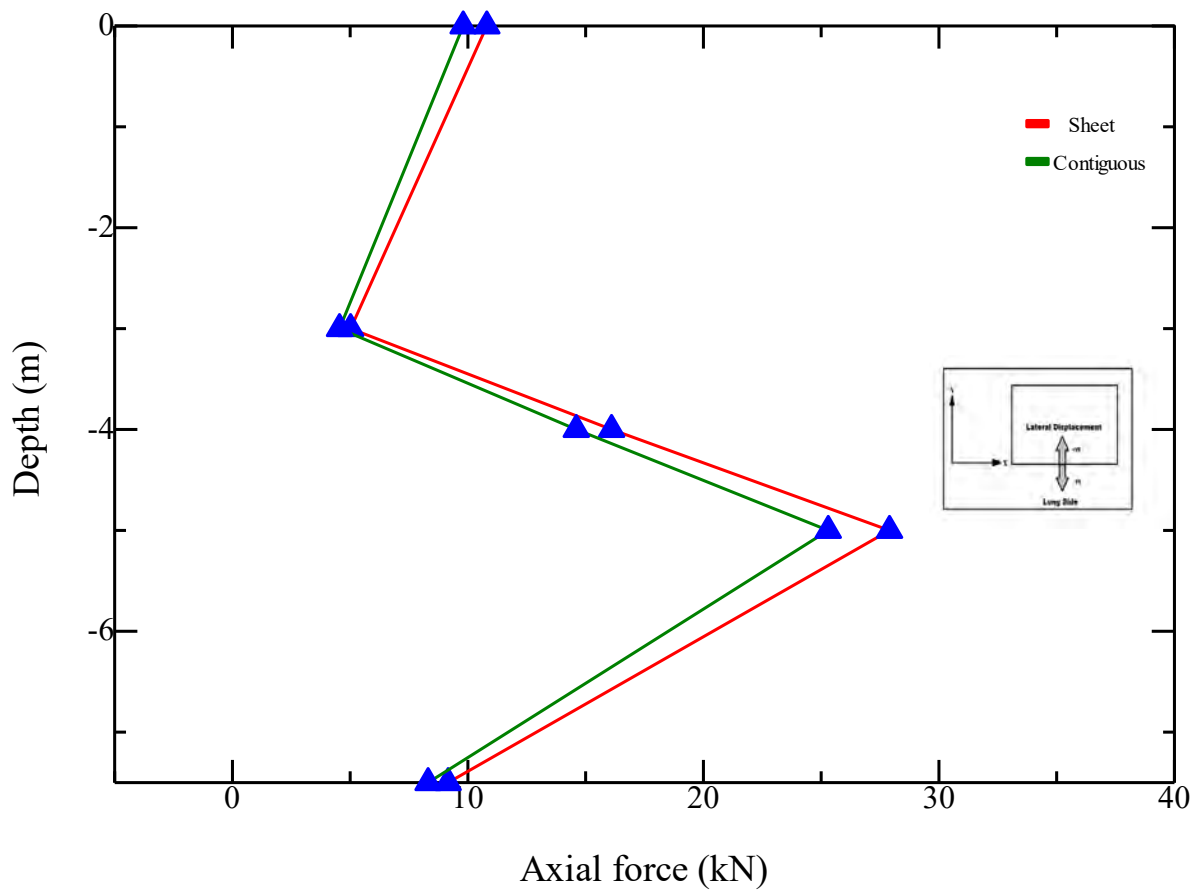


(b)

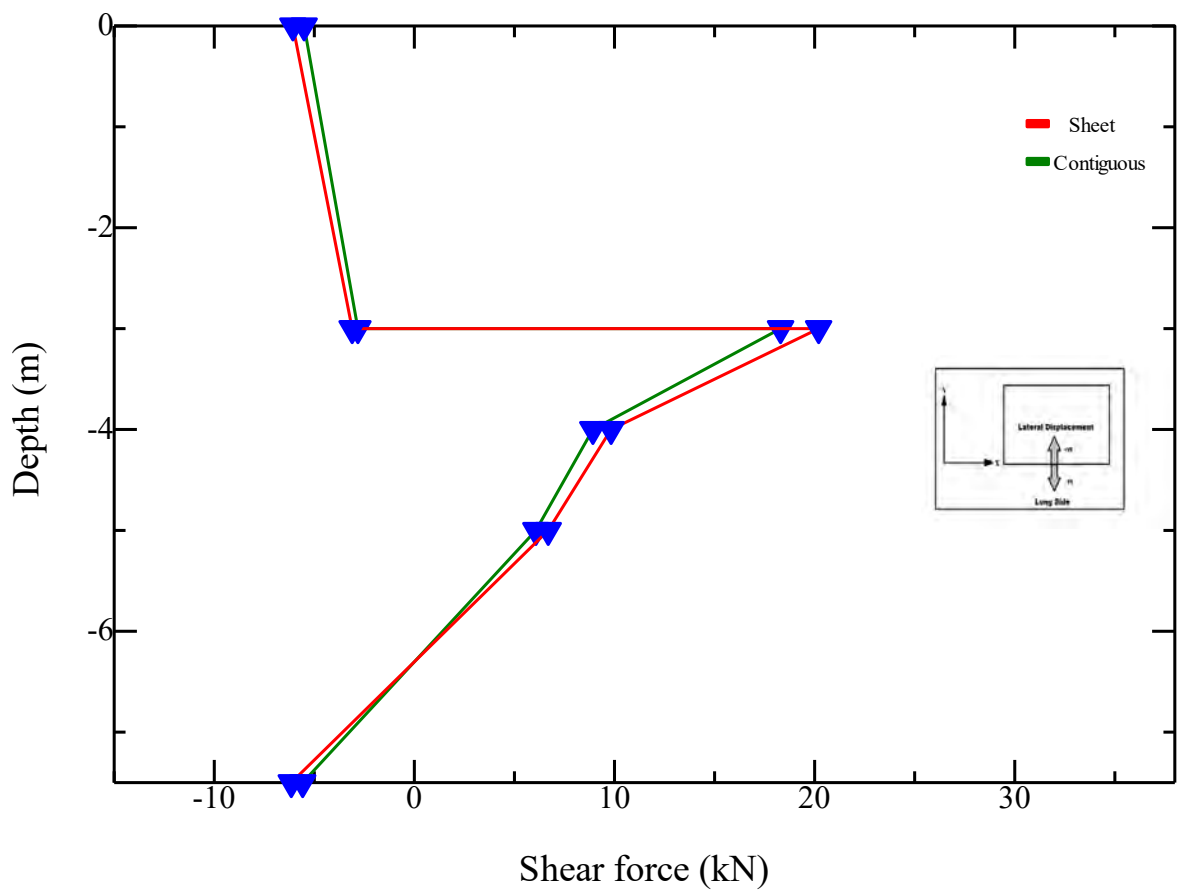


(c)

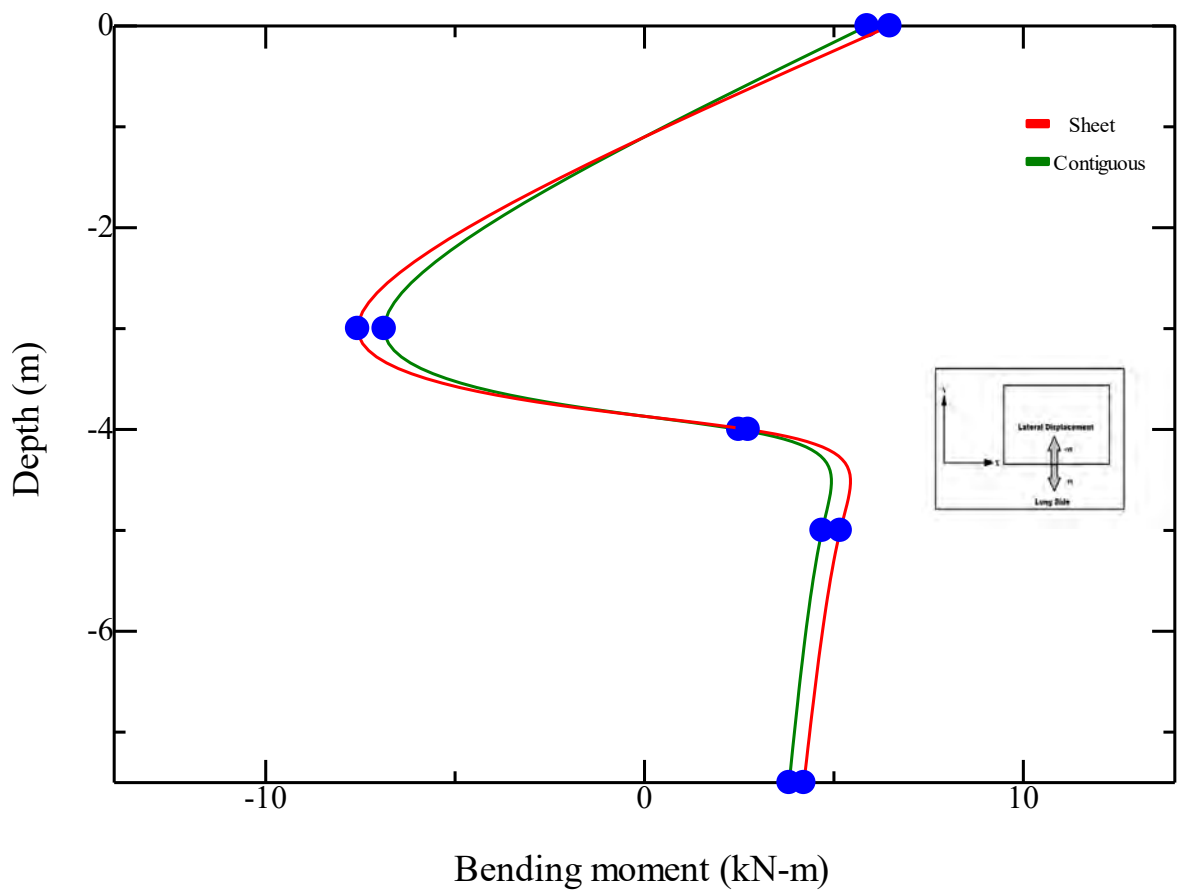
Fig. B-14 Internal forces in the short side of sheet pile and contiguous pile wall of Chittagong site having single basement system-(a) axial force (b) shear force (c) bending moment- HS model



(a)

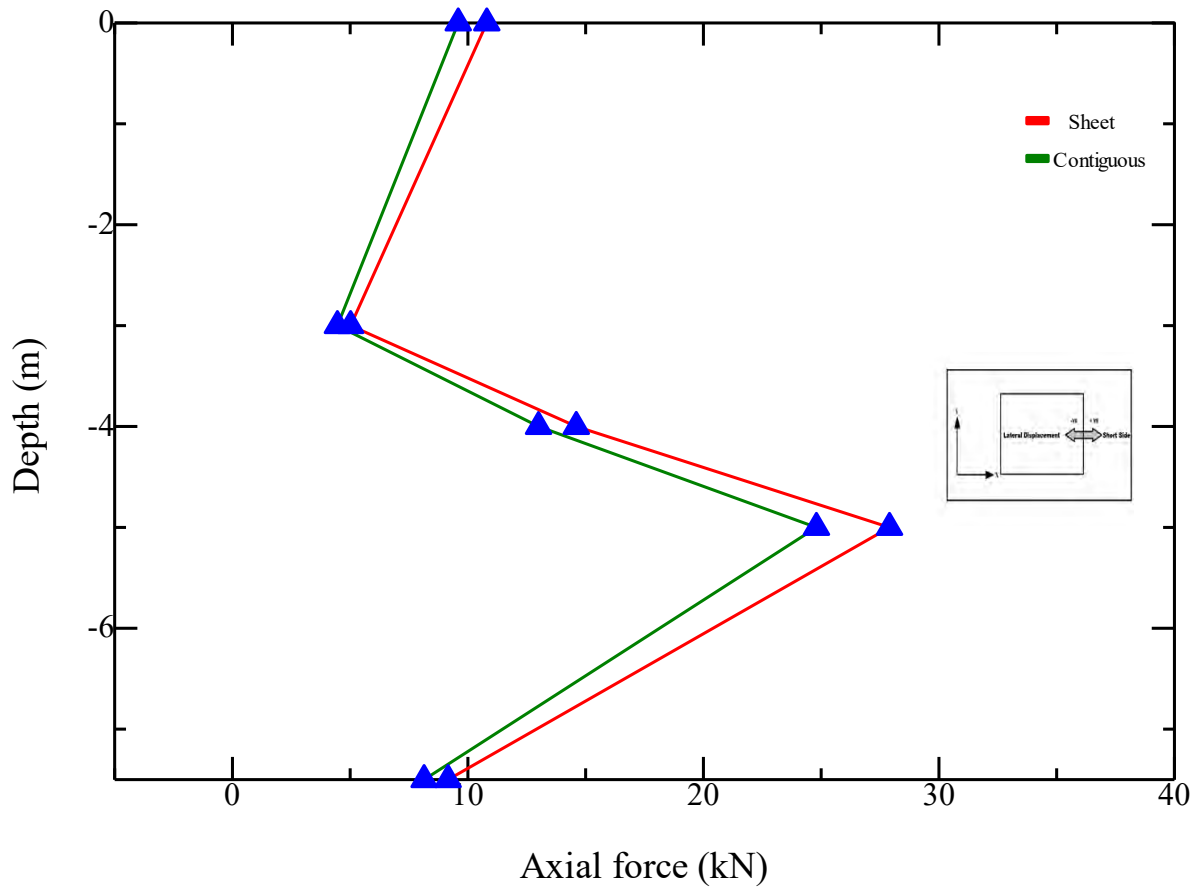


(b)

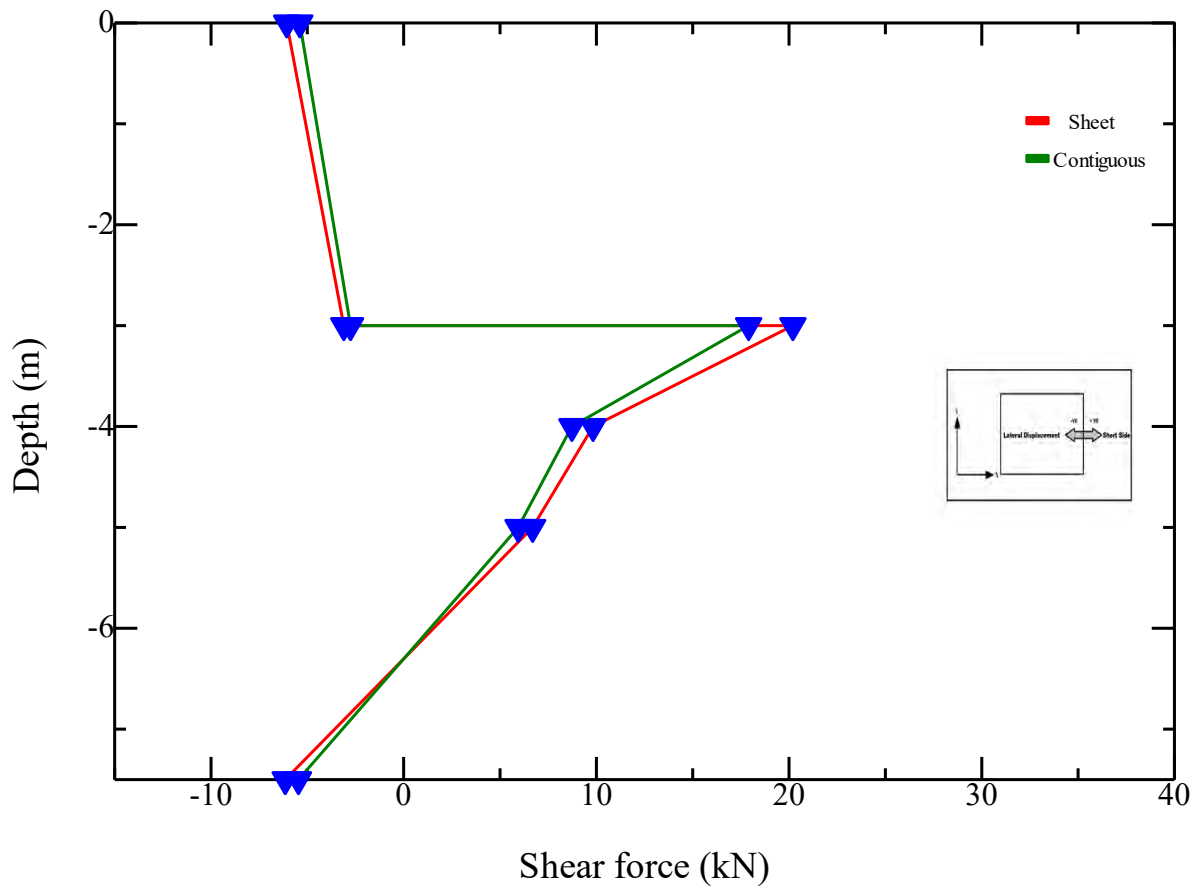


(c)

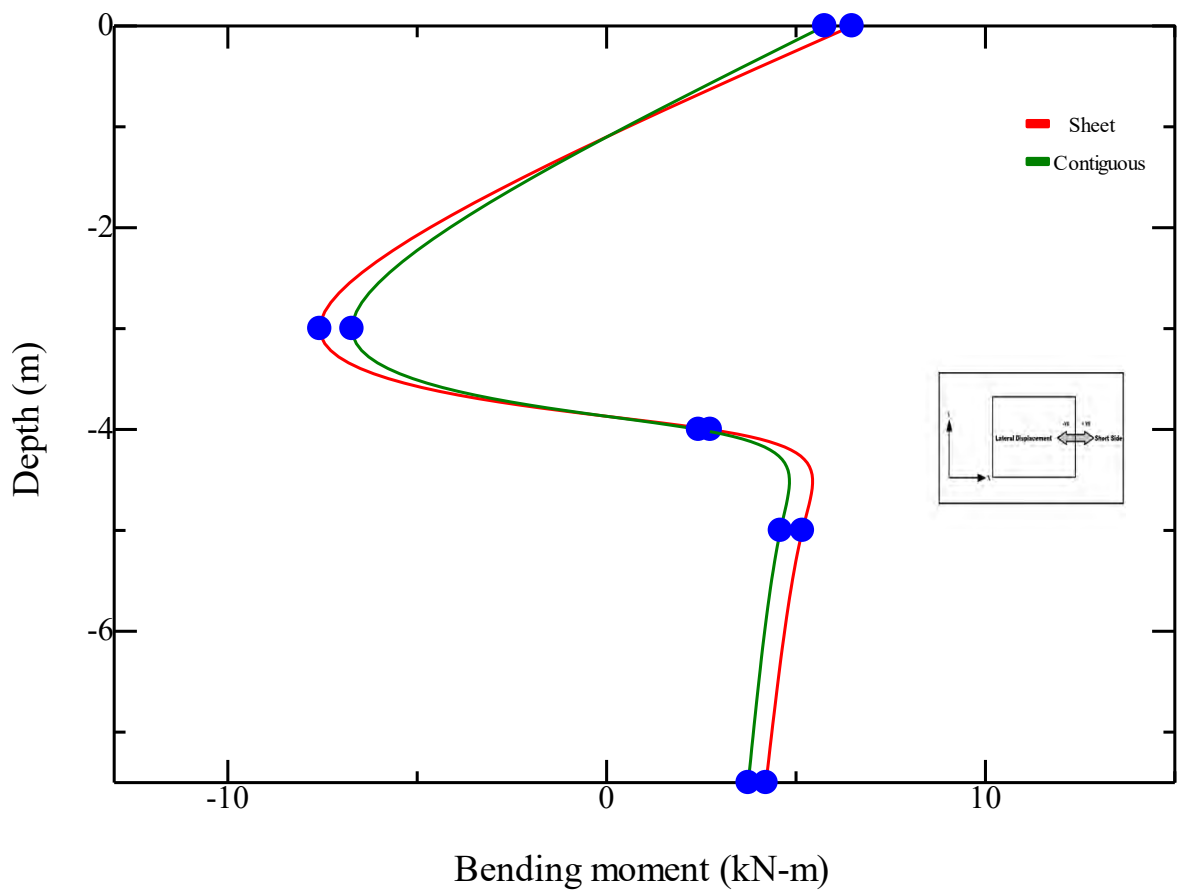
Fig. B-15 Internal forces in the long side of sheet pile and contiguous pile wall of Chittagong site having single basement system-(a) axial force (b) shear force (c) bending moment- MC model



(a)

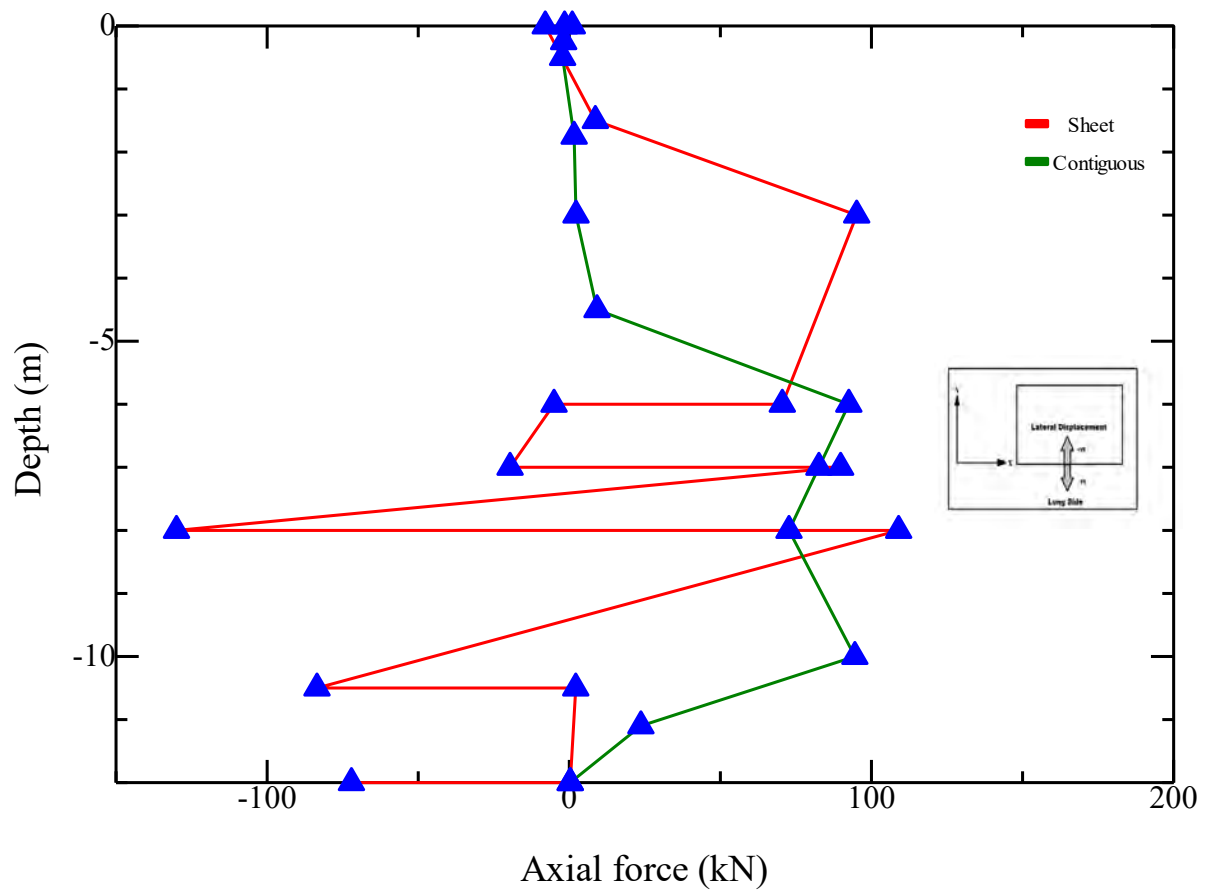


(b)

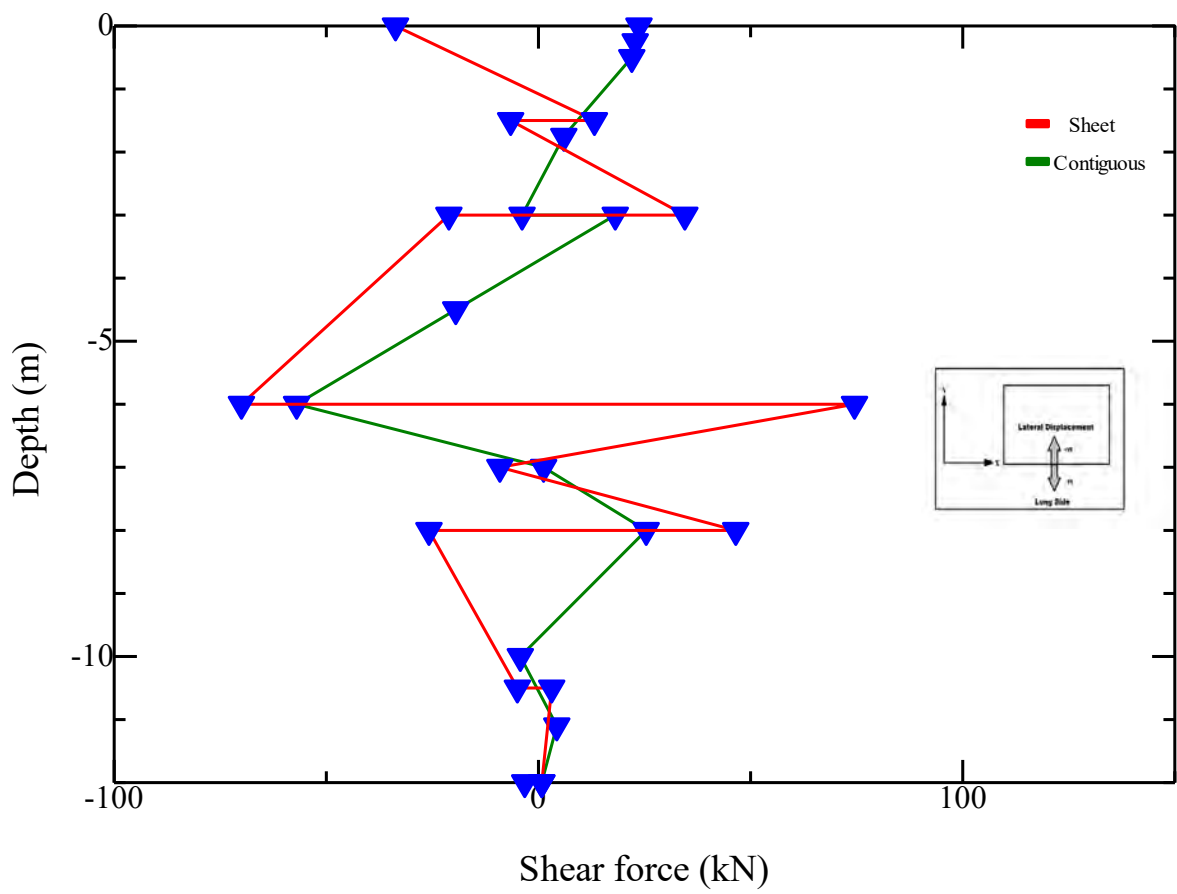


(c)

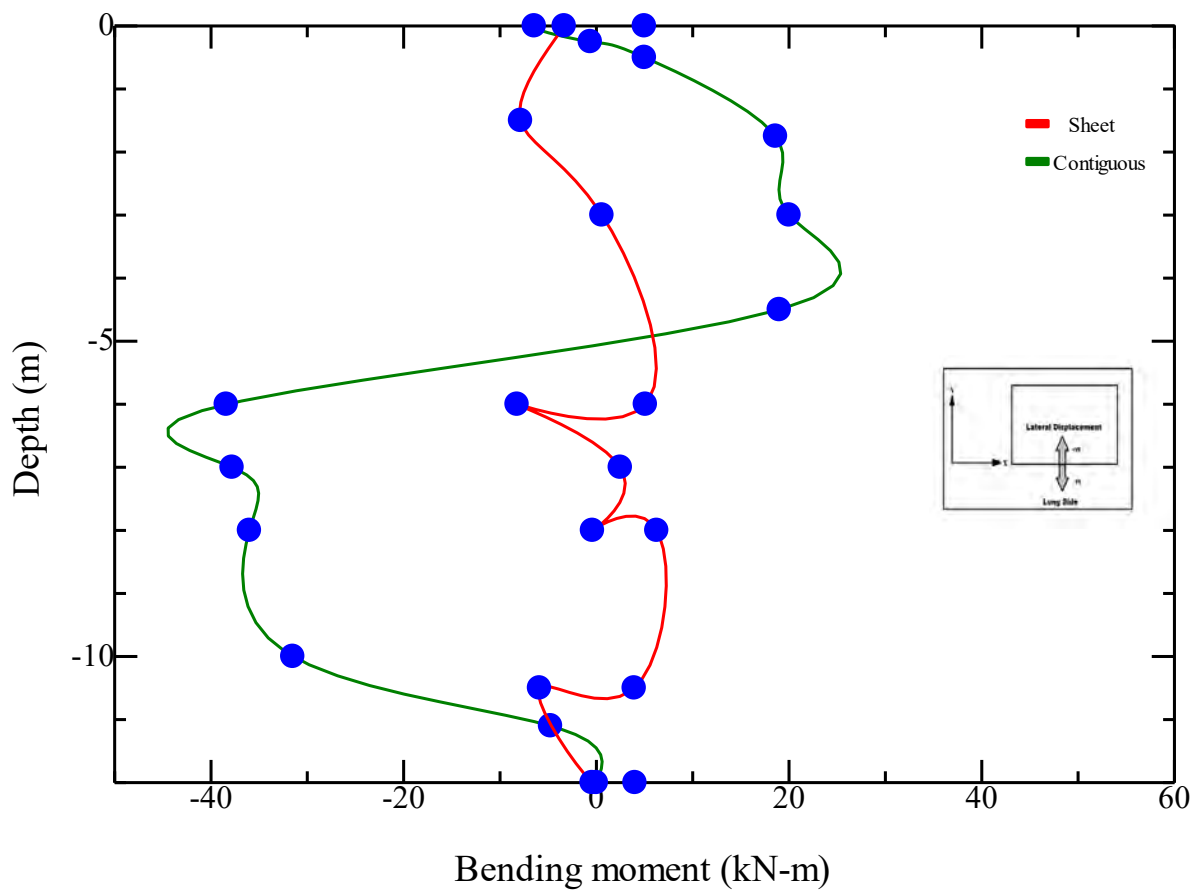
Fig. B-16 Internal forces in the short side of sheet pile and contiguous pile wall of Chittagong site having single basement system-(a) axial force (b) shear force (c) bending moment- MC model



(a)

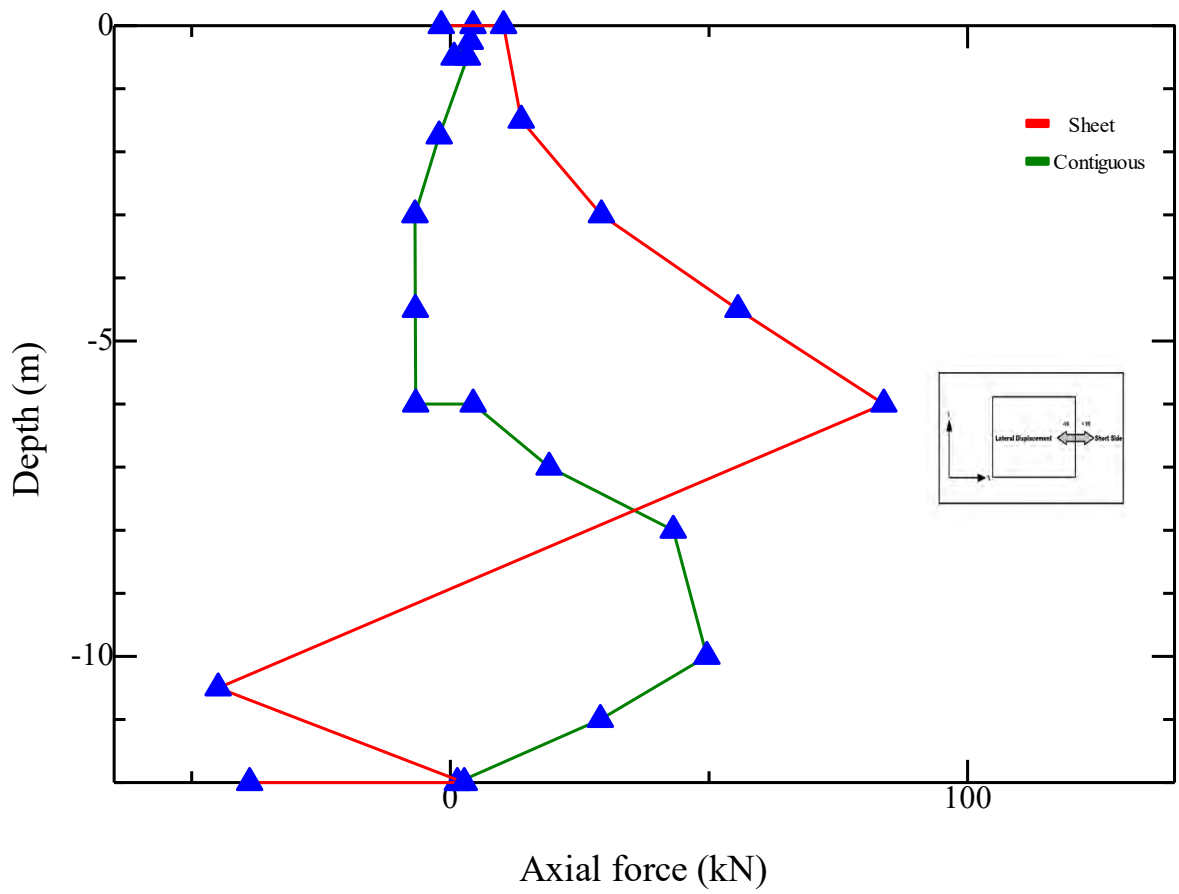


(b)

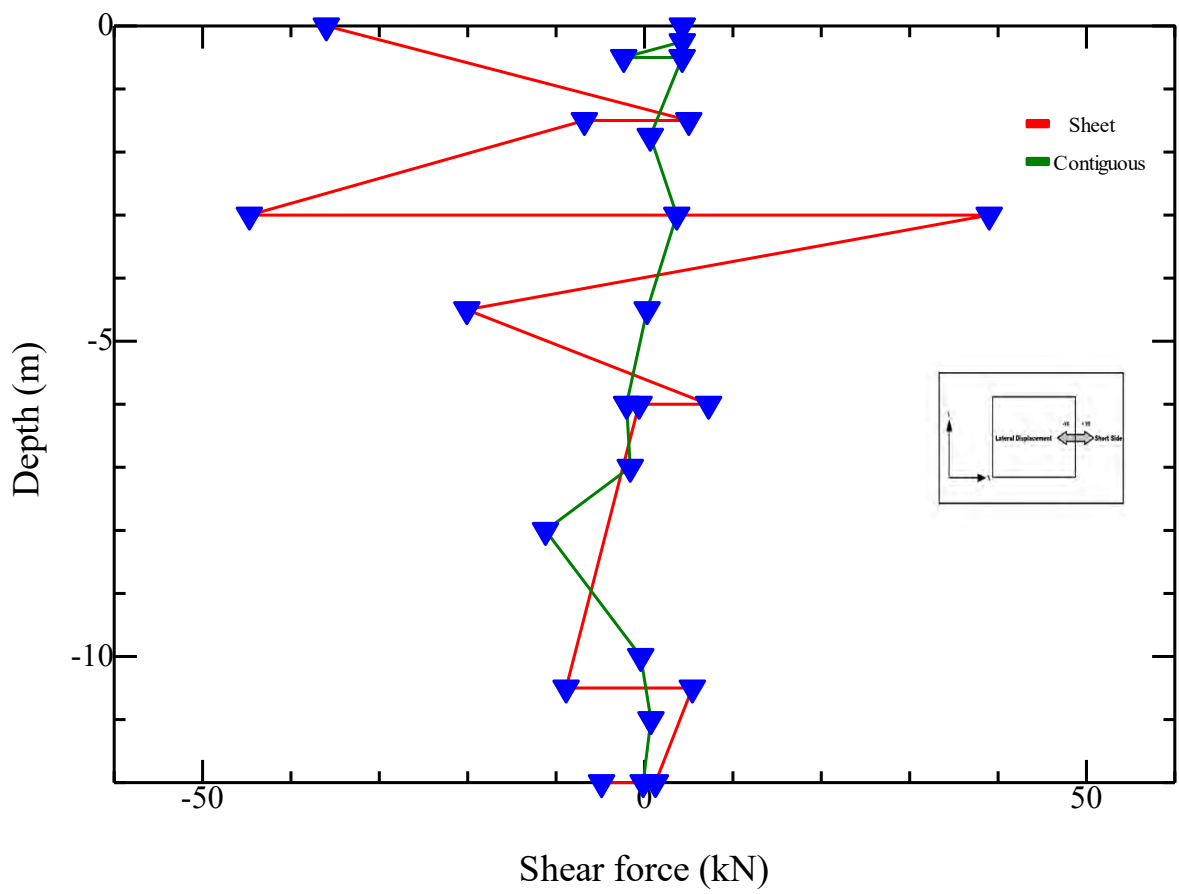


(c)

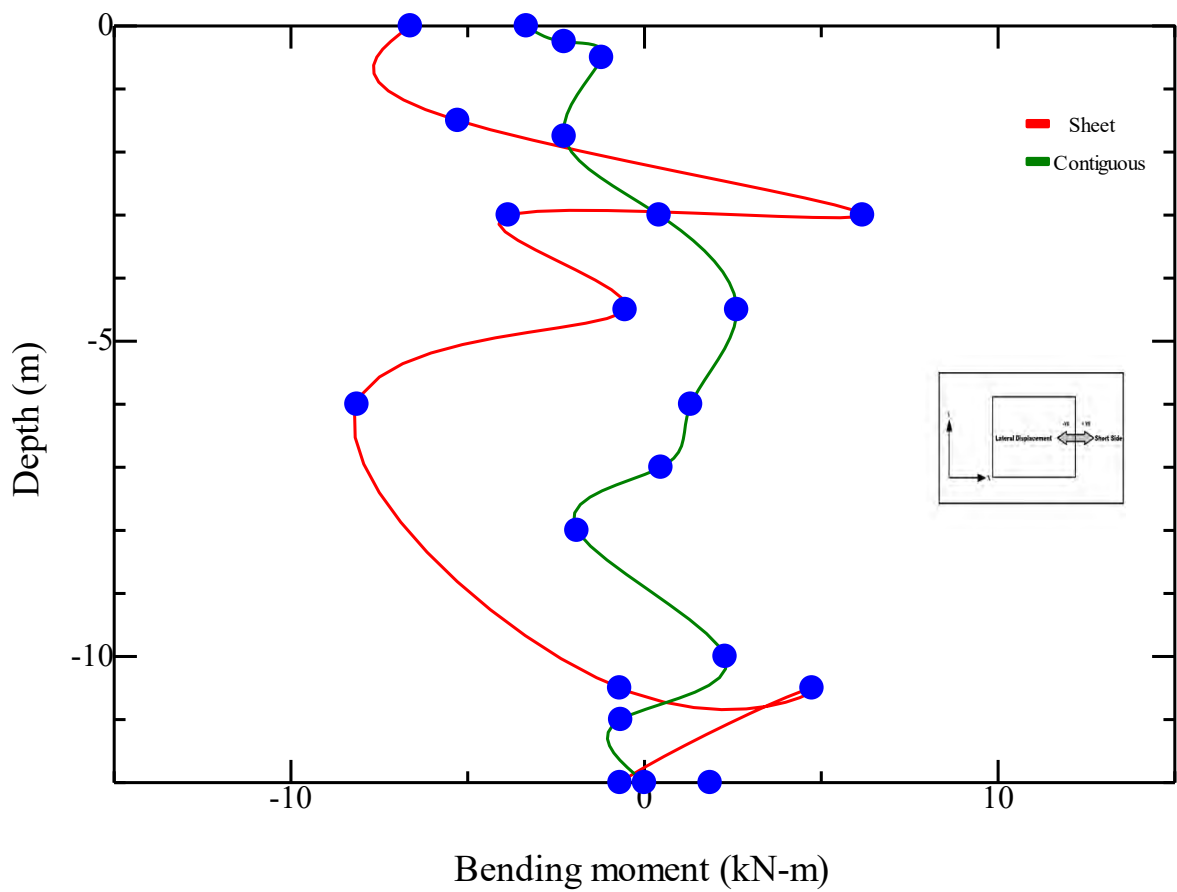
Fig. B-17 Internal forces in the long side of sheet pile and contiguous pile wall of Chittagong site having double basement system-(a) axial force (b) shear force (c) bending moment- HS model



(a)

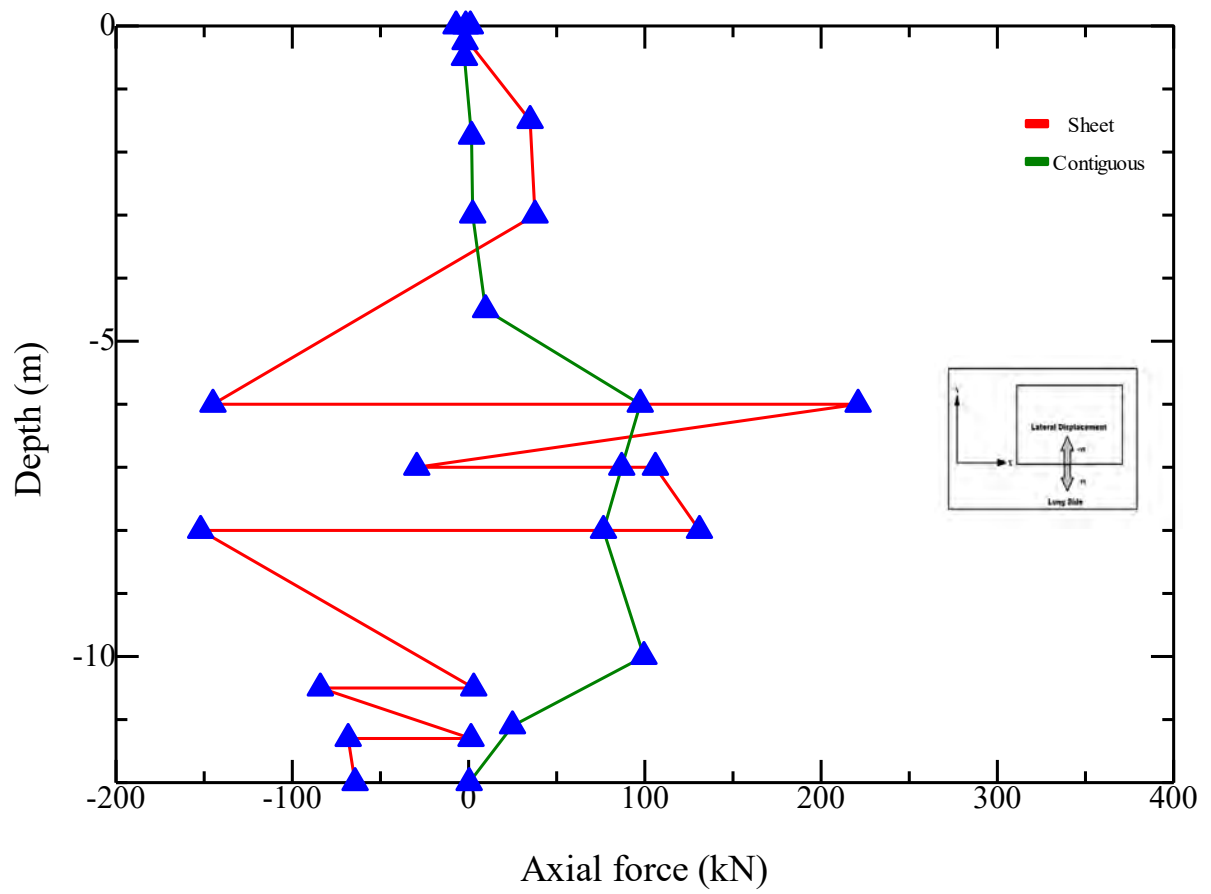


(b)

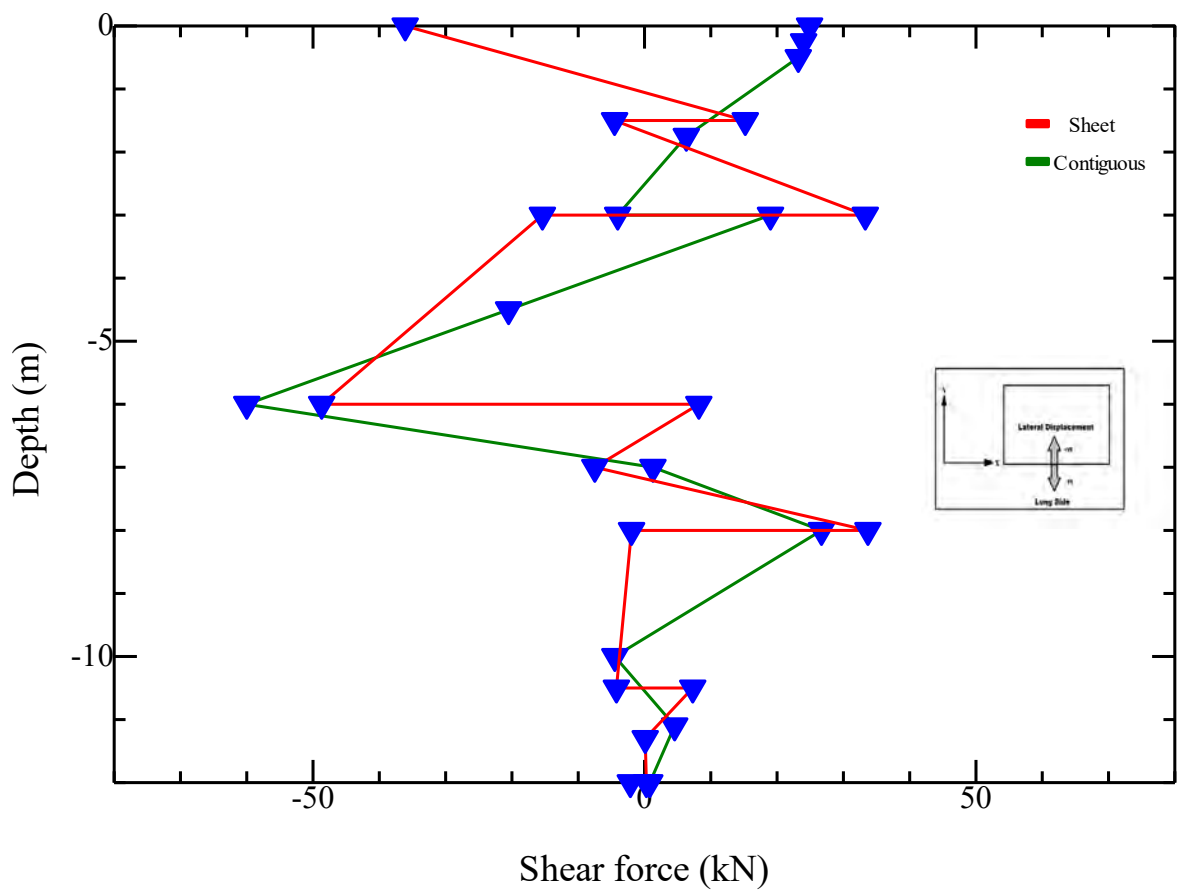


(c)

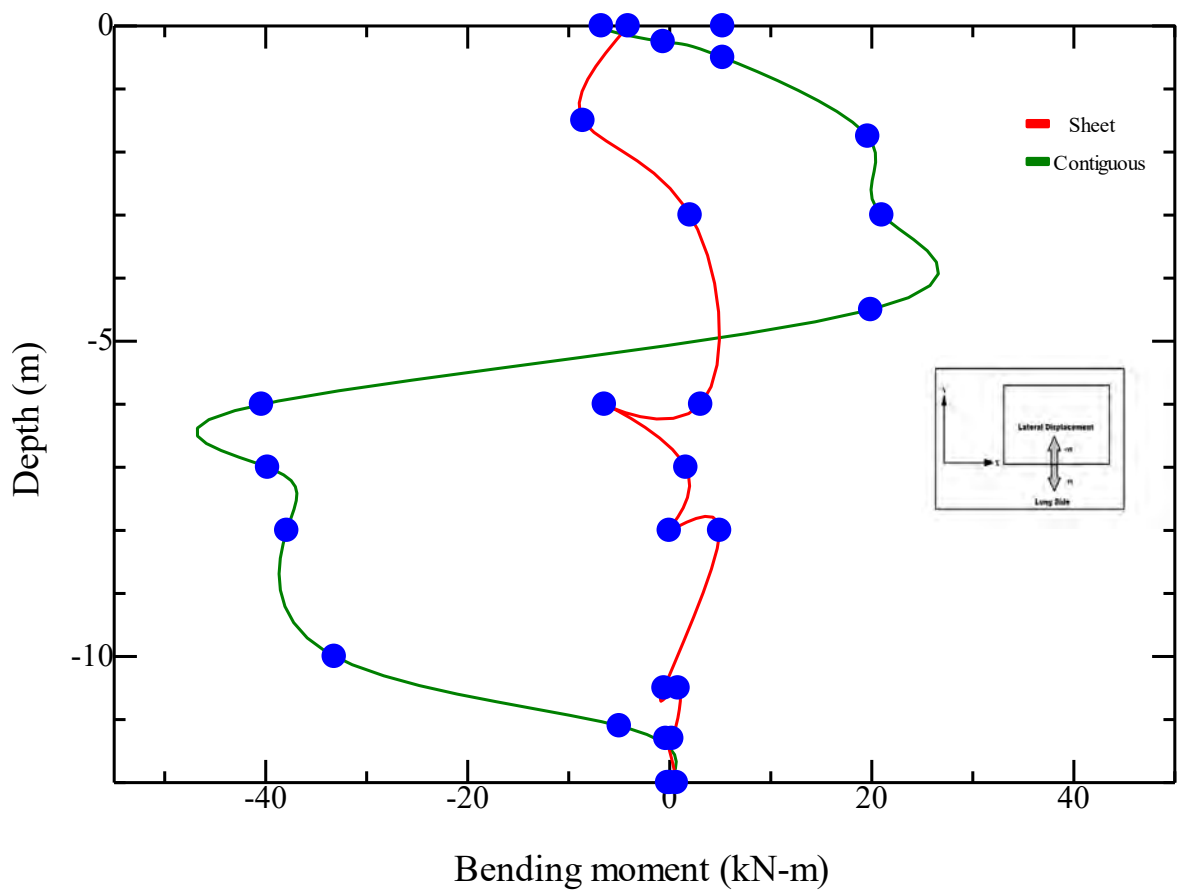
Fig. B-18 Internal forces in the short side of sheet pile and contiguous pile wall of Chittagong site having double basement system-(a) axial force (b) shear force (c) bending moment- HS model



(a)

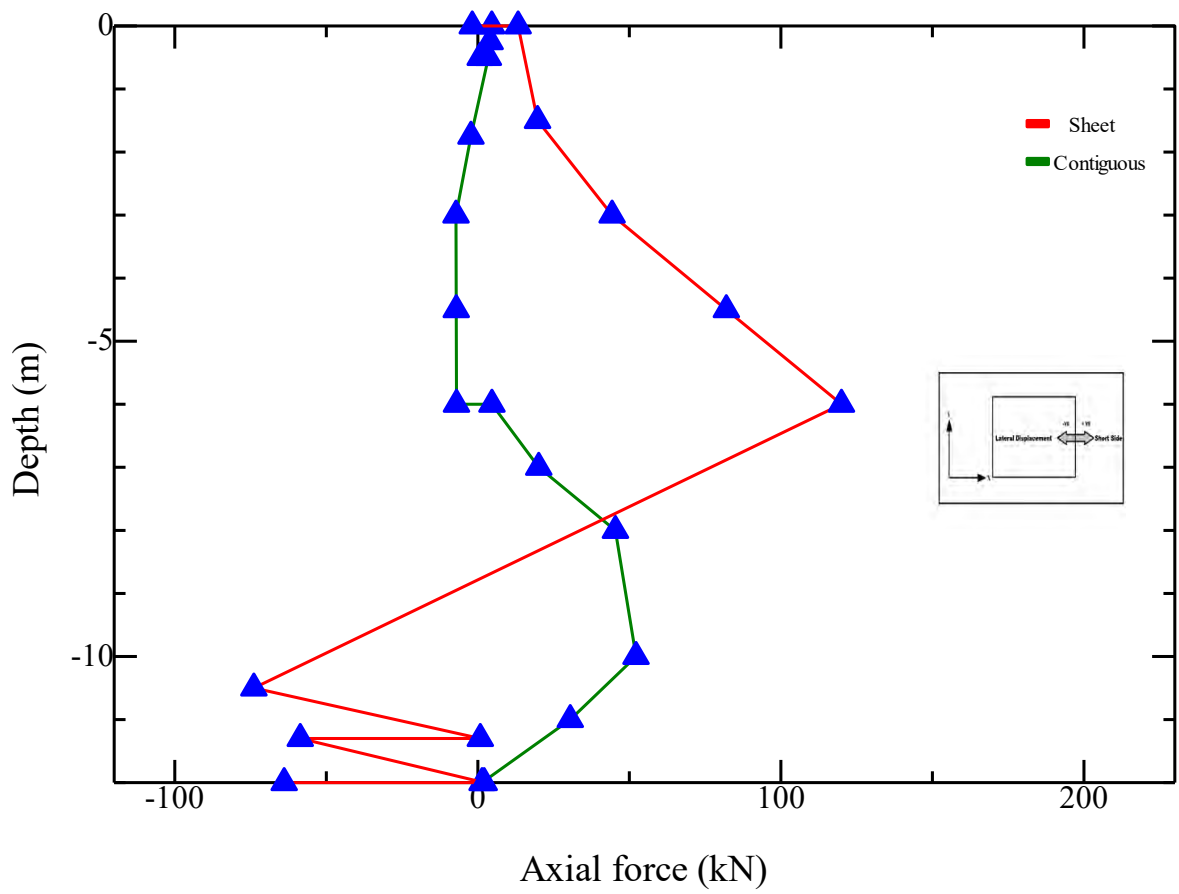


(b)

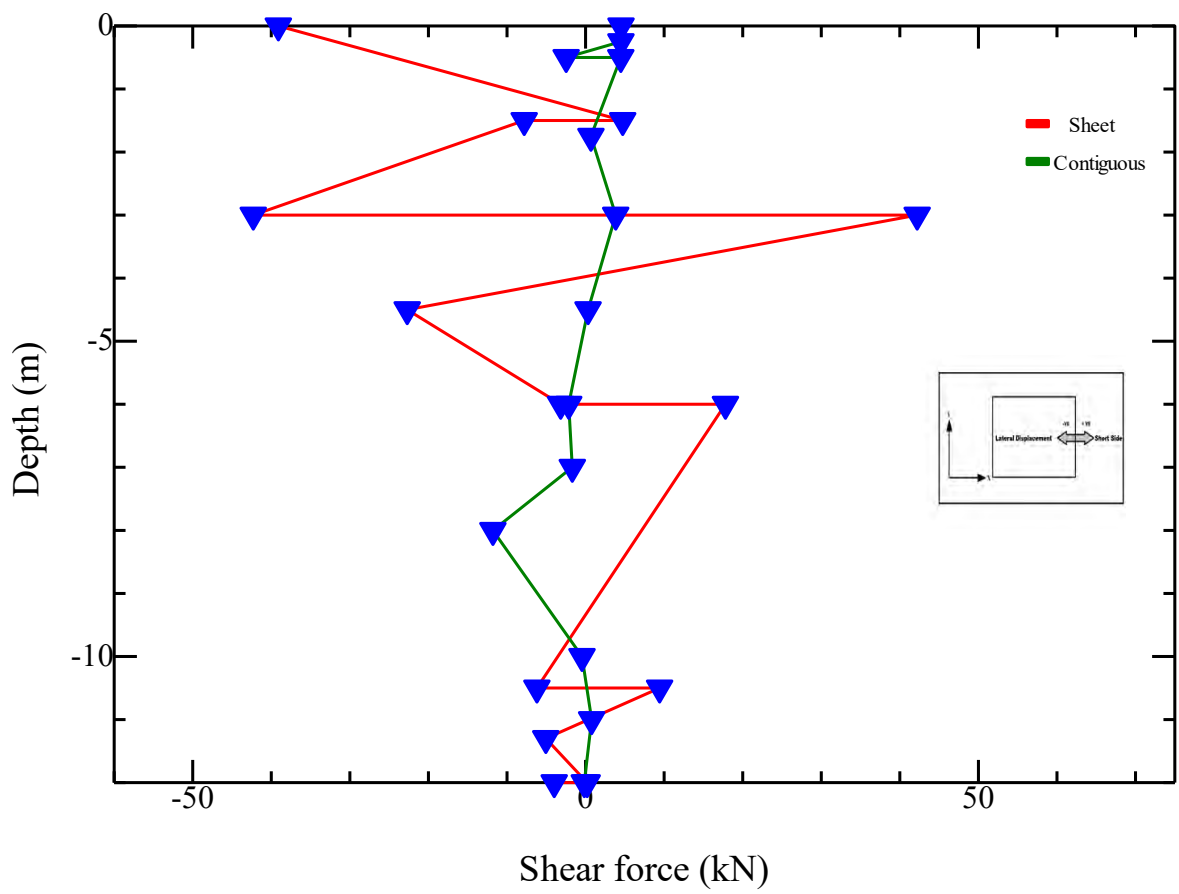


(c)

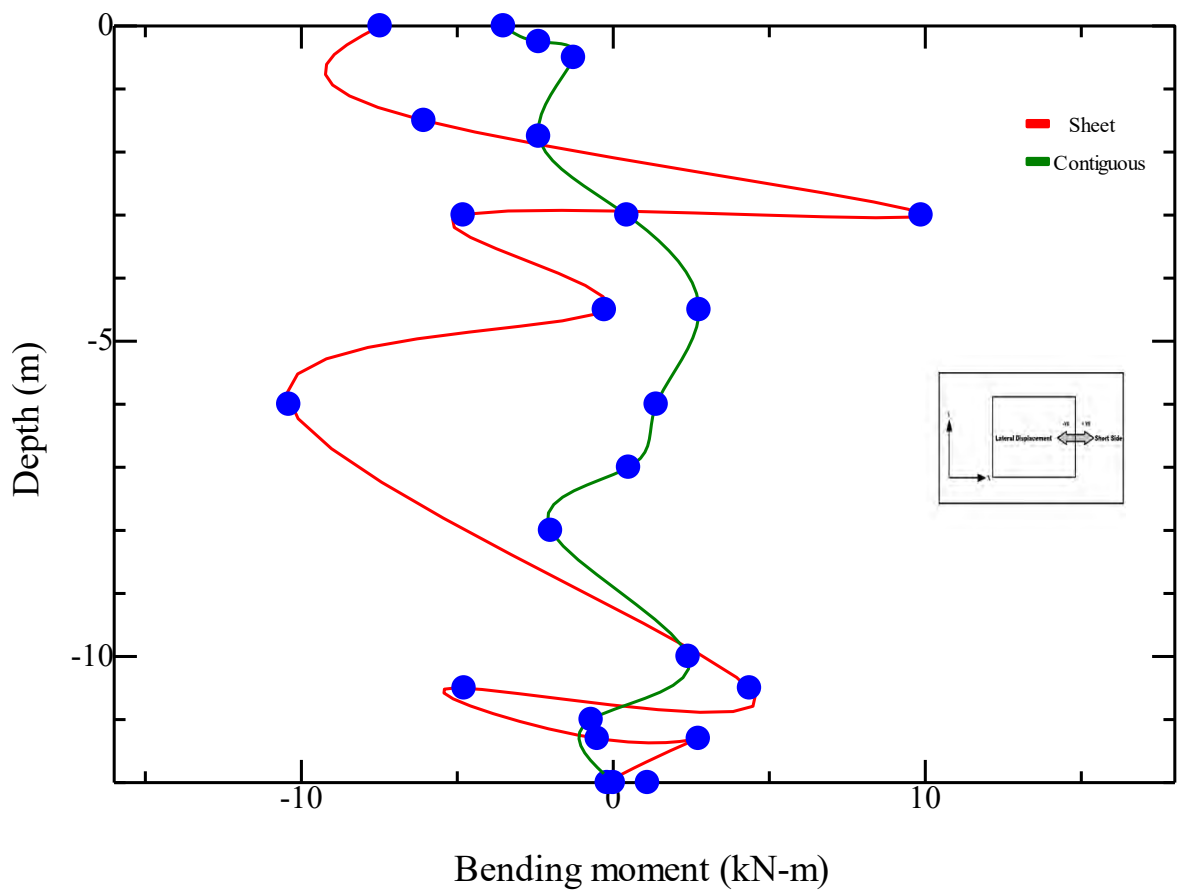
Fig. B-19 Internal forces in the long side of sheet pile and contiguous pile wall of Chittagong site having double basement system-(a) axial force (b) shear force (c) bending moment- MC model



(a)

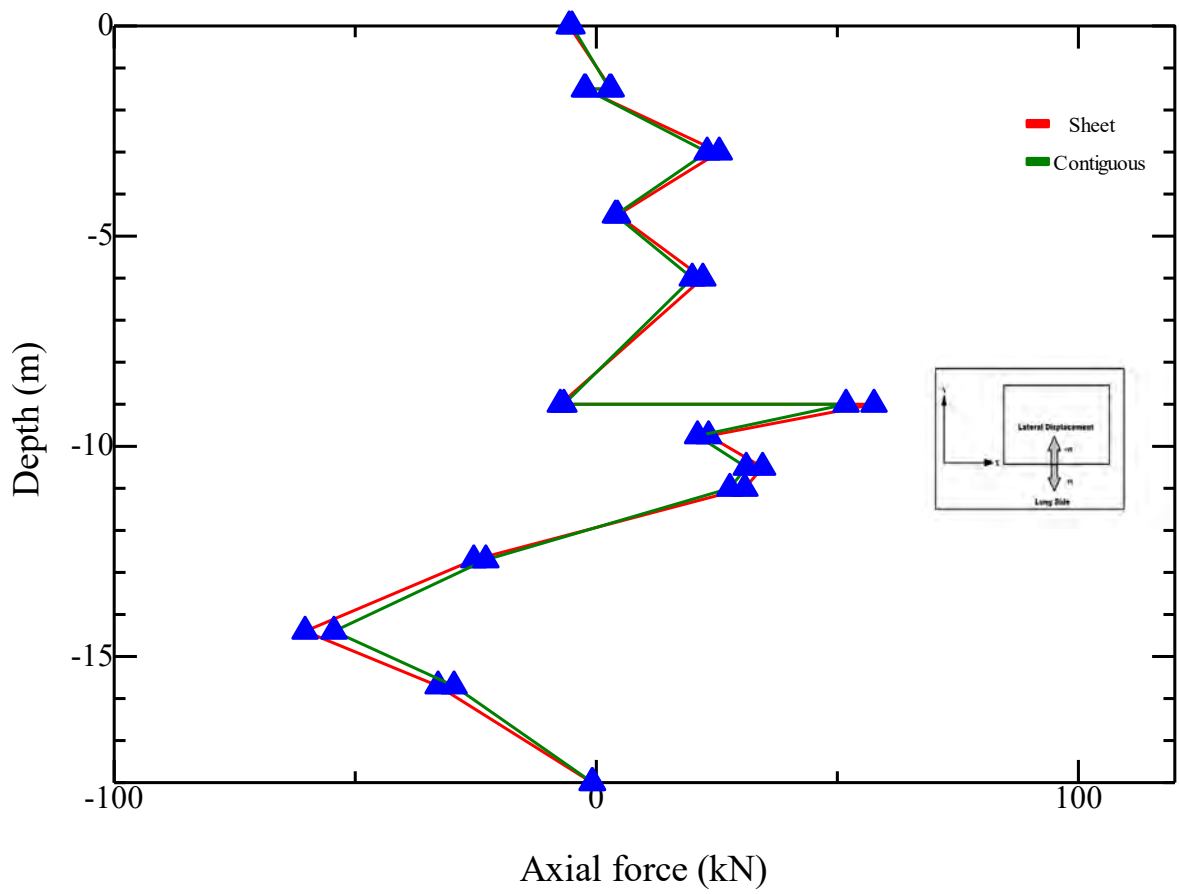


(b)

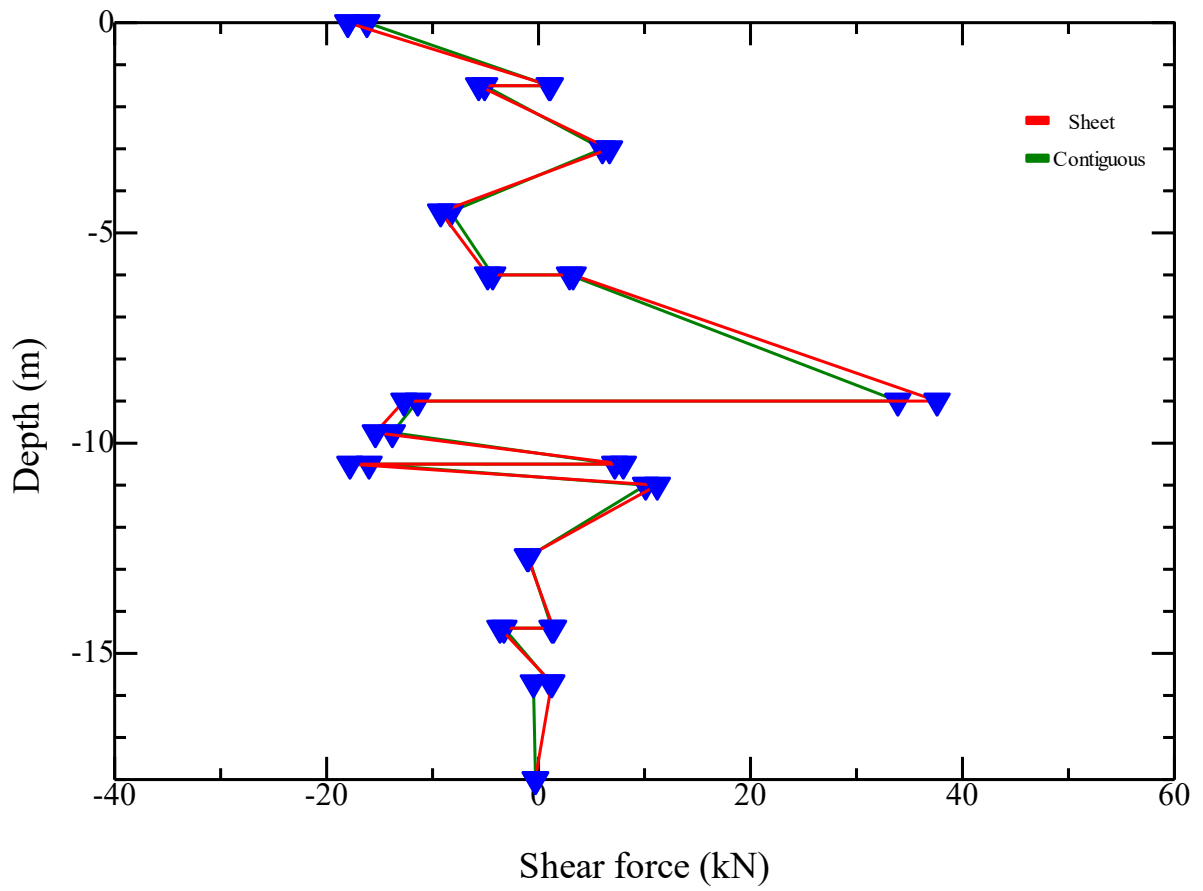


(c)

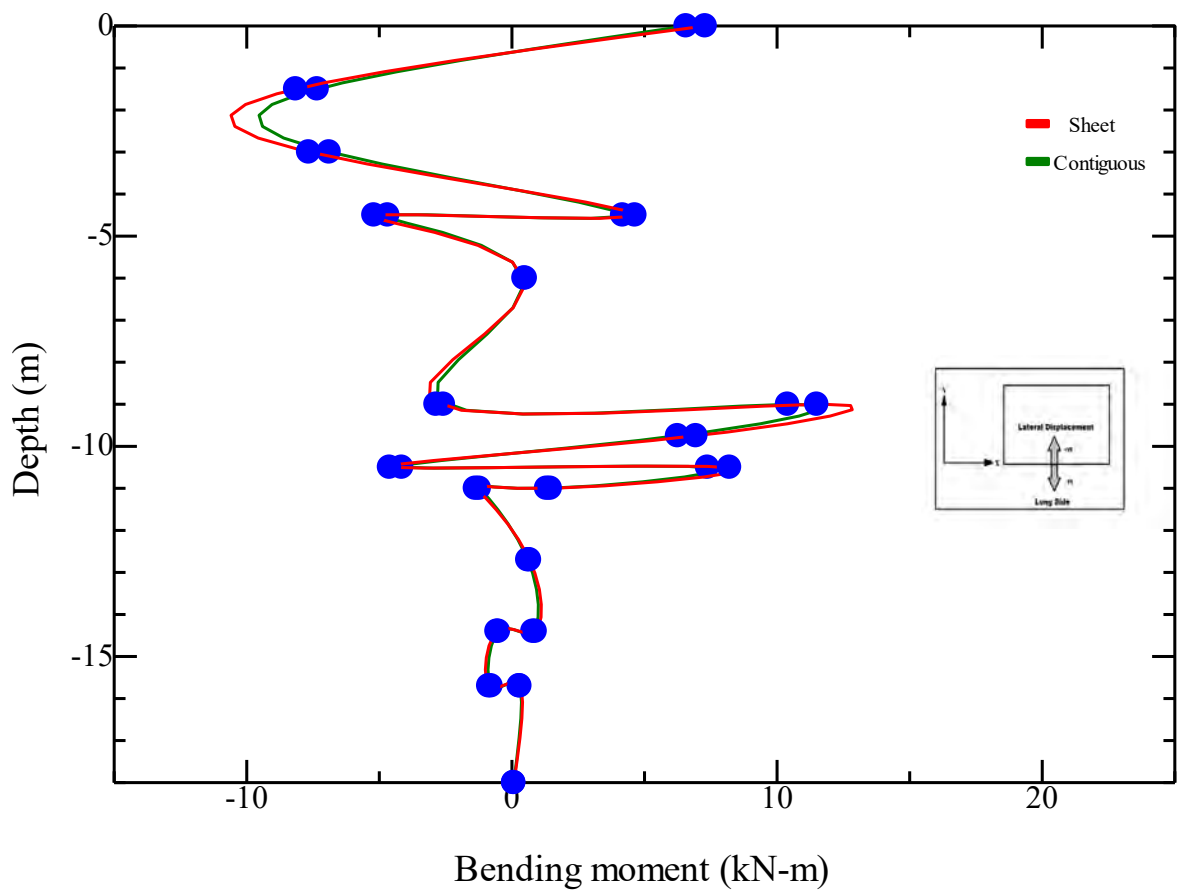
Fig. B-20 Internal forces in the short side of sheet pile and contiguous pile wall of Chittagong site having double basement system-(a) axial force (b) shear force (c) bending moment- MC model



(a)

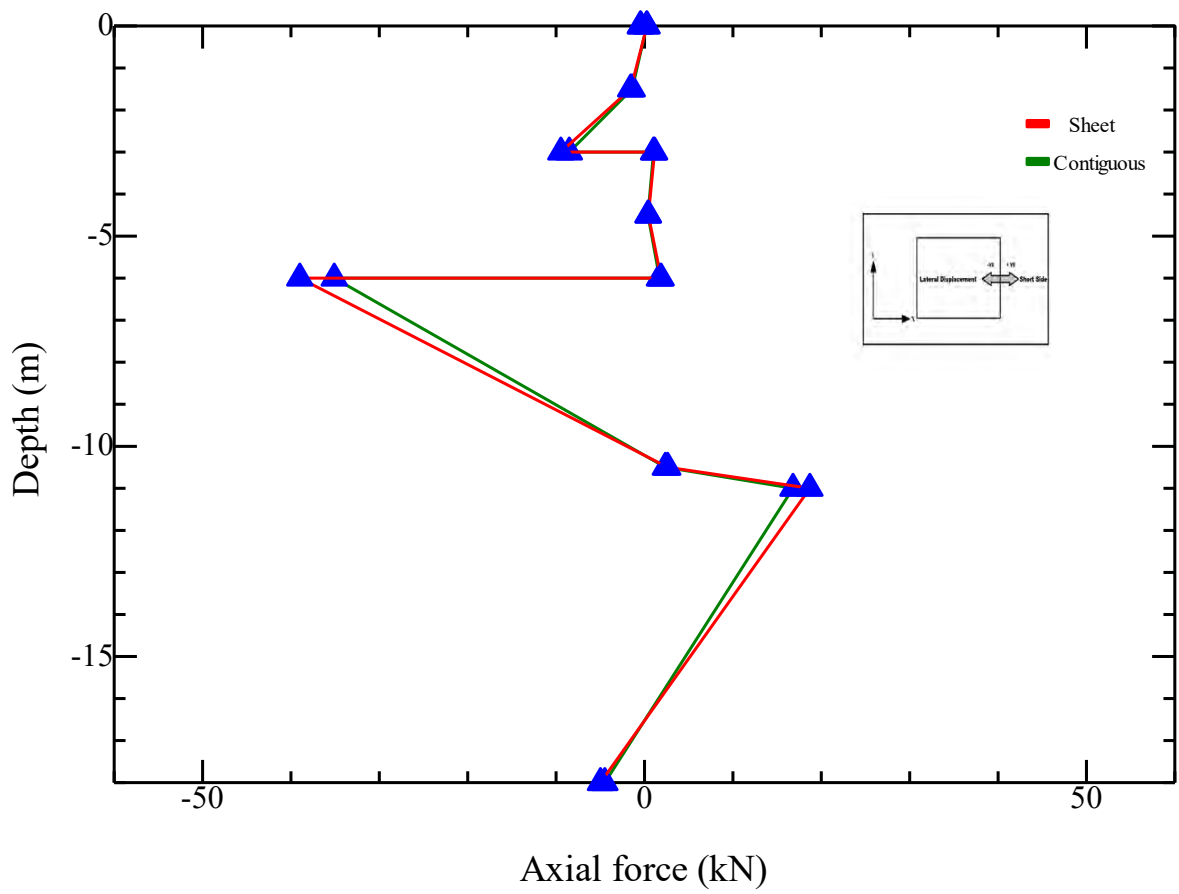


(b)

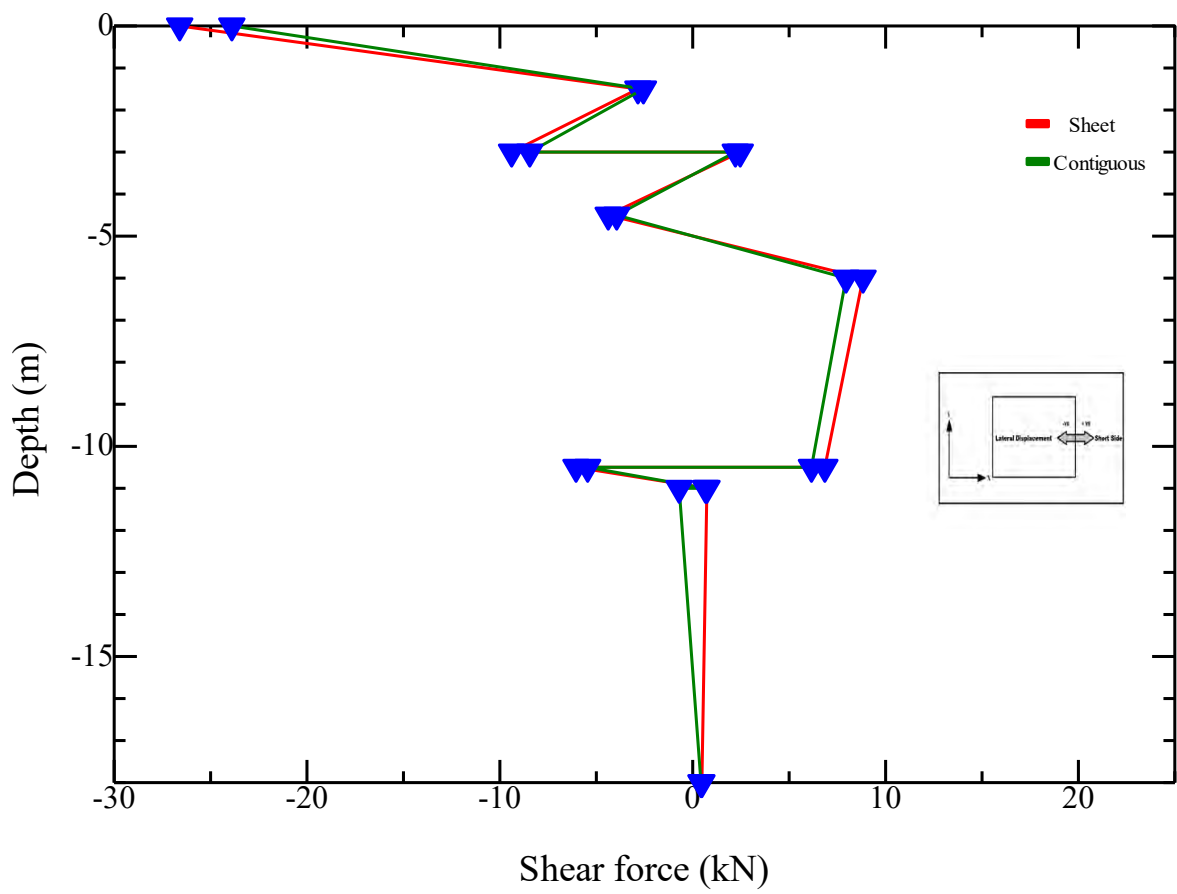


(c)

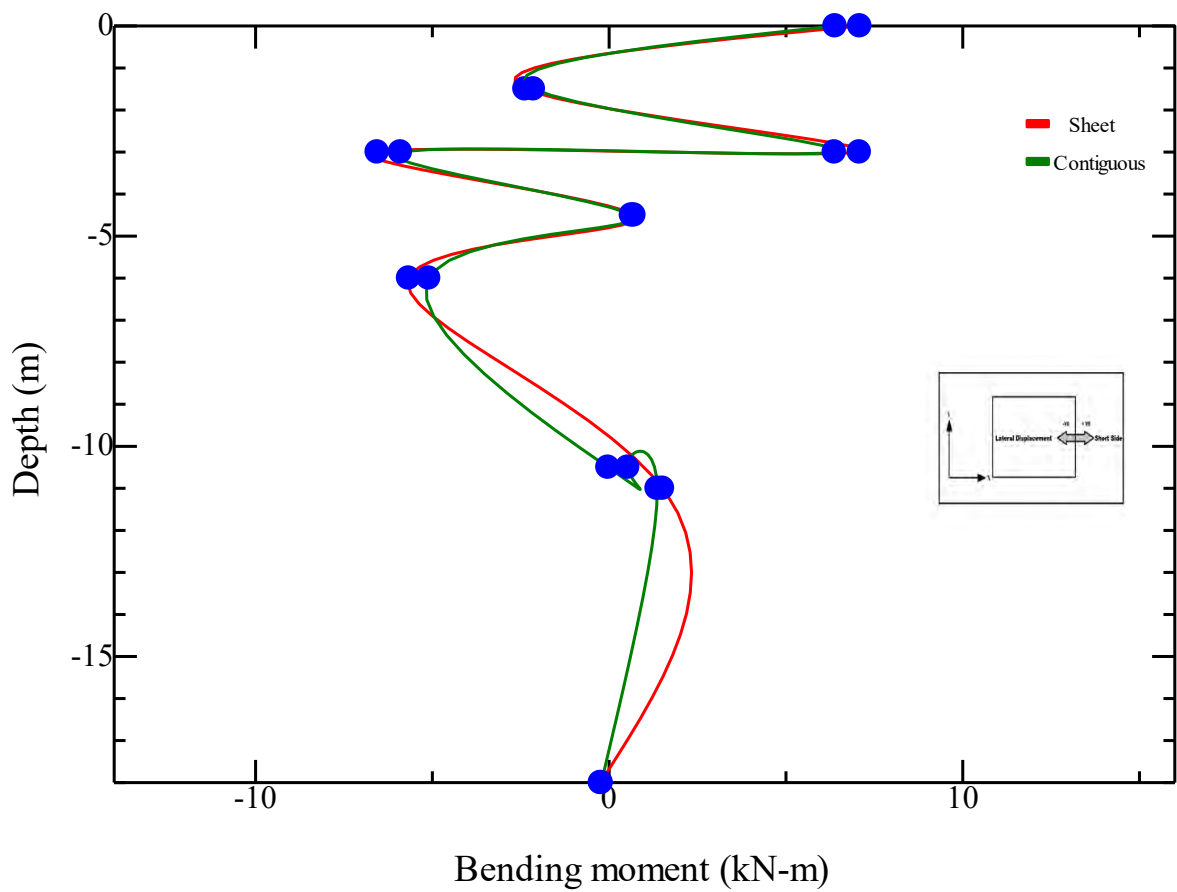
Fig. B-21 Internal forces in the long side of sheet pile and contiguous pile wall of Chittagong site having triple basement system-(a) axial force (b) shear force (c) bending moment- HS model



(a)

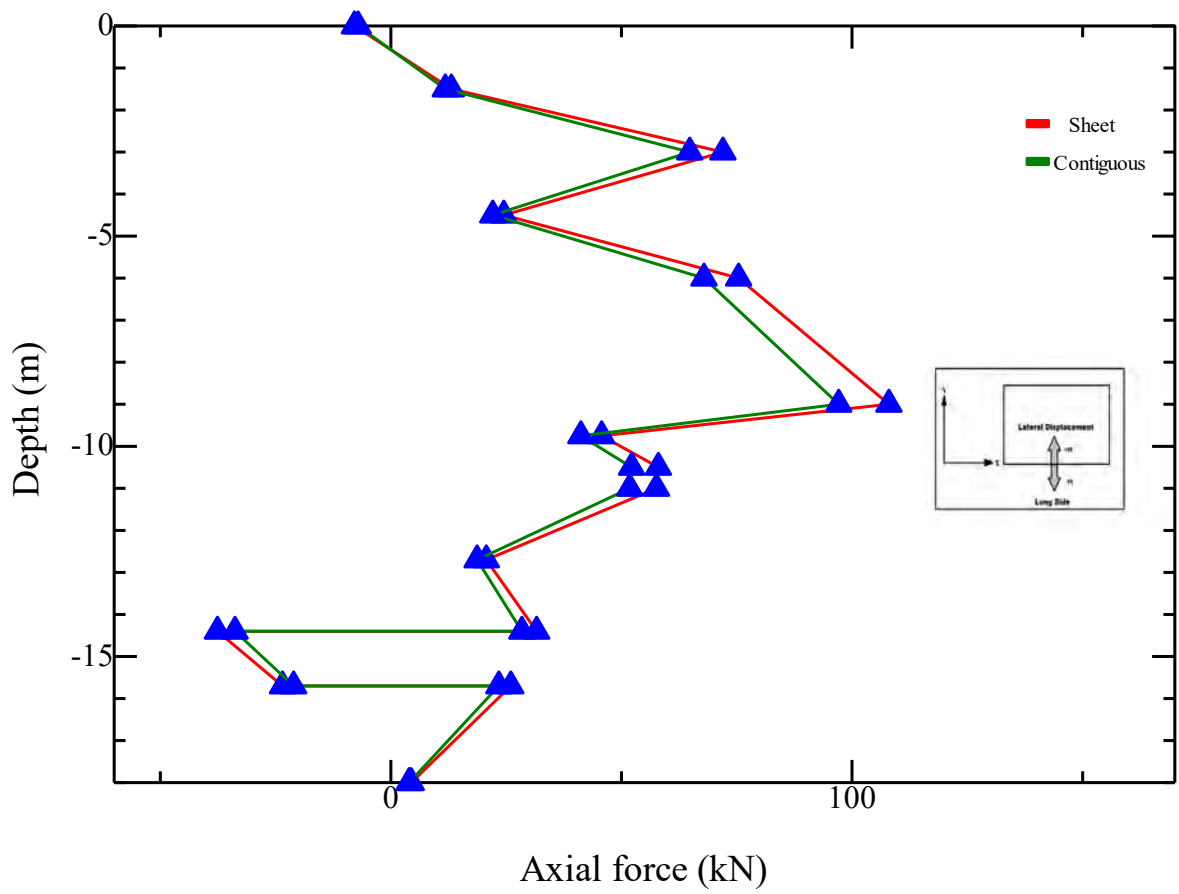


(b)

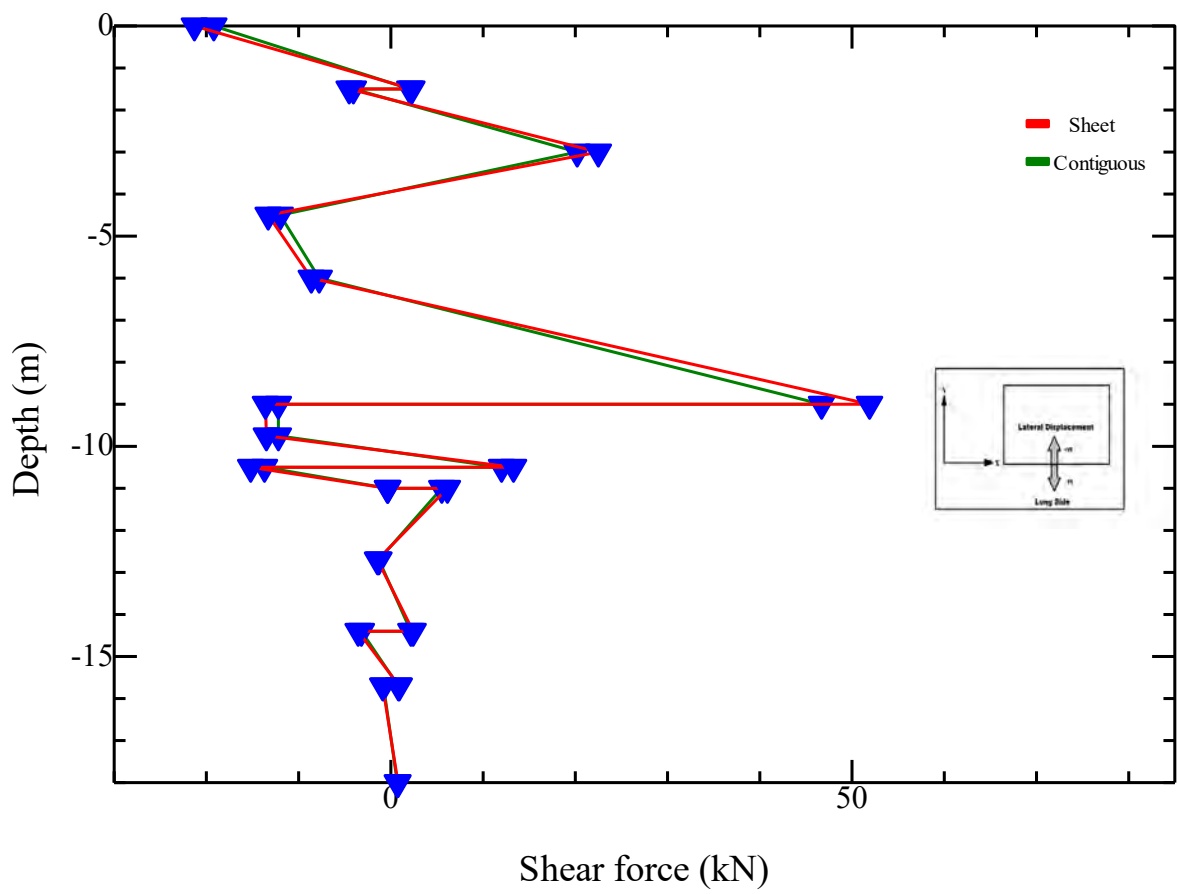


(c)

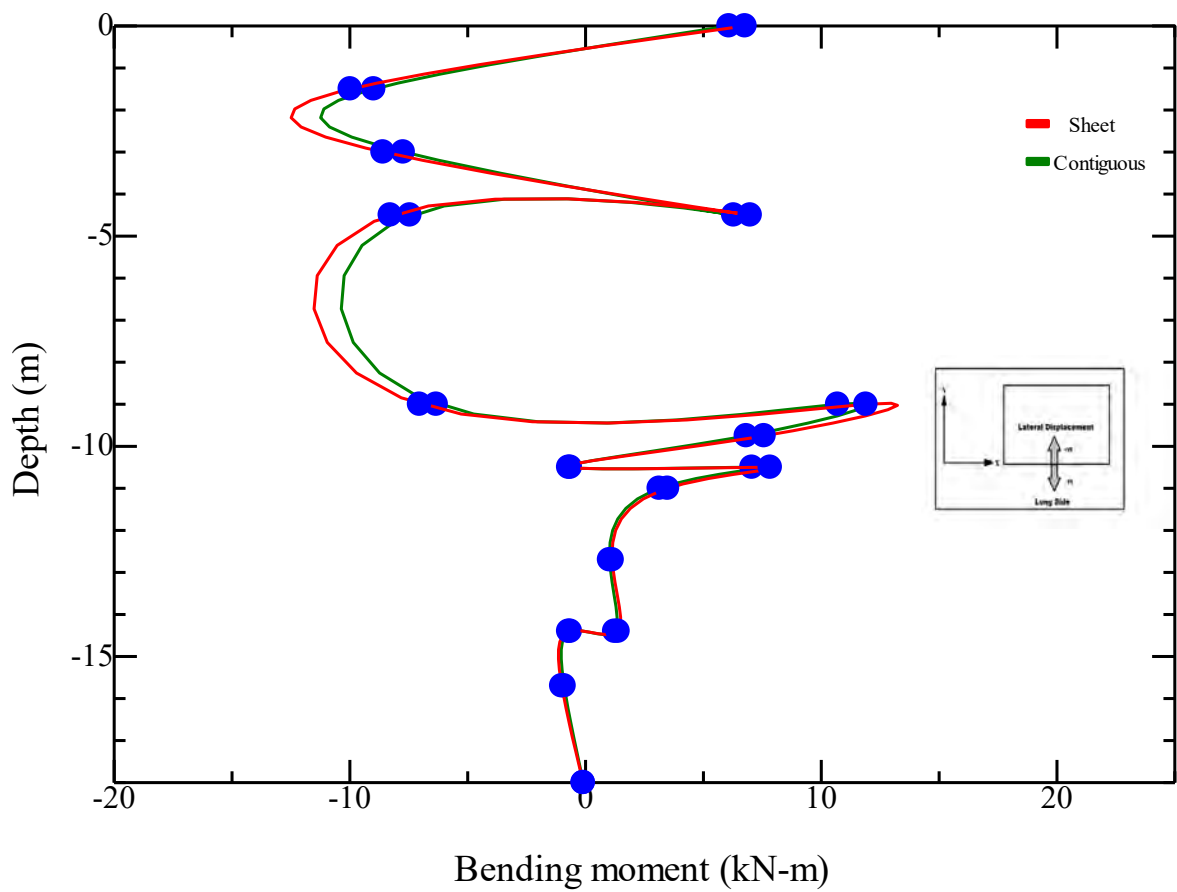
Fig. B-22 Internal forces in the short side of sheet pile and contiguous pile wall of Chittagong site having triple basement system-(a) axial force (b) shear force (c) bending moment- HS model



(a)

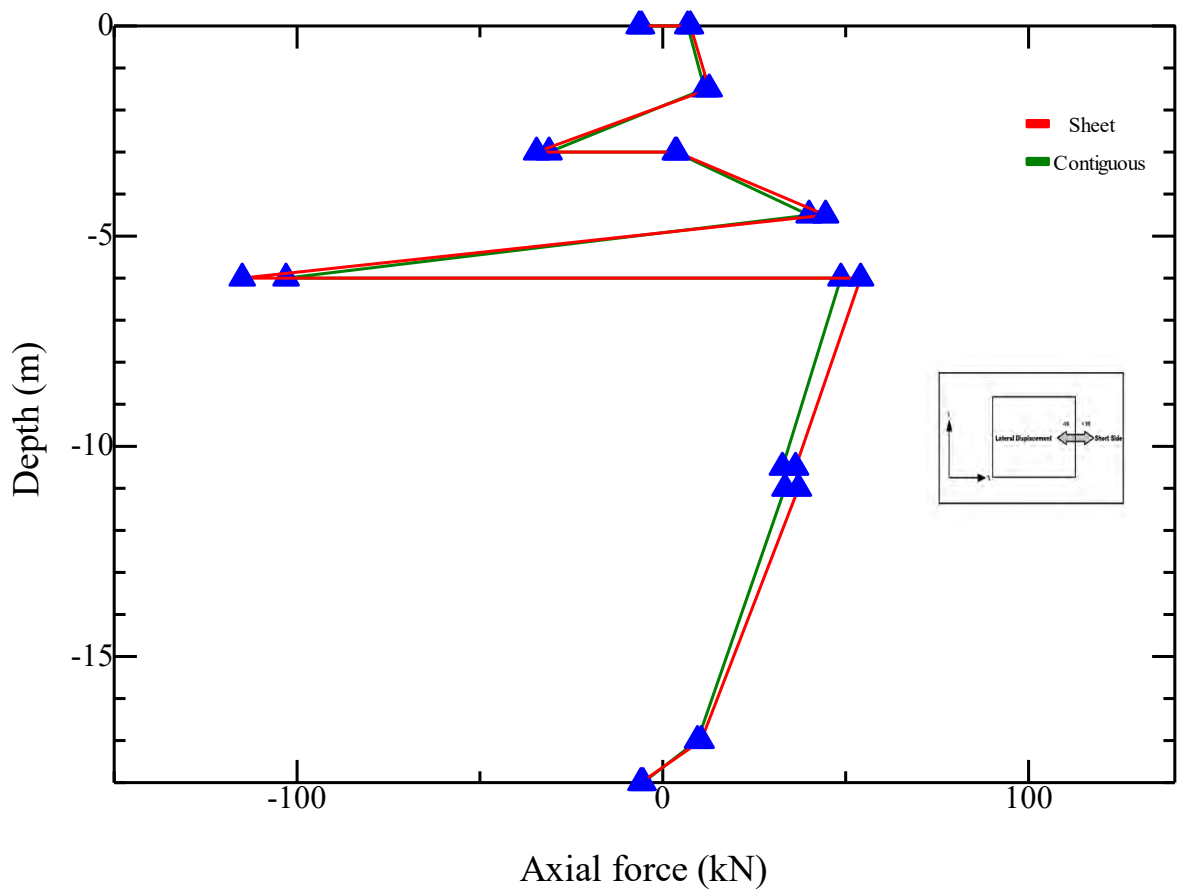


(b)

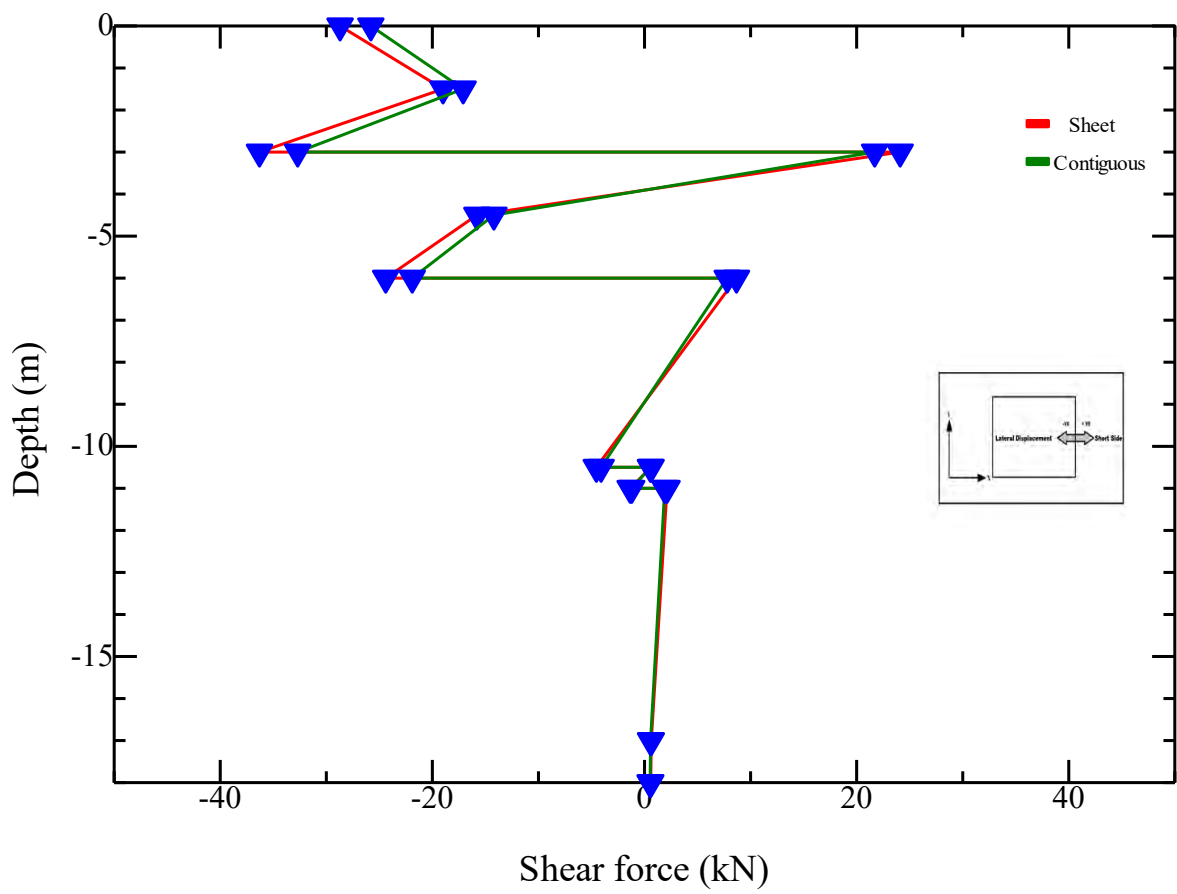


(c)

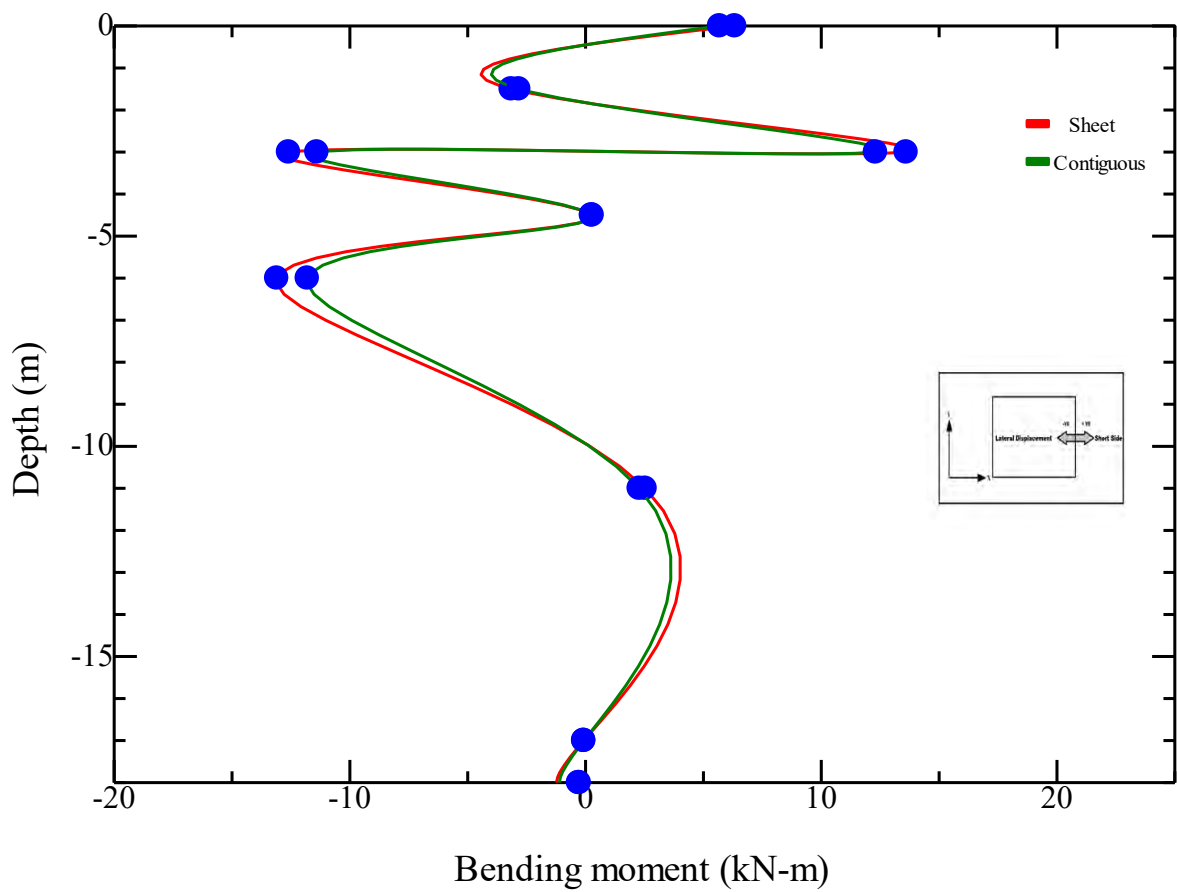
Fig. B-23 Internal forces in the long side of sheet pile and contiguous pile wall of Chittagong site having triple basement system-(a) axial force (b) shear force (c) bending moment- MC model



(a)



(b)

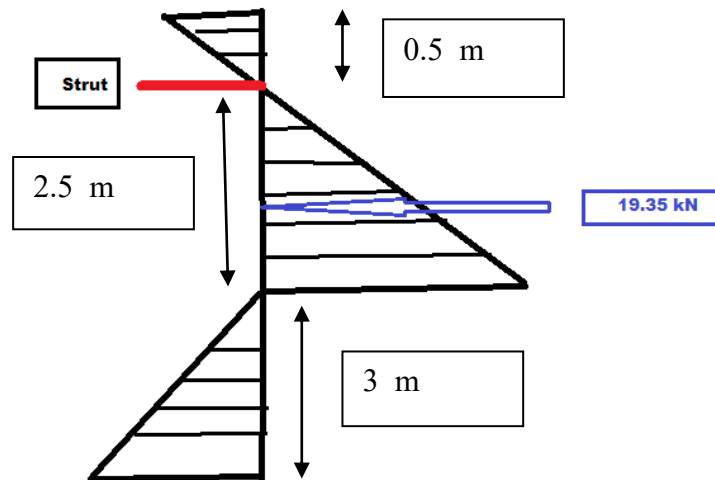


(c)

Fig. B-24 Internal forces in the short side of sheet pile and contiguous pile wall of Chittagong site having triple basement system-(a) axial force (b) shear force (c) bending moment- MC model

HAND CALCULATION OF BENDING MOMENT TO SHOW THE AGREEMENT WITH FEM MODEL

Case: Bending moment of contiguous pile in the single basement system of Dhaka site



Unit weight of soil, $\gamma = 18 \text{ kN/m}^3$

Cohesion, $c' = 31 \text{ kPa}$

Angle of friction, $\phi = 14^\circ$

Active Earth pressure co-efficient, $K_a = \frac{1 - \sin\phi}{1 + \sin\phi} = 0.61$

Passive Earth pressure co-efficient, $K_p = \frac{1}{K_a} = 1.83$

At zero depth, Pressure, $P = 2c\sqrt{K_a} = 2 \times 31 \times \sqrt{0.61} = 48.42 \text{ kN/m}^2$

At 3m depth, Pressure $P = \gamma \cdot H \cdot K_a - 2c\sqrt{K_a} = 15.48 \text{ kN/m}^2$

Force due to earth pressure = $0.5 \cdot 15.48 \cdot 2.5 \text{ kN/m} = 19.35 \text{ kN/m}$

Moment due to force = $0.67 \cdot 19.35 \cdot 2.5 = 15.96 \text{ kN-m}$

From FEM model the result is = 18 kN-m

Deviation is = 12% (Within acceptable range)